VARIOUS MODELLING TECHNIQUES IN SEISMIC RESPONSE OF ELEVATED CONCRETE WATER TANK CONSIDERING INTERACTIONS WITH SOIL AND WATER

GAREANE A. I. ALGREANE

THESIS SUBMITTED IN FULFILMENT FOR THE DEGREE OF DOCTOR OF PHILOSOPHY

FACULTY OF ENGINEERING AND BUILT ENVIRONMENT
UNIVERSITI KEBANGSAAN MALAYSIA
BANGI

2013

TEKNIK PEMODELAN PELBAGAI TINDAK BALAS SEISMIK BAGI TANGKI AIR KONKRIT TINGGI DAN INTERAKSI DENGAN TANAH DAN AIR

GAREANE A. I. ALGREANE

TESIS YANG DIKEMUKAKAN UNTUK MEMPEROLEH IJAZAH
DOKTOR FALSAFAH

FAKULTI KEJURUTERAAN DAN ALAM BINA
UNIVERSITI KEBANGSAAN MALAYSIA
BANGI

2013

DECLARATION

I hereby declare that the work in this thesis is my own except for quotations and summaries which have been duly acknowledged.

31 May 2013

GAREANE A. I. ALGREANE
P38312

ACKNOWLEDGEMENT

Every praises is due to the Almighty Allah alone, the Merciful and peace be upon his prophet who is forever a torch of guidance and knowledge for humanity as whole.

I would like to thank Allah for giving me this opportunity and patience to carry out this thesis.

I would like to express my greatest gratitude and deep appreciation to my advisors. Assoc. Prof. Dr. Siti Aminah bt Othman for being so generous with her time and Prof. Ir. Dr Othman A. Karim and Ir. Dr. Anuar Kasa for useful suggestion throughout the study

I am also indebted to Universiti Kebangsaan Malaysia (UKM) for providing me with the necessary facilities to carry out this research. Great appreciation is also extended to all my colleagues and friends and to all those who contributed directly and indirectly to the success of this study.

However, acknowledgements will be incomplete if it had not been for my friends who have devoted their life and efforts to us, who showered on us their love and moral support unconditionally and doubtlessly, prayed everyday for our success and prosperity.

ABSTRACT

Elevated tanks are lifeline structures because their functions are essential to remain functional in post-earthquake periods. These critical water storage and distribution facilities should be capable of surviving a major seismic event or sustaining only major damage that can readily be repaired. These facilities are needed to provide water for fire fighting, human consumption and sanitation. The irregular shape of the elevated tanks for which most of the mass confluent in the upper part of the tank makes it more sensitive to any dynamic load. Lack of real input seismic excitations at site, an artificial seismic excitation has been generated at bed rock based on Gasparini and Vanmarcke through SIMQKE software. The ground motion and response spectrum have been obtained based on one-dimensional nonlinear analysis site effects through software named as NERA. In this study circular and rectangular elevated water tanks have been chosen to conduct this study through two ways that widely used in the analysis of elevated tanks namely mechanical models and finite element models (FEM). In the case of mechanical models the study examined through software developed by authors the applicability of using these approaches, started from single degree of freedom (SDOF) idealization with and without soil structure interactions (SSI) effects. Also two degrees of freedom (2DOF) in which the fluid structure interactions (FSI) are considered according to Eurocode-8 (EC-8) also with and without SSI. Substructure approach has been adopted to assess the SSI effects in all mechanical models. The results of cases motioned before have been compared with FEM models implemented through LUSAS FEA 14.03 also in the cases with and without SSI effects. Added mass approach (Westergaard) has been used to account FSI in FEM models. The results of period of convective mode (T_c), period of impulsive mode (T_i) and level of forces (overturning moment and shear force) that created by using this approach is compared with FEM results. The results shows that simplified procedure that can be utilized for evaluating the dynamic characteristics and the dynamic response of elevated concrete water tank is adequate by using 2DOF, and inapplicable in the case of SDOF. Passed on the complexity implementation of Westergaard added masses approach, the authors suggested a modification to simplify Westergaard approach by making an alternative masses distribution to T_i and compare it with Westergaard method every case. The results show that minor effects due to the masses distribution are obtained. The circular tank has been chosen to study the linear and nonlinear seismic effects of the whole system (soil, foundation and tank), considering SSI (direct approach) and FSI based on integration dynamic analysis. The effects of state stresses in soil before and after the tank constructed have been studied extensively. The seismic load have been applied at two critical direction in which overturning moment and shear force are maximum, under two integration scheme named Newmark and Helber Hugi Tylor (HHT). The results show that the integration scheme and considering the state of stresses at soil does not affects the results significantly. All of the cases that mentioned above are conducted in two cases with embedment case and with no embedment. The total cases conducted in this study are 96, 12 mechanical cases and 84 FEM cases.

ABSTRAK

Tangki tinggi merupakan satu struktur perhubungan kerana fungsinya masih tetap berfungsi walaupun selepas gempa bumi.Tangki simpanan air kritikal ini dan juga pusat pengagihan mampu untuk bertahan daripada kejadian gegaran seismik utama ataupun hanya mengalami kerosakan yang boleh diperbaiki.Kemudahan ini amat diperlukan untuk menyediakan bekalan air untuk memadamkan api,kegunaan orang ramai dan sanitasi. Bentuknya juga tidak menentu kerana kebanyakan lebih besar di bahagian atas dan ini membuatkan ia lebih sensitif kepada mana-mana beban yang dinamik. Pengujaan seismik tiruan telah dihasilkan pada batuan dasar berdasarkan Gasparini dan Vanmarcke melalui perisian SIMQKE. Pergerakan tanah dan respon spektrum telah diperolehi berdasarkan analisis satu dimensi tak linear menerusi perisian dinamakan sebagai NERA. Di dalam kajian ini,bentuk tangki bulat dan segi empat tepat telah digunakan untuk menjalankan kajian ini melalui dua hala iaitu cara yang digunakan secara meluas bagi menganalisis model-model mekanikal dan unsur terhingga (FEM). Di dalam kes model-model mekanikal,kajian dilakukan melalui perisian yang dibangunkan oleh penulis untuk menguji kebolehgunaan mengunakan pendekatan ini bermula dengan darjah kebebasan tunggal (SDOF) dengan dan tanpa interaksi struktur tanah (SSI) serta kesannya. Terdapat dua darjah kebebasan (2DOF) di mana struktur cecair berinteraksi (FSI) dianggap menurut Eurocode-8 juga dengan dan tanpa SSI. Pendekatan sub struktur telah digunakan untuk menilai kesan SSI kepada semua model mekanikal. Keputusan daripada pemerhatian terdahulu dibandingkan dengan model FEM yang dibuat menggunakan LUSAS dan juga melalui proses dengan dan tanpa kesan SSI. Pendekatan jisim tambahan (Westergaard) telah digunakan untuk menganggar FSI dalam model-model FEM. Keputusan dari mod masa berolak, mod masa dedenyut dan juga tahap tekanan (momen terbalikan dan daya ricih) yang dicipta dengan pendekatan dan dibandingkan dengan keputusan FEM. Keputusan menunjukkan prosedur yang dipermudahkan digunakan untuk menilai ciri dinamik dan respon dinamik tangki air konkrit mencukupi dengan menggunakan 2DOF, dan tidak sesuai menggunakan SDOF. Berbalik kepada perlaksanaan kerumitan Westergaard,pendekatan penambahan jisim, penulis mencadangkan satu pengubahsuaian baru untuk memudahkan pendekatan Westergaard dengan membuat satu alternatif berkumpul taburan kepada dan bandingkan ia dengan kaedah Westergaard bagi setiap kes. Keputusan menunjukkan terdapat sedikit kesan disebabkan penyebaran jisim diperolehi.Tangki bulat telah dipilih untuk mengkaji linear dan kesan-kesan seismik tak linear keseluruhan sistem (tanah, asas dan tangki), dengan mempertimbangkan SSI dan FSI berdasarkan analisis dinamik integrasi. Kesan daripada tekanan di dalam tanah yang di namakan, keadaan in-situ dan keadaan tekanan tanah selepas tangki dibina,dengan menganggap keadaan tanah tidak mencair. Tekanan seismik telah digunakan pada dua arah kritikal di mana momen terbalikan dan daya ricih maksima di bawah dua integrasi skim dinamakan Newmark dan Helber Hugi Tylor. Keputusan menunjukkan skim integrasi dan anggapan keadaan had tekanan tanah tidak menunjukkan sebarang kaitan yang dapat mempengaruhi keputusan kajian tersebut. Semua kes yang disebutkan di atas dijalankan dalam dua kes yang berbeza iaitu kes pembebanan dan juga kes yang tiada pembebanan. Jumlah keseluruhan kes yang dijalankan di dalam kajian ini adalah 96, 12 kes mekanikal dan 84 kes FEM.

CONTENTS

LIST OF TABLES

LIST OF FIGURES

LIST OF SYMBOLS

V_{Base}	Base shear
M_o	Overturning moment
S_a	Spectral acceleration
W	Weight of structure
α_p	Base shear participation
g	Gravity acceleration
Δt	Time step
M	Structure mass and added hydrodynamic mass
C	Structural damping
K	Stiffness of the structure-foundation system
u	Displacement
$\dot{u}$	Velocity
$\ddot{u}$	Acceleration
P	Applied load
T_n	Shortest natural period of the structural system
$\propto, \beta, \gamma$	Weighting factors
q	Uniform pressure applied to the plate
K_{wk}	Modulus of sub-grade reaction
E_s	Young's modulus for the soil
ν_s	Poisson's Ratio for the soil
r_e	Radius of the equivalent plate
K_y	Vertical spring stiffness
K_θ	Rational spring stiffness
A_f	Vertical spring stiffness

A_t	Area of the soil surface
I_f	Inertial value of the base of the footing
$K_{winkler}$	Winkler spring stiffness
T	Fundamental period of a fixed-base structure
W_L	Weight of water + weight of tank + 2/3rd weight of staging frame
K_s	Stiffness of a staging based on fixed-base
m_i	Impulsive mass of liquid
m_c	Convective mass of liquid
m_w	Total mass of liquid tank
h_i	Height of impulsive mass above bottom of tank wall
K_c	Spring stiffness of convective mode
h	Maximum depth of liquid
h_c	Height of convective mass above bottom of tank wall
$\grave{h}_i$	Height of impulsive mass above bottom of tank wall
$\grave{h}_c$	Height of convective mass above bottom of tank wall
R	Radius of tank
K_{y-Sur}	Lateral springs with complex stiffness
$K_{\theta-Sur}$	Rotational springs with complex stiffness
G	Shear modulus
r_0	Radius of circular foundation
$\propto_\theta, \propto_y$	Coefficients of dimensionless
ν	Poisson ratio
B	Length of rectangular foundation
L	Width of rectangular foundation
e	Embedment height

d	Heights of soil layer resting on the rigid rock
$\mathrm{K}_{\mathrm{y-emb}}$	Horizontal correction factor of embedment of circular foundation
$\mathrm{K}_{\theta\mathrm{-emb}}$	Rocking correction factor of embedment of circular foundation
β_x	Translation along x-axis correction factor of embedment of rectangular foundation
β_y	Translation along y-axis correction factor of embedment of rectangular foundation
β_z	Translation along z-axis correction factor of embedment of rectangular foundation
β_{xx}	Rational along xx-axis correction factor of embedment of rectangular foundation
β_{yy}	Rational along yy-axis correction factor of embedment of rectangular foundation
β_{zz}	Rational along zz-axis correction factor of embedment of rectangular foundation
$\check{T}$	Flexible base period
L	Effective height of elevated tank
ξ	Flexible-base damping ratio
$\check{\xi}_0$	Contribution of the radiation damping, and the soil damping
ρ	Mass density of the water
ai	Westergaard pressure coefficient
A and B	Rayleigh damping factors
Tc	Period of convective mode
Ti	Period of impulsive mode
A_i	Amplitude
φ_i	Phase angle
G (ω)	Power spectral density function

$r_{S.P}$	Peak factor
S_V	Target velocity of the response spectrum
ξ_s	Fictitious time-dependent damping factor

LIST OF ABBREVIATIONS

FEM	Finite Element Method
SSI	Soil Structure Interaction
FSI	Fluid Structure Interaction
UBC	Uniform Building Code
IBC	International Building Code
EC-8	Euro Code part 8
LUSAS	London University Stresses Analysis System
SDOF	Single Degree of Freedom
Two DOF	Two Degree of Freedom
MDOF	Multi Degree of Freedom
HHT- α	Hilbert, Hughes and Taylor α Method
BEM	Boundary Element Method
CG	Center of Gravity
ATC	Applied Technology Council
NEHRP	National Earthquake Hazards Reduction Program
ACI	American Concrete Institute
SEER	Engineering Seismology and Earthquake Engineering Research

CHAPTER I

INTRODUCTION

1.1 OVERVIEW

Earthquake is a complex natural phenomenon in which the researchers is trying to understand, from the early history of mankind. Despite of scientific study of the subject for the last 100 years or so, it is felt that we are still in the infancy of our knowledge on the subject.

The parameters affecting this phenomenon are so large and varying and also covering different branches of science, we can at best arrive at a simplified model of the problem amenable to human perception and try to arrive at a solution which would in all probability survive this nature's assault with some limited damage.

The basic objective of an earthquake resistant design is not to make the structure foolproof but to limit its damage to the extent of minimizing the loss of human life and property. Though earthquake is a global phenomenon, yet there are some countries in the world like USA, Japan, Turkey, India, Iran, New zealand etc that are severely affected by earthquakes leading to significant loss of human life and properties, while there are others whose geological characteristics are considered seismically inert like Malaysia, United Kingdom, Australia, UAE, Libya etc. which have no significant history of earthquakes. Based on the above, it is evident that there are countries where significant research and investigation have been carried out to develop procedures for earthquake resistant design of structures. Countries like USA, Japan, India, Mexico etc. have contributed significantly on this issue. Whilst in

Malaysia the research of the earthquake resistant only started recently due to seismic activities in recent years.

Prior to about 2002, Malaysia was considered to be a low seismic risk area. In recent years, however, there has been an increasing awareness of seismicity, which can be attributed to recent concern about the potential for a major earthquake resulting from the subduction zone of the Sunda-Arc and Sumatran fault shown in Figure 1.1 (Azlan et al. 2006). The later event is considered to be a speculative event on basis of present knowledge. The net effect of the increasing awareness of earthquake hazard has been a general upward revision of design seismic coefficients and ground accelerations.

The effects caused by the Sumatran earthquake in 2002, has drawn attention to an ongoing problem in Malaysia with regard to seismic vulnerability. Some of the regions that affected by the earthquake were not classified as seismic areas, and structures were built without seismic provisions. Therefore, the failure of structures may exceed as what have been expected in the region with a low magnitude earthquake. The cracks on some of structures in Penang alerted the country to the vulnerability of critical structures such as schools, hospitals, tanks and etc.

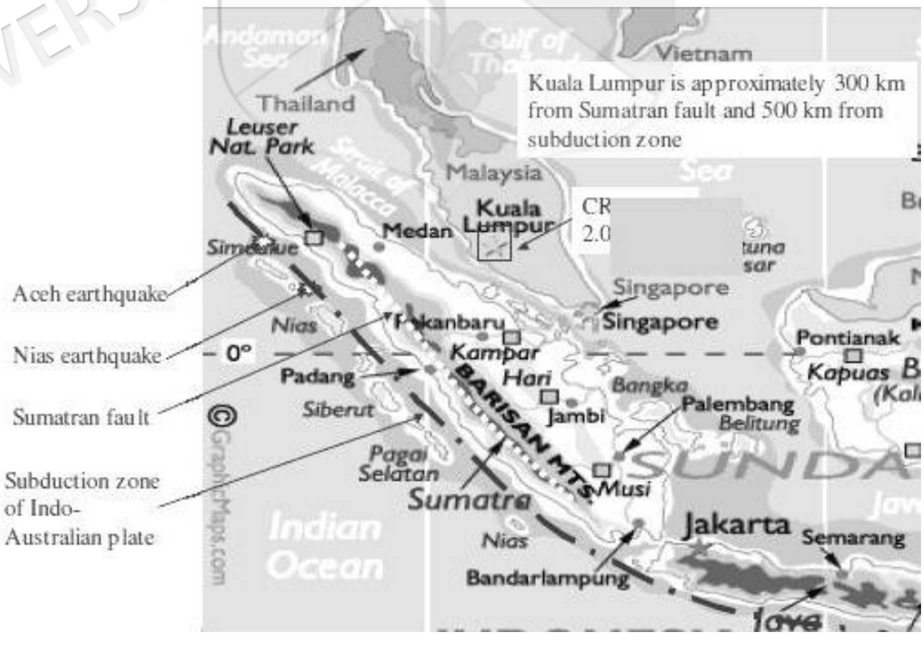

FIGURE 1.1 Location of Sumatran fault and the Sunda-Arc subduction zone

Source: Bellier 1999

Water supply and distribution facilities are classified as lifeline structures because their functions are essential in post-earthquake periods. These critical water storage and distribution facilities should be capable of surviving a major seismic event or sustaining only major damage that can readily be repaired. These facilities are needed to provide water for fire fighting, human consumption and sanitation. Catastrophic-type facilities not only deprive the public of these services but further endanger public health and safety.

Today water tanks have taken on many shapes (rectangular, circular) and configurations (elevated, ground) that most common among these is a cylindrical tank with a roof of either a one or two-way slab or a partial spherical dome or rectangular shapes. The construction material usually either steel, reinforced concrete or in some cases composite, this type of structures usually built with typical shapes and configuration as shown in Figure 1.2.

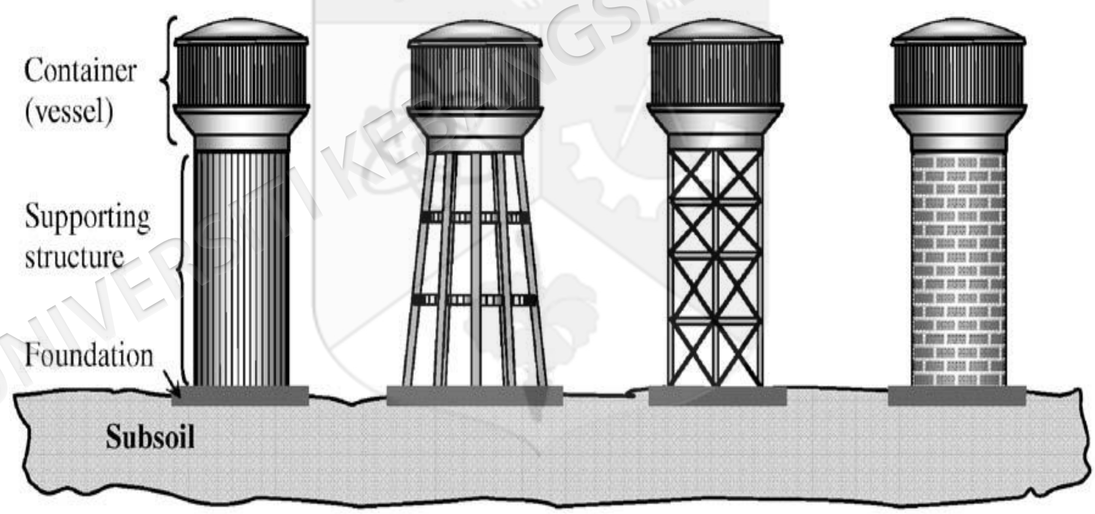

FIGURE 1.2 Various structures circular elevated water tank

Source: Livaoglu 2006

1.2 BACKGROUND

In the late 1950s and early 1960s, the seismic force design of tanks was based on a single lateral force coefficient applied to the tank as a rigid body in manner similar to that used in design of one and two story structure. By the mid to late 1960s, it was recognized that the fluid motion in the tank could contribute significantly to its response and a lateral force coefficient was applied only to the rigid impulsive component of the tank fluid and not to the convective or sloshing component. It was not until the 1970s that the influence of soil tank interaction and tank flexibility were recognized as significant design considerations for earthquake. By the 1970s, it become apparent that building code lateral force coefficients were often a poor approximation to actual ground motion conditions for design of structures that did not exhibit the same type of earthquake behavior and posses similar seismic overload capacity in the form of ductility and redundant load paths as conventional seismic building construction (Ronald & Eguchi 1986). The failure of such structures due to earthquakes are results of shear forces created at the base of the elevated tank or overturning moments as shown in Figure 1.3.

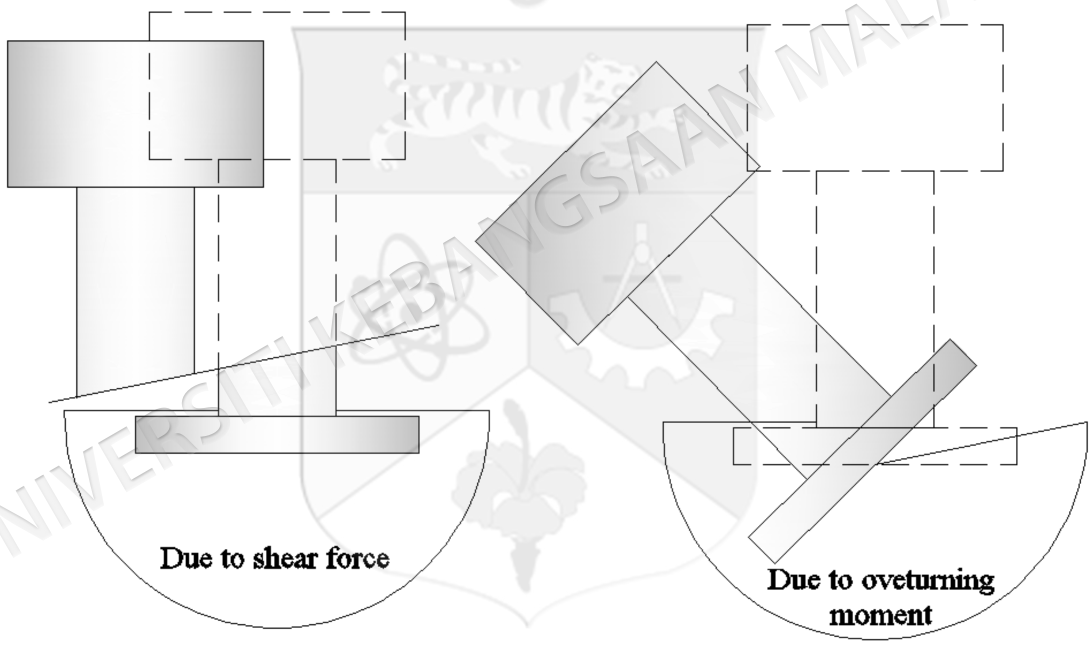

FIGURE 1.3 Failure of elevated water tank due to seismic loads

1.3 PROBLEM STATEMENT

To analyze the elevated concrete water tanks under seismic loads through finite element method (FEM), the engineers facing difficulties to include into account some of variable that may play a major role in the response of elevated tank to the seismic loads, such as soil structure interaction (SSI) and fluid structure interaction (FSI), due to that the engineers resorts to use of approximate methods that lacking some of realistic in which the mass of elevated tank and water and part of staging lumped in one single degree of freedom (SDOF) or two degree of freedom (two-DOF)

It is well known that most of FEM software does not contain flow elements in their elements library which is used to simulate FSI based on some of ways having more realistic approaches. Avoiding the lacking of flow elements, added mass approach in which the mass inside the tank gets divided to two parts passed on Housner's approach namely sloshing part and rigid part. The difficulties are how to simulate the sloshing part in which needs some of linkage elements (stiffness element) that not available in some of FEM commercial software, and adding the mass of rigid part according to Westergaard added mass approach in which not easy to implement.

In the case of SSI, the modeling is relatively easier than water because there are several ways supported in most conventional FEM software of which can be performed easier and the familiarity of most engineers to SSI is more than FSI, because it's usually considered in analysis of building. But the effects of SSI in the case of FEM and mechanical models needs to be re-evaluated and compare with approaches assumed to be having a high accuracy of modeling namely "nonlinear direct dynamic analysis with considered SSI and FSI" under Malaysian seismic data

The evaluation process needs to include a range of variables and see their effects on the process of analysis and proposes outlines for the analyzing of elevated concrete water tanks.

1.4 RESEARCH OBJECTIVES

To achieve the aforementioned need, four objectives were focused in this study:

(1) To establish a comparative study in order to evaluate various models of elevated water tank based on single degree of freedom (SDOF), two degree of freedom (two-DOF) and FEM models in case of fixed and SSI consideration through free vibration and direct dynamic analysis, in case of embedment and no embedment;

(2) To propose suitable alternative modification, in order to simplify the SSI techniques, for saving the computation time and efforts;

(3) To study the effects of nonlinear SSI on the response of elevated concrete water tank with two dynamic analysis scheme, namely Newmark and Tylor in two critical directions of seismic analysis; and

(4) To study the consideration effects of in-situ soil stress before and after the tank constructed on the whole seismic response of elevated concrete water tank.

1.5 SCOPE OF RESEARCH

The scope of work carried out in this study was limited to:

(1) Circular and rectangular elevated concrete water tank.

(2) Analytical modes namely single degree of freedom, single degree of freedom with SSI, two degree of freedom with FSI and two degree of freedom S-FSI.

(3) Three dimensional finite elements model based of fixed base with FSI consideration using added mass approach with free vibration response spectrum and time history analysis.

(4) Three dimensional finite elements with accounting three dimensional continuums SSI and FSI using transient nonlinear dynamic analysis.

(5) All cases were modeled with embedment and no embedment

(6) Malaysian seismic data (low intensity of earthquake)

1.6 THESIS ORGANIZATION

The thesis is organized in seven chapters. A brief description of the content of each chapter is given below.

Chapter I provide the general background and motivation for this work. The objectives of the research, scope of research, problem statement and the organization of the thesis are presented.

Chapter II provides thorough information about the background needed for conducting this research. It presents information about SSI, FSI and method of dynamic analysis, dynamic analysis of elevated tank approaches and provided the previous studies in this area.

Chapter III explains the research program and discusses the methodology used to the developed models. This chapter also describes the models development steps of building the models (analytical and FEM) and focuses on the development and description of the prototype simple software used in the analysis of analytical models.

Chapter IV presents information about the generation of ground motions. It also focuses on background information about local site effect. Also present the results of ground motion generations and nonlinear local site effects generation.

Chapter V starts with exhibited the cases to be conducted in this study. Then the modal parameters identification of elevated tanks (Circular and rectangular) according with the methodology that presented in the chapter III.

Chapter VI focuses on presenting and discussions of the results obtained in this thesis.

Chapter VII highlights the conclusions obtained from the analyses of the results, and gives recommendations for future work.

CHAPTER II

LITERATURE REVIEW

2.1 INTRODUCTION

Few issues of structural response due to static loads remain unresolved. Therefore, a further sophisticated procedure for static analyses and design is difficult to justify on the basis of either safety or economy. On the other hand, seismic loading and response of structures are far from being sufficiently understood especially for hydraulic structure where soil and water play an important role. The analysis process, which leads to the evaluation of seismic actions as load applied on structure with accounting the soil and water interactions and the methods of analysis as input data and deformations as output of the analysis, involves knowledge from several sub-disciplines in engineering, such as engineering seismology, geotechnical engineering, structural analysis and computational mechanics (Elnashai and Sarno 2008). Therefore, to perform reliable seismic analyses of structural systems, a conceptual framework, such as shown in Figure 2.1, is required. This framework includes the essential components summarized below:

- Ground motion and load modelling;
- Structural modelling;
- Foundation soil and water modelling;
- Method of analysis;
- Performance levels;
- Output for assessment

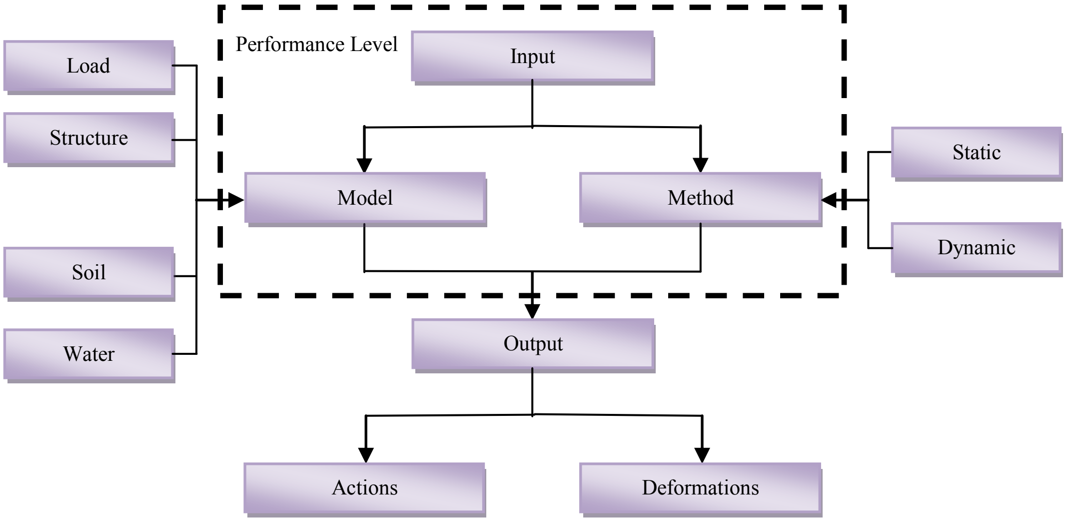

FIGURE 2.1 Conceptual frameworks for seismic analysis of hydraulic structures
Source: Elnashai and Sarno 2008

Several types of loads may be applied to a structure during its lifetime. These include primarily dead and live loads. Dead loads may be modelled reliably through Gaussian distributions and exhibit low coefficients of variation. Live loads exhibit higher variability and their statistical representation depends significantly on the type of live load considered. However, when an earthquake hits a structure, it is unlikely that all live loads would be at their respective maximum value. Therefore, load combination models are an important part of the definition of actions on structures.

Dead loads considered in static and dynamic analyses are due to the own weight of the structure as well as partitions, finishes and any other permanent fixtures. Live loads, on the other hand, are non - permanent and represent the use and occupancy. Seismic codes provide characteristic values of design loads.

Lateral loads, such as wind and earthquakes, occur only occasionally. Seismic loads are generated by the mass of the structure when accelerated by earthquake ground motion. As such, these loads are a function of the characteristics of both earthquake and structure. When calculating seismic loads, the weight of the structure does not correspond to the full dead and live load together, since this would be over conservative in view of the low probability of an earthquake occurring while the structure is at maximum live load. Furthermore, some live loads may not be rigidly fixed to the supporting system and do not necessarily move in phase with the rest of the structure. Therefore, it is appropriate to define percentages of dead and live loads when considering the tributary seismic weight and corresponding mass (Elnashai and Sarno 2008). To investigate the earthquake effects on the structure, there are numerous approaches that can be adopted in the seismic codes such as Uniform Building Code (UBC), International Building Code (IBC) Euro Code Part 8 (EC-8)

2.2 SEISMIC ANALYSIS APPROACHES

Evaluation of the structures response to the earthquake ground motions can be evaluated in phases from the simple to complexity progressing and regular use as shown in Figure 2.2. The simplest approach knows as seismic coefficient method, then equivalent lateral force method, response spectrum– modal analysis procedure, time history-modal analysis procedure, linear time history – direct integration, and finally nonlinear time history-direct integration. The literature review on such methods used is discussed below.

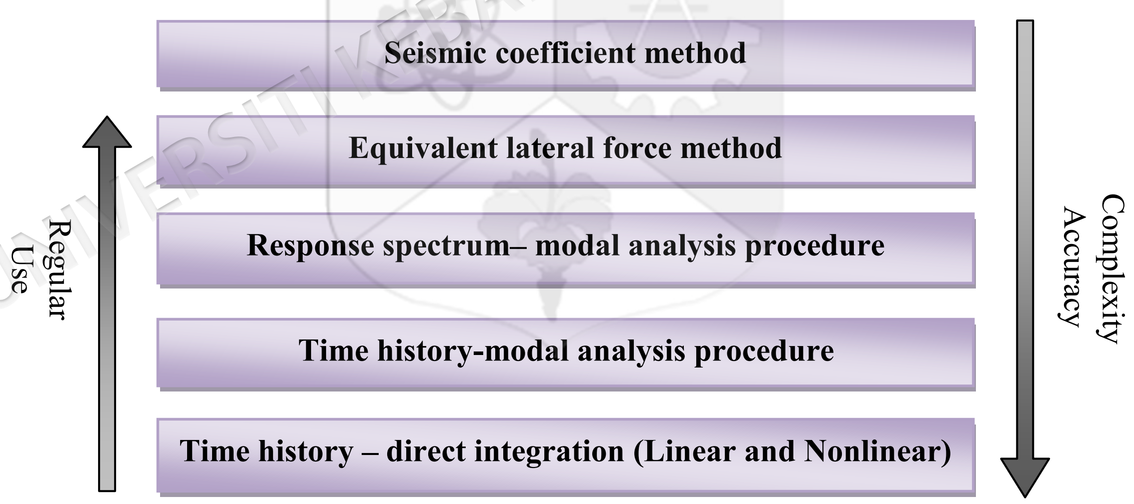

FIGURE 2.2 Methods of seismic analysis

2.2.1 Seismic Coefficient Method

In this method, the seismic load is treated as static load and combined with hydrostatic pressures in the reservoir of the tank, and gravity loads. It is conventionally used to evaluate seismic stability of structures. According to UBC and EC-8 this method may still be used in the preliminary design and stability analyses. The inertia forces acting on the tank are computed as the product of the structural mass, added-mass of water, and the effects of dynamic soil, multiply with seismic coefficient. In representing the effects of ground motion by static lateral forces, the seismic coefficient method neither accounts for the dynamic characteristics of the structure-water-soil system nor for the characteristics of the ground motion. The method, however, should be used with caution if the interaction between the structure and soil-pile foundation is significant. The seismic coefficient method is part of the Linear Static Procedure (US army group of engineering 2007).

2.2.2 Equivalent Lateral Force Method

This method is widely used for the seismic design of structures. The concept is based on fact that the structure response is predominant in the first mode. In the case of elevated concrete water tanks, similar procedures have been developed for preliminary seismic analysis (Fenves and Chopra 1986) using standard mode shapes and natural frequencies. In such cases especially the elevated water tank, the first (fundamental) mode of vibration could contribute as much as 80% or more to the total seismic response of the structure. Therefore, the period and general deflected shape of the first mode are sufficient for estimating inertia forces or equivalent lateral loads needed for the seismic design or evaluation. The equivalent lateral force method is illustrated in Figure 2.3. The steps of the analysis are described as follows:

(1) Determine the period of vibration for the first mode as in Figure 2.3a. This can be done using a general formula developed for the particular structure under consideration based on what is known about the stiffness of the structure-foundation system *(K)* and the total system mass (*M* = structure mass + added hydrodynamic mass).

(2) Determine the spectral acceleration (S_a) for an equivalent single degree-of-freedom system (SDF) as shown in Figure 2.3b. This can be done using the period of vibration determined in Step 1 in combination with a standard or

site-specific acceleration response spectrum. In some cases, as for buildings, the spectral acceleration will be represented by a standard spectrum in equation form as part of a base shear formula. The base shear formula will also account for the base shear participation factor described in the following step.

(3) Once the spectral acceleration (S_a) has been determined, the total inertial force on the structure due to the design ground motions (represented by the design response spectrum shown in Figure 2.3b) can be estimated using Equation (2.1). When spectral acceleration and the total mass are known, the base shear participation (α_p) can be estimated from the structure deflected shape and mass distribution.

$$V_{Base} = \alpha_p (S_a) \frac{W}{g} \tag{2.1}$$

(4) The analytical model of the structure can be represented by a series of lumped masses as shown in Figure 2.3c. The total inertial force (base shear) is then distributed along the height of the structure at each lumped mass location. The magnitude of each inertial force is obtained from the product of the mass participation factor, multiply with the lumped mass, multiply with the spectral acceleration (S_a), multiply with the value of the mode shape at the lumped mass location

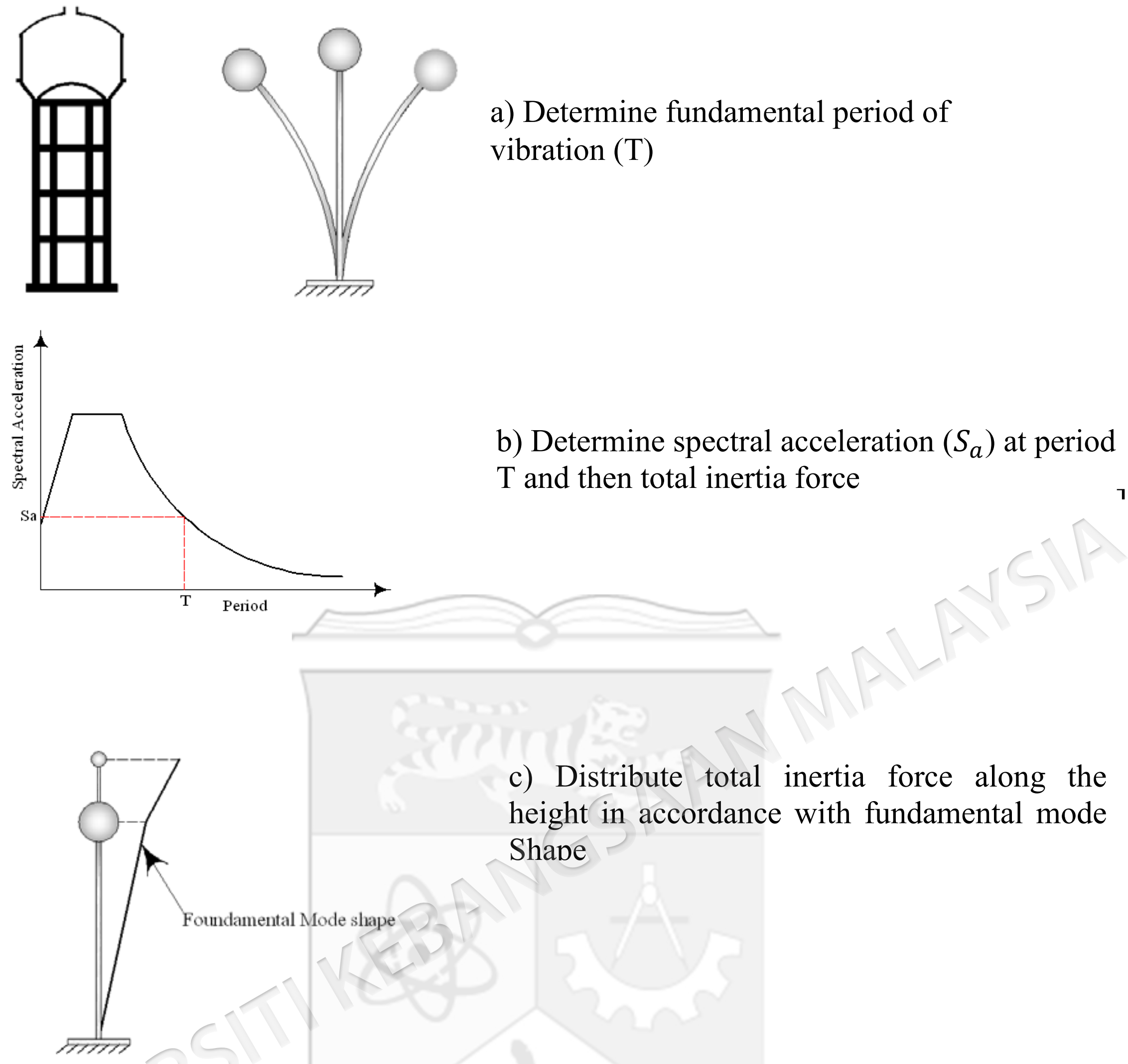

FIGURE 2.3 Illustration of equivalent lateral force method

The first-mode mass participation factor is the same for each lumped mass location and can be determined based on the mass distribution and deflected shape. The mode shape value will either be provided in the equivalent lateral force method, or will be incorporated in a base shear distribution formula as done for buildings. Once all the inertial forces have been determined, the analysis can proceed in the same procedure as any static analysis.

2.2.3 Response Spectrum – Modal Analysis Procedure.

This method is similar to equivalent lateral force method, except that it is the most basic and truly dynamic method of analysis. The number of modes required varies for each analysis however; all modes with significant contribution to the total response of the structure should be included. Usually the numbers of modes are adequate if the total mass participation of the modes used in the analysis is at least within 90-percent of the total mass of the structure. Modal analysis is usually performed using computer software, and it is capable of determining the periods of vibration and mode shapes for all contributing modes. Most structural analysis programs such as LUSAS have this capability, and for many reasons this type of analysis is preferred over the equivalent lateral force method of analysis which is limited to a single mode. The response-spectrum modal analysis procedure however has limitations and time history analysis is usually recommended for final design and evaluation in conformance when:

1- The computed response-spectrum stresses or section forces exceed the allowable values, thus indicating nonlinear response might occur

2- Estimation of the level of nonlinear behaviour and thus damage is necessary to assess acceptability of the design or seismic safety of an existing structure.

2.2.4 Time History-Modal Analysis Procedure

This procedure is similar to that described for the response spectrum – modal analysis procedure, except that earthquake demands are in the form of acceleration time histories, rather than response spectra and the results are in terms of displacement and stress (or force) histories. Peak values of various response quantities are extracted from the response histories. Time history-modal analysis provides valuable time dependent information that is not available in the response spectrum–modal analysis procedure. Especially important is the number of excursions beyond displacement levels where the structure might experience strength degradation (strain softening). As with the response spectrum–modal analysis procedure, the time history-modal analysis is limited to a linear elastic response. The nonlinear response of a structure is computed by the time-history method using the direct integration procedure.

2.2.5 Linear and Nonlinear Time history – Direct Integration Procedure

Linear and nonlinear time history analysis, involves direct integration of the equations of motion, and therefore it is the most powerful method available for evaluating the response of structures to earthquake ground motions. It is a step-by-step numerical integration procedure, which determines stresses (or forces) and displacements for a series of short time increments from the initiation of loading to any desired time (Chopra 2006). The time increments are generally taken of equal length for computational convenience. The condition of dynamic equilibrium is established at the beginning and end of each time increment. The motion of the system during each time increment is evaluated on the basis of an assumed response mechanism. The advantage of this method is that it can be used for both linear and nonlinear analyses. In the case of nonlinear analyses, structure properties (including nonlinear behaviour) can be modified during each time increment to capture response behaviour appropriate to that deformed state.

There are many numerical integration procedures have been developed. However, only a very brief summary of the most common methods are presented here to show how they are applied in seismic analysis of hydraulic structures. Direct integration methods are generally classified as either explicit or implicit. In general, linear time-history analyses of hydraulic structure are usually conducted using implicit methods. However, explicit methods are briefly discussed here and they are included in some commercial computer programs such as LUSAS.

2.2.6 Explicit Methods

The basic concept that common to most explicit methods is to write the equations of motion for the beginning of the time step, approximately the initial velocity and acceleration terms by finite difference expressions, and then solve for response at the end of time step (LUSAS 2007). The response values calculated in each step depend only on quantities obtained in the preceding step. Therefore, the numerical process proceeds directly from one step to next. Explicit methods are very convenient, but they are only conditionally stable and will "blow up" if time step is not sufficiently small. The following method is used in the explicit approach.

The central difference method is a very simple of explicit method that uses the following finite-difference expressions for approximation of the initial velocity and acceleration terms (Clough and Penzien 1993, Bathe and Wilson 1976)

$$\left(\frac{1}{\Delta t^2}M + \frac{1}{2\Delta t}C\right)u_{t+\Delta t} = P - \left(K - \frac{2}{\Delta t^2}M\right)u - \left(\frac{1}{\Delta t^2}M - \frac{1}{2\Delta t}C\right)u_{t-\Delta t} \quad (2.2)$$

Equation (2.1) shows that the stiffness matrix does not appear in the coefficient of $u_{t+\Delta t}$, and thus factorization of the (effective) stiffness matrix will not be required. If mass and damping matrices are diagonal, even the matrices need not be assembled. In that case the solution is obtained at the element level which allows solving very large structural systems without substantial computer resources. These advantages make the central difference method convenient and efficient. However, the method is only conditionally stable and its stability depends on the choice of time step Δt. To obtain a stable solution, Δt must be $< T_n/\pi$, where T_n is the shortest natural period of the structural system. If the central difference method is used with a $\Delta t > T_n/\pi$ the solution will increase exponentially. This may not be a limiting factor for a SDOF system, because more than π or 3 steps are needed to adequately define one vibration cycle. However, the size of time step would be an issue for the MDOF systems where very short-period modes of vibration (compared with time step of input loading) are essential to the dynamic response of the system. In these situations extremely small time step would make the explicit methods undesirable.

2.2.7 Implicit Methods

In an implicit method the expressions for new values at $t + \Delta t$ used equilibrium equations at $t + \Delta t$, and thus include one or more values pertaining to that same step (LUSAS 2007). Examples of various implicit integration methods are presented below.

2.2.8 Newmark-β method

The Newmark-β method is a step-by-step procedure with the following integration equations for the displacement and velocity at time step $t + \Delta t$ (Clough and Penzien 1993, Bathe and Wilson 1976).

$$u_{t+\Delta t} = u_t + \Delta t \dot{u}_t + \Delta t^2 \left[\left(\frac{1}{2} - \beta \right) \ddot{u}_t + \beta \ddot{u}_{t+\Delta t} \right] \tag{2.3}$$

$$\dot{u}_{t+\Delta t} = u_t + \Delta t [(1 - \gamma) \ddot{u}_t + \gamma \ddot{u}_{t+\Delta t}] \tag{2.4}$$

Where β and γ are weighting factors and can be chosen to obtain optimum stability and accuracy.

1- If $\beta = 1/4$ and $\gamma = 1/2$ the Newmark-β method is unconditionally stable (i.e. regardless of the size of the time step). In this case the acceleration within the time step Δt is constant and is usually referred to as the Newmark's constant-average acceleration scheme.

2- If $\beta = 1/6$ and $\gamma = 1/2$ the Newmark-β method is identical to the linear acceleration method, in which the acceleration varies linearly within each time step. The linear acceleration method, however, is only conditionally stable. The linear acceleration method will be unstable unless $\Delta_t / T_n \leq \sqrt{3/\pi} = 0.55$ This restriction has no effect in the analysis of SDOF systems because a shorter time steps than $\Delta_t / T_n = 0.55$ is needed for satisfactory representation of the dynamic response and input, but may require extremely short time step for analysis of MDOF systems having short periods of vibration.

3- In general assuming a linear acceleration within each time step gives a better approximation of the dynamic response and provides more accurate results than the constant acceleration method.

2.2.9 Wilson θ method

For a general type of structure the period of the highest mode is related to the properties of the individual elements. An element with relatively small mass results in a very short period of vibration, with the effect of requiring an extremely short time step of integration, as discussed above.

Although the unconditionally-stable constant acceleration method can be used in this situation, for accuracy reasons an unconditionally-stable linear acceleration method such as the Wilson θ-method (Clough and Penzien 1993, Bathe and Wilson 1976) is more desirable. The Wilson θ-method is based on the assumption that the acceleration varies linearly over an extended computational interval $\tau = \theta\Delta_t$, where $\theta \geq 1$. For $\theta = 1$, the method reverts to the standard linear acceleration method, but for $\theta > 1.37$ it becomes unconditionally stable. However, the Wilson θ–method tends to damp out the higher modes and could produce large errors when contributions of higher modes are significant. Therefore, the use of this method is no longer recommended.

2.2.10 The Hilbert, Hughes and Taylor α method (HHT- α method)

The HHT-α method (Hughes 1997) is a generalization of the Newmark-β method and reduces to the Newmark-β method for α = 0. The finite-difference equations for the HHT-α method are identical to those of the Newmark-β method. The equations of motion are modified, however, using a parameter α.

$$M\ddot{u}_{t+\Delta t} + (1+\alpha)C\dot{u}_{t+\Delta t} - \alpha C\dot{u}_t + (1+\alpha)Ku_{t+\Delta t} - \alpha Ku_t = (1+\alpha)f_{t+\Delta t} - \alpha f_t \qquad (2.5)$$

With α = 0 the HHT-α method reduces to the constant acceleration method. If -1/3 ≤ α ≤ 0, β = (1-α2)/4, and γ =1/2-α, the HHT-α method is second-order accurate and unconditionally stable. The HHT-α method is useful in structural dynamics simulations incorporating many degrees of freedom, and in which it is desirable to numerically attenuate (or dampen-out) the response at high frequencies. Decreasing α (below zero) decreases the response at frequencies above 1/ (2Δt), provided that β and γ are defined as above.

2.3 SOIL-STRUCTURE INTERACTION

Soil-structure interaction (SSI) is where structural elements and the ground displacements are dependent upon one another. SSI is present in many civil engineering problems due to the contact between structure and ground. All structures are affected by SSI with varying emphasis in the earthquake excitation. To handle SSI there are numerous approaches beginning with the complex method and progressing to the simpler, namely Direct, Substructure, Macro-element model, Simple physical models and impedance functions (Nasser 2009) as shown in Figure 2.4

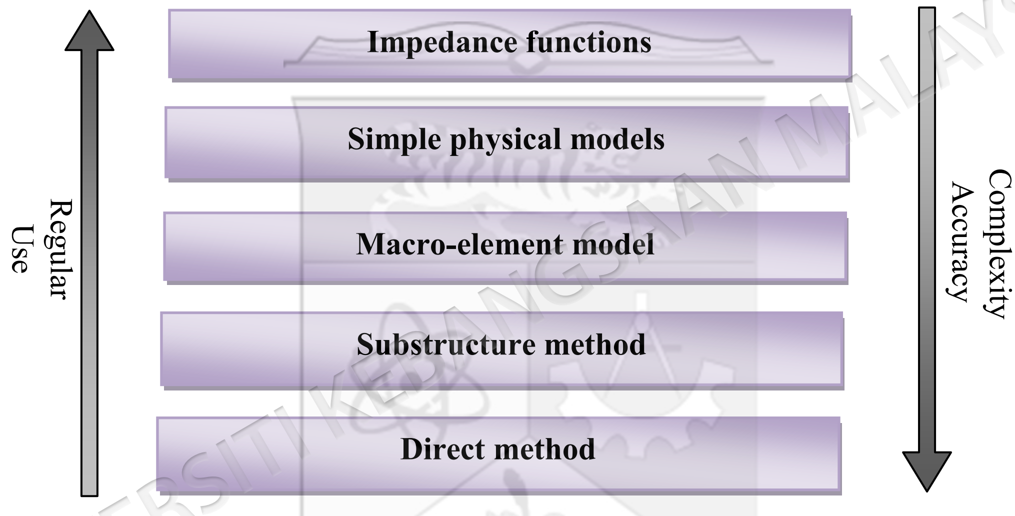

FIGURE 2.4 Approaches commonly used for soil structure interaction

Source: Nasser 2009

2.3.1 Modelling of the Ground

The two main types of ground are soil and rock. The model of a structure is more likely to be realistic if the deformation of the rock support is neglected than if the effect of a soil support is neglected. An elastic model for rock may be realistic in some situations, but the real behaviour of jointed rock is complex (Macleod 2005).

Soil tends to be non-homogeneous, with mechanical properties that may be time-dependent, functions of water content and nonlinear relation to stress and strain. To address these features requires advanced analysis.

It is generally thought that the structure is easy to model relative to the soil, but the real behavior of a structure depends on the cladding, the internal partitions, temperature effects, etc., which is difficult to represent it through a model.

Even though it is very difficult to produce a predictive model does not mean that it is not possible to take account of SSI. The needs to use of an approximate model may be better than no attempt to model the interaction. Figure 2.5 shown the approaches that commonly used in the modeling of soil profiles

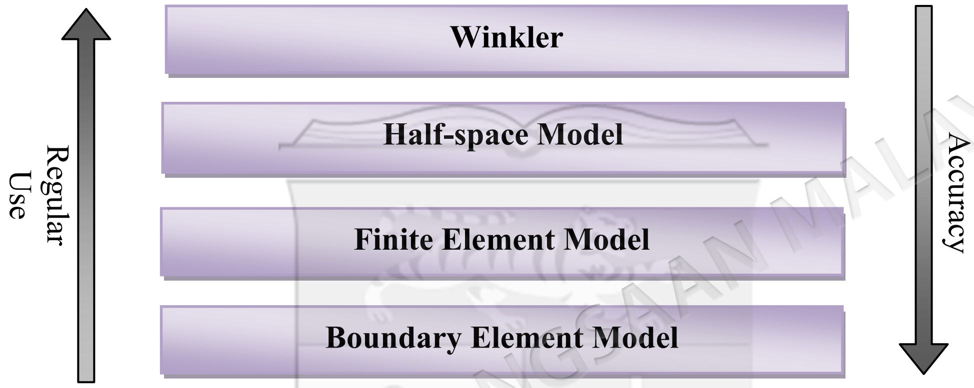

FIGURE 2.5 Approaches commonly used for soil modelling
Source: Macleod 2005

2.3.2 Winkler model for soil behavior

Figure 2.6 illustrates the deformation of a Winkler support. If a vertical load is applied to a rigid plate, the soil surface is assumed to move downwards with a linear elastic response over the area of the plate but does not deform beyond the plate boundaries (Macleod 2005).

This neglects shear transfer in the soil which makes the deformation extend beyond the limits of the plate, as shown in Figure 2.6(b). Over the area of the load, the soil acts as a simple spring with the load deformation relationship

$$q = K_{wk}\delta \qquad (2.6)$$

where q is the uniform pressure applied to the plate (equal to the reaction pressure of the soil on the plate), K_{wk} is often denoted as the 'modulus of sub-grade reaction' but denoted here as the Winkler stiffness (it is based on plate bearing tests and has units of KN/m^3), and is the deformation of the soil surface.

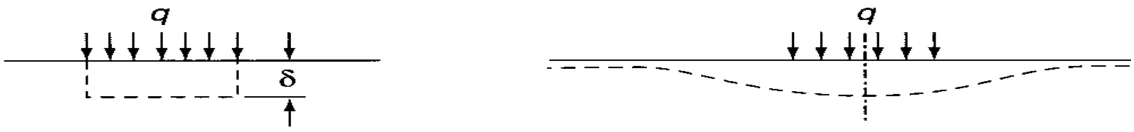

(a) (b)

FIGURE 2.6 Displacement patterns: (a) Winkler displacement (b) displacement with shear transfer

2.2.3 Validation information for the Winkler model

A 1978 Institution of Structural Engineers' report on structure soil interaction stated that the Winkler model cannot be recommended for the analysis of rafts and continuous footings. A later edition of this report does not even mention the model. The model is, however, recommended for use in design of combined footings and mats (ACI 2002).

The main negative feature of the Winkler model is that results from it can be significantly different from those obtained by measurement, i.e. it cannot be treated as a predictive model. In particular, it gives poor predictions of soil pressure at the edges of foundations (Wolf 1994). However, the method:

1- Is easy to implement using a structural analysis package

2- May give better results than by ignoring the effect of soil stiffness in an analysis of the structure

But the disadvantages of this approach are:

1- No prediction of soil movements at a distance from the foundation element is given.

2- No shear transmission between adjacent springs, therefore no prediction of differential settlement (no "dished" profiles under uniform load)

3- Difficulty in determining spring stiffness (k) leading to uncertainty in predicted total or average settlements

2.3.4 Values for K_{wk}

Table 2.1 gives typical values for K_{wk}. It is possible to relate K_{wk} to the elastic properties of the soil using (Hemsley 1998)

$$K_{wk} = \frac{2E_s}{\pi r_e(1-\nu_s^2)} \tag{2.7}$$

in which E_s is Young's modulus for the soil ν_s is Poisson's ratio for the soil and r_e is the radius of the equivalent plate.

TABLE 2.1 Typical values of Winkler stiffness for soils

Soil	$K_{wk}(\frac{KN}{m^3})$
Lose sand	4800-16000
Medium dense sand	9600-80000
Dense sand	64000-128000
Clay medium dense sand	32000-80000
Salty medium dense sand	24000-48000
Calyey soil	
$q_u \lesssim 200N/m^2$	12000-24000
$200 < q_u \lesssim 400N/m^2$	24000-48000
$q_u > 800N/m^2$	>48000

2.3.5 Implementing the Winkler model

Most structural analysis software such as LUSAS allows elastic spring supports which are effectively adequate in some cases, using Winkler springs as shown in Figure 2.7.

In some cases the derivation of the element stiffness matrix includes a Winkler support, and the Winkler stiffness is part of the data for the element.

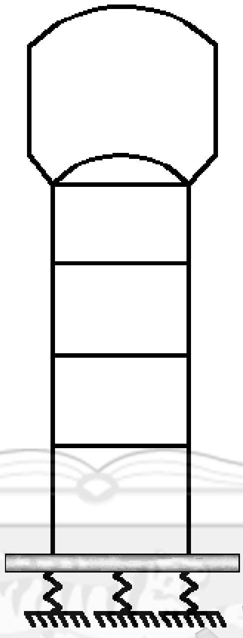

FIGURE 2.7 Winkler model concepts

A single footing can be modeled as a rigid block supported on a Winkler spring with

$$K_y = K_{wk}A_f \tag{2.8}$$

$$K_\theta = K_{wk}I_f \tag{2.9}$$

where K_y is the vertical spring stiffness, K_{wk} is the Winkler stiffness, A_f is the vertical spring stiffness, K_θ is the rotational spring stiffness and I_f is the inertia value of the base of the footing (about the same axis as K_θ is defined). For a three dimensional model, rotational springs about two axes can be defined. The value of Winkler spring stiffness at a node under a raft is calculated using

$$K_{winkler} = K_{wk}A_t \tag{2.10}$$

where K_{wk} is the Winkler stiffness and A_t is the area of the soil surface which is tributary to the node.

2.3.6 Half space models

The concept of a half space model (Figure 2.8) is that a grid of nodes is defined at the ground surface and a stiffness matrix for the soil is defined at that level. This is added to the stiffness matrix for the structure to produce a model that incorporates both the soil and the structure. Such models are not normally implemented in structural analysis software. Linear elastic and non-linear models can be used.

The surface described by Hemsley (1998) is a potentially elastic model for defining a half space model. The stress in the soil is estimated using homogeneous conditions, but the strains caused by these stresses are integrated by taking into account variation of properties within the depth of the soil.

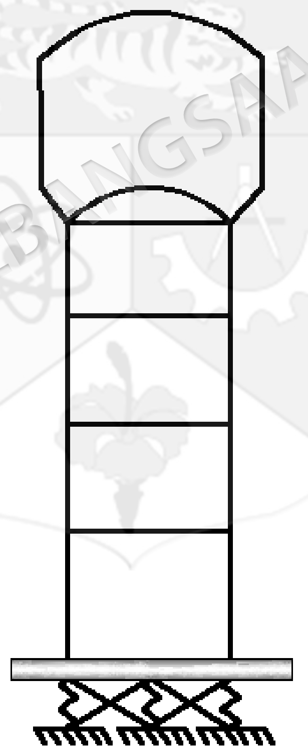

FIGURE 2.8 Half space concepts model

2.3.7 Finite element models

In the SSI analysis the soil can be treated as an elastic medium and modeled with finite element model as shown in Figure 2.9. Due to advancement of computer technology it is now become a realistic option for SSI modeling, especially if elastic properties are utilized. The following types of elements can be used

1- Three dimensional model using three dimensional elements.

2- For long structures, a plane strain model can be used.

3- Axisymmetric elements can be used for circular systems with axisymmetric loading.

Using 3D finite elements has the disadvantage that the order of solution may be high, although this may not be significant with modern computing power. Variation in the material properties both horizontally and vertically is easily catered in finite clement model. It is necessary to define limits to the extent of the finite soil model. Desal and Abel (1972) quotes from other sources the following rules.

$$H_S/B_S{:}4.0\text{-}6.0 \tag{2.11}$$

$$V_S/B_S{:}10.0\text{-}12.0 \tag{2.12}$$

where B_s is the plan dimension of the structure, H_s is the horizontal distance from the centre of the structure to the limit of the soil model and V_s is the vertical distance from the base of the structure to the limit of the soil model i.e. the depth of the soil model (Figure 2.10).

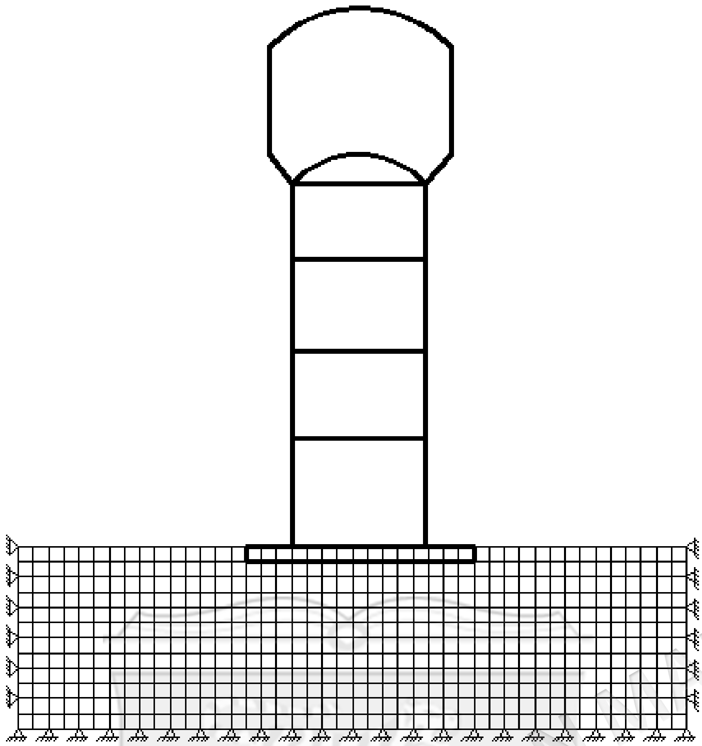

FIGURE 2.9 Modeling soil through FEM

2.3.8 Validation information for modeling the soil as linear elastic

Soil behavior is highly non-linear and irreversible. The linear elastic model is insufficient to capture the essential feature of soil. The use of linear model may, however, be considered to model strong massive structure in the soil or bedrock layers. Stress states in the linear elastic model are not limited in any way, which means that the model shows infinite strength (PLAXIS 2008)

- Significant change in the water content of the soil after loading is likely to invalidate the elastic assumption for predictive analysis.

- In general, the results will tend to be indicative rather than predictive.

- Linear elasticity tends to give better results for cohesive soils than for cohesion-less soils.

- Linear elasticity will give better results than the Winkler model.

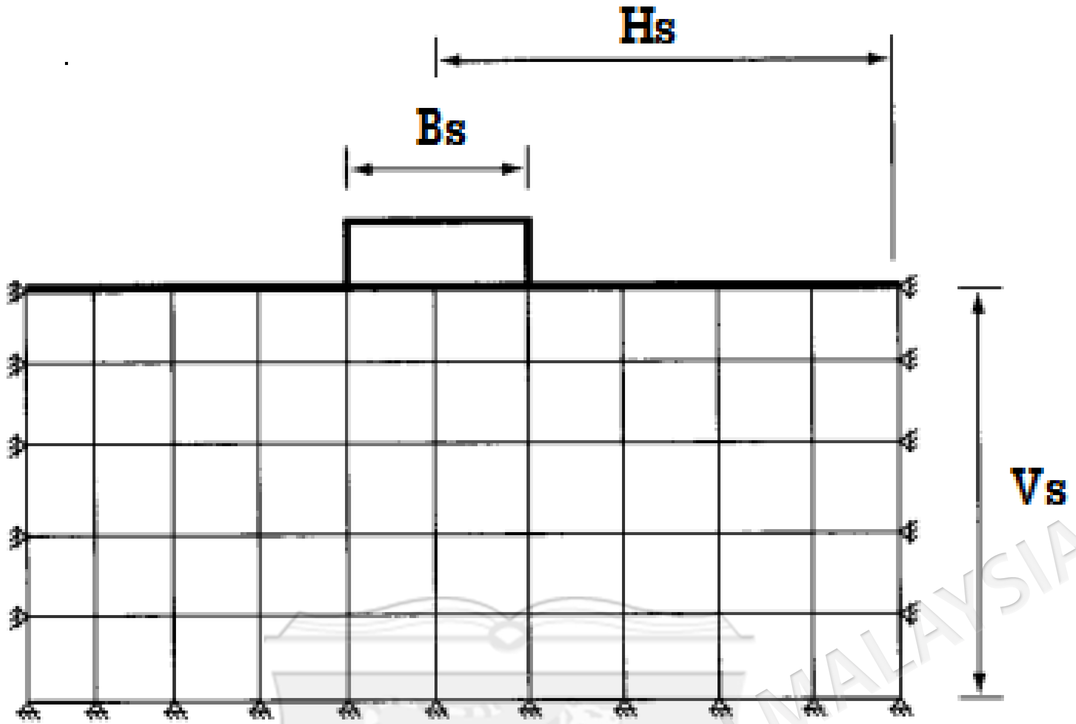

FIGURE 2.10 Limits of finite model of soil.

- Linear elasticity will tend to give better results for short-term loading than for long-term loading.
- Due to the confining pressure, E values for the soil will increase with depth.

2.3.9 Boundary element models

Boundary Element Methods (BEM) based on boundary integral equations are very well suited for dynamic SSI problems and have become widely used for this type of problems as shown in Figure 2.11. Unbounded regions are naturally represented. The radiation of waves towards infinity is automatically included in the model, which is based on an integral representation that valid for internal and external regions.

The first BEM application for SSI problems was presented by Dominguez (1978). The direct formulation of the BEM was applied to compute dynamic stiffness of foundations. The frequency domain formulation was used to obtain stiffness of rectangular foundations resting on, or embedded in, a viscoelastic half-space. Otternstrener and Schmid (1981) and Otternstrener (1982), followed the same approach to study, dynamic stiffness of foundations and cross-interaction between two foundations. Non-homogeneous soils have been studied by Abascal and Dominguez (1986). Apsel and Luco (1983) used an indirect BEM in combination with semi-explicit Green's functions to compute stiffness of circular foundations embedded in a layered half-space. Dynamic stiffness of circular foundations on the surface or embedded in layered soils have been computed using the direct BEM by Alarcon et al. (1989) and Emperador and Dominguez (1989). Karabalis and Beskos (1984) computed dynamic stiffness of surface foundations excited by nonharmonic forces using the time domain BEM. Also in the time domain, Mohammadi and Karabalis (1990) studied the use of adaptive discretization techniques and compared "relaxed" versus "non-relaxed" boundary conditions. The BEM has also been used to compute dynamic stiffness of foundations when soil-foundation separation exists, by Hillmer and Schmid (1988), and Abascal and Dominguez (1990). Unfortunately for commercial reason LUSAS is only based on FEM.

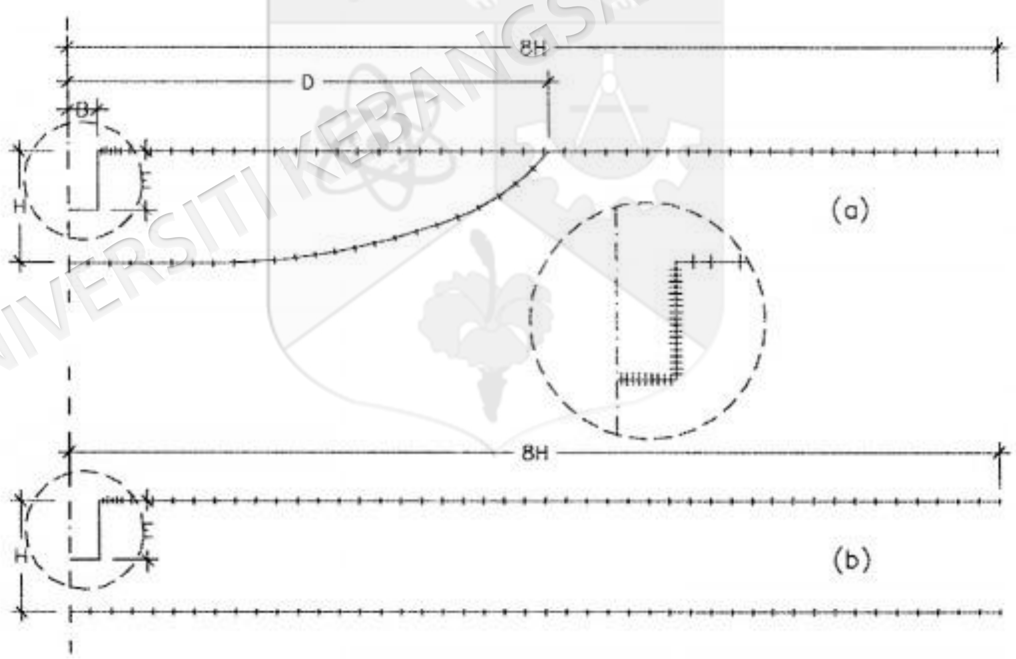

FIGURE 2.11 Boundary element discretization for foundations embedded in alluvial deposits on compliant bedrock: (a) semi-elliptical; (b) layered deposit

2.3.10 Soil structure interaction methods

There are two classical approaches for modelling the problem of SSI which are referred as the direct and substructure approaches. The substructure approach is computationally more efficient and the system is divided into two subsystems as shown in Figure 2.12b, superstructure that may include a portion of non-linear soil around the foundation (near-field) and a substructure that includes the unbounded soil around the superstructure (far-field). The subsystems are connected by a general SSI. The analysis of foundation input motion is required when using the substructure approach, which is normally referred to as kinematic interaction analysis. In the second step, the stiffness and damping characteristics of the soil are characterized using either relatively simple impedance function models for rigid foundations or a series of springs and dashpots distributed around the foundation. Distributed springs are needed when accounting for foundation flexibility.

In direct approach, the computational model consists of the whole structure including foundations and soil media as shown in Figure 2.12a. The system in this approach is excited by a complex and incoherent wave field. From a computational point of view this problem is difficult to solve, particularly when the system contains significant nonlinearities, and hence the direct approach is rarely used in practice.

Powerful software such as LUSAS can be very helpful in the research of SSI since the application of numerical methods is significantly broader than that of analytical methods. Foundation flexibility, non-homogeneity, nonlinearity, kinematic interaction, and possible partial uplift of foundation are now included in the examination of the SSI phenomena.

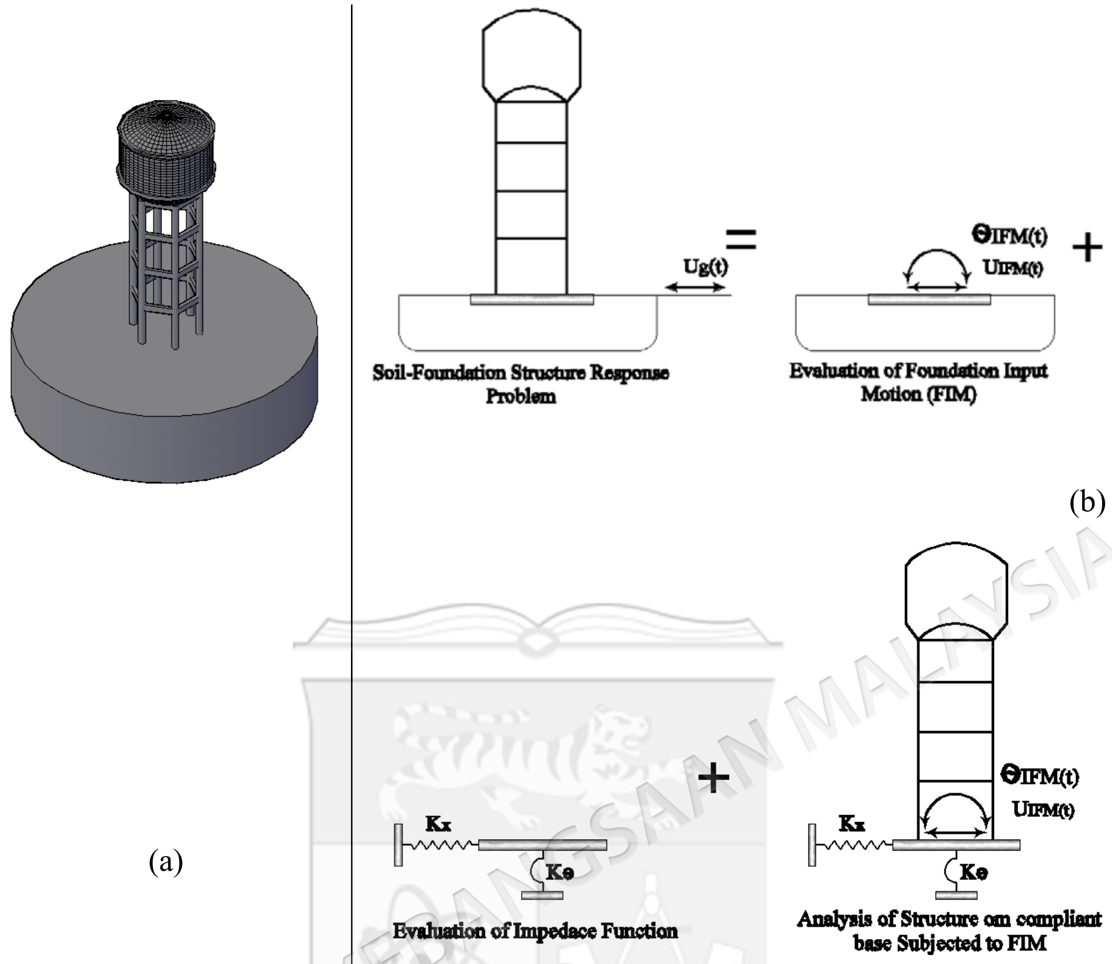

FIGURE 2.12 Soil structure interaction (a) direct approach, (b) substructure approach

2.3.11 Modelling of the nonlinear material behaviour

Modelling of the material behaviour in SSI analyses covers a wide range of soil behaviour. In the static analysis of interaction problems, the elasto-plastic range covers more than the elastic range in which Mohr-Coulomb and Drucker - Baker criterions are the most common failure criterion encountered in geotechnical engineering. In the case of dynamic SSI analysis the complicated soil behaviour under cyclic and dynamic loads have to be considered. One can distinguish between implicit and explicit models for application under seismic loads. The resulting numerical error from these models should be small for the given limited number of seismic loading cycles. At present, the most commonly used cyclic models are those based on strain (Figure 2.13).

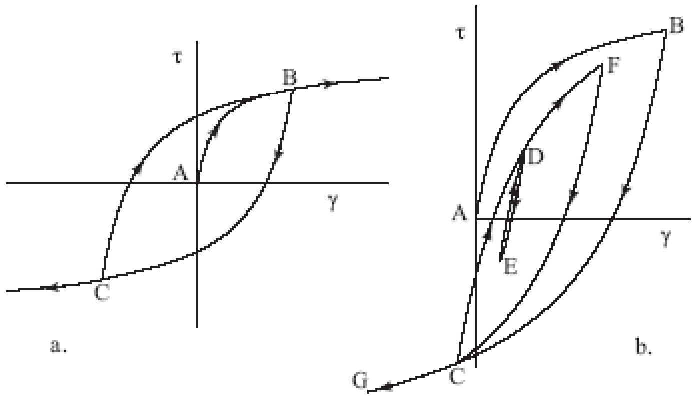

FIGURE 2.13 Masing rule for stress-strain response.

2.3.12 Simplified models

The simplest SSI models are those in which the structure is supported by a rigid foundation where only six additional degrees-of-freedom (three translations and three rotations) are required. Numerical models take into account the effects of foundation flexibility.

The mechanical behaviour of subsoil during an earthquake appears to be quite erratic and complex. It would seem impossible to describe this behaviour by any mathematical law that would conform to the actual observations. For this reason, simple models are preferred and used in most cases since the results obtained would appear reasonable

Many attempts have been made to improve these models by some suitable modifications to simulate the physical behaviour of soil more closely. Along this line, John Wolf (1994) extended the concept of the truncated cones and developed lumped-parameter models to simulate the behaviour of shallow and embedded foundations. Brief overviews of these models are as follows.

2.3.13 Macro-element approach

This method is based on the concept of generalized stress and strain variables. The concept has significant advantages since it simplifies the SSI problem without releasing the important response characteristics of the system.

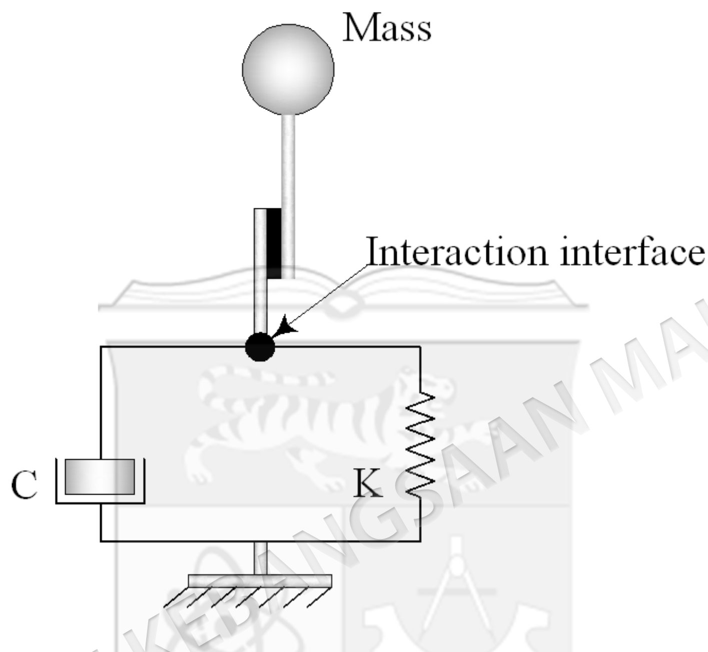

FIGURE 2.14 Structure of macro-element models

In the case of a lumped mass supported by a circular rigid foundation, which is the system (soil-foundation-structure) is subject to seismic excitation. The macro-element can be introduced as a change in the scale of the considered system, in which the foundation and the near field soil is replaced with a plastic hinge and expressed by a macro-element. The motion of this representative point describes the motion of the rigid foundation as shown in Figure 2.14

2.3.14 Simple physical models (Cone model for soil medium)

In a dynamic SSI analysis a bounded structure (which may be linear or nonlinear), consisting of the actual structure and an adjacent irregular soil if present, will interact with the unbounded (infinite or semi-infinite) soil which is assumed to be linear elastic. The most striking feature in an unbounded soil, which is never encountered in a bounded medium, is, in general, the radiation energy towards infinity, leading to so-called radiation damping even in such a linear system. Mathematically, in a frequency-domain analysis, the dynamic stiffness relating amplitude of the displacements to those of the interaction forces in the nodes of the structure soil interface of the unbounded soil is complex for all frequencies. As is well known, this occurs when the unbounded soil consists of a homogeneous half-space (Wolf 2002). Therefore, a cone model has been proposed by Meek and Wolf (1994) for evaluating the dynamic stiffness and effective input motion of a foundation on the ground. Compared to more rigorous numerical methods, this cone model required only simple numerical manipulation within reasonable accuracy (Wolf 1994; Takewaki 2003).

Simple physical models to represent the unbounded soil can be applied as follows: in certain cases, the effect of the interaction of the soil and the structure on the response of the latter would be negligible and thus need not to be considered. This applies, for example, to a flexible high structure with the small mass where the influences of the higher modes on the seismic response remain small. Exciting the base of the structure with the prescribed earthquake motion is then possible. For load applied directly to the structure, the soil in this case can be represented by a static spring or the structure can even be regarded as built-in (Wolf 1994, 2002). When a homogeneous half-space statically loaded, the static vertical displacement varies with the increasing depth which is known as a Boussinesq theory. The shape is also like a truncated cone as shown in Figure 2.15, for dynamic loading.

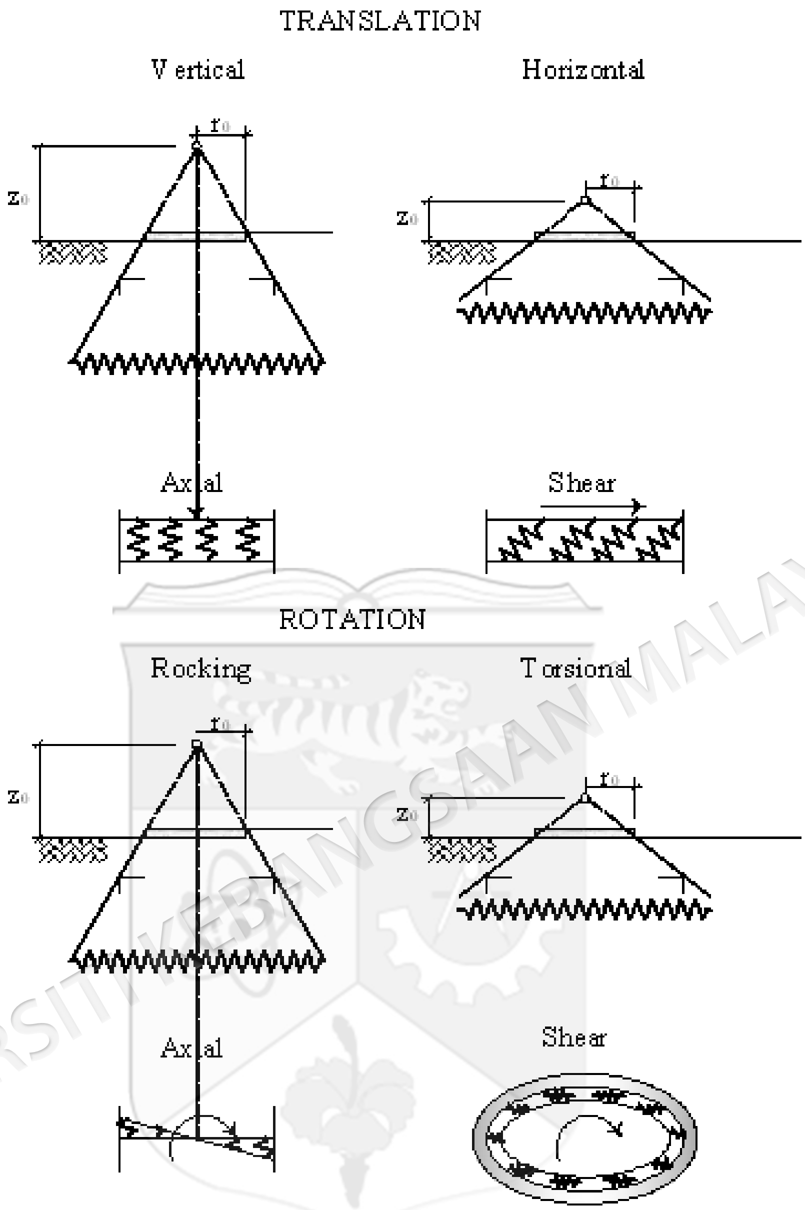

FIGURE 2.15 Cone for various degrees of freedom with corresponding apex ratio (opening angle), wave-propagation velocity and distortion

Source: Wolf 1094

2.3.15 Impedance functions

The method is used in the analysis of foundation vibrations and/or in general for SSI problem. In comparison to the cone model, impedance functions are, in general, based on the solution of three-dimensional or two-dimensional wave equation in the unbounded half-space. The analysis of dynamic SSI effect is done by separating the whole system into two parts; a lumped parameter system and a spring-dashpot combination which substitutes the soil media. The spring represents the stiffness of soil whereas the dashpot encloses the radiation damping of soil as shown in Figure 2.16.

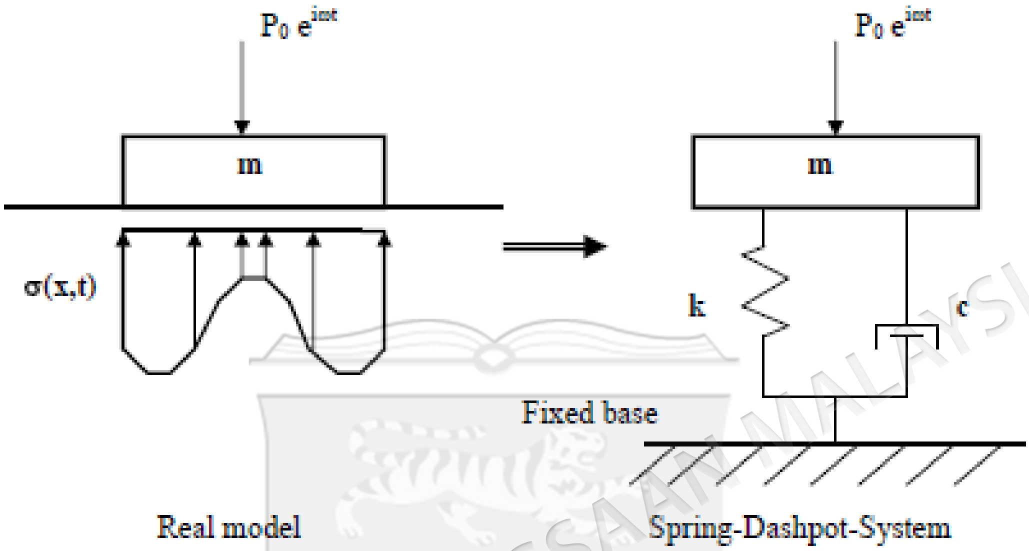

FIGURE 2.16 Principal of the impedance function

2.4 FLUID STRUCTURE INTERACTION (FSI)

The analysis of hydraulic structure such as elevated concrete water tank under dynamic load of FSI problems can be investigated by using different approaches such as added mass (Westergaard 1931 or velocity potential), Lagrangian (Wilson & Khalvati 1983), Eulerian (Zienkiewicz & Bettes 1978), and Lagrangian Eulerian approach (Donea et al. 1982) as shown in Figure 2.17, these analysis can be carried out in the FEM or by the analytical methods. The added mass approach can be investigated by using some of conventional FEM software such as SAP 2000, STAAD Pro and LUSAS, whilst the other approaches of analyses need special programs that include fluid elements such as ANSYS, ABAQUS ADINA, ALGOR and etc.

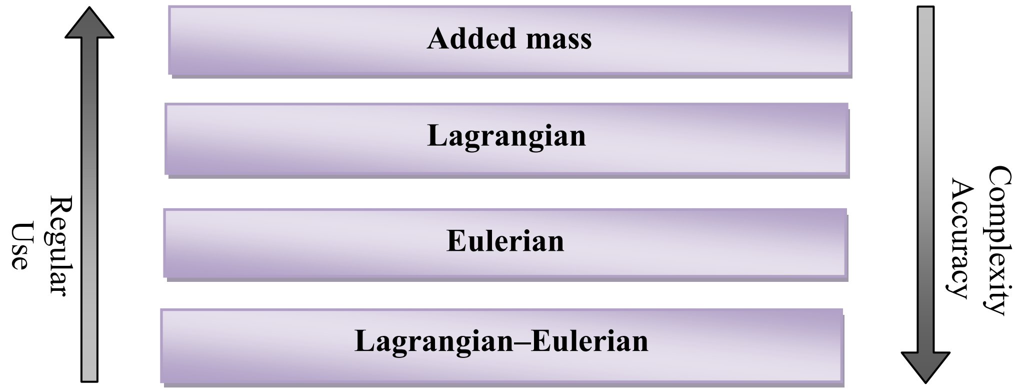

FIGURE 2.17   Approaches commonly used for fluid structure interaction

In this study added mass approach is adopted to conduct all the FSI effects in which the tank reservoir and water interact through hydrodynamic pressures at the tank-water interface. The hydrodynamic pressures are affected by the energy loss at the reservoir boundary. The complete formulation of the FSI produces frequency-dependent terms that can be interpreted as an added force, an added mass, and an added damping (Chopra 2006). The added hydrodynamic mass influences the structure response by lengthening the period of vibration, which in turn changes the response spectrum ordinate and thus the earthquake forces. The added hydrodynamic damping arises from the radiation of pressure wave tanks and also from the refraction or absorption of pressure waves at the reservoir bottom. The added damping reduces the amplitude of the structure response especially at the higher modes. If the water is assumed incompressible, hydrodynamic effects are simply represented by added mass coefficients. Depending on the level of sophistication needed the added hydrodynamic mass may be computed using Westergaard, velocity potential, or finite-element procedures.

2.5 STRUCTURAL MODELLING OF ELEVATED CONCRETE WATER TANK

Structural models of elevated concrete water tank are idealizations of the prototype and are intended to simulate the response characteristics of systems. Three levels of modelling are generally used for earthquake response analysis of the elevated tanks as shown in Figure 2.18. These are summarized below in ascending order of complexity and accuracy:

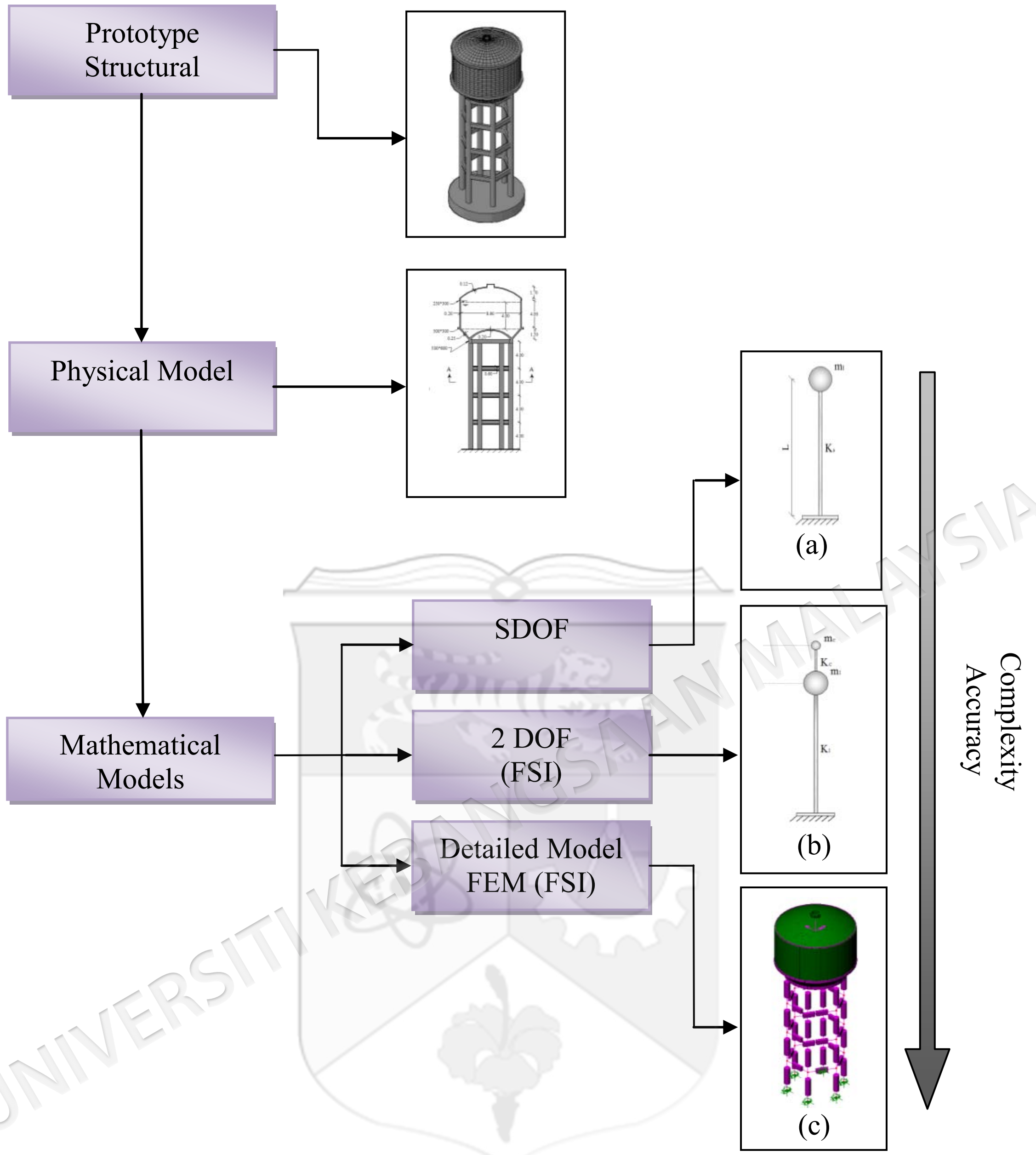

FIGURE 2.18 Structural modelling of elevated tanks for earthquake response analysis based on fixed base approach

The characteristics of the three levels of tank modelling mentioned above are summarized in Table 2.2 .Their comparison is useful for the selection of an appropriate method of discretization while considering the objective of the analysis, the accuracy desired and the computational resources available (Elnashai & Sarno 2008). Following is a brief description of structural idealization for seismic analysis of elevated tanks.

TABLE 2.2 Comparisons between different levels of elevated tank models (relative measure)

Model type	Discretization type	Tridimensional effects	Complexity Accuracy	Computational demand
Substitute	SDOF	Usually not accommodated	Low	Low
Stick	2DOF (FSI)	Accommodated	Medium	Medium
Detailed	MDOF (FSI)	Accommodated	High	High

In the case of single degree of freedom (SDOF) as shown in the Figure 2.20(a), there are two significant issues should be discussed for this concept. The first issue is related to the behaviour of the fluid. If the container is completely full of water, this prevents the vertical motion of water sloshing therefore the elevated tank must be treated as a SDOF system in such a case. When the fluid in the container (vessel) oscillates, this concept fails to characterize the real behaviour. The other issue is related to the supporting structures. As the ductility and the energy-absorbing capacities are mainly regulated by the supporting structure, this is important for the seismic design of elevated tanks. The ACI 371R-98 (1995) suggests that the single lumped mass model should be used when the water load (Ww) is 80% or more of the total gravity load (WG) that includes: the total dead load above the base, water load and a minimum of 25% of the floor live load in areas that are used for storage.

In the case of 2DOF, the equivalent spring-mass models have been proposed by some researchers to consider the dynamic behaviour of the fluid inside a container as shown in Figure 2.20 (b). The fluid is replaced by an impulsive mass that is rigidly attached to the tank container wall and by the convective masses that are connected to the walls through the springs of stiffness. According to the literature, although only the first convective mass may be considered (Housner 1963), additional higher-mode convective masses may also be included (Chen and Barber 1976, Bauer 1964) for the ground-supported tanks. A single convective mass is generally used for the practical design of the elevated tanks (Haroun and Housner 1981, Livaoglu and Dogangun 2005) and higher modes of sloshing have negligible influence on the forces exerted on the container even if the fundamental frequency of the structure is in the vicinity of one of the natural frequencies of sloshing (Haroun and Ellaithy 1985). A simplified analysis procedure has been suggested by Housner (1963) for fixed-base elevated tanks as shown in Figure 2.19. In this approach, the two masses (m_c and m_l) are assumed to be uncoupled and the earthquake forces on the support are estimated by considering two separate SDOF. The mass of m_c represents only the sloshing.

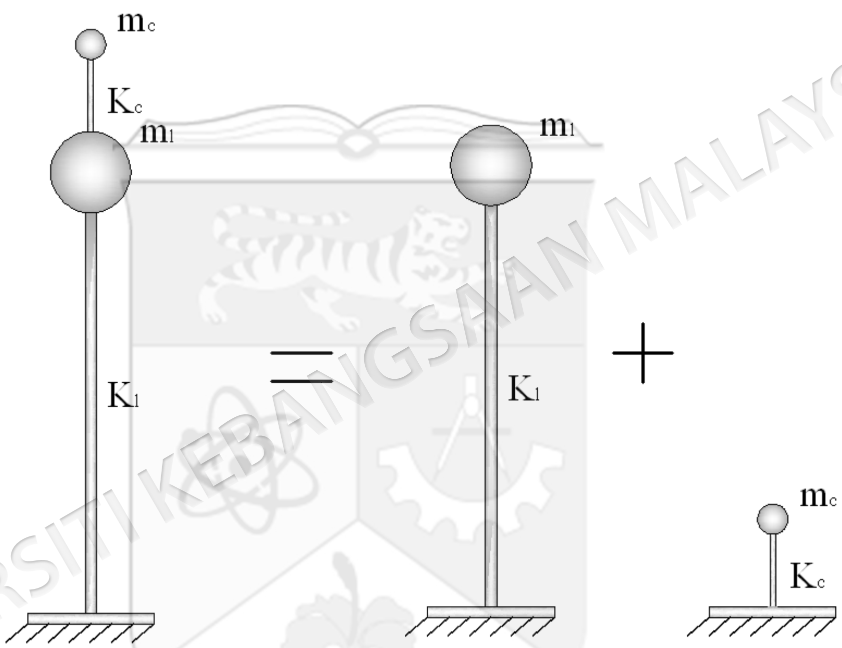

(a)Two mass idealization of elevated tank (b)Equivalent uncoupled system

FIGURE 2.19 Two mass idealization for elevated tank

It has generally been recognized that the interaction between soil and structure can indeed affect the response of structures, especially for structures on relatively flexible soil. Although the SSI may be more important for elevated tanks due to most of the masses being lumped above the ground level and the foundation being supported on a relatively small area, few studies on this subject (Dieterman 1988, Livaoglu 2005, Livaoglu and Dogangun 2005) have been carried out. The majority of the research devoted to estimate the behaviour of the fluid and the supporting structure by using the fixed base assumption (Dutta et al. 2000a, 2001). In the models shown in Figure

2.18(a) and 2.20(b), the interaction problem for structure-soil systems is based on tanks on rigid foundation and homogeneous soil which are adopted in this thesis in the mechanical models. Lateral and rocking vibrations are considered, because effects of these motions are generally more important than vertical and torsional vibrations, which are neglected in this study.

The dynamic interaction with the foundation introduces flexibility at the base of the model and could provide additional damping mechanisms through material and radiation damping. The tank also interacts with the retained water through hydrodynamic pressures at the structure-water interface. This interaction is coupled in the sense that motions of the tank generate hydrodynamic pressures that affect deformations (or motions) of the structure, which in turn influence the hydrodynamic pressures. Often SSI and FSI effects can be accommodated in the special FE models developed for elevated tanks evaluation as shown in Figure 2.20(c). Since foundation properties, structural properties, and boundary conditions can vary, it is advisable to systematically vary parameters that have a significant effect on structure response until the final results cover a reasonable range of possible responses that the structure could experience during the design earthquake. The response of the whole system (soil and tank) in case of direct method is used under severe ground shaking may approach or exceed the yield state especially at the soil. This means that in a linear-elastic dynamic analysis the use of effective stiffness is more appropriate than the initial elastic stiffness used in the static analysis, and that the damping should be selected consistently with the expected level of deformation and the extent of nonlinear behaviour.

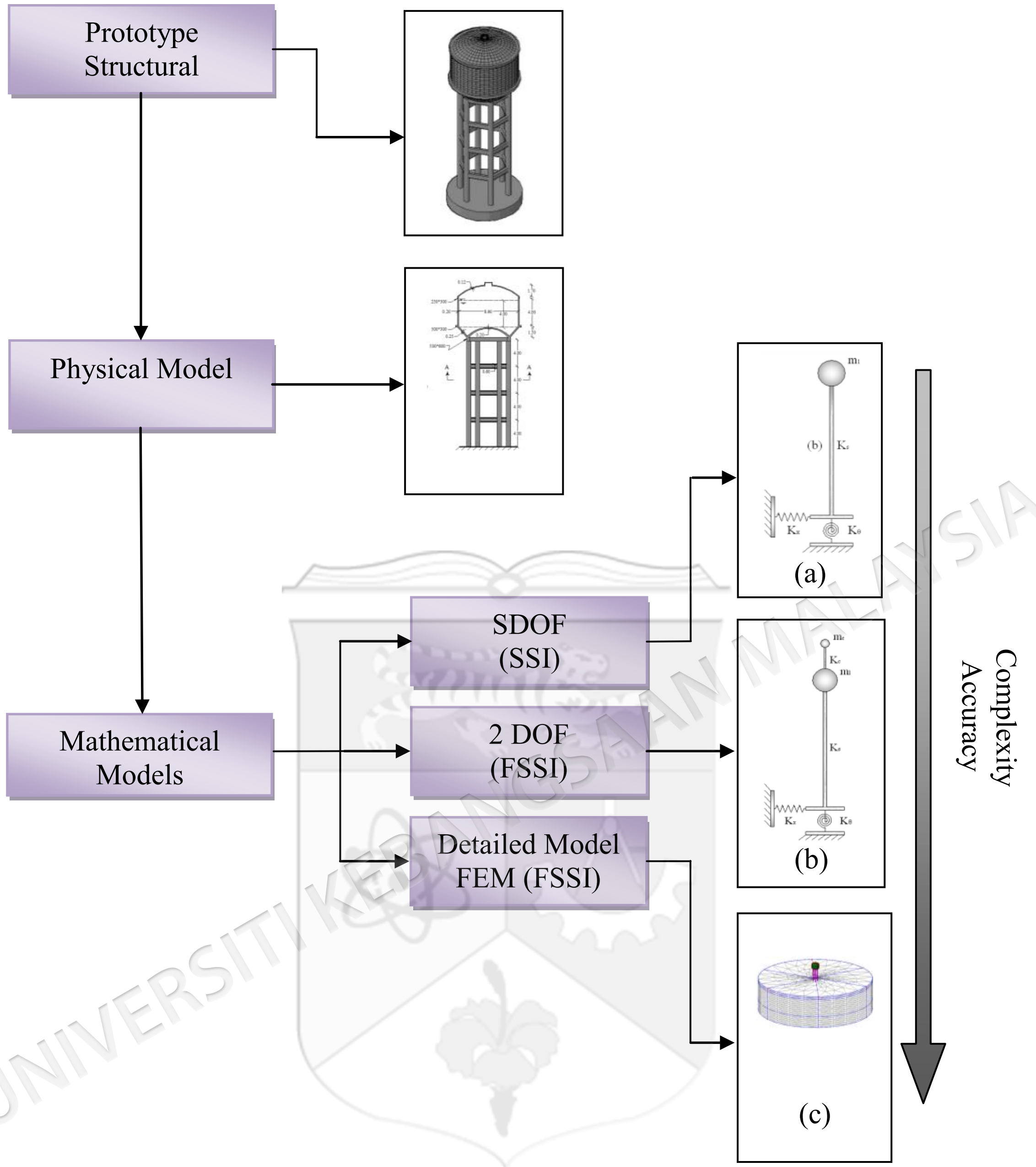

FIGURE 2.20 Structural modelling of elevated tank for earthquake response analysis with soil interaction effects

2.6 PREVIOUS STUDIES OF SEISMIC RESPONSE OF ECWT

Numerous studies have been carried out on the seismic behaviour of storage tanks however most of these studies has focused on the ground level tanks. Very few studies focused on the behaviour of underground tanks (Goto and Shirasuna 1980), rectangular tanks (Dogangun and Livaoglu 2004) or elevated tanks. Most studies were investigating the seismic behaviour of elevated tanks as summarized below.

Haroun and Housner (1981) developed a three-mass model of ground-supported tanks that takes tank-wall flexibility into account. Here, as the elevated tanks are considered to be reinforced concrete, the flexibility of the walls is ignored and the third-mass is not considered for the simplified models.

Haroun and Ellaithy (1985) developed a model including an analysis of a variety of elevated rigid tanks undergoing translation and rotation. The model considers fluid sloshing modes, and it assesses the effect of tank wall flexibility on the earthquake response of the elevated tanks

Resheidat and Sunna (1986) investigated the behaviour of a rectangular elevated tank considering the soil foundation structure interaction during earthquakes. They neglected the sloshing effects on the seismic behaviour of the elevated tanks and the radiation damping effect of soil.

Haroun and Temraz (1992) analysed models of two-dimensional X-braced elevated tanks supported on the isolated footings to investigate the effects of dynamic interaction between the tower and the supporting soil-foundation system but they also neglected the sloshing effects.

Marashi and Shakib (1997) carried out an ambient vibration test for the evaluation of the dynamic characteristics of elevated tanks.

Dutta et al. (2000a) studied the supporting system of elevated tanks with reduced torsional vulnerability and they suggested approximate empirical equations for the lateral, horizontal and torsional stiffness for different frame supporting systems.

Dutta et al. (2000b) study aims to estimate the range of variation of time for usually constructed elevated concrete water tank with frame-type staging for assessing their torsional vulnerability. Closed-form expressions for torsional and lateral stiffness of tank stagings are derived and verified by standard FE software. These expressions are used for studying the variation of time for feasible ranges of influencing parameters.

Dutta et al. (2001a) also investigated how the inelastic torsional behavior of the tank system with accidental eccentricity varies with increasing number of panels. Subsequently,

Dutta et al. (2001b) studies the possibility of implies torsional behaviour of elevated water tanks due to such small accidental eccentricity in inelastic range through detailed case studies; using two simple idealized systems with two coupled lateral/torsional degrees of freedom and, strength-deteriorating and elasto-plastic hysteresis models.

Mandal and Dutta (2002) presents a limited parametric study to evaluate the effectiveness of each of these configurations in changing. A systematic stepwise approach is proposed for checking torsional vulnerability of the tanks and choosing a suitable configuration. Since the magnitude and direction of eccentricity for elevated water tanks is often not known, configuration-based solution may be preferable to the conventional

Dutta et al. (2003) presented the effect of SSI on two dynamic characteristics namely, the impulsive lateral period which regulates lateral seismic behaviour and the impulsive torsional-to-lateral period ratio which regulates torsional vulnerability of the structure. The analytical expressions for these two dynamic characteristics have been derived considering the effect of soil-flexibility for elevated concrete water tank with these alternate configurations. These formulations have been validated against the results of finite element analysis for a few example tanks.

Shrimali and Jangid (2003) investigated the earthquake response of elevated liquid storage steel tanks isolated by the linear elastomeric bearings under real earthquake ground motion. Two types of isolated tank models are considered in which the bearings are placed at the base and top of the steel tower structure. Their study accounted the sloshing of water; the seismic response is obtained by the linear transient dynamic analysis using Newmark scheme, the time period of tower structure

Dutta et al. (2004) showed that soil-structure interaction (SSI) could cause an increase in base shear particularly for elevated tanks with low structural periods. This study also concluded that ignoring the effect of SSI could result in potential large tensile forces in some of staging columns due to seismic loads.

Livaoglu and Dogangun (2004) exhibit a simple procedure for fluid-elevated tank-foundation/soil systems and, by this way, investigate behaviour of the elevated tanks during earthquake excitation. Fluid modelled as lumped masses as impulsive and convective masses proposed by Housner. The substructure method was selected to consider SSI effects. Mode superposition method is used for dynamic analysis of all elevated tank systems. Both time domain and frequency domain are performed to analyze the systems. The procedure presented in this paper can be easily used for frequency domain analysis when compared to more rigorous numerical methods.

Damatty et al. (2005) is motivated by the lack of procedures for the seismic analysis and design of such structures. It reports the first experimental study conducted on a small-scale combined liquid-filled conical shell model. Shake table testing is conducted to determine the fundamental frequencies as well as the frequencies of vibration of the modes during which the cross section of the tank remains circular.

Livaoglu and Dogangun (2006a) provide firstly a synthesis work related to the dynamic behaviour of elevated tanks is presented and then seismic analyses of sample elevated tanks with circular frame and cylindrical shell supporting systems are carried out. To analyze and evaluate of seismic behaviour of the tanks, modal analysis method is used considering requirements of Turkish Earthquake Code (TEC) and Eurocode 8 version which are became valid in the same period of time (1998). Four local site classes defined in TEC-98 and three local site classes in EC-8 are considered in the seismic analysis. The results for both supporting systems restrained on the local site classes are compared each other. Some conclusions and discussions related to the local site classes effects on the dynamic behaviour of elevated tanks are given at the end of the study.

Livaoglu and Dogangun (2006b) submit a synthesis work related to how the ground types defined in Eurocode-8 (EC-8 Part: 1 2006) and Turkish Earthquake Code (TEC-06) affect response of the elevated tanks and secondly to evaluate the performance of supporting system according to the ground types. For this purpose, an elevated tank with a frame supporting system which has been commonly used in recent years by the Ministry of Public Works and Settlements is e selected in the analyses. For taking into account FSI a procedure which is proposed by EC-8 is adapted to the study. By using this procedure the elevated tank-fluid system is modelled with FE technique. The model is analyzed via the Response spectrum analysis for evaluating the ground type effects on the behaviour of tanks. Finally, consequences of analyses carried out in this paper show that the ground types defined in EC-8 generally give fewer results than the corresponding one in TEC-06. Furthermore it is seen from the results that the supporting system of the elevated tanks doesn’t have an adequate performance for a lot of ground types investigated in this study.

Livaoglu and Dogangun (2006c) conducted a comprehensive review of simplified seismic design procedures for elevated tanks and the applicability of general-purpose structural analyses programs to FSSI problems elevated concrete water tank. In this study ten models are evaluated by using mechanical and FE modelling techniques. An added mass approach for the FSI, and the massless foundation and substructure approaches for the SSI are presented. The applicability of these ten models for the seismic design of the elevated tanks with four different subsoil classes are emphasized and illustrated. Figure 2.21 shows comparisons of the periods of the convective mode and impulsive mode according to subsoil class.

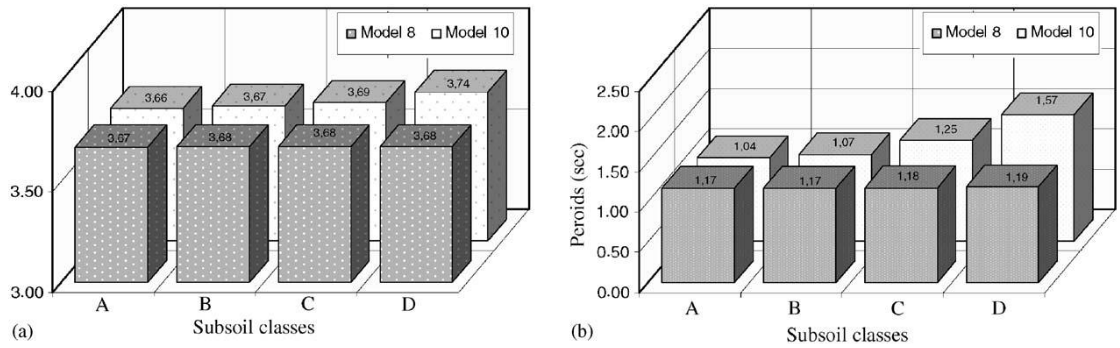

FIGURE 2.21 Comparisons of the periods of (a) the convective mode and (b) impulsive mode according to subsoil class

Livaoglu and Dogangun (2007a) investigate the effects of foundation embedment on the seismic behaviour of fluid-elevated tank-foundation–soil system with a structural frame supporting the fluid containing tank. Six different soil types defined in the well-known seismic codes were considered. Both the sloshing effects of the FSI and SSI of the elevated tanks located on these six different soils were included in the analyses. Fluid-elevated tank-foundation–soil systems were modelled with the FE technique. The FSI was taken into account using Lagrangian fluid FE. Viscous boundary condiation was used to include elevated tank-foundation–soil interaction effects. The models were analyzed for the foundations with and without embedment. Figure 2.22 shows maximum calculated displacements along the height of the elevated tank with embedment different embedment and different soil type

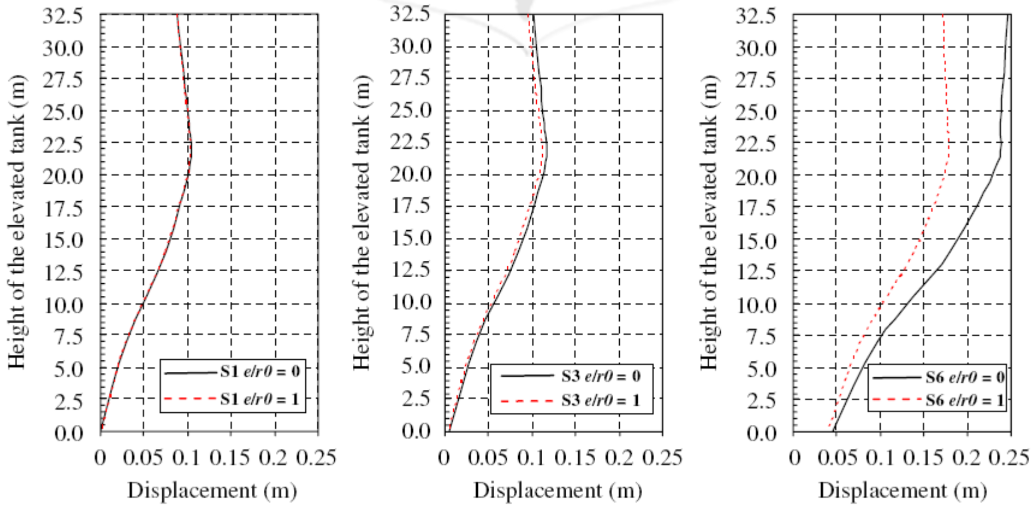

FIGURE 2.22 Maximum displacements along the height of the elevated tank with embedment different embedment and different soil type

Livaoglu and Dogangun (2007b) study the changing supporting system of elevated tanks to what extent may be effective. As examples two different types of supporting system are selected for this subject. The first is frame and the second is cylindrical shell supporting system. After that seismic analyses were performed considering FSI. Conclusions from the analyses result showed that supporting system may considerably change the seismic behaviour of the elevated tanks

Livaoglu and Dogangun (2008) investigate how SSI affects sloshing response of the elevated tanks with frame staging system on different soil conditions. For this purpose, the elevated tanks with frame staging system which are built on six different soil profiles are analyzed for both embedded and surface foundation cases. Thus, considering these six different profiles described in well-known earthquake codes as supporting medium, a series of transient analysis have been performed to assess the effect of both FSI and SSI. Fluid-Elevated Tank-Soil/Foundation systems are modeled with FE technique. In these models FSI is taken into account by implementing Lagrangian fluid FE approximation into the general purpose structural analysis computer code ANSYS. A 3-D FE model with viscous boundary is used in the analyses of elevated tanks-soil/foundation interaction. Formed models are analyzed for embedment and no embedment cases. Finally results from analyses showed that SSI for the elevated tanks affected the sloshing response of the fluid inside the vessel.

Shakib et al. (2010) study three reinforced concrete elevated water tanks, with a capacity of 900 cubic meters and height of 25, 32 and 39 m were subjected to an ensemble of earthquake records.

The behaviour of concrete material was assumed to be nonlinear. Seismic demand of the elevated water tanks for a wide range of structural characteristics was assessed. The obtained results revealed that scattering of responses in the mean minus standard deviation and mean plus standard deviation are approximately 60% to 70 %. Moreover, simultaneous effects of mass increase and stiffness decrease of tank staging led to increase in the base shear, overturning moment, displacement and hydrodynamic pressure equal to 10 - 20 %, 13 - 32 %, 10 - 15 % and 8 - 9 %, respectively.

Wieschollek et al. (2011) describes the results of a survey on existing European and American Codes with regard to their applicability to spherical liquid storage tanks and provides comparison of design outcomes according to these codes. The investigations were performed on an example of an existing spherical tank which was selected to be representative for the current practice. The studies comprised numerical FE modelling and calculation as well as simplified models for the estimation of the dynamic properties of the tank structure. The applicability of behaviour factors was discussed based on proposals made by Eurocode 8. Particular attention was paid to the influence of sloshing effects for which no guidance is given in the codes. The sloshing effects were investigated according to the current state of the art based on available publications. Finally the resistance of the tank was compared to the action effect determined from the European and American codes. The comparison of action effects obtained with and without consideration of sloshing effects showed a rather important influence of these effects on the final results.

From the above studies show that very limited research was carried out on the SSI effects on the behaviour of elevated tanks, and a number less is considered FSI which are conduced based on linear dynamic analysis.

Table 2.3 gives an idea of some of the most important summary of previous studies since the late 1981s.

TABLE 2.3 Summary of previous studies by other researchers

Paper aims	Authors	Year
Developed a three-mass model of ground-supported tanks that takes tank-wall flexibility into account	Haroun and Housner	1981
Developed a model including an analysis of a variety of elevated rigid tanks undergoing translation and rotation	Haroun and Ellaithy	1985
Investigated the behaviour of a rectangular elevated tank considering the soil foundation structure interaction during earthquakes	Resheidat and Sunna	1986
Analysed models of two-dimensional X-braced elevated tanks supported on the isolated footings	Haroun and Temraz	1992
Carried out an ambient vibration test for the evaluation of the dynamic characteristics of elevated tanks	Marashi and Shakib	1997
Studied the supporting system of elevated tanks with reduced torsional vulnerability	Dutta et al	2000
Estimated the range of variation of time for usually constructed elevated concrete water tank with frame-type staging for assessing their torsional vulnerability	Dutta et al	2000
Investigated how the inelastic torsional behaviour of the tank system with accidental eccentricity varies with increasing number of panels.	Dutta et al	2001
Studied the possibility of implies torsional behaviour of elevated water tanks due to such small accidental eccentricity in inelastic range	Dutta et al	2001
Presented a limited parametric study to evaluate the effectiveness of each of these configurations in changing	Mandal and Dutta	2002
Presented the effect of SSI on two dynamic characteristics of elevated tank	Dutta et al	2003
Investigated the earthquake response of elevated liquid storage steel tanks isolated by the linear elastomeric bearings under real earthquake ground motion	Shrimali and Jangid	2003
Showed SSI could cause an increase in base shear particularly for elevated tanks with low structural periods	Dutta et al	2004

Continued...

...Continuation

Exhibit a simple procedure for fluid-elevated tank-foundation/soil systems	Livaoglu and Dogangun	2004
Reports the first experimental study conducted on a small-scale combined liquid-filled conical shell mode	Livaoglu and Dogangun	2005
Dynamic characteristics of combined conical-cylindrical shells	Damatty et al	2005
Provide firstly a synthesis work related to the dynamic behaviour of elevated tanks	Livaoglu and Dogangun	2006
Study the effects of local site classes on the dynamic behavior of elevated tanks with frame and shaft supporting structures	Livaoglu and Dogangun	2006
Conducted a comprehensive review of simplified seismic design procedures for elevated tanks	Livaoglu and Dogangun	2006
Study the effect of foundation embedment on seismic behavior of elevated tanks considering fluid–structure-soil interaction	Livaoglu and Dogangun	2007
Study the changing supporting system of elevated tanks	Livaoglu and Dogangun	2007
Investigate how SSI affects sloshing response of the elevated tanks with frame staging system on different soil conditions	Livaoglu and Dogangun	2008
Study three reinforced concrete elevated water tanks, with a capacity of 900 cubic meters and different heights	Shakib et al	2010
Describes the results of a survey on existing European and American Codes	Wieschollek et al	**2011**

2.7 SUMMARY

This chapter starts with a general idea of the analysis of hydraulic structures under the influence of dynamic loads. And then view the dynamic methods that commonly used to analyze of such structures under dynamic loads with considered the regular to use and the difficulty. This chapter also reviewed SSI including the soil modelling approaches and FSI also here the regular to use and difficulty was viewed. After giving the reader an idea of all that sections, finally the chapter viewed the previous studies in the analysis of elevated concrete water tank.

CHAPTER III

METHODOLOGY

3.1 INTRODUCTION

The understanding of modeling steps of the elevated concrete water tanks starts from SDOF to two DOF (rectangular, circular, and rectangular with embedment and circular with embedment) in which easy to implement according with seismic codes regulations. Modeling steps through FEM needs a good understanding to FEM as a numerical method including modeling steps of FEM related with static and dynamic analysis and nonlinearity mechanism. LUSAS FEA software is adopted to perform all FE models in this study in which its dynamic options cover all of the dynamic analysis that required for this study.

Figure 3.1 shows the flow chart of study process that adopted in this study in which states from data collections namely documents, typical shapes of elevated tanks and Malaysian seismic hazard studies with soil profile to identifying of the problem.

In the phase one the seismic data that collect as response spectrum to calculate the tome history motion at bedrock artificially to be used for accounting the local site effects and obtained the response spectrum at the ground and 4m embedment.

In the phase two calculating of parameters of the models (mechanical and FEM) such as mass of convective mode and mass of impulsive mode, stiffness of staging and .etc, the response spectrum in case of ground and 4m embedment that calculated in the phase one can be used to calculate the base shear and overturning moment at the base of elevated tank in case of no embedment and embedment.

For the FEM cases and after obtained the parameters of the models from phase one and phase two to study the effects of Westergaard modifications as free vibration analysis

In phase three calculating the response of elevated tank based on FEM with considering SSI and FSI in case of linear and nonlinear based on H. H. Tylor and Newmark in two critical directions

In phase four calculation the construction stages effects for circular tank brfore the tank constructed and after the tank constructed

In phase five makes some outlines and suggest some of future woke the upcoming researchers

In this study two elevated concrete water tanks adopted, square and circular shape. The circular elevated concrete water tank has a capacity of 250 m^3 with the top of water level at about 21.8 m above ground. The tank is spherical in shape, 8.6 m in diameter and 7.85 m in height at its centre. The support consists of 6 vertical circular columns and the columns are connected by the circumferential beams at regular intervals, of 4,8,12 and 16 m as shown in Appendix (I), the density of concrete is 25 KN/m^3.

A square shape water container of 1255 m^3 capacity is supported on reinforced concrete staging of 16 columns of 400x400 mm with horizontal bracings of 200 x 450 mm at three levels. Details of staging configuration are shown in Appendix (I). The density of concrete used is $25kN/m^3$.

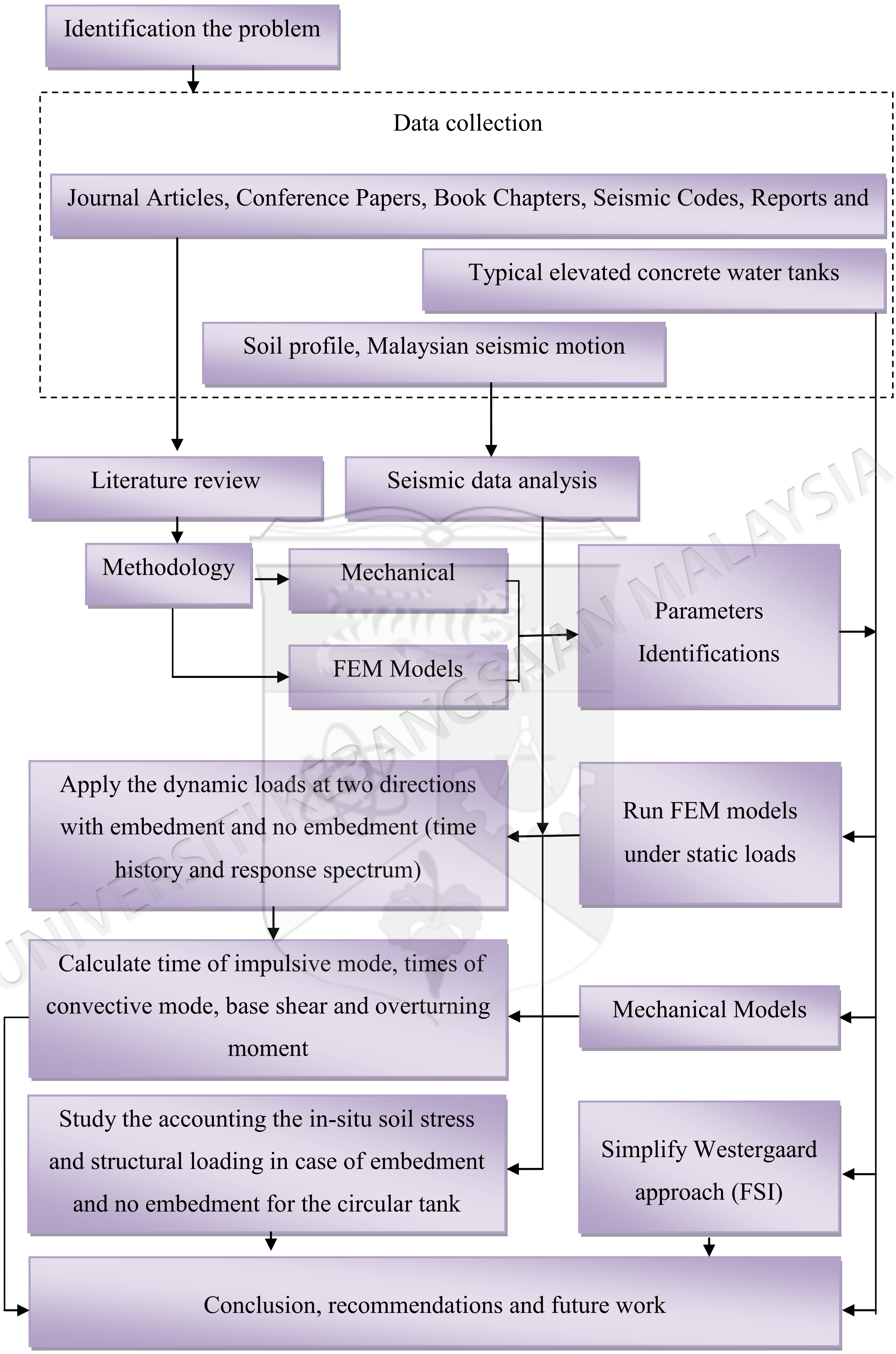

FIGURE 3.1 Flow chart of the study

3.2 MECHANICAL ANALYSIS OF ELEVATED TANK

This section described the seismic procedures of estimating the response of elevated tank (base shear and overturning moment) which are adopted by most of seismic codes. The flowing section gives the modeling steps that used in this study.

3.2.1 Single Degree of Freedom

In this case the tank is idealized as an equivalent SDOF system (Figure 3.2). Four parameters are needed to define the SDOF system: effective mass M_l, effective height H, effective stiffness K_s and effective damping ξ .The height H defines the location of the equivalent or effective mass M_l of the SDOF system. The equivalence used to estimate K_s and ξ assumes that the displacement of the original structure is the same as that of the SDOF model. This approach is frequently used for inelastic structures (Gulkan & Sozen 1974; Shibata & Sozen 1976; Kowalski et al. 1995; Priestley 2003).

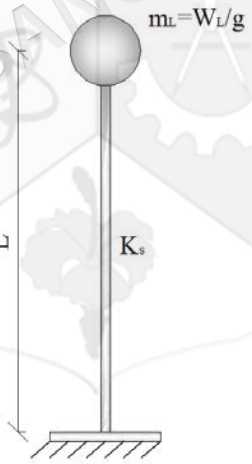

FIGURE 3.2 Single lumped mass model fixed base approach

The fundamental period T of the elevated water tank with SDOF can be obtained by Equation (3.1) (Chopra 2006).

$$T = 2\pi\sqrt{\frac{W_L}{gK_s}} \tag{3.1}$$

in which W_L = weight of water + weight of tank + 2/3rd weight of staging frame, and K_s is lateral stiffness of the staging and it can be defined as the force required to be applied at center gravity (CG) of tank as to get a corresponding unit deflection. FE software can be used to model the staging as shown in Figure 3.3 Since container portion is quite rigid, a rigid link is assumed from top of staging to the CG of tank. In FE model of staging, length of rigid link can also be performed manually by using standard structural analysis methods (stiffness matrix).

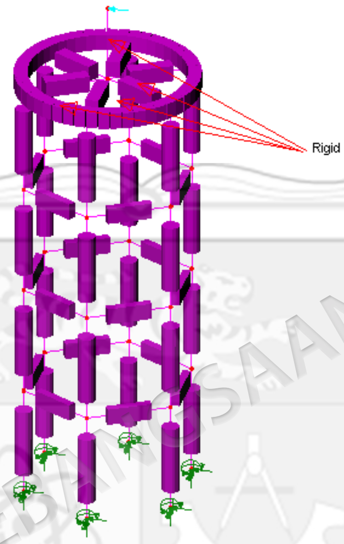

FIGURE 3.3 FE model of staging in LUSAS FEA 14.03

3.2.2 Two Degree of Freedom FSI

Seismic response of elevated tanks depends on complex FSI that may result in global overturning moments and base shear induced by horizontal inertial forces as shown in Figure 3.4. Hence the seismic behavior of elevated water storage tanks subjected to earthquake are characterized by two predominant modes of vibration, the first mode is that of sloshing mass of the liquid (convective mass) m_c; the second mode is that of the combined structure and non-sloshing mass of liquid (impulsive mass) m_i.

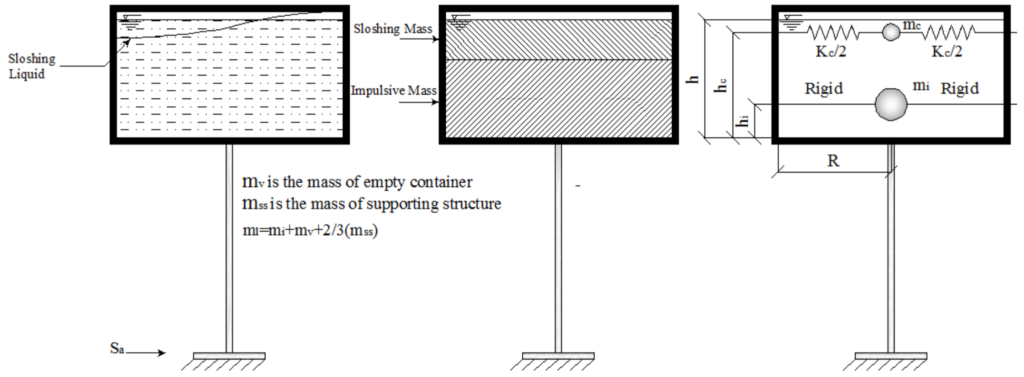

FGURE 3.4 Typical elevated tank with liquid divided into impulsive and sloshing mass

Using Table 3.1, initially developed by Housner (1963) for cylindrical tanks and subsequently modified as a result of analytical refinements and testing, to estimate the proportion of sloshing mass to fixed liquid mass, mode periods, and other dynamic parameters. The analytical approach is simplified if tank shell can be considered rigid relative to the sloshing liquid as shown in Figure 3.5

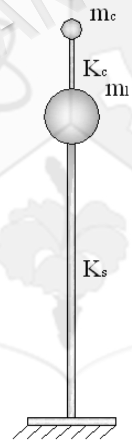

FIGURE 3.5 Considering of FSI suggested

TABLE 3.1 Recommended design values for the first impulsive and convective modes of vibration as a function of the tank height-to-radius ratio (h/R)

h/R	C_i	C_c	m_i/m_w	m_c/m_w	h_i/h	h_c/h	$\grave{h}_i/h$	$\grave{h}_c/h$
0.3	9.28	2.09	0.176	0.824	0.400	0.521	2.640	3.414
0.5	7.74	1.74	0.300	0.700	0.400	0.543	1.460	1.517
0.7	6.97	1.60	0.414	0.586	0.401	0.571	1.009	1.011
1.0	6.36	1.52	0.548	0.452	0.419	0.616	0.721	0.785
1.5	6.06	1.48	0.686	0.314	0.439	0.690	0.555	0.734
2.0	6.21	1.48	0.763	0.237	0.448	0.751	0.500	0.764
2.5	6.56	1.48	0.810	0.190	0.452	0.794	0.480	0.796
3.0	7.03	1.48	0.420	0.158	0.453	0.825	0.472	0.825

Source: Euro Code Part-8

In which m_w, is a total mass of liquid tank, m_i is impulsive mass of liquid, m_c is convective mass of liquid, K_c is spring stiffness of convective mode, h is maximum depth of liquid, h_i is height of impulsive mass above bottom of tank wall (without considering base pressure), h_c is height of convective mass above bottom of tank wall (without considering base pressure),$\grave{h}_i$ is height of impulsive mass above bottom of tank wall (considering base pressure), $\grave{h}_c$ is height of convective mass above bottom of tank wall (considering base pressure). K_c can be determined using following equation

$$K_c = m_c \frac{g}{R} 1.84 tanh \frac{1.84.L}{R} \tag{3.2}$$

3.2.3 Soil Structure Interaction of the Mechanical Models

As described in Chapter II section 2.3.2, two physical phenomena comprise the mechanisms of interaction between the structure, foundation, and soil, namely kinematic and inertial interaction. Inertia developed in the structure due to its own vibrations gives rise to base shear and moment, which kinematic turn cause displacements of the foundation relative to the free-field.

In case of inertial interaction procedure the simplified analytical formulations which are calibrated in this thesis against "empirical" data are based on the sub-structure approach that described in chapter II section 2.3.2. Analyses of inertial interaction effects predict the variations of first-mode (convective and impulsive) period and damping ratio between the actual (SSI) case (which incorporates the flexibility of both the foundation-soil system and the structure) and a fictional (fixed-base) case (which incorporates only the flexibility of the structure). The SSI modal parameters can be used with a free-field response spectrum to evaluate design base shear forces for the elevated tank. The analyses for kinematic interaction predict frequency-dependent transfer function amplitudes relating foundation and free-field motions. SSI provisions in the Applied Technology Council (ATC 1978) and the National Earthquake Hazards Reduction Program (NEHRP) (BSSC 1997) seismic design codes are similar to portions of the inertial interaction analysis procedures described in this chapter section 2.3.2. Kinematic interaction effects are neglected in the code provisions, meaning that free-field motions and foundation input motion are assumed to be identical.

3.2.4 Circular and Rectangular Foundations

The systems (soil/foundation) commonly employed in simplified analyses of inertial interaction of the elevated tanks. The base of the tank is allowed to translate relative to the free-field an amount y and rotate an amount θ. The impedance function is represented by lateral and rotational springs with complex stiffnesses K_{y-Sur} and $K_{\theta-Sur}$, which gives rise to base shear and moment respectively.

Static stiffness of this truncated cone for circular foundation can be obtained as in Table 3.2

TABLE 3.2 Static stiffness values of rigid circular foundation

Stiffness	Stiffness of foundation at surface
Horizontal K_{y-Sur}	$\frac{8Gr_0}{2-\nu} \propto_y$
Rocking $K_{\theta Sur}$	$\frac{8Gr_0^3}{3(1-\nu)} \propto_\theta$

Source: Wolf 1994

in which G is shear modulus, r_0 is radius of circular foundation, is poisson ratio, $\propto_\theta$ and $\propto_y$ are the coefficients of dimensionless

For stiffness value of other geometrical shape like square and rectangular are given by Wolf 1994 and for arbitrary shape are given by Dobry and Gazetas (1986) and Gazetas and Tassoulas (1987) as shown in Table 3.3 and Figure 3.5

TABLE 3.3 Static stiffness values of rigid rectangular foundation

Degree of freedom	Stiffness of foundation at surface
Translation along x-axis $K_{x,Sur}$	$\frac{GB}{2-\nu}[3.4\left(\frac{L}{B}\right)^{0.65} + 1.2]$
Translation along y-axis $K_{y,Sur}$	$\frac{GB}{2-\nu}[3.4\left(\frac{L}{B}\right)^{0.65} + 0.4\left(\frac{L}{B}\right) + 0.8]$
Rotational along xx-axis $K_{\theta x,Sur}$	$\frac{GB^3}{1-\nu}[0.4(\frac{L}{B}) + 0.1]$
Rotational along yy-axis $K_{\theta y,Sur}$	$\frac{GB^3}{1-\nu}[0.47\left(\frac{L}{B}\right)^{0.24} + 0.034]$

Source: Wolf 1994

in which B and L as shown in Figure 3.6

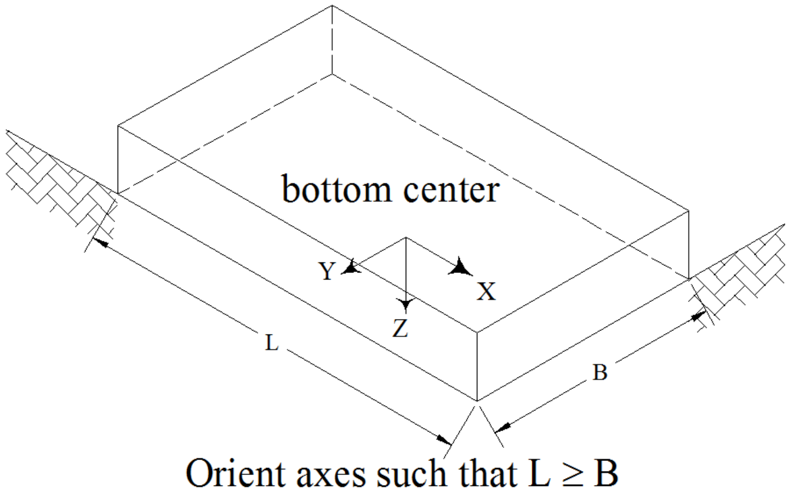

FIGURE 3.6 Parameters of rectangular dimension

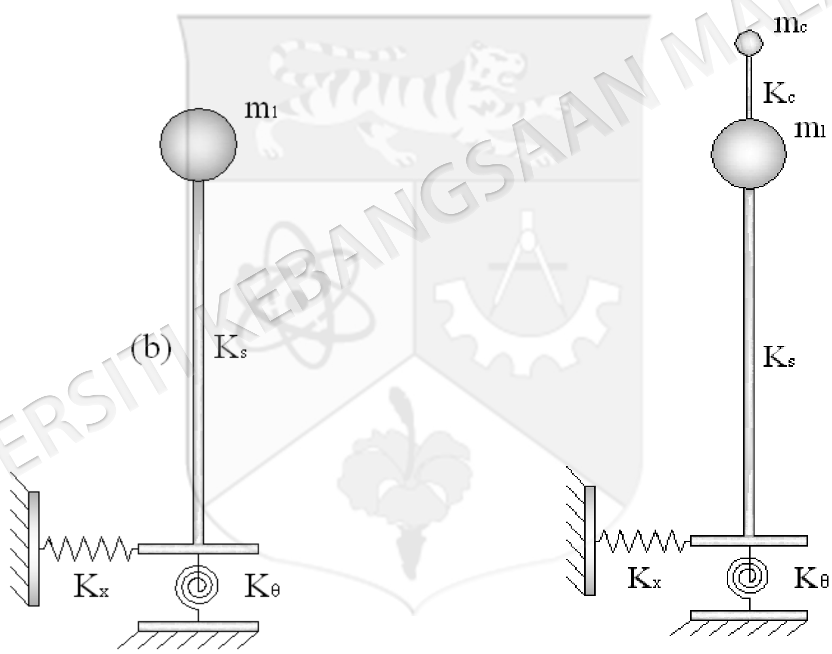

FIGURE 3.7 Simplified model for analysis inertial interaction

3.2.5 Foundation Embedment

Foundation embedment effects were investigated by Elsabee and Morray (1977) for the case of a circular foundation embedded to a depth e into a homogeneous soil layer of depth. It was found that the static horizontal and rocking stiffness for such foundation as presented in Table 3.4 and Table 3.5

TABLE 3.4 Correction factor of embedment of circular foundation,

Stiffness	**Correction factor of embedment**
Horizontal	$\mathrm{K}_{\mathrm{y-emb}} = \left(1 + \frac{1}{2}\frac{r_0}{d}\right)\left(1 + \frac{e}{r_0}\right)\left(1 + \frac{e}{d}\right)$
Rocking	$\mathrm{K}_{\theta\mathrm{-emb}} = \left(1 + \frac{1}{6}\frac{r_0}{d}\right)\left[1 + 2.3\frac{e}{r_0} + 0.58\left(\frac{e}{r_0}\right)^3\right]\left(1 + 0.7\frac{e}{d}\right)$

in which d: heights of soil layer resting on the rigid rock (d $=\propto$ for embedment no rock) e embedment height (Figure 3.8)

TABLE 3.5 Correction factor of embedment of rectangular foundation

Degree of freedom	**Correction factor of embedment**
Translation along x-axis	$\beta_x = \left(1 + 0.21\sqrt{\frac{D}{B}}\right).\left[1 + 1.6\left(\frac{hd(B+L)^{0.4}}{BL^2}\right)\right]$
Translation along y-axis	$\beta_y = \beta_x$
Translation along z-axis	$\beta_z = \left[1 + \frac{1}{21}\frac{D}{B}\left(2 + 2.6\frac{B}{L}\right)\right].\left[1 + 0.32\left(\frac{d(B+L)^{2/3}}{BL}\right)\right]$
Rational along xx-axis	$\beta_{xx} = 1 + 0.25\frac{d}{B}\left[1 + 2\frac{d}{B}\left(\frac{d}{D}\right)^{-0.2}\sqrt{\frac{B}{L}}\right]$
Rational along yy-axis	$\beta_{yy} = 1 + 1.4\left(\frac{d}{L}\right)^{0.6}\left[1.5 + 3.7\left(\frac{d}{L}\right)^{1.9}\left(\frac{d}{D}\right)^{-0.6}\right]$
Rational along zz-axis	$\beta_{zz} = 1 + 2.6\left(1 + \frac{B}{L}\right)\left(\frac{d}{B}\right)^{0.9}$

in which d: heights of soil layer resting on the rigid rock (d =∝ for embedment no rock) e embedment height and height, $h =$ depth of centroid of effective sidewall contact (Figure 3.8)

$$K_{emb} = \beta . K_{sur}$$

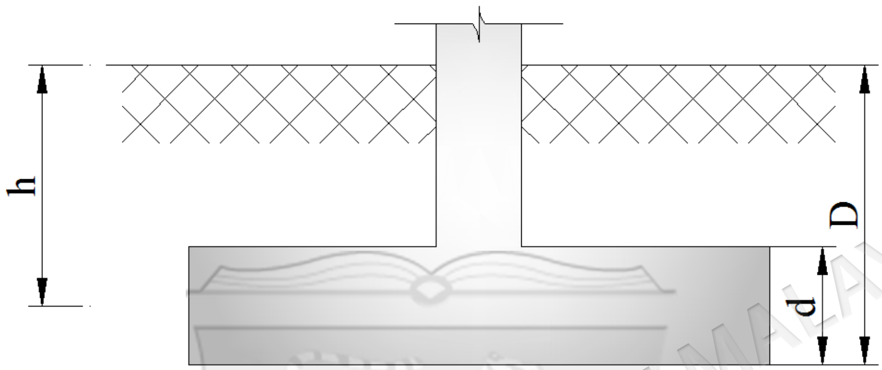

FIGURE 3.8 Parameters of embedment in foundation

The flexible base period $\breve{T}$ is evaluated from Veletsos and Meek (1974)

$$\breve{T} = T\sqrt{1 + \frac{K_s}{K_y}\left(1 + \frac{K_y L^2}{K_\theta}\right)} \quad (3.3)$$

where:

T is the fundamental period of a fixed-base structure, K_s is the stiffness of a staging based on fixed-base and L is the effective height that is taken as 70% of the height to the level where the gravity load is effectively concentrated.

The flexible-base damping ratio has contributions from the viscous damping in the tank as well as radiation and hysteretic damping in its foundation. Jennings and Bielak (1973) expressed the flexible-base damping as

$$\breve{\xi} = \breve{\xi}_0 + \frac{\xi}{\left(\frac{\breve{T}}{T}\right)^3} \quad (3.4)$$

where $\check{\xi}_0$ represents the contribution of the radiation damping, and the soil damping shown in Figure 3.9 shall be determined by averaging the values obtained from solid lines and the dash lines.

The procedures are shown in ACSE 7-02, and they can also be found in Veletsos (1977), Veletsos and Shivakumar (1993) and Stewart and Fenves (1998)

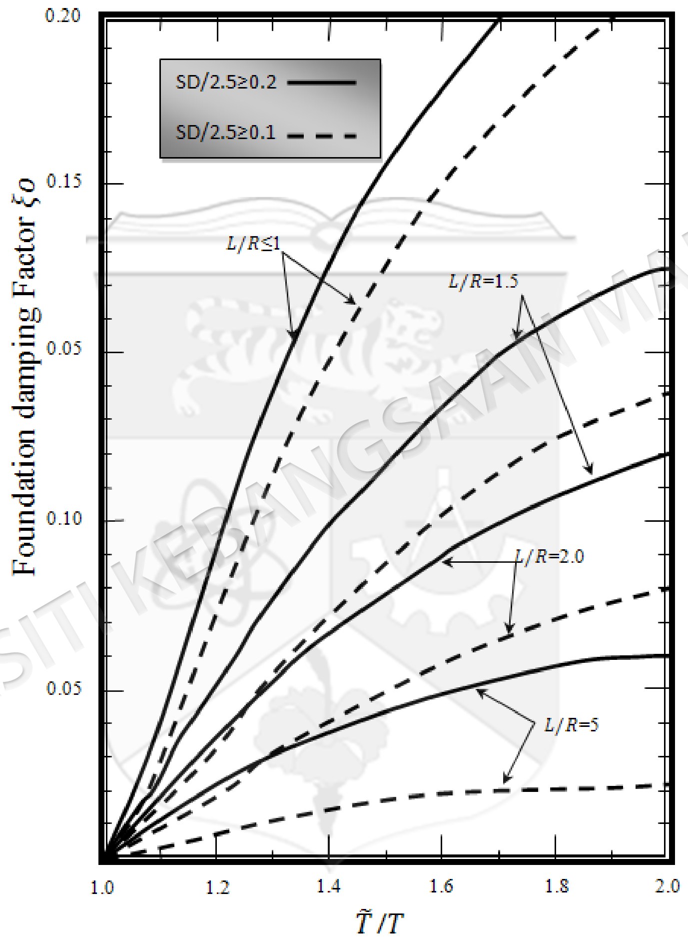

FIGURE 3.9 Foundation damping factor

Source: IBC 2003

3.3 THE FINITE ELEMENT METHOD (FEM) OVERVIEW

In the FEM, the actual structures are modelled as an assembly of finite small parts. Each part is called an element with specified geometry as shown in Figure 3.10

The complicated solution of the actual structure is approximated by a simple solution of a model that includes piecewise-continuous simple solutions. The finite element procedure produces many algebraic equations that can be solved by computer.

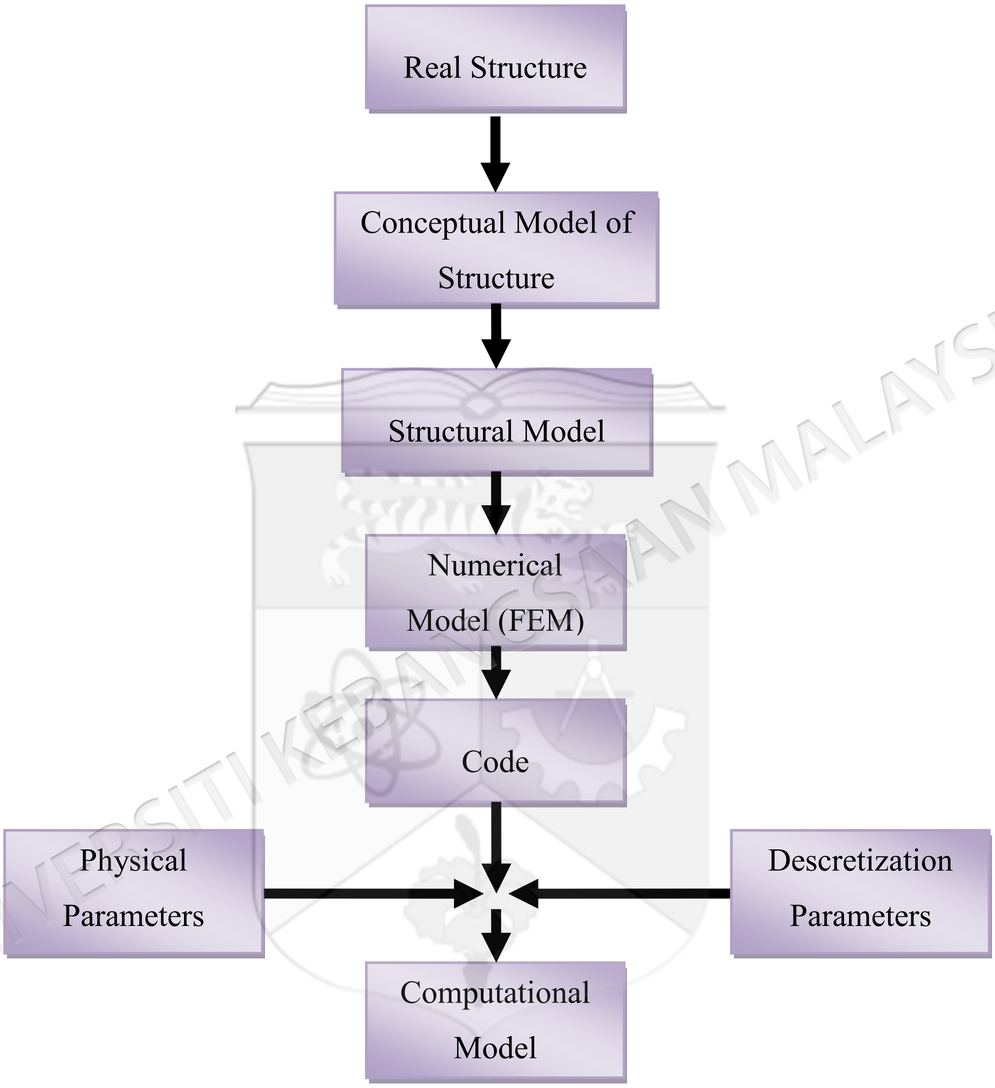

FIGURE 3.10 Path from the real structure to the computational model

The elements connect to the others by nodes. Each node has some degrees of freedom (DOF), the number of DOF depends on the model (in the real structure there are infinite DOF). The algebraic equations are solved to determine the DOF. For the structure and geotechnical problems, the DOF usually are displacements.

Within each element, the unknown function of the state variable is defined approximately, and these individually defined functions match each other at the element nodes and then the unknown function is approximated over the entire domain.

The primary difference between the FEM and other methods such as is that in the FEM, the approximation is defined in a relatively small region. Finding an admissible function satisfying the boundary conditions for the entire domain is often difficult; however, in the FEM, admissible functions are satisfied in the element domain with simple geometry and pay no attention to complications at the boundaries. The elements can have different types, shapes and physical properties so that the finite element method can give the close physical resemblance between the actual structure and its finite element model. A FE analysis typically involves the following procedures applied to analysis of structure and geotechnical problems:

- Divide the problem domain into finite elements.
- Selection of nodal displacement parameter and element interpolation functions.
- Formulate the properties of each element.
- Assemble elements to obtain the FE model.
- Apply the known load.
- Add boundary conditions: The boundary conditions are the known displacements of nodes.
- Solve simultaneous linear algebraic equations to determine nodal displacements.
- Calculate the strains from nodal displacements and stresses from strains.

The complete process described in this section can be represented as a loop that starts by creating element stiffness matrices K_i and finishes by calculating element forces as shown in Figure 3.11. The result is accepted if the applied loads and the calculated reactions agree.

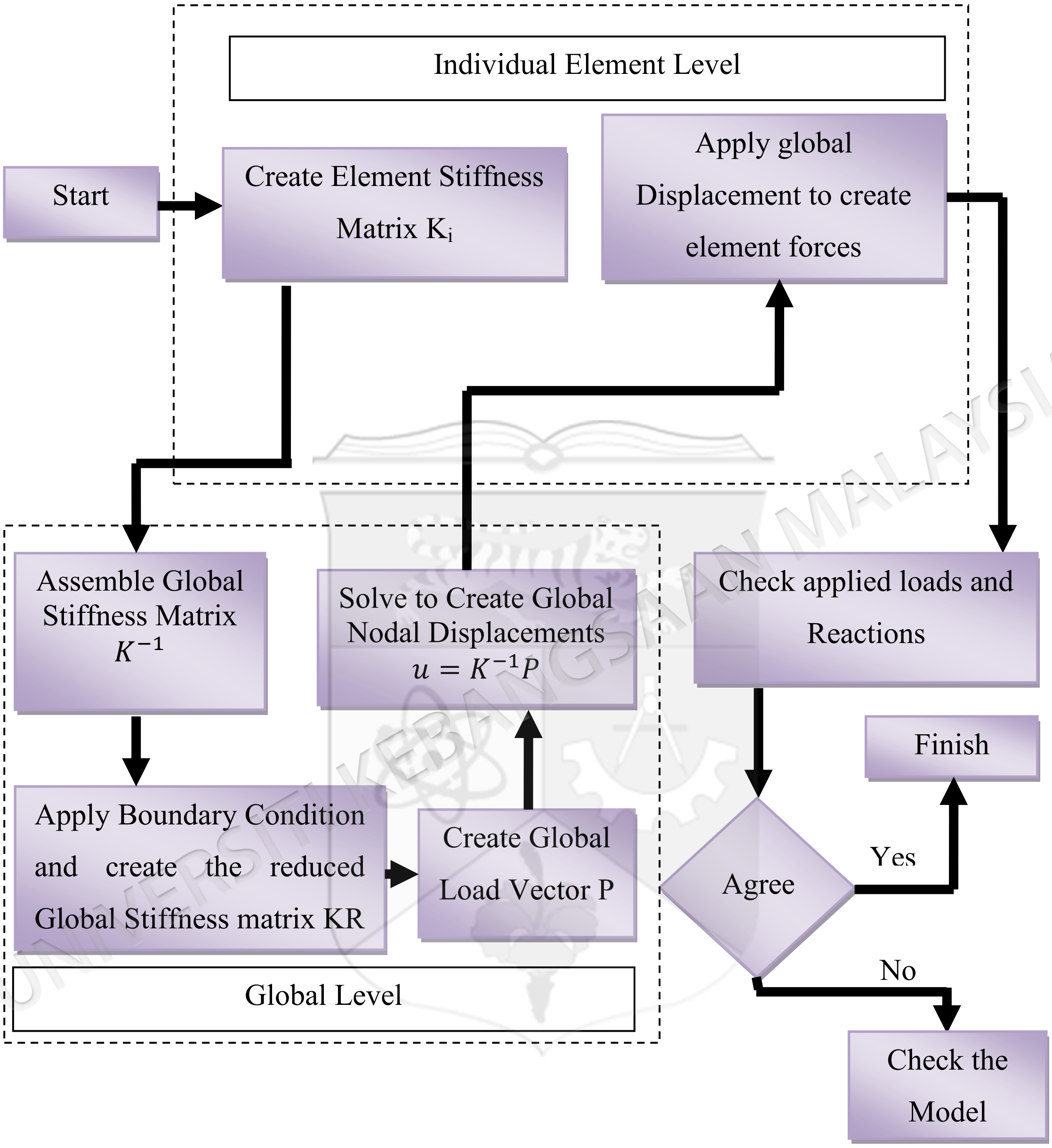

FIGURE 3.11 Analysis loop based on FEM

Source: Morris and Rahman 2008

Yet most of the steps undertaken by mainstream FE systems follow the steps outlined above. However, in most cases the analysis loop is extended as the process, for the static analysis case, concludes with the calculation of element strains and stresses. Thus the loop is augmented by additional steps that are undertaken at the element level as shown in Figure 3.12.

This direct approach employs a very simple method to create an element stiffness matrix. In reality, a more complex approach is used to create these matrices using shape functions that approximate the displacement field within an element.

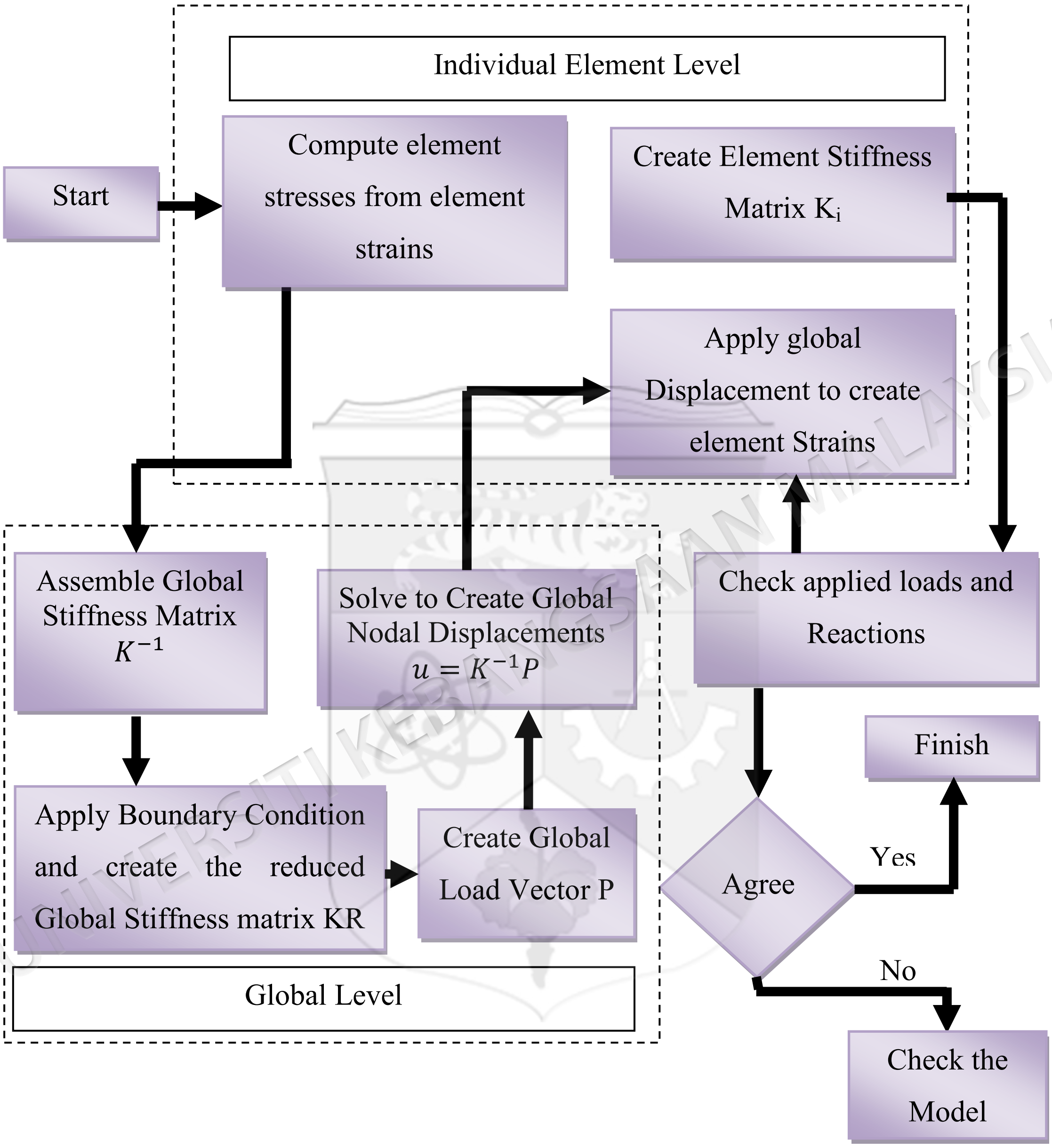

FIGURE 3.12 Augmented analysis loop

Source: Morris and Rahman 2008

In the case of free vibration dynamic analysis the analysis loop associated with this type of free vibration analysis is shown in Figure 3.13 in which stiffness (K_i) and mass (K_i) matrices are created as first step to obtain the frequencies (ω_i) and mode shapes (U_i).

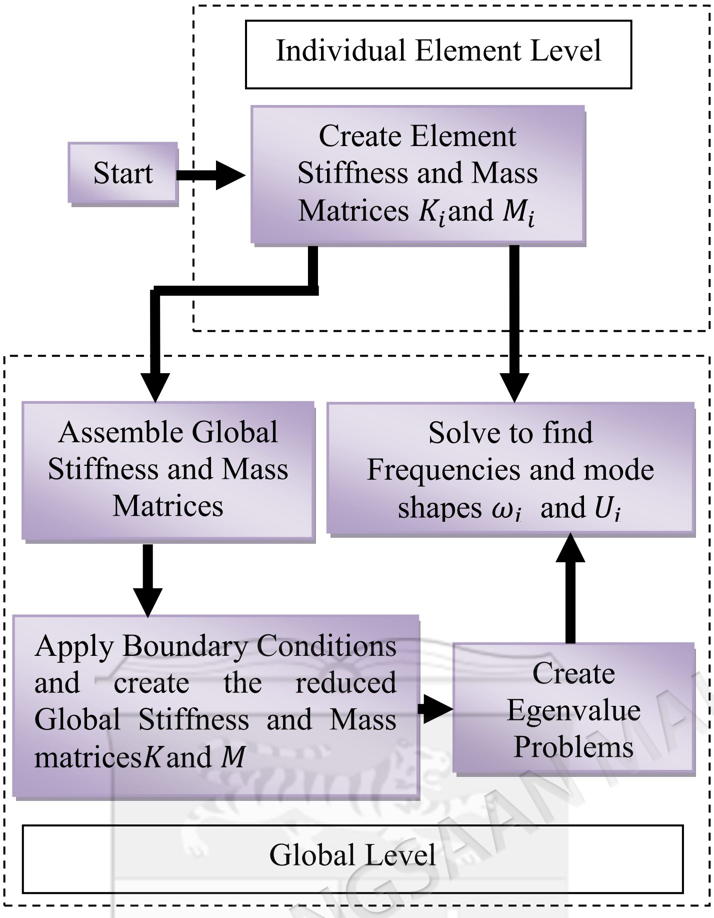

FIGURE 3.13 Free vibration analysis loop

3.4 MODELLING PROCEDURES IN LUSAS

Generally any arbitrary structure such as elevated water tanks subjected to dynamic loads can be carried out through FEM package in which some of software lacking some elements in their elements library. In this study, LUSAS covers all facilities that presented in the figure such as with the ability of conducting static and dynamic models with higher level of accuracy. Modelling involves creating a geometric representation of a structure and defining its characteristic behaviour in terms of its physical properties such as material, loading, and support. The model is created as a graphical representation consisting of several known positions in 3D space and the connections between them. Collectively this is known as the geometry of the model. Geometry consists of points, lines, surfaces and volumes. A volume needs surfaces to enclose it and define its boundary. Similarly a surface needs lines to form its perimeter and lines need points to define their ends. The shape of a surface between its boundary lines, and the shape of a line between its end points can be simple (straight lines, flat surfaces) or complex, depending on the manner in which it was created as shown in Figure 3.14.

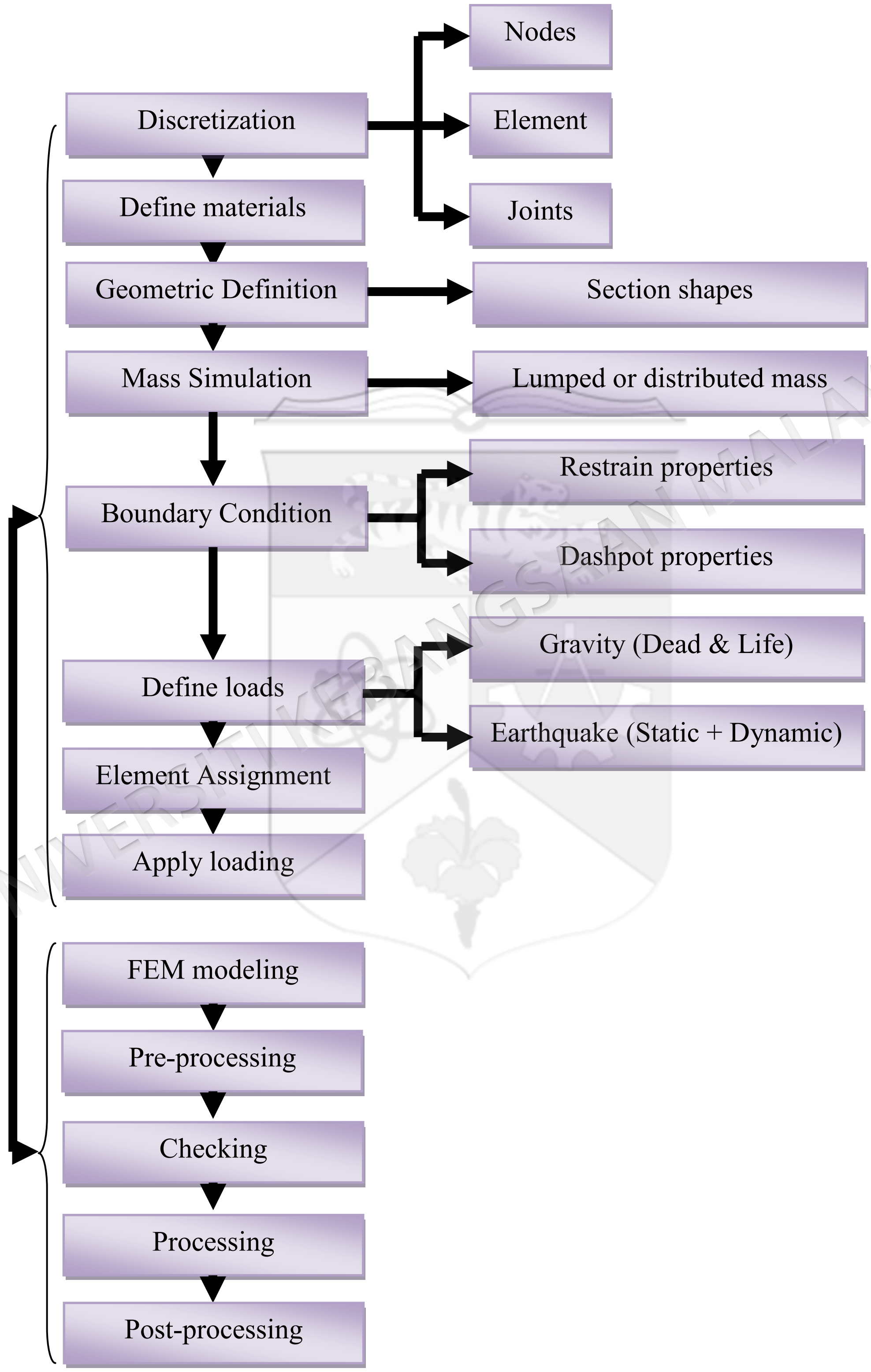

FIGURE 3.14 Typical seismic FEM analysis algorithms

In this section, the description modelling steps of most comprehensive elevated tank case which are consists of 1) tank super structure and foundation with FSI added mass approach 2) substructure with nonlinear SSI (direct approach) effects, and 3) with considered three analysis stages.

3.4.1 Dynamic Option Tools in LUSAS

Generally the dynamic tools in LUSAS software can be presented in the flowchart as shown in Figure 3.15, in which it cover most of the dynamic facilities such as modal dynamic analysis. The common forms of modal analysis (using the eigenmodes system), are natural frequency analysis, eigenvalue (Linear) buckling analysis, spectral (seismic) response analysis, harmonic (forced) response analysis and transient dynamic analysis (direct integration) which is widely used in the analysis of SSI.

Solving the equation of motion using direct integration must follow two assumptions which allow this to be transformed into linear simultaneous equations in which the dynamic equilibrium equation is satisfied at discrete time points within the solution time interval. These points are 'dt' apart, and the interval between them is referred to as a 'time-step', the variation of displacement, velocity and acceleration within these time intervals is postulated (Bathe 1982). LUSAS having two facilities to evaluate the solution of the equation of dynamic equilibrium which are implicit and explicit (LUSAS User Manual 2007), implicit dynamic analysis is used to solve "low velocity" problems where low frequency effects dominate the response. Typical applications for this analysis include seismic analysis or plant and structures including SSI (Bathe 1982; Beshara & Virdi 1991), low velocity impact and analysis of deformable blast panels. LUSAS has a highly accurate state-of-the-art facility based on the second order Hilber-Hughes-Taylor algorithm (LUSAS User Manual 2007), this algorithm is self-starting (meaning no preliminary static solution is required) and allows variable time steps to be used. It is unconditionally stable for linear problems enabling large time steps to be taken without loss in stability. An automatic time step computation is available if required. The implicit dynamics option is available for all implicit element types with either consistent or lumped mass idealization and may also be combined with the other analysis options.

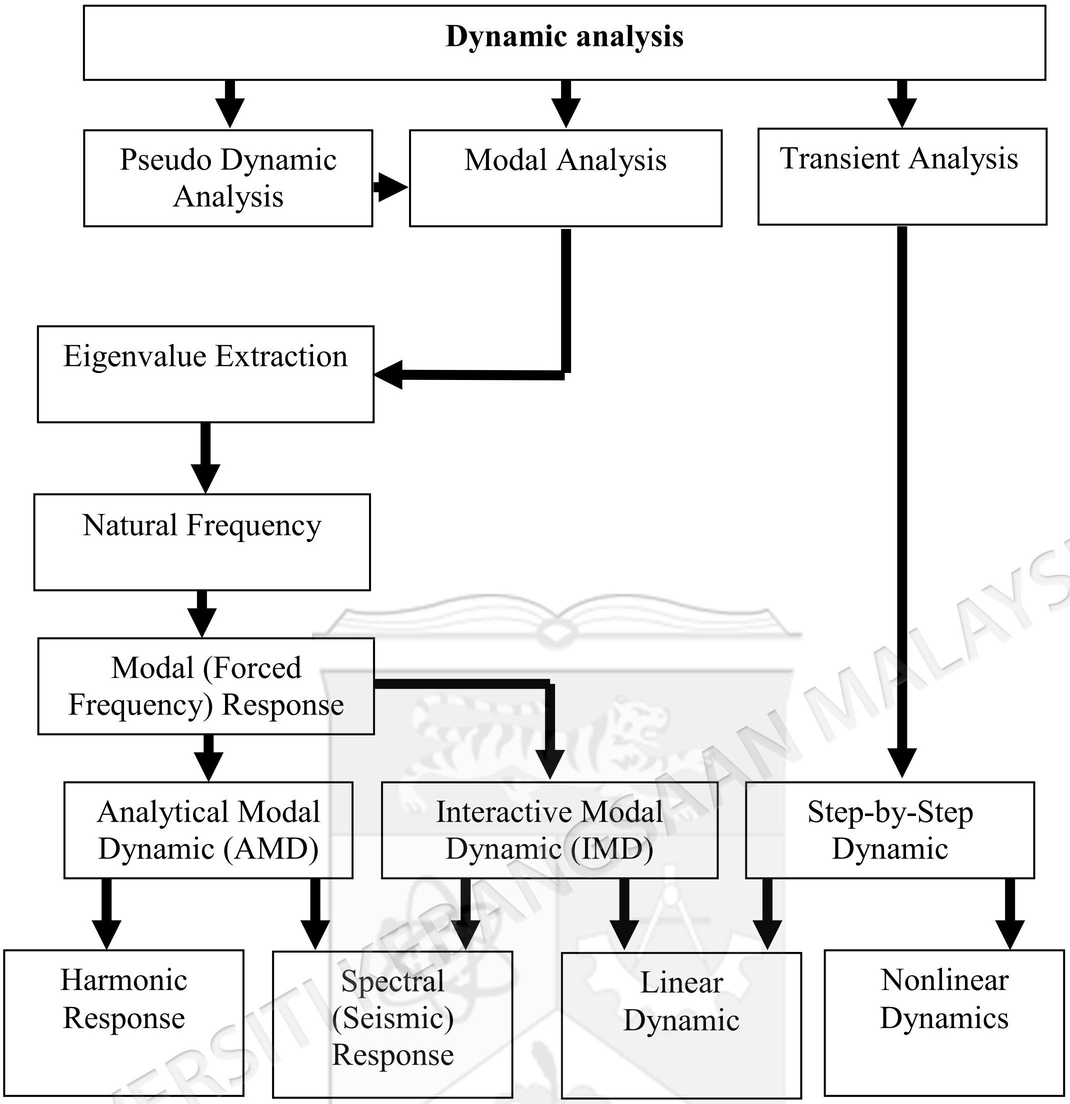

FIGURE 3.15 Dynamic options in LUSAS software

3.4.2 Elements to be used in Modelling

The LUSAS element library contains several types classified into groups according to their function. The available element groups in LUSAS are; bar elements, beam elements, continuum elements (2-D and 3-D), plate elements, shell elements, membrane elements, joint elements, field elements and interface elements.

This section is providing a brief description of the element types used in the elevated concrete water tanks modelling; a more detailed element description can be studied in the LUSAS Theory Manual and in the LUSAS Element Reference Manual.

3.4.3 Beam Elements (BMS3)

There are numerous types of beam elements available in the beam section in the LUSAS element library. The beam elements are commonly used to model plane and space frame structures.

BMS3 is a straight beam element in 3D for which shear deformations are included. The geometric properties are constant along the length. The number of node is 3 with end release conditions with 6 DOF at end nodes. The third node is used to define the local xy-plane as shown in Figure 3.16.

BMS3 is not able to described non-linear behaviour such as geometric or material effects, but can if combined with other elements be included in a non-linear analysis (3D continuum soil element). Linear, eigen, and dynamic analysis procedures are fully supported with this element.

The element can be used to model 3D frame structure with the QSI4, curved thin shell elements.

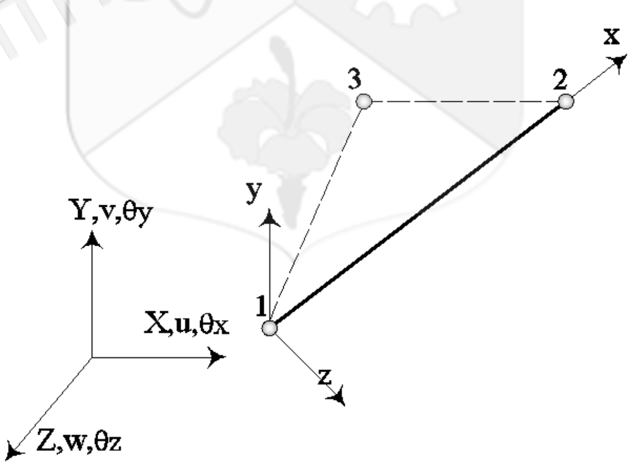

FIGURE 3.16 Quadrilateral 3D thick beam element with denoted degrees of freedom. (LUSAS, 2007)

3.4.4 Shell Elements (QSI4)

There are numerous types of shell elements available in the shell section of the LUSAS element library. The shell elements are commonly used to model 3-D structures, capturing both flexural and membrane effects.

QSI4 (Figure 3.17) is a quadrilateral thin shell 3D which includes a high performance incompatible model. The elements take into account both membrane and flexural deformations. As required by thin plate theory, transverse shearing deformations are excluded. An average thickness value for each element is obtained from the specified nodal thicknesses. Since the elements are formulated in local element axes, directional material properties may be defined relative to the element orientation.

QSI4 is not able to described non-linear behaviour such as geometric or material effects, but can if combined with other elements be included in a non-linear analysis. Linear, eigen, and dynamic analysis procedures are fully supported with this element.

.

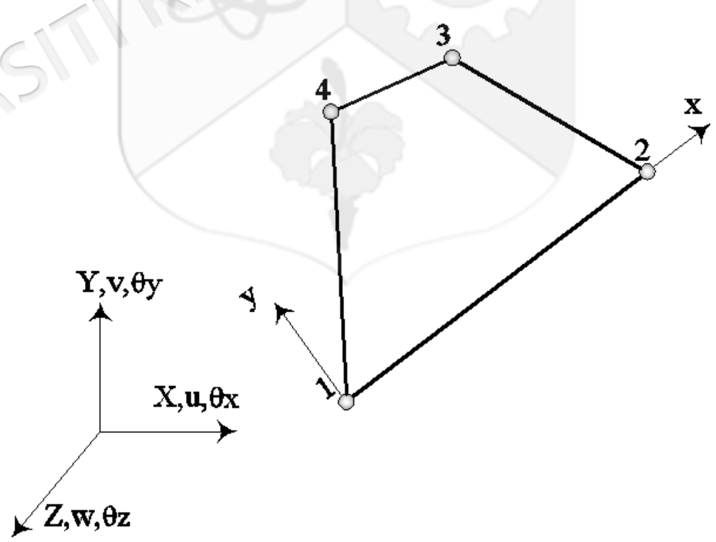

FIGURE 3.17 Quadrilateral shell elements (QSI4) with denoted degrees of freedom. (LUSAS, 2007)

3.4.5 Joint Elements

Joint elements (Figure 3.18) may be used to connect nodes of different element with elastic springs. The springs can be given any desired configuration concerning translational and rotational stiffness. The joint elements will, via an interface mesh, connect nodes of different elements. An initial gap between the nodes is allowed, but to maximise the efficiency of the joint element and capture the time variation the gap should be minimised.

The stiffness matrix corresponding to the joint element does not rely on engineering beam theory, implying that joint elements are independent of both shear forces and joint length. Even though the joint elements remain geometrically linear, they are able to be included in non-linear analyses due to assumed infinitesimal strains and the neglecting large deformations effects.

Joint elements are valid for both 2-D and 3-D modelling. The connection is represented by a line joint in 2-D while modelling in 3-D requires a surface joint mesh to be generated. There are two methods of applying the surface joint mesh, either by a single joint where the joint mesh is assigned to a single line or by connecting the elements with multiple nodes by means of a joint mesh interface. The method using a single line is more suitable when only a few joints are desired due to the required definition of each joint.

The joint mesh interface utilise a master and slave connection to tie the desired lines or surfaces together. The joint properties are applied by assigning them to the selected master feature, describing the behaviour of the joint. To create a joint with rotational degrees-of-freedom, the geometric properties of the joint are required to be assigned due to the eccentricity present. Additionally, the joint mesh requires that material properties are defined.

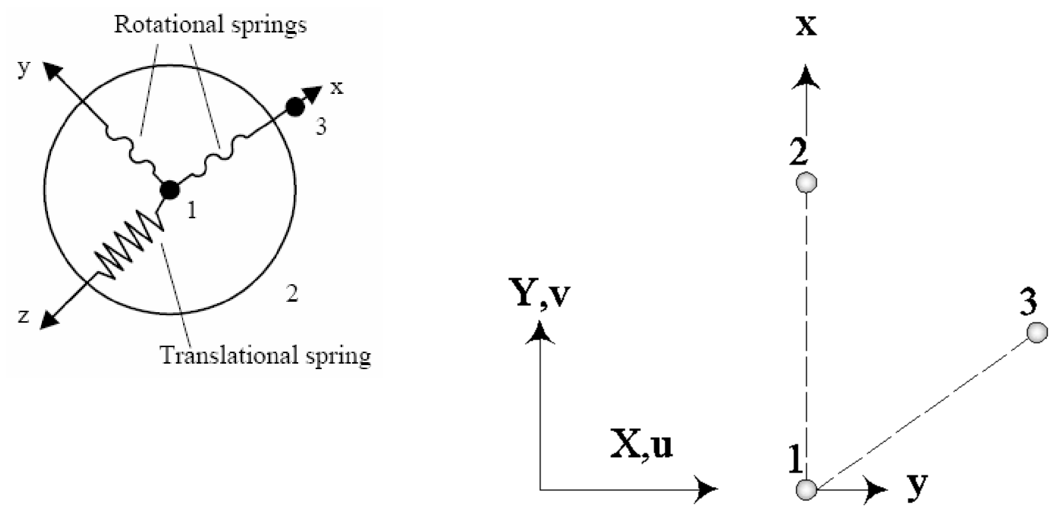

FIGURE 3.18 Joint three-dimensional elements for plate bending elements. The joint element consists of rotational springs in x- and y-direction and a translational spring in z-direction (LUSAS, 2007).

3.4.6 3D Continuum Elements (HX8)

3D continuum elements are used to model fully 3-dimensional structures. Tetrahedral, pentahedral and hexahedral solid elements are available to model full 3-dimensional stress fields. A family of 3D isoparametric solid continuum elements with higher order models capable of modelling curved boundaries. The elements are numerically integrated.

HX8 (Figure 3.19) Geometrically is capable of modelling initial stresses which used for modelling in-situ soil stresses, also having ability to described nonlinear behaviour such as geometric and material effects. Linear, nonlinear (Capable to use Drucker-Prager as yield criteria), eigen, and dynamic (implicit dynamic scheme) analysis procedures are fully supported with this element.

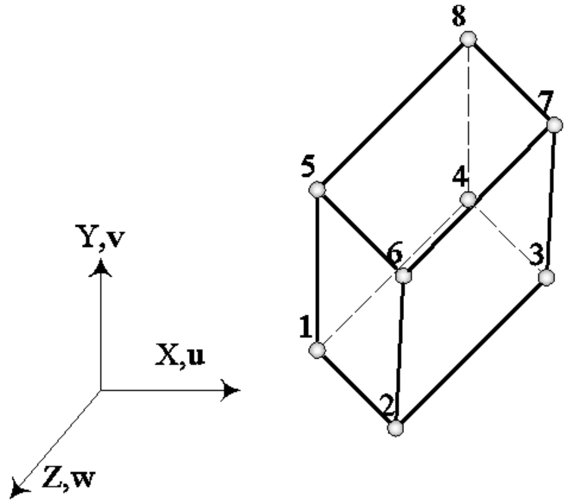

FIGURE 3.19 Hexahedra three dimensions elements (HX8) with denoted degrees of freedom (LUSAS, 2007)

3.4.7 Wastergaard Method Added Mass Approach

The Westergaard added mass procedure is one of the methods that are used to incorporate the hydrodynamic effect in the analysis for computer codes without a fluid element formulation. With the hydrodynamic water pressure on the vertical face of a rigid structure opposite in phase to the ground acceleration, these hydrodynamic pressures are equivalent to the inertia force of an added mass moving with the tank (Chopra 2012). The Westergaard (1931) procedure adding an additional water mass to the mass matrix is obtained by different techniques like Housner's expressions and EC-8.

This method was originally developed for the dams but it can be applied to other hydraulic structure under earthquake loads i.e. tanks (Livaoglu & Dogangun 2006). In this thesis the impulsive mass is obtained according to EC-8 (Table 3.1) technique is added to the tanks walls according to Westergaard approach as shown in Figure 3.21 using Equation (3.5)

$$m_{ai} = [\frac{7}{8}\rho\sqrt{h(h - y_i)}]A_i \tag{3.5}$$

In which ρ is the mass density, h the depth of wall and $\ddot{u}_g$ the imposed ground acceleration

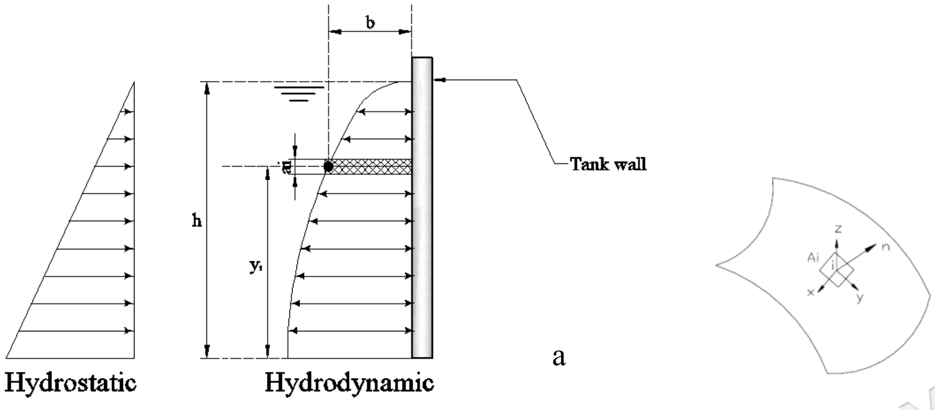

FIGURE 3.20 (a) Westergaard added mass concept, (b) normal and cartesian directions of curve linear surface

In the case of Intze tank where the walls having sloped and curved contact surface, Equation (3.6) should be compatible with the tank shape by assumes the pressure is still expressed by Westergaard's original parabolic shape, but the orientation of the pressure is normal to the face of the structure and its magnitude is proportional to the total normal acceleration at that point is recognized. In general, the orientation of pressures on a 3-D surface varies from point to point; and if expressed in Cartesian coordinate components, it would produce added-mass terms associated with all three orthogonal axes. Following this description the generalized Westergaard added mass at any point i on the face of a 3-D structure is expressed by (Kuo 1982).

$$m_{ai} = \tau_i A_i \lambda_i^T \lambda_i = \tau_i A_i \begin{bmatrix} \lambda_X^2 & & Sym \\ \lambda_Y \lambda_X & \lambda_Y^2 & \\ \lambda_Z \lambda_X & \lambda_Z \lambda_Y & \lambda_Z^2 \end{bmatrix} \tag{3.6}$$

$A_i =$ Tributary area associated with node i

$\lambda_i = (\lambda_X, \lambda_Y, \lambda_Z)$ is the normal direction cosines as shown in Figure 3.20 (b)

$ai =$ Westergaard pressure coefficient given by

$$m_{ai} = [\frac{7}{8}\rho\sqrt{h_i(h_i - y_i)}] \quad (3.7)$$

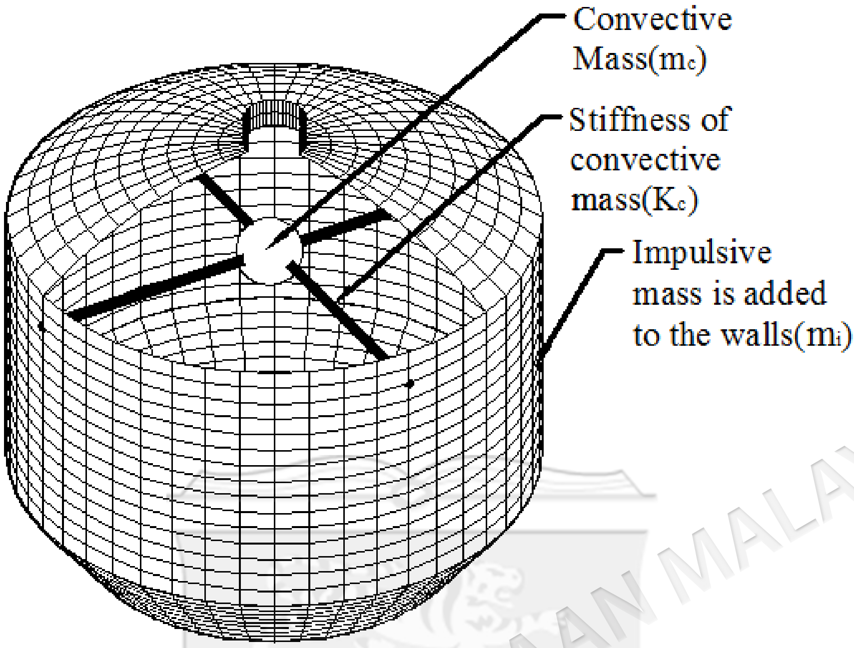

FIGURE 3.21 The finite element models for the FSI

3.4.8 Damping

LUSAS enables the application of both viscous damping and structural modal damping ratios when defining the elevated tank structure's total damping. A combination of the two types of damping is also allowed. However, structural damping cannot be used in modal response analysis in the time domain. The damping ratio expressed with a percentage of the critical damping, can either be user specified or automatically calculated by the software. The provided estimation of the modal damping is only available if relevant damping data is included in the eigenvalue analysis. Any arbitrary damping ratio can be individually assigned to each mode. For dynamic analysis of structures with a damping greater than the prescribed maximum ratio a direct step-by-step integration is suggested.

The most usual approximation for C is the so-called Rayleigh damping (Clough and Penzien 1975) as shown in Figure 3.25, given by a linear combination of mass and stiffness matrices.

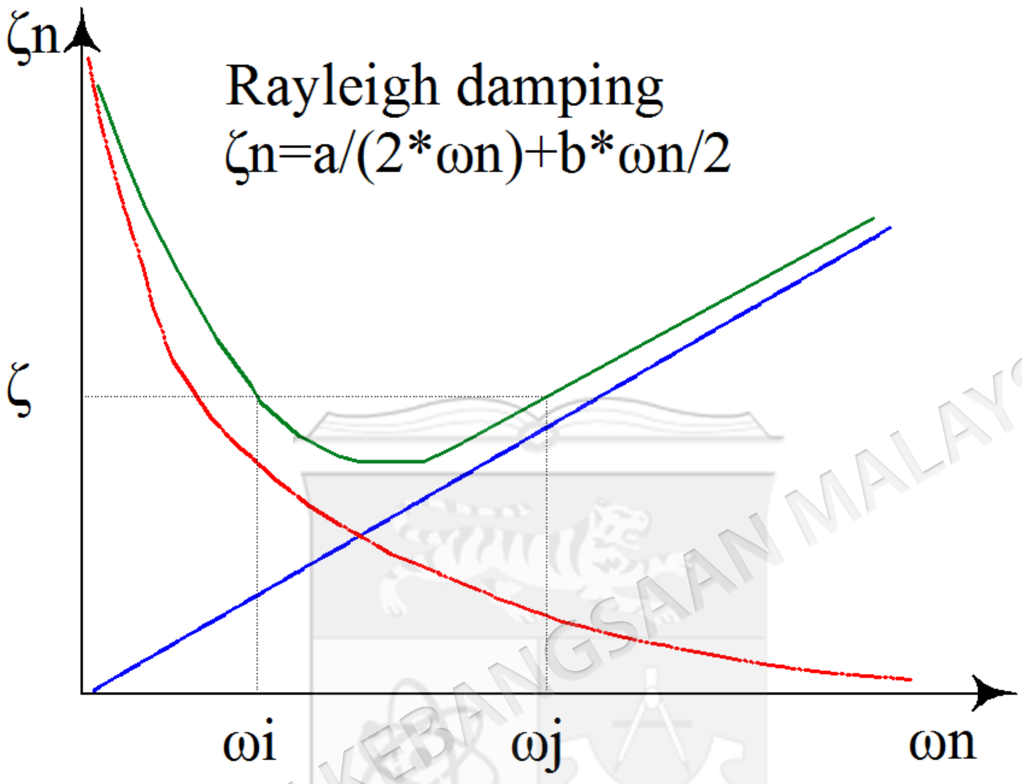

FIGURE 3.22 Rayleigh damping parameters

ξ and ω shown in Figure 3.22 are Rayleigh damping factors, so-called numerical damping; K is the stiffness matrix. It is apparent that the two Rayleigh damping factors ξ and ω can be evaluated by the solution of a pair of simultaneous equations if the damping ratios associated with two specific circular frequencies (modes) are known. In addition, it is generally assumed that the same damping ratio applies to both chosen circular frequencies.

Such an assumption leads to a constant damping ratio for entire system (soil +foundation + tank), which is not usually pertinent to soils, whose damping depends strongly on the development of share strains and may vary abruptly over the geometrical domain of integration. For this reason, and when the shear strains are lower than the threshold value, a variable damping solution can be adopted, in which the Rayleigh assumption holds good.

3.4.9 Boundary Condition

The actual problem determines to what extent boundaries become necessary. In many cases of soil structure interaction analysis the structures under consideration are situated at, or close to, the free surface and the soft soil layers at the surfaces are bounded by hard rocks at the bottom. So we can take advantage of two real elementary boundaries, a zero displacement boundary at the bottom. Thus, the unbounded domain extends only in the horizontal directions and only remaining vertical boundaries cause problems.

3.4.10 Elasto-Plastic Models

The elasto-plastic models available within LUSAS can be broadly divided into two families. The older models are based on classical continuum formulations in which the plastic strains are integrated according to a strict interpretation of the flow rules governing their evolution. Recent developments in numerical analysis have reinterpreted the classic laws in a search for greater numerical efficiency and have led to the concept of "consistency" of formulation. These methods have the advantage of improved stability for large load steps and quadratic convergence in the global Newton-Raphson iterations. Within the framework of the consistent formulation, time dependent inelastic straining has also been modelled. The models available within LUSAS are as described in the following section.

2.3.11 Material Model used for the Soil Elements

It is required that stress-strains relationship of a material passing from linear zone to nonlinear zone under various loads should have failure criteria. Choosing acceptable failure criteria related to the class of material and type of loading is important in reaching to the correct result in structured analysis. For this purpose, miscellaneous criteria such as Mohr-Coulomb failure criterion, Tresca failure criterion, Von Misses failure criterion and Drucker-Prager failure criterion have been used (Figure 3.23 and Figure 3.24). It is substantial that nonlinear behaviours of soils having a different characteristic in comparison to structure systems should be regarded with grave concern from the viewpoint of soil-structure interaction. The reason why the behaviour of soils is different than other materials is the increase in their sliding resistance in connection with the stress level and the difference on the behaviour under tensile stress from the one under pressure stress. Therefore, considering a failure criterion to supply the conditions of the soil is unavoidable. Hence, for soil element is generally used Drucker-Prager elasto-plastic failure criterion (Chen and Mizuno 1990).

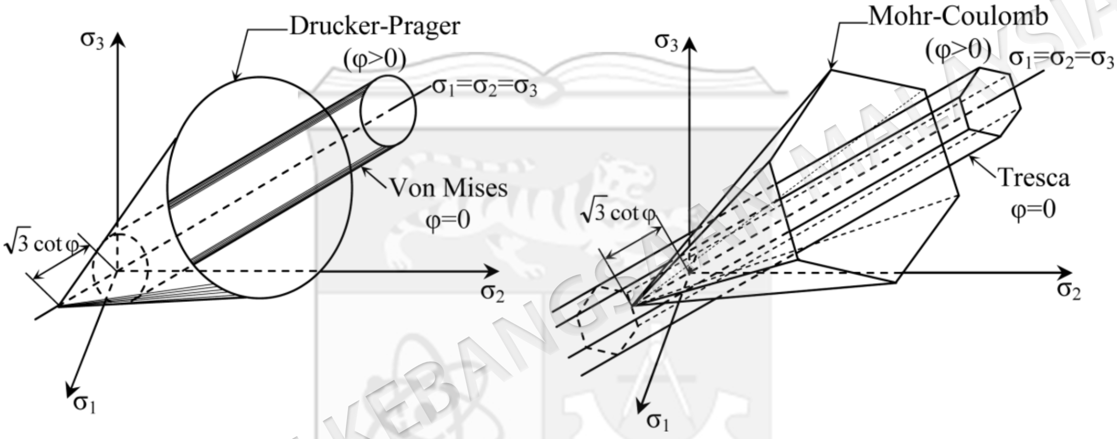

FIGURE 3.23 Schematic failure surfaces at the principal stress space for different failure criteria

Source: Gursoy 2009

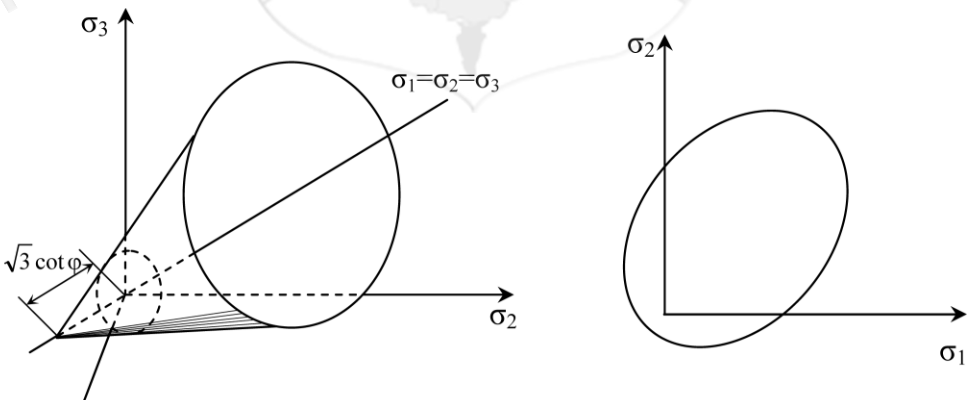

FIGURE 3.24 Drucker-Prager schematic failure surfaces at two dimensional principal stress planes and at three dimensional principal stress spaces

Source: Gursoy 2009

3.4.12 Nonlinear Incremental-Iterative Procedure

In the present analysis an incremental loading procedure combined with Newton-Raphson method has been used for solving the nonlinear equations involved in a plasticity analysis. In this method the load is applied in increments, but in each increment successive iterations are performed, but in each iteration the stiffness matrix is updated, after each iteration, the step potion of the total loading that is not balanced is calculated and used in the next step to compute an additional increment of displacement (Figure 3.25). The solution converged in the equilibrium after the number of iterations when the restoring force equals to the applied loads (or at least to within some tolerance)

.

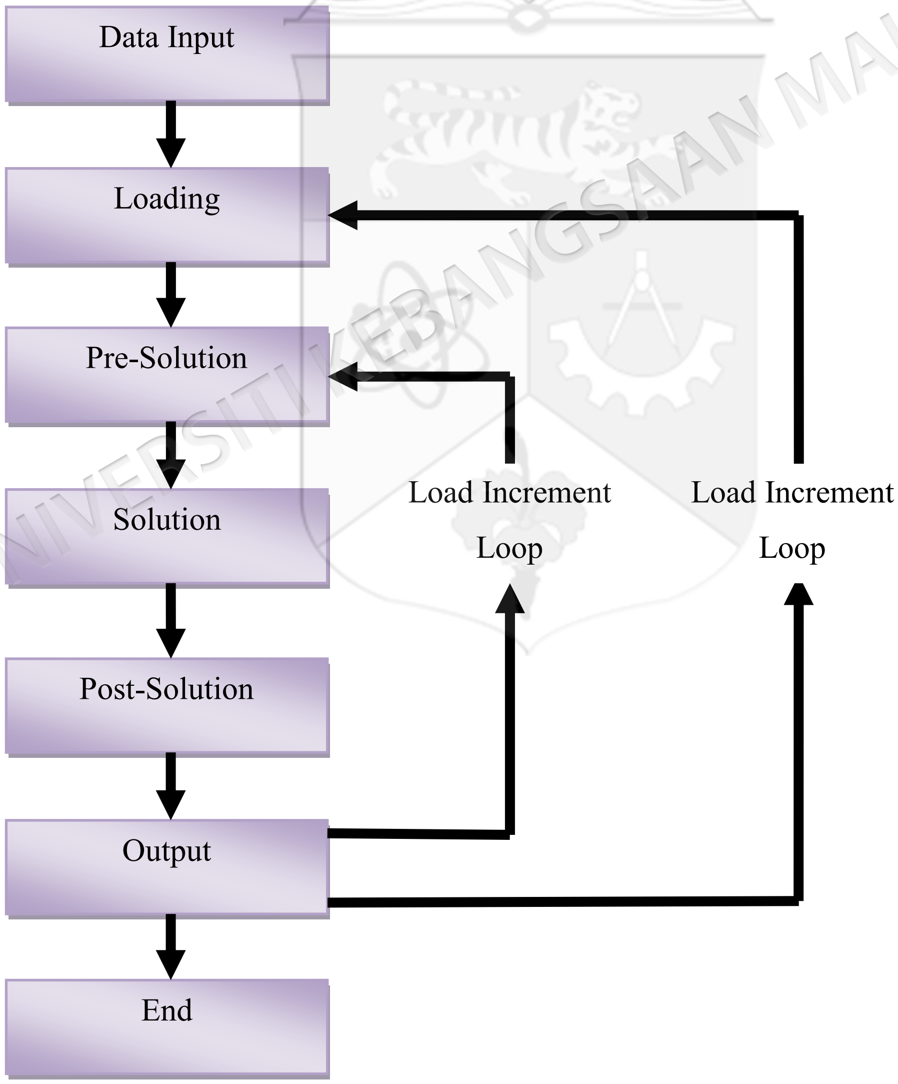

FIGURE 3.25 Typical nonlinear program executions

3.4.13 Numerical Analysis of Elevated Tank

This section describes how the modelling procedures are performed for the three stages of the static and seismic analysis.

This analysis process is divided into three stages:

1- Perform the initial state of stress (in-situ soil stress) of the soil before tank is constructed.

2- Perform the state of stress with structural loading (self weight + water in reservoir)

3- Perform the seismic load in the case of the soils do not liquefy (Drucker-Prager elasto-plastic failure criterion)

Each stage is described separately in the following sections.

3.4.14 Initial Stress (in-situ soil stress) Stage

In this stage the analysis is started from the state of soil before the tank is constructed. In this study the construction process such as excavation and filling are ignored because it has minor effect compared to whole initial stress analysis, therefore the tank is assumed placed in one stage. The initial state (Figure 3.26) of stress in the soil can be characterized by the volumetric weight of the soil and the lateral pressure ratio. This ratio is defined as the quotient of the horizontal (principal) effective stress and the vertical effective stress. It should be noted that the initial stress must be set as first load case and cannot be altered throughout the analysis.

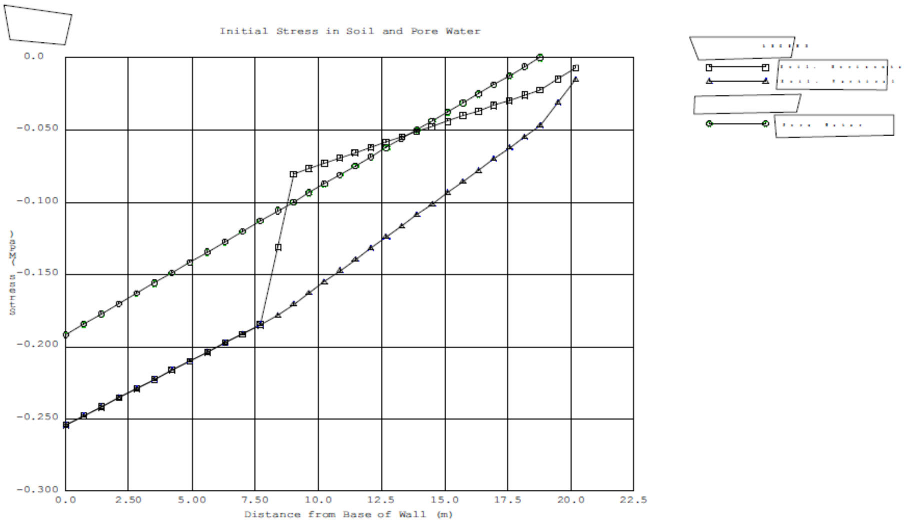

FIGURE 3.26 Typical initial stresses profile

In this study the in-situ stresses of the soil and Young's Modulus are modelled wary with depth. The variations entered ensure that stresses increase negatively with depth while the Young's Modulus increases positively with depth.
Initial loads:-

1- Initial stresses of soil in three directions (x,y,z)

2- Self weight of soil

3.4.15 Structural Loading Stage

In this stage incorporate the state of stress of the soil with the reservoir level of the tank raised to its full height. The static equilibrium state in this stage is now calculated for the new state of stress. The model in this stage is now solved for this applied condition,

Structural loads:-

1- Hydrostatic pressure of water
2- Self weight of the tank and foundation

3.4.16 Seismic Analysis Stage

In this stage perform a seismic load, with assumption that the soils do not liquefy, with the respect the source of nonlinearity, in this case concern over the soil behaviour suggested that material nonlinearity should be assigned to this part of the structure.

When the loading cannot be considered instantaneous or where inertia and damping forces are significant a dynamic analysis is required. Generally, the dynamic solution is obtained by performing numerical step-by-step integration in the time domain. A variation of the displacements and the velocities are assumed as the solution progress with each time increment. The simultaneously solved set of equations within each time-step represents the response at discrete time instances when dynamic equilibrium is fulfilled. When the initial conditions are known, successive application of the procedure produces the dynamic response of the structure.

3.4.17 Transient Dynamic Analysis

There are several different methods available for solving the dynamic equilibrium equations using direct integration. The algorithms are described in chapter II section 2.2.5. The choice of which integration scheme to apply onto a specific model is highly dependent on the complexity of the structure and the type of analysis required.

An explicit integration scheme generates a stable result if the time-step is shorter than the critical length. Explicit algorithms permit de-coupling of the equilibrium equations which implies that an inversion of the stiffness matrix is not needed. This characteristic makes the explicit algorithms more suited for analyses which require small time-steps, irrespective of the stability requirements. When an explicit direct integration is desired, LUSAS applies the central difference integration scheme (Figure 3.15), described in chapter II section 2.2.7. The central difference method is particularly effective when a uniform discretisation of lower order elements is used.

The implicit algorithms are unconditionally stable allowing the time-step to increase with a retained convergence. The total number of time instances where equilibrium is calculated can therefore be reduced. The computational effort at each time-step is more extensive due to the required inversion of the stiffness matrix. Generally, an implicit integration is preferred for inertial problems where the total response is governed by relatively low frequencies. The main reason for this is that the time-step is commonly set to be greater than the critical length preventing optimal accuracy for the higher modes. The higher modes have less influence on the total response implying that the total accuracy is condensated. The Hilber-Hughes-Taylor implicit integration and Newmark scheme, described in Chapter II section 2.2.7, is used in this the study

3.4.16 Eigenvalue Analysis

If solving the dynamic problem by means of modal analysis, the extraction of natural frequencies and natural modes are required. The natural frequencies and eigen modes are determined by an eigenvalue analysis.

There are different methods available in LUSAS to extract the eigenvalues and eigenvectors (Figure 3.15) from large systems of equations. The algorithms of the methods have several common features. The algorithms initially determine which DOF will provide the greatest contribution to the structural response. Thereafter, a transformation matrix and a reduced set of equations are assembled.

Finally, the eigenvalues and eigenvectors of the reduced system are extracted and are thereafter transformed to represent the complete system.

The solution is completed by calculating error estimations of the precision provided by the eigenvalues and corresponding eigenvectors. A normalisation of the eigenvectors is recommended in order to decrease the duration of the dynamic analysis.

Table 3.6 conclude the compassion between analytical model dynamic, interactive modal dynamic and transient dynamic analysis (step by step) that available in LUSAS software

TABLE 3.6 Comparison between the three types of dynamic analysis that is available in LUSAS software

Analytical Model Dynamic (AMD)	**Interactive Modal Dynamic(IMD)**	**Transient Dynamic (Step-by-Step)**
Response of all nodes at specific pre-determined (solved) frequencies	Response of all nodes at specific general frequency	Response of all nodes at all (solved) frequencies
Response of specific nodes at all pre-determined (solved) frequencies	Response of specific nodes over specified frequency range	

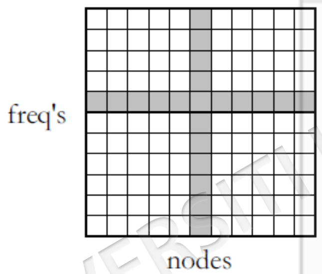

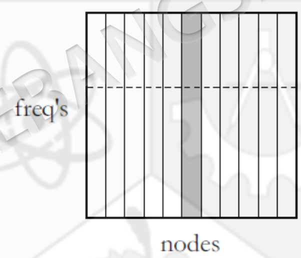

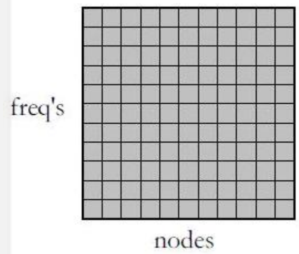

3.4.19 Numerical Analysis through FEM

In this section, the linear and non-linear dynamic analysis of an elevated tank is presented, several linear analyses were made to investigate the performance of an elevated tank through the implicit time stepping FE dynamic analysis.

The investigation focuses upon how the responses vary with: (1) the size of time step; (2) the density of the soil mesh. The results obtained from linear time stepping FE analysis show that the dynamic response of structures depend on the parameters of the integration algorithm, e.g. time step size; and the density of the mesh. The results also show that the model used is capable of predicting the linear dynamic behavior of elevated tank.

In this section, artificial earthquake time-history which is generated from the USH following the issues of selecting most suitable parameters for earthquake generation as studied in Chapter IV, are used for the linear and non-linear dynamic analysis. Figure 3.27 shows the characteristics for the nonlinear dynamic response of elevated tank using LUSAS software.

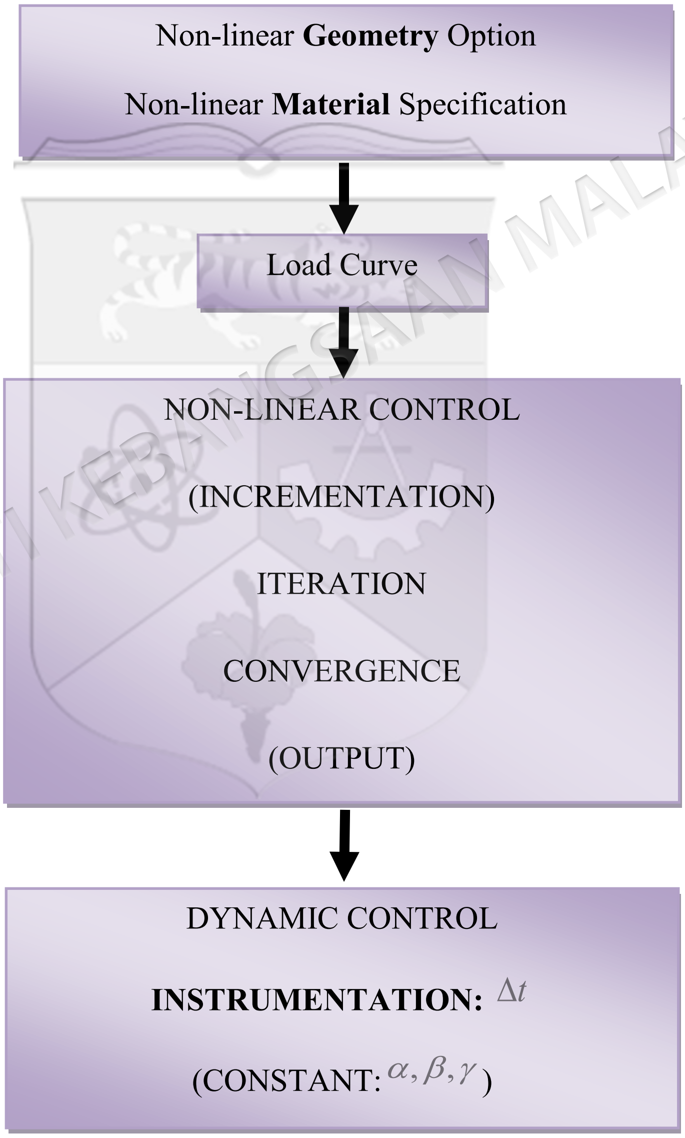

FIGURE 3.27 Nonlinear dynamic analysis in LUSAS

3.5 PROGRAM TOOL DEVELOPMENT

In this section developed prototype software by the author that can be used by the engineers to determine the dynamic responses of the structures natural frequencies and time histories based on Newmark approach as analysis scheme.

3.5.1 Considerations in Development

The followings are some of the considerations included in the development of the prototype program:

1- By input number of DOF for masses stiffness and damping values the user can evaluate the natural frequencies (Tc and Ti)

2- By input β and γ which are the values of Newmark integration, the user can determine the time history response of the tank (displacement and acceleration) at every level been considered

3.5.2 Description of the Program

The following sections describe the prototype program

3.5.3 Introduction

The developed software is to assist engineers and researchers in dynamic analysis of structures. Program is intended to introduce the dynamic analysis of practitioners who are unfamiliar with the concepts and process of dynamic analysis.

3.5.4 Overview of Prototype Steps

The tasks required to determine natural frequencies and time histories response of the structures is assigned according to the steps listed below, and followed by brief description of each step.

1- Load data

2- Natural frequencies

3- Time histories response prediction

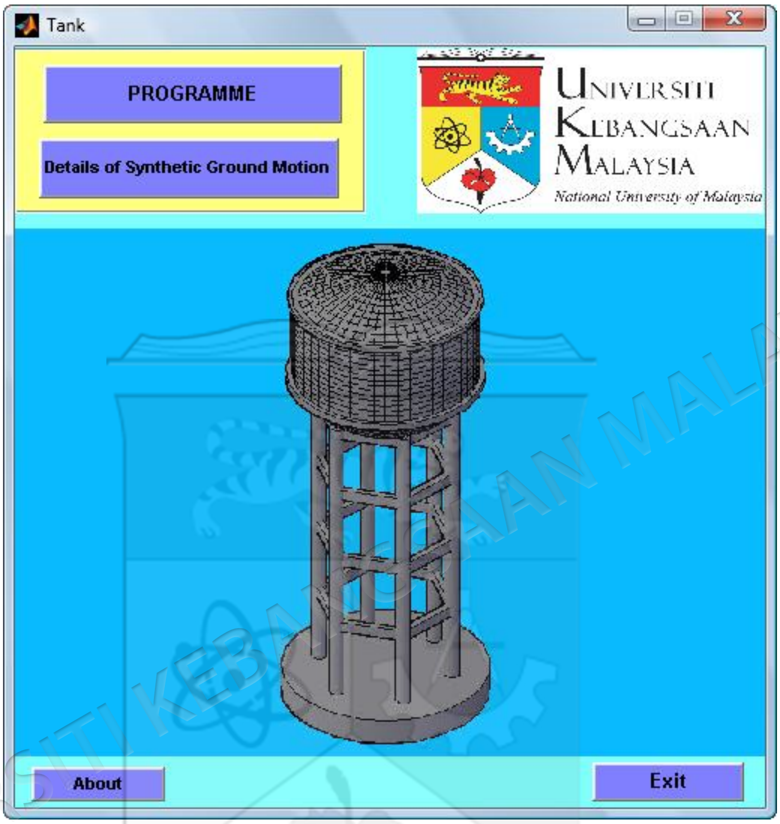

FIGURE 3.28 Main menu of the prototype

Figure 3.28 shows the main menu of the prototype program. The main menu shows two icons where in the upper box is for executing the program and the lower box is to shows the information of the earthquake to be used as shown in Figure 3.29

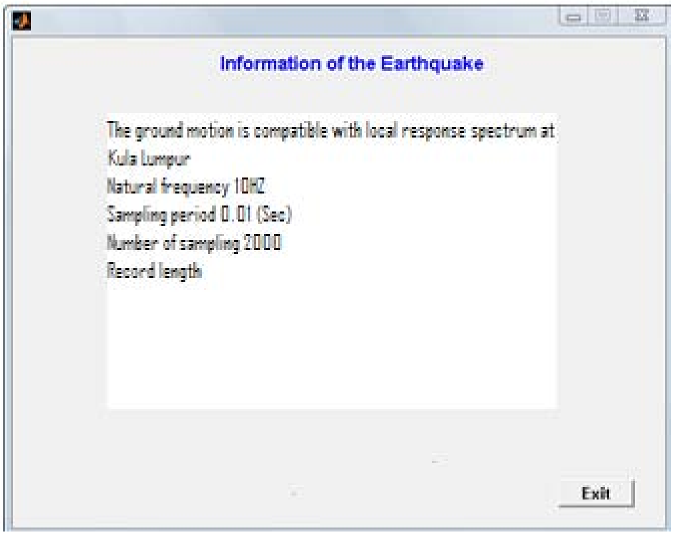

FIGURE 3.29 Earthquake information

1- **Load data.** As shown in Figure 3.30 user can input the rows of data mass stiffness and damping by pushing button is used to loaded data labeled as Input,

2- **Natural frequencies.** For the analysis of natural frequencies and time histories responses a push button is used.

3- **Time histories response prediction.** To plot the time history response of the structure needs to input additional data namely Newmark integrations (β and γ) time period and any number of lumped mass required for the analysis for particular earthquake as shown in Figure 3.30

Input Data

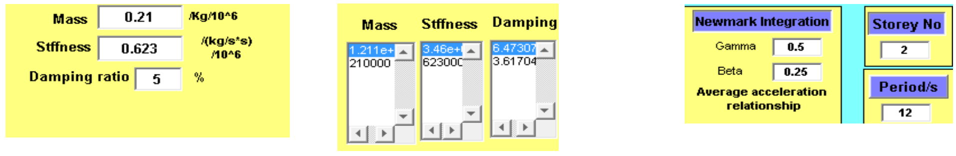

Output Results

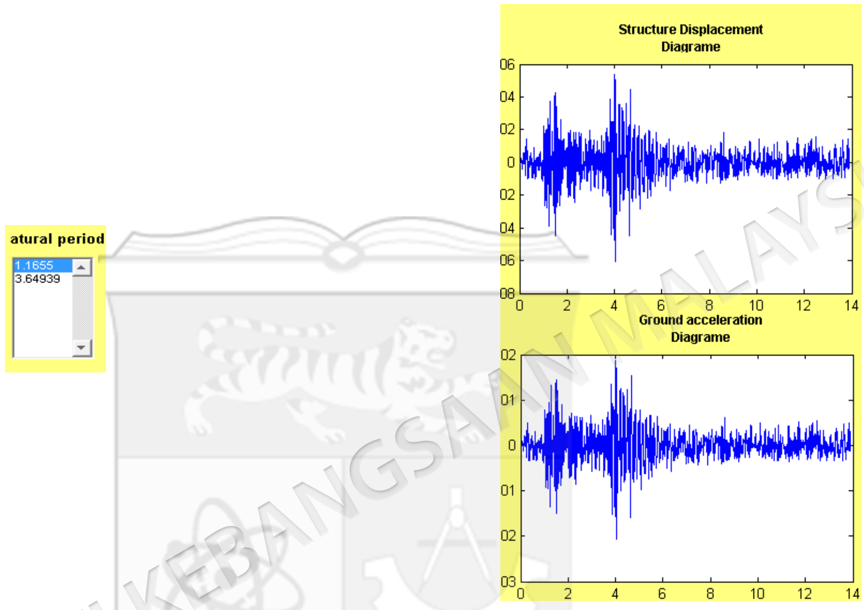

FIGURE 3.30 Load data and obtained results

3.6 ADVANTAGES AND DISADVANTAGES OF THE PROGRAM

The advantages of developed program are:

- Program is easy to use.
- Program saves time and decrease design cost.
- Generates and presents a good quality graphics.
- The Program can be used for unlimited of degree of freedom

However the disadvantage of this developed Program that the Program is run under MATLAB environment.

3.7 VERIFICATION OF THE PROGRAM

In order to ensure the accuracy of the developed program, therefore verification with the analytical solutions (mechanical model) must be carried out. Table 3.7 shows the comparison results of the period of convective (T_c) and impulsive modes (T_i).

TABLE 3.7 Verifying of program results

Mode	Program	Reference (Livaoglu 2006)	Deviation (%)
Tc	3.649	3.69	1.11
Ti	1.166	1.166	0

3.8 SUMMARY

In this chapter, a review of various theoretical aspects of the numerical modelling of the elevated tanks were described and discussed. The two ways that widely used to model elevated tanks, namely mechanical models and FEM models were proposed to be used for the numerical analysis in this thesis, and the steps of structural modelling were deeply discussed in the case of embedded and no embedded with and without considering SSI for all cases. The chapter also considers the development and brief descriptions of the prototype model. Overview of the prototype steps in predicting natural frequencies and time histories response are also discussed. Some advantages and disadvantages of the developed program are also presented.

CHAPTER IV

GENERATION OF ARTIFICIAL TIME HISTORIES AND LOCAL SITE EFFECTS

4.1 INTRODUCTION

Earthquake ground motions are usually recommended to be used for dynamic analysis and design of structure with irregular shapes such as elevated tanks, dams and irregular building as well as evaluation of the response of earth structures in terms of stability, deformation, and liquefaction potential (Priestley et al. 1996; Bommer & Ruggeri 2002). Lacking of real ground motions recorded at the site, earthquake ground motion should be generated. This chapter provides background information on selection of the ground motions, and generation the artificial ground motion compatible with local (Malaysian) response spectrum to be used in linear and nonlinear time history analysis. This methodology was introduced by Gasparini and Vanmarcke (Gasparini & Vanmarcke 1976) in which the basis of procedures coded in the software called SIMQKE.

This chapter also reviews the mathematical process about local site effect based on one-dimensional nonlinear analysis of earthquake site response and also this procedure coded in program called NERA (**N**onlinear **E**arthquake **R**esponse **A**nalysis).

4.2 SELECTION AND SCALING OF EARTHQUAKE GROUND MOTION

The selection or scaling of ground motions is critical task to choose or develop an appropriate ground motion. The main challenges in their development are to ensure that they are consistent with the target parameters and also realistic. This is not as easy as it might appear; many motions that appear reasonable in the time domain may not when examined in the frequency domain, and vice versa. Many reasonable looking time histories of acceleration produce quality of an artificial ground motion is very difficult to discern by eye. The generating of the earthquake ground motions can be evaluated by three fundamental types (Bommer & Ruggeri 2002) as following sections.

4.2.1 Modification of Actual Ground Motion Records

Perhaps the simplest approach to the generation of artificial ground motions is the modification of actual recorded ground motion. Maximum motion levels, such as peak acceleration and peak velocity, have been used to rescale actual strong motion records to higher or lower levels of shaking. Krinitszky and Chang, (1979) recommended that the scaling factor (the ratio of the target amplitude to the amplitude of the record being scaled) should be kept close to 1, and always between 0.25 and 4.0, and the analysis can be conducted with several scaled records. Vanmarcke, (1979) noting that simple amplitude scaling fails to account for differences in important characteristics such as frequency content and duration. He also suggested that limits on the scaling factor should be related to the type of problem to which the resulting motion is to be applied. For analysis of linear elastic structure, the limits of Krinitszky and Chang, (1979) were considered suitable, but for liquefaction a scaling factor range of 0.5 to 2.0 was recommended.

4.2.2 Generation of Synthetic Ground Motion

This type of rescaling procedure requires careful selection of the actual motion to be used. A desirable ground motion record will have a peak acceleration or velocity close to the target value, and have magnitude, distance, and local site characteristics that are similar to those of the target motion. Computer programs (Dussom et al. 1991; Ferritto 1992) that contain, or at least interact with, strong motion databases are available to aid in the selection of actual ground motions for rescaling.

There have been significant developments on the generation of synthetic ground-motion accelerograms by Zeng et al. (1994), Atkinson and Boore (1997), Beresnev and Atkinson (1998), and Boore (2003). However, their applications, in terms of determining the many parameters required to characterise the earthquake source, generally require the engineer to engage the services of specialist consultant in engineering seismology. The determination of the source parameters for previous earthquakes invariably carries a high degree of uncertainty, and the specification of these parameters can involve a significant degree of expert judgement (Bommer & Acevedo 2004).

4.2.3 Generation of Artificial Motions

To generate artificial ground motions compatible with local response spectrum of long duration without significantly changing the frequency content, was carried out by Seed and Idriss (1969), have spliced parts of actual ground motion records together. Procedures of this type must also be used with caution. Careful examination of the reasonableness of spliced motions in both time and a frequency domain is advised.

Gasparini and Vanmarcke (1976), approach is adopted in this thesis to generate a power spectral density function from the smoothed response spectrum, and then to derive sinusoidal signals having random phase angles and amplitudes. The sinusoidal motions are then summed and an iterative procedure can be invoked to improve the match with the target response spectrum, by calculating the ratio between the target and actual response ordinates at selected frequencies. The power spectral density function is then adjusted by the square of this ratio, and a new motion is generated. The attraction of the approach is obvious because it is possible to obtain acceleration time-series that are almost completely compatible with the local elastic design spectrum, which in many cases will be the only information available to the design engineer regarding the nature of the ground motions.

Based on the above reviews, it can be revealed that real ground motions by definition are free from the problems associated with either synthetic records or artificial spectrum-compatible records. However, even real recorded ground motions are now widely available as mentioned above, it is noted that a significant gap in the present day collection of ground motions is that shaking in vicinity of the causative fault in a truly great (Richter magnitude scale 8) earthquake has rarely been recorded (Bommer & Acevedo 2004). Individual real earthquake records are limited in the sense that they are conditional on a single realisation of a set of random parameters (magnitude, focal depth, attenuation characteristics, frequency content, earthquake duration, etc), a realisation that will likely never occur again and that may not be satisfactory for analysis and design purposes. In addition, even today with the large number of real ground motions recorded during the past three decades, it may still be difficult to find groups of strong earthquake time-histories that fulfil the requirements of certain magnitude and distance for design earthquake conditions.

4.3 METHODOLOGY AND FORMULATION OF THE GASPARINI AND VANMARCKE APPROACH

Selection of appropriate seismic excitations that compatible with design response spectrum in particular region could affect the results significantly (Azlan et al. 2005). In this study, the procedure of artificial earthquake generation developed by Gasparini and Vanmarcke (Gasparini & Vanmarcke 1976) is adopted. The procedure is based on periodic function expanded into a series of sinusoidal waves (Housner 1955).

$$x(t)\sum_{i=1}^{n} A_i \sin(\omega_i t + \varphi_i) \tag{4.1}$$

where A_i is the amplitude and φ_i is the phase angle of the i^{th} contributing sinusoidal. The amplitudes A_i are related to power spectral density function G (ω) in the following way:

$$A_i = \sqrt{2\int_0^{\omega} G(\omega_i).\, d\omega} \tag{4.2}$$

The relationship between G (ω) of seismic excitation and response spectrum can be expressed as following

$$G(\omega_i) \approx \frac{1}{\omega_i\left(\frac{\pi}{4\xi_s} - 1\right)} \left\{ \frac{\omega_i^2 (S_V)_{S.P}^2}{r_{S.P}^2} - \int_0^{\omega} G(\omega) d\omega \right\}^{\frac{1}{2}} \tag{4.3}$$

where $r_{S.P}$ is the peak factor; S_V is the target velocity of the response spectrum; ω_i is the circular frequency of the i^{th} contributing sinusoid; ξ_s is the fictitious time-dependent damping factor for duration t. The definitions of these parameters can be found in Gasparini and Vanmarcke (1976)

To simulate the transient character of real earthquakes, the steady-state motions are multiplied by a deterministic envelope function $I(t)$. The artificial motion $X(t)$ becomes:

$$X(t) = a(t) = I(t) \sum_n A_n - \sin(\omega_n t + \phi_n) \tag{4.4}$$

There are three different envelope intensity functions available such as trapezoidal, exponential, and compound (Gasparini & Vanmarcke 1976). The procedure then artificially raises or lowers the generated peak acceleration to match exactly the target peak acceleration that has been computed by using seismic hazard analysis

In this study the response spectrum is obtained from seismic hazard analysis by other researchers (Azlan et al. 2005), this data included the target and calculated response spectrum at the bed rock, and artificial seismic excitation compatible with its target response spectrum.

4.4 LOCAL SITE EFFECT

Usually the ground response analyses is used to predict the surface ground motions for development of design response spectra, to evaluate the dynamic stresses and strains for evaluation of liquefaction hazards, and to determine the earthquake induced forces for design of earth structures. Once the source and travel path effects are determined in conjunction with the seismic hazard analysis, the problem becomes to determine the response of soil deposit to the motion of the bedrock immediately beneath it. The development of site-specific design ground motions, which reflects the strength as shown in Figure 4.1

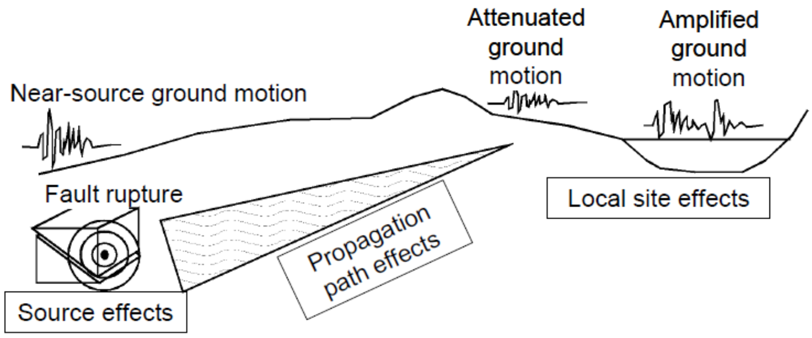

FIGURE 4.1 Schematic diagram of source of ground motion

Usually (equivalent linear or nonlinear) of one-dimensional analysis are performed for the site-specific profiles using the rock motions as input motion, to compute the time histories at the ground surface. Response spectra of calculated ground surface motions are statically analysed or interpreted in some manner to develop ‘design spectrum’ for the site. The time histories from the ground response analysis can be used directly to represent the ground surface motions or artificial time histories can be developed to match the design spectrum according to the methodology presented in Figure 4.2

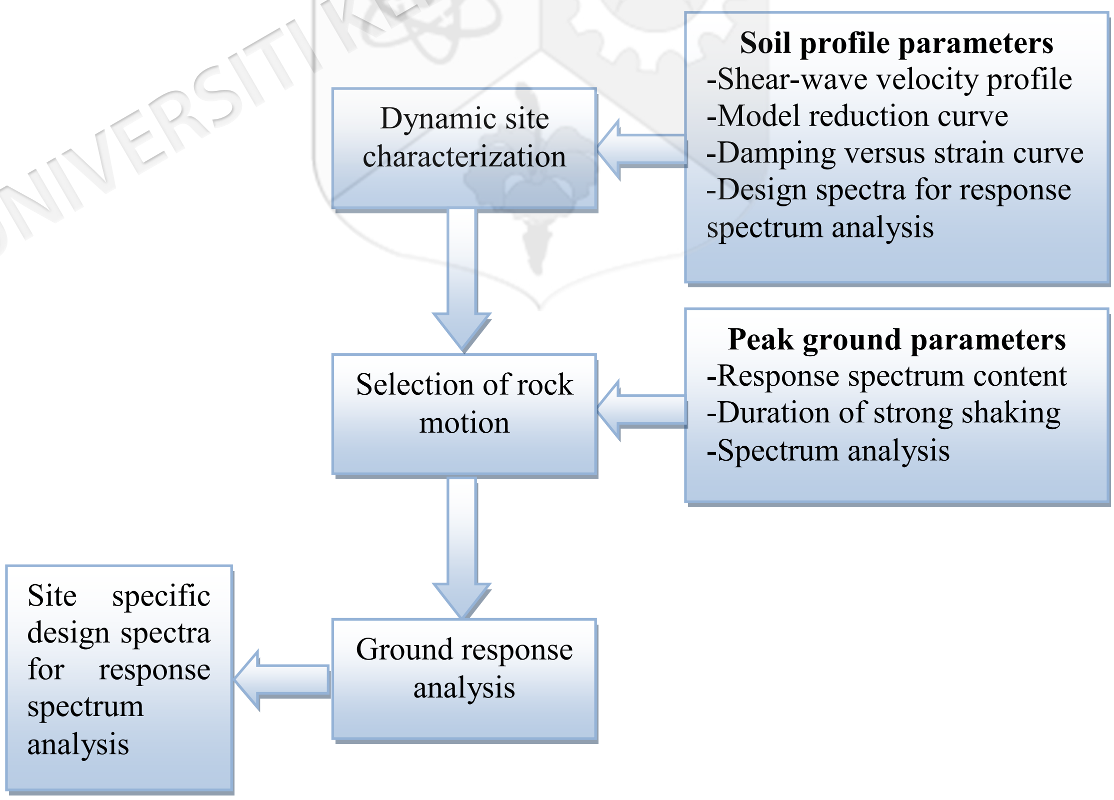

FIGURE 4.2 Site specific ground response analyses

If the soil layers are on an incline 3-Dimensional or 2-Dimensional methods should be used to analyze the dynamic site response. If the interfaces of soil layers are horizontal in all directions, 1-Dimensional finite element or wave propagation theory can be developed to analyze the dynamic response of soil deposit during an earthquake as shown in the Figure 4.3.

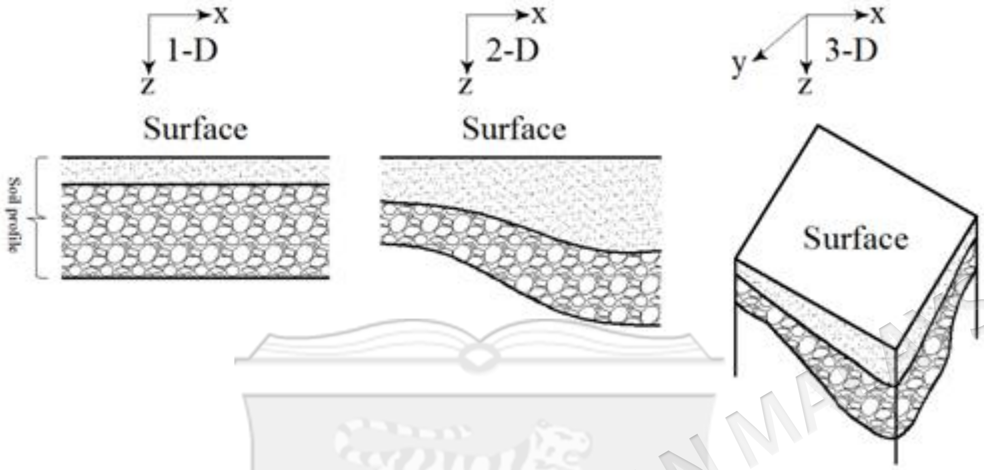

FIGURE 4.3 Subsurface geology could be referred as one-dimensional, two-dimensional or three-dimensional

Source: Smith 2001

Theory presented below only considers the soil deposits with horizontal interface for both convolution and de-convolution.

Currently, the 1-D finite element method is only used to determine the ground or any depth of soil deposit motion if bedrock motions are known. Finite element method can be solved for both linear and nonlinear problems. If the motion on ground surface or at any depth is known, 1-D wave propagation theory can be used to determine the bedrock motion or the motion at any other depth. 1-D wave propagation theory is only used for linear solution. For nonlinear solution, equivalent linear properties of the soils can be used (Schnabel et al. 1970; Idriss & Sun 1991).

An earthquake ground motion can be decomposed into the sum of a series of simple harmonic loading functions by using Fourier transform. The solutions for harmonic loading are available and used to compute the total response for a linear system based on the principle of superposition. The seismic function can be represented by sum of a finite of harmonic motions.

4.5 1D WAVE PROPAGATION THEORY

The seismic waves that propagate through the soil layers during earthquakes accrued and can affected any structures that constructed on the surface. The earthquake that accrued before such as Loma Prieta (1989) and Northridge (1994) has clarified the role of local site effects in modifying the characteristics of the motion data. It is well known that characteristic of soil layers can cause significant effects on the seismic excitation at bedrock through its propagating in the soil layers which is lead to a different effects on structures rested at the surface. Therefore, in the case of linear behaviour of the soil layers, it is assumed that the surface motion will be amplified proportionally to the input motion. Whilst, in the non-linear behaviour the soil will have a tendency to damp out the shaking energy for large amplitude motion. The nonlinear modifications of the artificial seismic excitation are conducted in this study through finite difference method software named NERA, which is based on one dimensional nonlinear site response analysis.

The stress-strain relationship can be represented in following expression for a Kelvin-Voigt model, shown in Figure 4.4:

$$\tau = G\gamma_s + \eta \frac{\partial \gamma}{\partial t} \tag{4.5}$$

where in Equation (4.5) τ is shear stress, γ_s is shear strain, and η is viscosity. Under harmonic motion, the shear strain can be written by

The one dimension system using thin element of a Kelvin-Voigt model is shown in Figures 4.4

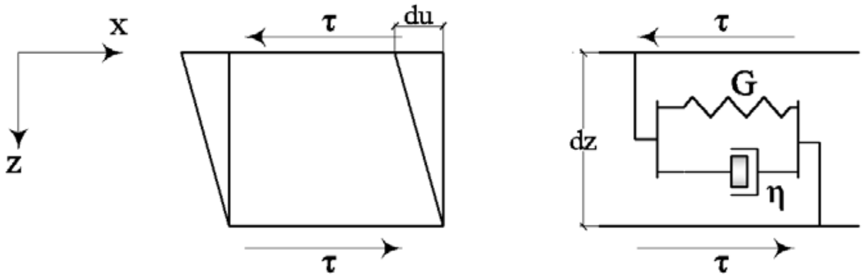

FIGURE 4.4 Thin element of a Kelvin-Vvoigt model subject to horizontal shearing

Source: Kramer 1996

In case of equivalent linear analysis in frequency domain analysis, the input motion is represented by the Fourier series and uses transfer functions for the solution of wave equations based on the principle of superposition so that the nonlinear stress-strain behaviour of soil is not allowed. The nonlinear behaviour of soil can be represented by the shear modulus reduction curve in which shear modulus depends on shear strain level. The actual nonlinear, inelastic behaviour of soil can be approximated by equivalent linear soil properties (Kramer, 1996). In the linear approach, shear modulus and damping factor are the constants in each soil layer and the equivalent values need to be determined, which are consistent with the level of strain induced in each layer during earthquake. For the transient motion of an earthquake, it is common to characterize the strain level in terms of an effective shear strain, which is usually taken as 65 percent of the peak strain.

In equivalent linear analysis, the iterative solution is employed. In the first solution, the shear strain and damping ration are calculated from zero shear strain. In the following iteration, effective shear strain is taken as 65 percent of peak shear strain and the shear modulus and damping ratio corresponding to effective shear strain are then use for the next iteration. This process is repeated until the effective shear strain does not change much from one iteration to the next.

4.6 EQUIVALENT VISCOUS DAMPING

Dynamic testing on soil indicated that the soil damping ratio associated with the area bounded by hysteretic stress-strain loops is essentially independent of cyclic frequency. In time domain analysis, which is used in soil-structure interaction analysis, only velocity-proportional viscous damping can be used in the form of dashpot embedded within the material elements (Kwok et al. 2007). Currently, the use of viscous damping in time domain analysis is not a convenient approximation in comparison to frequency domain analysis. Kwok et al. (2007) and Stewart and Kwok (2008) recommended the procedures for the specification of Rayleigh damping in time domain analysis using mode superposition method. There are two sources of viscous damping including modal damping ratio and viscous damping. Modal damping ratio is used in mode superposition, and viscous damping is used in direct method of solving the dynamic equilibrium equation. The selection of modal damping ratio are presented detail by Kwok et al. (2007).

Currently, there is no guideline for using viscous damping in direct method. In the following, recommended procedures for the specification of viscous damping will issues for current practice.

4.7 MAIN STEPS TO GENERATE AND EVALUATE THE GROUND MOTION

The main steps can be illustrated in Figure 4.5 which are:-

Step A:- Generate an artificial ground motion at the bedrock compatible with local response spectrum (bedrock of Kuala Lumpur) that conducted by SEER.

Step B: -Extract the amplification factor for the ground motion based on the soil profile and the ground motion conducted in **step A** using one dimension site response analysis.

Step C: - Extract the surface ground motion.

Step D: - Evaluate the local (Malaysian) response spectrum from the surface ground motion that conducted in **step C**

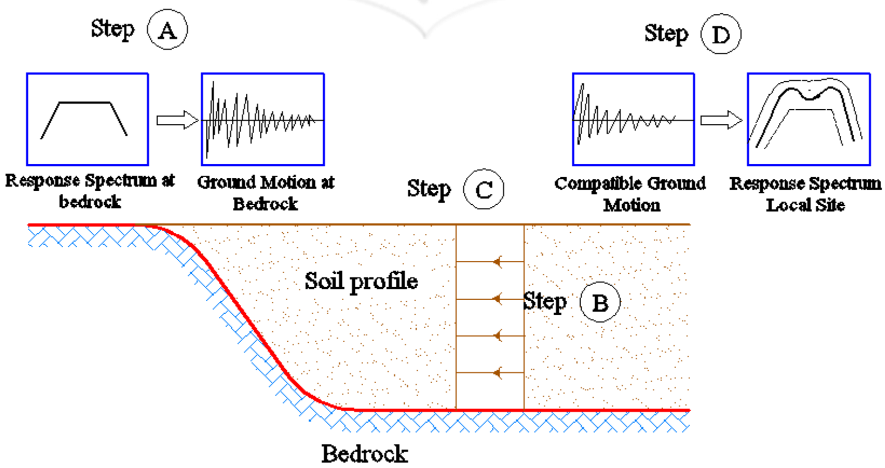

FIGURE 4.5 Main steps to generate and evaluate the ground motion

4.8 INPUT GROUND MOTION CHARACTERISTICS

The intent of selecting a suite of time-history is that the structure is analyzed by ground motions that are representative of what the structure could experience, with better compatible spectral values at these frequencies. It is also necessary that the spectra produced not significantly exceed the site-specific design response spectrum

.

A key requirement of the specification is the ability to withstand a seismic event consistent with a 1 in 2500 years return period, without loss of containment. This requirement has been interpreted as a 0.149g and ZPA earthquake (Figure 4.6), compatible with the Malaysia Hard Site response spectrum that conducted by SEER as shown in Figure 4.7

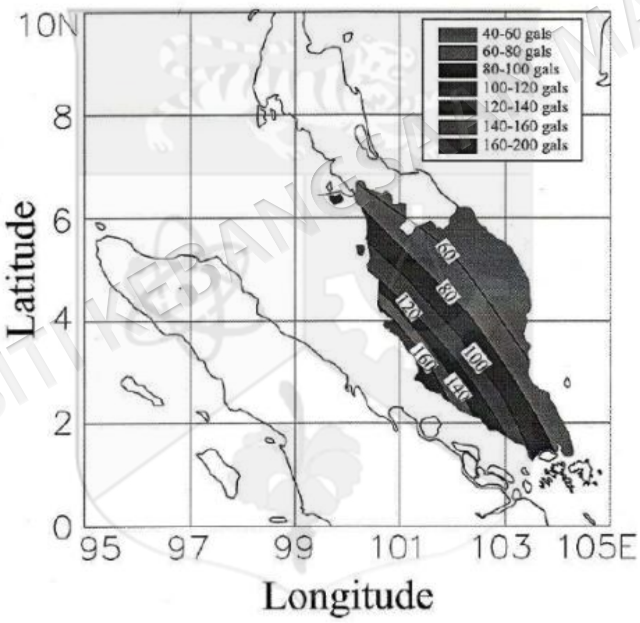

FIGURE 4.6 Macrozonation map for peninsular Malaysia for 2500 year return period

Source: JKR Seismic Design Guidelines 2007

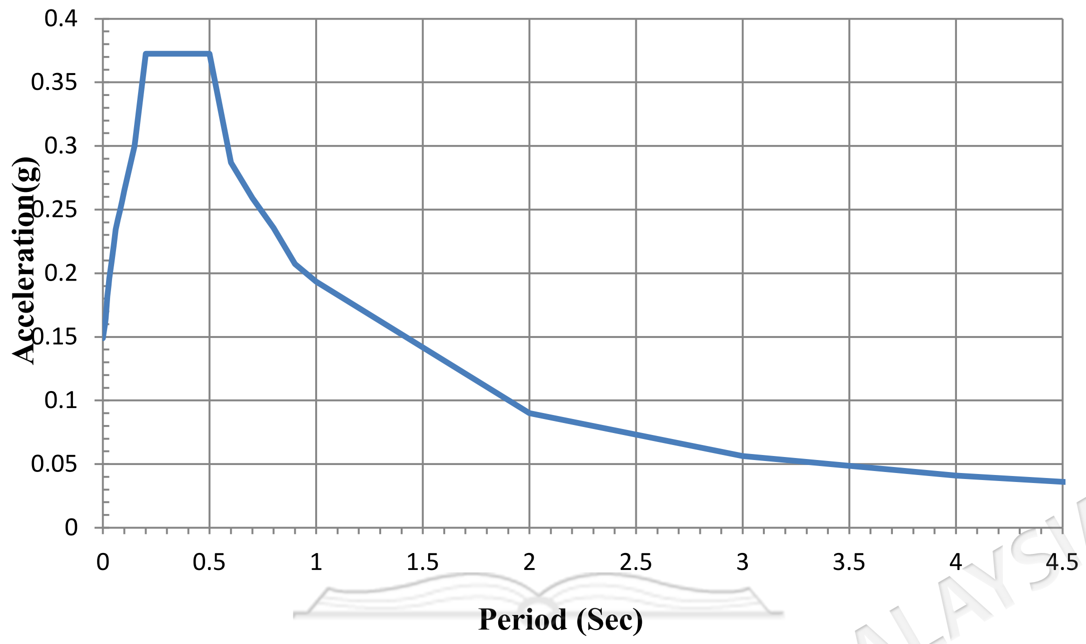

FIGURE 4.7 Target response spectrum conducted by SEER at bedrock of Kuala Lumpur (Azlan 2005)

4.9 GENERATION OF ARTIFICIAL GROUND MOTION

The generation of artificial ground motion using SIMQKE software and based on Gasparini and Vanmarcke approach as shown in flow chart is presented in Appendix II.

4.10.1 Properties of Generated Motions

To generate a suitable earthquake time-history that more compatible and identical with target response spectrum can only be generated if the program parameters and properties of an earthquake that affect the generated earthquake are chosen with height accuracy. Table 4.1 presented the parameters that influences from the characteristics of artificial earthquakes such as the power spectral density function, earthquake duration, maximum frequency ranges, and time intervals; and from the program parameters such as the iteration technique and frequency content to the generated earthquakes.

TABLE 4.1 Characteristics for earthquake generation

Characteristics	**Input values**
Target response spectrum	Reference (Azlan et al 2005)
Duration	20s
Peak Ground Acceleration (PGA)	0.149g
Frequency range	0.25 - 33.33 (Hz)
Intensity envelope function	A compound intensity envelope function (Jennings et al. 1968)
Generated response spectrum for damping	5%
Iteration number	6

With respect to the power spectral density function $G(\omega)$ derived from response spectrum (Figure 4.9), the generated $G(\omega)$ reasonably presents a typical spectral density function of a real earthquake in the case of damping $\xi = 0.05$. Artificial earthquake-like ground motion with duration ≤ 20 seconds should be considered to ensure the generated $G(\omega)$ on a typical form of real earthquakes and to leave the long-period structures enough time to perform steady-state response. The maximum frequency range of 0.2 Hz to a maximum frequency ≤ 33.33 Hz can be chosen for the generation of artificial earthquake, choosing this parameter is based almost on literature of earthquake engineering on the maximum frequency of real recorded earthquakes. The discretization interval in duration 0.02 of an artificial earthquake cannot be chosen freely but must be small enough in order to close describe the wave form and frequency content of the earthquake motion. Iteration number 1 to 6 cycles (seeds of random number as defaulted in the program), are used together to compatible the computed response spectrum with the response spectrum in an allowable tolerance.

It can be said again that suitable sets of artificial time-history (Figure 4.9) is obtained in the manner that their corresponding response spectra are well compatible with the target response spectrum,

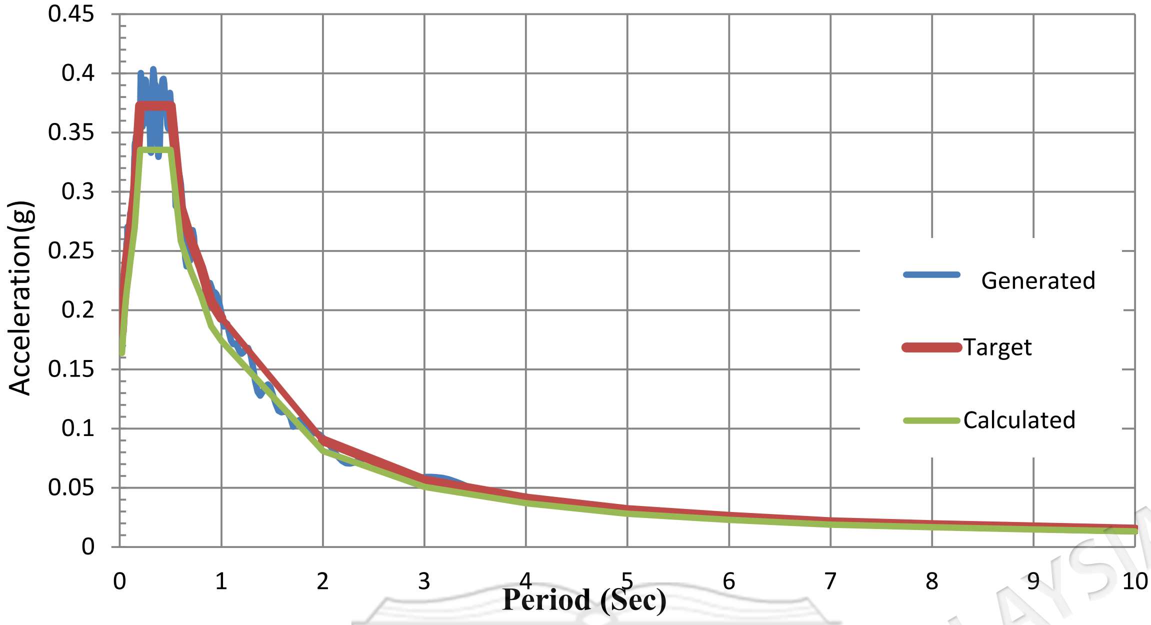

FIGURE 4.8 Target and calculated response spectrum at the bed rock of Kula Lumpur

From Figure 4.8 the compatibility between the computed response spectrum and the target one should not be expected to be convergent at all frequencies. The convergence at high frequency range is easiest to obtain even with no cycling technique used (Nguyen 2006), as the central frequency is located in this range. It will be enough to consider the artificial time-history if elevated concrete water tank to be analyzed having its fundamental periods in this area.

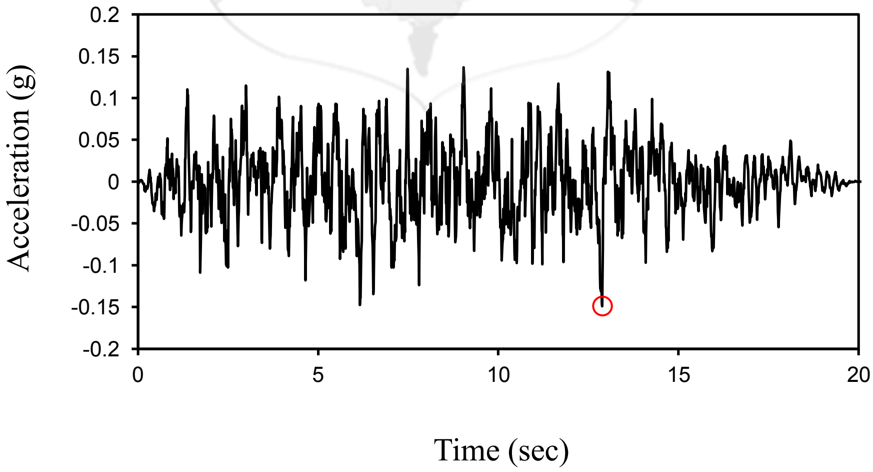

FIGURE 4.9 Numerical generation of artificial seismic motion compatible with target response spectrum of the bedrock of Kuala Lumpur

4.10 NONLINEAR LOCAL SITE EFFECT PARAMETERS

The determination of the model input ground motion representing the real site motion is a critical task for our analyses. For the appropriate use of the rock record of Kuala Lumpur earthquake in the case fixed base and SSI effect, the record needed to be modified to take into account the soil site-specific effects. To do so, the record then assigned as outcrop on the bedrock to the computer program NERA and the output taken within the top of the clay layer of NERA model

The artificial seismic excitation was assigned as outcrop on the bedrock to NERA model, and the output of ground motion shown in Figure 13 was taken within the top. Figure 4.11 and Figure 4.12 summarizes the soil profile and some selected parameters used for NERA runs. The flowing paragraphs are concerned on mathematical process of one dimensional wave propagation theory

The data of the soil profile (Figure 4.10) from the borehole collected as soil type, thickness of the soil layer and standard penetration test (SPT) are derived from a borehole located at Kuala Lumpur and Logistic Region located in the path where the smart tunnel being constructed. From the data, unit weight of each layer type and the shear wave velocity are determined.

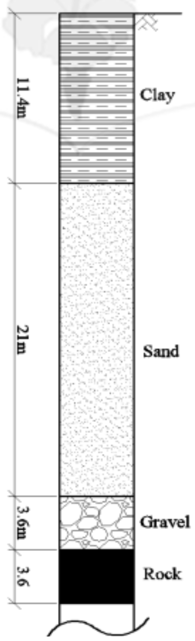

FIGURE 4.10 Soil profile collected

Several researchers have proposed correlations between G_{MAX} or v_s and N-STP, several parameters obtained from laboratory testing or in-situ testing. Numerous researchers have investigated the relationship between maximum shear modulus or shear wave velocity and N-value of Standard Penetration Test (SPT). Most of the studies were performed in Japan. Since then, some similar studies have been reported in the United States. Some of the correlations compiled by Barros (1991) are listed in Table 4.2

TABLE 4.2 Correlation between G_{MAX} or V_s and N-STP (Barros, 1991)

Reference	**Correlations** $\boldsymbol{G_{MAX}(Kpa)}$	**Correlations** $\boldsymbol{V_s(m/sec)}$	**Number of data**	**r**	**Soil type**
Ohsaki &Iwasaki (1973)	$G_{MAX} = 11500N^{0.8}$		220	0.89	All(Japan)
Ohta & Goto (1978)		$V_s = 85.3N^{0.341}$	289	0.72	All(Japan)
Imai & Tonouchi (1982)	$G_{MAX} = 14070N^{0.68}$		1654	0.87	All(Japan)
		$V_s = 96.9N^{0.314}$	1654	0.69	All(Japan)
Seed et al (1983)	$G_{MAX} = 6220N$				Sand (USA)
Sykora &Stokoe (1983)		$V_s = 101N^{0.29}$	229	0.84	Sand (USA)

In this study determination of Vs were calculated from N-SPT by estimating the average of two empirical formula that values based on two empirical formula that suggested by Olisaki and Iwasaki (1973), Imai and Tonouchi (1982). This approach is used based on the following reason:

1. The seismic tests were not sufficient either to develop a new empirical formula or to choose the most suitable formula for converting the N-value to vs.

2. The average value was used in order to cover the epistemic uncertainties due to this insufficient data.

3. Those two formulas were chosen because their coefficients of correlation are higher than Ohta and Goto (1978)

It is assumed that the soils are not susceptible to liquefaction during a seismic event. The full soil parameters profile are shown in Figure 4.11

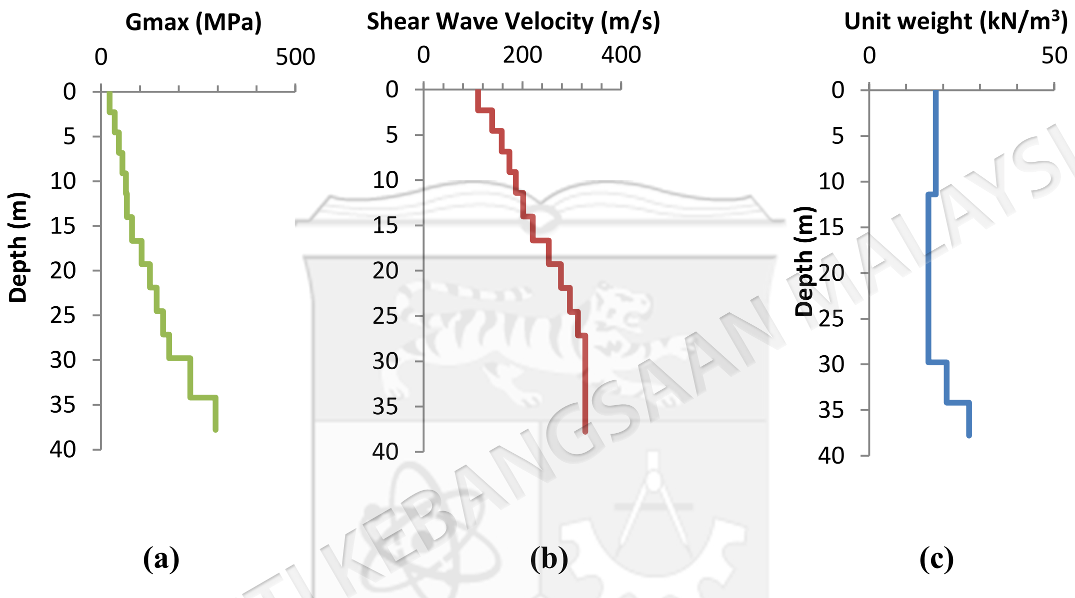

FIGURE 4.11 Parameters of soil profile at the site

In this study the soils dynamic characteristic assumed to be governed of modules reduction factor (G/G_{max}) and damping ration curves, as shown in Figure 4.12.

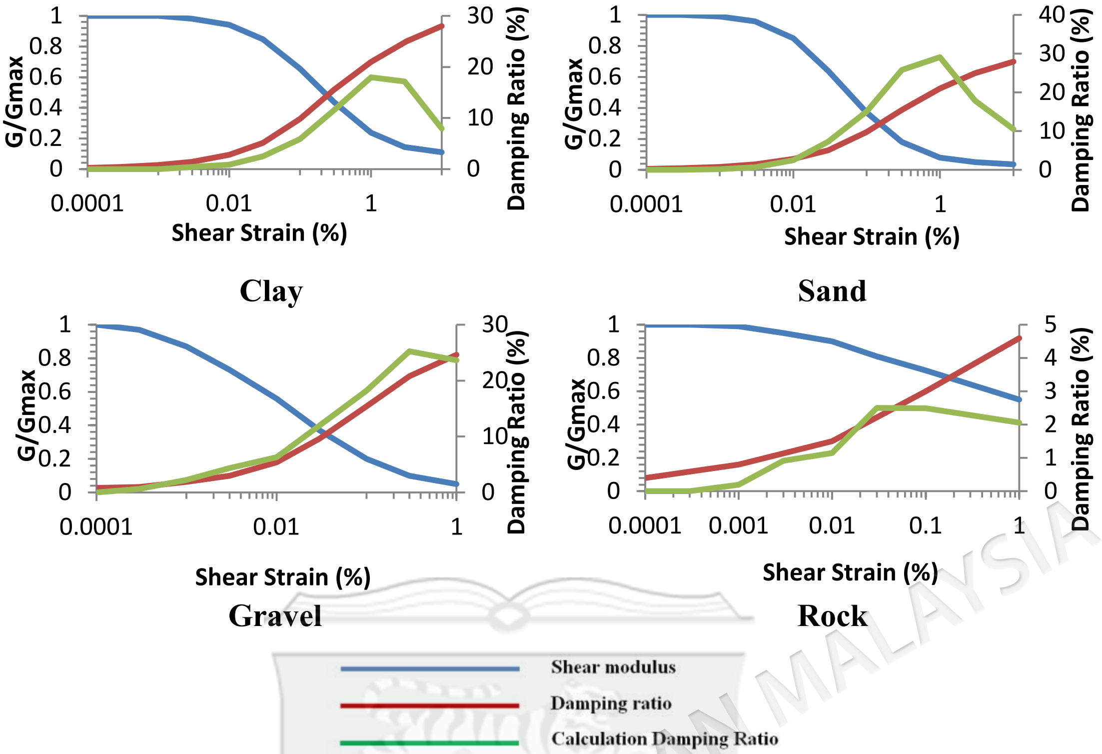

FIGURE 4.12 Material properties of the soil profile

The results of analysis in Figures 4.9 and Figure 4.13 where generally the accelerations at the bedrock were amplified on the surface by 30% which indicated that the selection of appropriate time histories is one of the most critical in ground response analysis. While the selection of time histories could change the results of accelerations at the surface significantly (refer to Appendix III for soil profile data)

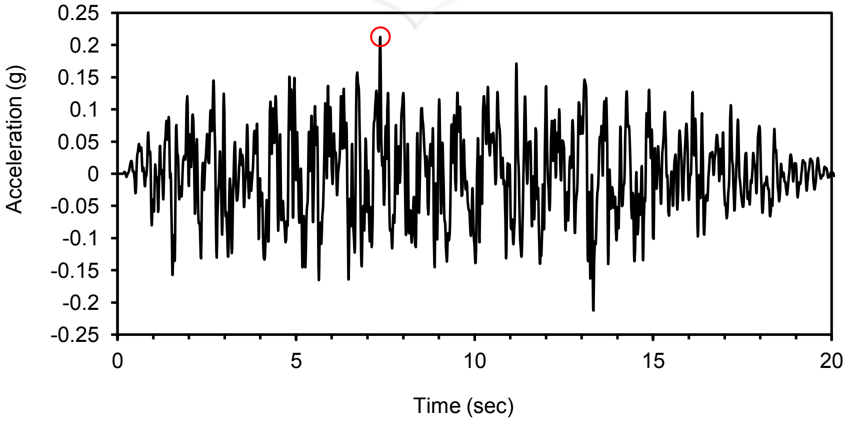

FIGURE 4.13 Output ground motion time history

Based on analysis, and according with UBC 97 for which average Vs for upper 100 feet of soil profile, Vs.30= 269 m/s (180-360), generally the site can be classified as stiff soil or site class D (Figure 4.14). Similarly in case of 4 m embedment that is shown in Figure 4.15

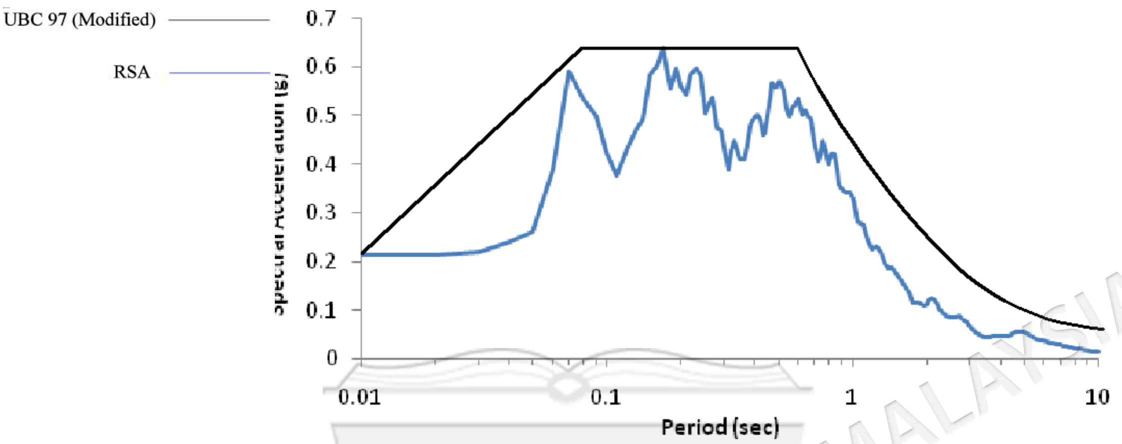

FIGURE 4.14 Period (s) Vs response spectrum acceleration (g) at surface (site class: D)

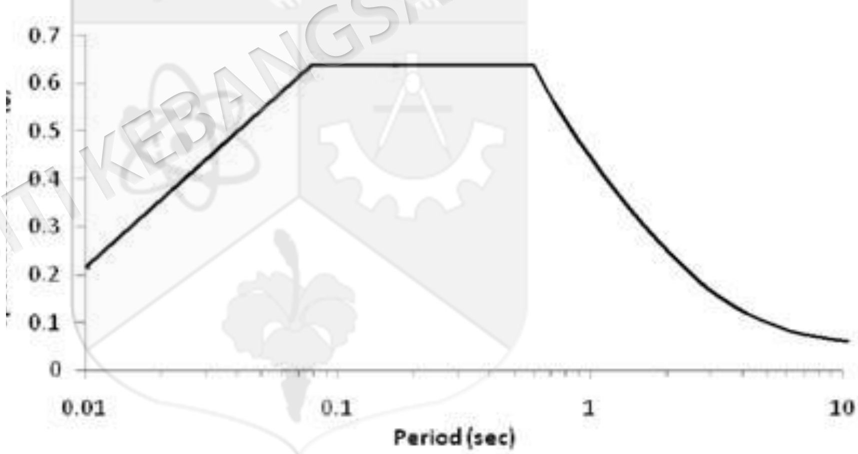

FIGURE 4.15 Period (s) Vs response spectrum acceleration (g) at 4 m of embedment (site class: D)

4.11 SUMMARY

In this chapter, a review of various theoretical aspects of the selection and scaling of earthquake ground motion, and focused on formulation of the Gasparini and Vanmarcke approach. This chapter also discussed the local site effect and one dimensional wave propagation theory. The ground motion time history characteristic and parameters used for inputting nonlinear local site effects were also discussed.

CHAPTER V

PARAMETERS IDENTIFICATIONS

5.1 INTRODUCTION

This chapter started with discussion in details the cases to be conducted in this study (mechanical and FEM models). Then the modal parameters identification of elevated tanks (circular and rectangular) in case of mechanical and FEM models are presented. The difficult tasks are identifying the SSI parameters (mesh size and time step) for which the identification of some parameters are still challenged especially in the case of nonlinear direct integration. This chapter shows the evaluating process of these parameters to obtain reasonable results.

5.2 CASES TO BE CONDUCTED IN THIS STUDY

In this study 96 cases are analyzed to cover the objectives, 12 mechanical models and 84 FEM models. The mechanical models analysis consists of SDOF and 2DOF models for case of embedment and no embedment. The following paragraphs described these cases started from Table 5.1 to Table 5.6 Where FV denoted free vibration method, RS denoted response spectrum method, TH denoted time history, and BC denoted boundary condition.

5.2.1 Cases of Mechanical Models with no Embedded (Circular and Rectangular)

Table 5.1 shows the mechanical models adopted in this study, with the case of the embedment is equal to zero. The models are categorized as two cases of SDOF and 2DOF in the case of fixed base and flexible foundation (SSI) as boundary conditions

(BC), for circular and rectangular tank. The dynamic analysis in this case performed in two steps namely 1) Free vibration (FV) and 2) response spectrum (RS).

TABLE 5.1 Cases considered for mechanical models with no embedment

esaC	ksy T knaC	Category	Analysis Type		FSI	BC	
			FV	RS		Fixed	SSI
1	r aCcuriC	SDOF	✓	✓	×	✓	×
2		SDOF	✓	✓	×	×	✓
5		2DOF	✓	✓	✓	✓	×
6		2DOF	✓	✓	✓	×	✓
3	r auuinacriC	SDOF	✓	✓	×	✓	×
4		SDOF	✓	✓	×	×	✓
7		2DOF	✓	✓	✓	✓	×
8		2DOF	✓	✓	✓	×	✓

5.2.2 Cases of Mechanical Models with Embedded (Circular and Rectangular)

Table 5.2 shows the cases of mechanical models adopted in this study with the case of the embedment equal to 4 m for both circular and rectangular tanks. The models are categorized as two cases of SDOF and 2DOF in the case of fixed base and flexible foundation for circular and rectangular tank. The same steps of dynamic analysis approaches are adopted FV and RS.

TABLE 5.2 Cases considered for mechanical models with embedment

esaC	ksy T kna C	Category	Analysis Type		FSI	BC	
			FV	RS		Fixed	SSI
13	r aCcuriC	SDOF	✓	✓	×	×	✓
14		2DOF	✓	✓	✓	×	✓
15	r auuinacriC	SDOF	✓	✓	×	×	✓
16		2DOF	✓	✓	✓	×	✓

5.2.3 Cases of FEM Models (Rectangular)

Table 5.3 and Table 5.4 shows FE cases (multi degree of freedom) of the rectangular tank adopted in this study in the case of no embedment and the embedment equal to 4m respectively. Due to the symmetrically of the rectangular tank considered, the seismic load is applied in one direction in cased of fixed base and flexible base. The same dynamic analysis steps adopted FV and RS plus time history (TH)

TABLE 5.3 Cases of FE models with no embedment for rectangular tank

Case	Analysis Type					FSI	BC	
	FV	RS	TH	LD	ND		Fixed	SSI
11	✓	✓	×	×	×	✓	✓	×
12	✓	✓	×	×	×	✓	×	✓
19	×	×	×	✓	×	✓	×	✓
20	×	×	×	×	✓	✓	×	✓

TABLE 5.4 Cases of FE models with embedment for rectangular tank

Case	Analysis Type					FSI	BC	
	FV	RS	TH	LD	ND		Fixed	SSI
17	✓	✓	×	×	×	✓	×	✓
21	×	×	×	✓	×	✓	×	✓
22	×	×	×	×	✓	✓	×	✓

5.2.4 Cases of FEM Models (Circular)

In these cases as shown in Table 5.5 and 5.6, in which: A is referred to stage A (In-situ Soil stresses +Structural Loading+ Seismic Loading), B is referred to (Structural Loading+ Seismic Load) and C referred to (Seismic Loading) Whilst, the analysis scheme approach used are NM is Newmark and HT is Helber Huge Taylor, and the seismic loads are applied at critical directions as mentioned in chapter III section 3.3.6

TABLE 5.5 Construction stage cases of circular tank with no embedment

Cases	Seismic load		Analysis Stages			Analysis Scheme		Direction		Analysis Type					FSI	BC	
	B	G	A	B	C	NM	HT	I	II	FV	RS	TH	LD	ND		Fixed	SSI
9	×	✓	-	-	-	-	-	-	-	✓	✓	×	×	×	✓	✓	×
10	✓	×	-	-	-	-	-	-	-	✓	✓	×	×	×	✓	×	✓
	✓	×	×	×	✓	✓	×	✓	×	×	×	×	✓	×	✓	×	✓
	✓	×	×	✓	✓	✓	×	✓	×	×	×	×	✓	×	✓	×	✓
	✓	×	✓	✓	✓	✓	×	✓	×	×	×	×	✓	×	✓	×	✓
	✓	×	×	×	✓	✓	×	×	✓	×	×	×	✓	×	✓	×	✓
	✓	×	×	✓	✓	✓	×	×	✓	×	×	×	✓	×	✓	×	✓
	✓	×	✓	✓	✓	✓	×	×	✓	×	×	×	✓	×	✓	×	✓
	✓	×	×	×	✓	×	✓	✓	×	×	×	×	✓	×	✓	×	✓
	✓	×	×	✓	✓	×	✓	✓	×	×	×	×	✓	×	✓	×	✓
23	✓	×	✓	✓	✓	×	✓	✓	×	×	×	×	✓	×	✓	×	✓
	✓	×	×	×	✓	×	✓	×	✓	×	×	×	✓	×	✓	×	✓
	✓	×	×	✓	✓	×	✓	×	✓	×	×	×	✓	×	✓	×	✓
	✓	×	✓	✓	✓	×	✓	×	✓	×	×	×	✓	×	✓	×	✓
	✓	×	×	×	✓	✓	×	✓	×	×	×	×	×	✓	✓	×	✓
	✓	×	×	✓	✓	✓	×	✓	×	×	×	×	×	✓	✓	×	✓
	✓	×	✓	✓	✓	✓	×	✓	×	×	×	×	×	✓	✓	×	✓
	✓	×	×	×	✓	✓	×	×	✓	×	×	×	×	✓	✓	×	✓
	✓	×	×	✓	✓	✓	×	×	✓	×	×	×	×	✓	✓	×	✓
	✓	×	✓	✓	✓	✓	×	×	✓	×	×	×	×	✓	✓	×	✓
	✓	×	×	×	✓	×	✓	✓	×	×	×	×	×	✓	✓	×	✓
	✓	×	×	✓	✓	×	✓	✓	×	×	×	×	×	✓	✓	×	✓
24	✓	×	✓	✓	✓	×	✓	✓	×	×	×	×	×	✓	✓	×	✓
	✓	×	×	×	✓	×	✓	×	✓	×	×	×	×	✓	✓	×	✓
	✓	×	×	✓	✓	×	✓	×	✓	×	×	×	×	✓	✓	×	✓
	✓	×	✓	✓	✓	×	✓	×	✓	×	×	×	×	✓	✓	×	✓

TABLE 5.6 Construction stage cases of circular tank with embedment

Cases	Seismic load		Analysis Stages			Analysis Scheme		Direction		Analysis Type					FSI	BC	
	B	G	A	B	C	NM	HT	I	II	FV	RS	TH	LD	ND		Fixed	SSI
18	✓	×	-	-	-	-	-	-	-	✓	✓	×	×	×	✓	×	✓
	✓	×	×	×	✓	✓	×	✓	×	×	×	×	✓	×	✓	×	✓
	✓	×	×	✓	✓	✓	×	✓	×	×	×	×	✓	×	✓	×	✓
	✓	×	✓	✓	✓	✓	×	✓	×	×	×	×	✓	×	✓	×	✓
	✓	×	×	×	✓	✓	×	×	✓	×	×	×	✓	×	✓	×	✓
	✓	×	×	✓	✓	✓	×	×	✓	×	×	×	✓	×	✓	×	✓
	✓	×	✓	✓	✓	✓	×	×	✓	×	×	×	✓	×	✓	×	✓
	✓	×	×	×	✓	×	✓	✓	×	×	×	×	✓	×	✓	×	✓
	✓	×	×	✓	✓	×	✓	✓	×	×	×	×	✓	×	✓	×	✓
25	✓	×	✓	✓	✓	×	✓	✓	×	×	×	×	✓	×	✓	×	✓
	✓	×	×	×	✓	×	✓	×	✓	×	×	×	✓	×	✓	×	✓
	✓	×	×	✓	✓	×	✓	×	✓	×	×	×	✓	×	✓	×	✓
	✓	×	✓	✓	✓	×	✓	×	✓	×	×	×	✓	×	✓	×	✓
	✓	×	×	×	✓	✓	×	✓	×	×	×	×	×	✓	✓	×	✓
	✓	×	×	✓	✓	✓	×	✓	×	×	×	×	×	✓	✓	×	✓
	✓	×	✓	✓	✓	✓	×	✓	×	×	×	×	×	✓	✓	×	✓
	✓	×	×	×	✓	✓	×	×	✓	×	×	×	×	✓	✓	×	✓
	✓	×	×	✓	✓	✓	×	×	✓	×	×	×	×	✓	✓	×	✓
	✓	×	✓	✓	✓	✓	×	×	✓	×	×	×	×	✓	✓	×	✓
	✓	×	×	×	✓	×	✓	✓	×	×	×	×	×	✓	✓	×	✓
	✓	×	×	✓	✓	×	✓	✓	×	×	×	×	×	✓	✓	×	✓
26	✓	×	✓	✓	✓	×	✓	✓	×	×	×	×	×	✓	✓	×	✓
	✓	×	×	×	✓	×	✓	×	✓	×	×	×	×	✓	✓	×	✓
	✓	×	×	✓	✓	×	✓	×	✓	×	×	×	×	✓	✓	×	✓
	✓	×	✓	✓	✓	×	✓	×	✓	×	×	×	×	✓	✓	×	✓

5.3 PARAMETERS OF MODAL PROPERTIES OF CIRCULAR AND RECTANGULAR TANKS

In this case the parameters of modals properties exhibited in Table 5.7 are used in the analysis of the elevated tanks for both case of mechanical and FEM according to methodology presented in Chapter III section 3.2.

TABLE 5.7 Model properties of circular and rectangular tank

Parameter	Circular	Rectangular
m_c	$112.5\ Ton$	$579.0\ Ton$
m_i	$373.1\ Ton$	$808.0\ Ton$
K_c	$450\ N/m$	$1420\ N/m$
K_s	$17800\ N/m$	$5200\ N/m$

5.4 IDENTIFICATION PARAMETERS OF THE ALTERNATIVE MASSES DISTRIBUTED.

As shown in Figure 5.1, the distribution of masses that suggested by authors are placed at level of center of gravity of the empty container of elevated tank in both cases circular and rectangular in the FE models. The impulsive mass are divided to six cases (4, 8, 16, 24, 48 and model number six the impulsive mass distributed equally along the walls of elevated tanks). The values of suggested impulsive masses for each model are presented in Table 5.8 for rectangular and circular tanks.

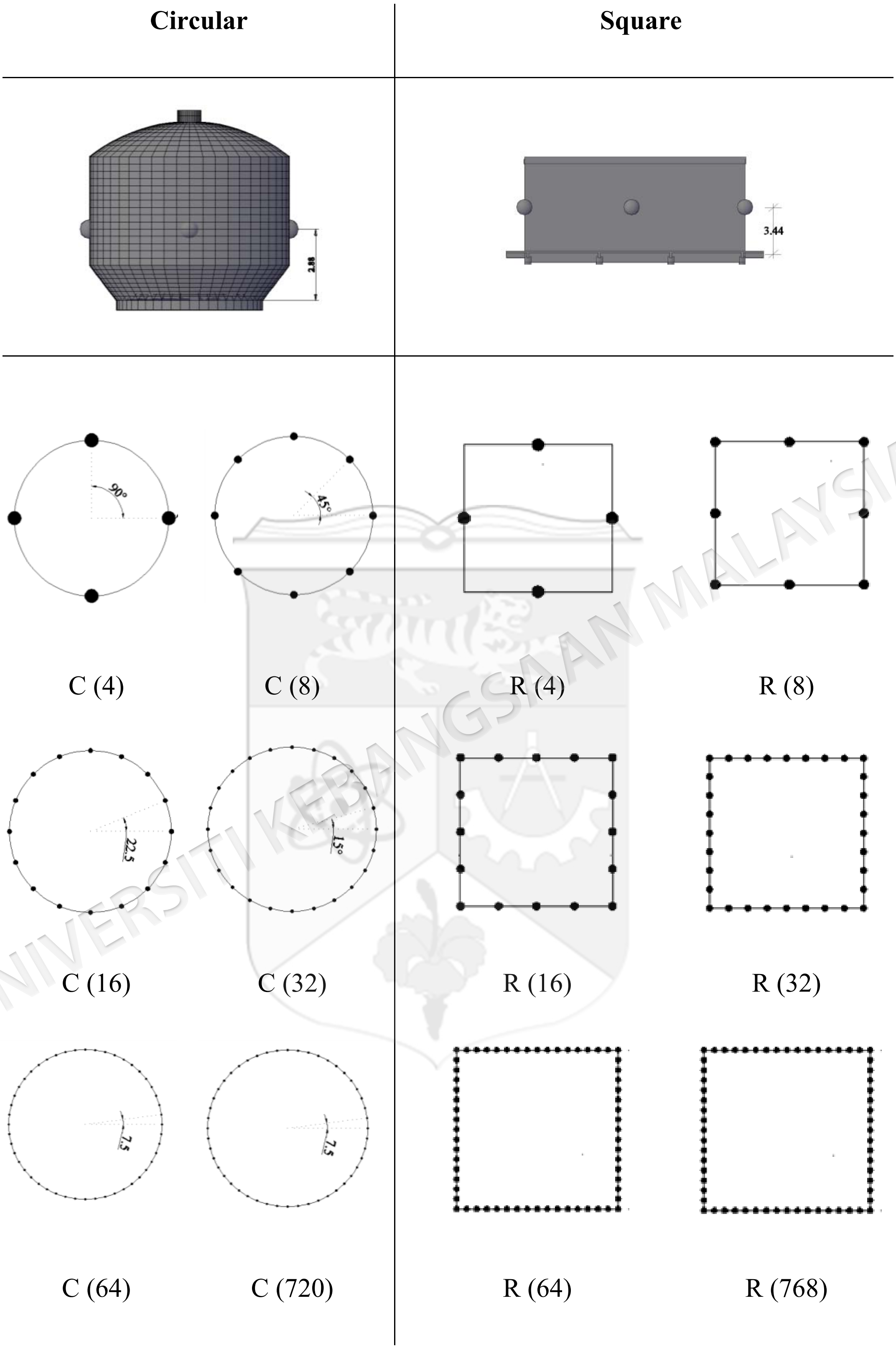

FIGURE 5.1 Alternative masses distribution in case of circular and rectangular tanks.

TABLE 5.8 Model parameters modification of impulsive mass rectangular and circular elevated tank

Models	Impulsive mass Circular (Ton)	Models	Impulsive mass Rectangular (Ton)
C(4)	35.15	R (4)	168.89
C(8)	17.58	R (8)	84.45
C(16)	8.79	R (16)	42.22
C(32)	5.86	R (32)	21.11
C(64)	2.93	R (64)	10.56
C(720)	0.18	R (768)	0.938

5.5 PARAMETER IDENTIFICATIONS FOR FEM LINEAR AND NON-LINEAR DIRECT DYNAMIC ANALYSIS

In order to obtain an effective solution for seismic response, or a non-linear dynamic response in particular, it is important to choose an appropriate time integration scheme. This choice mainly depends on the parameters including integration solution, time step and FEM mesh. Therefore, this section is concerned about the selection of these parameters. The aims is to choose a set of suitable parameters which will give reasonable results for practical purposes and significantly reduce the computational efforts for large number of analyses required in this study.

5.5.1 Finite Element Mesh

The selection of an appropriate FE mesh size especially for top soil layer at vertical direction and the choice of an effective integration scheme for the response solution are closely related and must be considered together. The mesh should be able to capture the highest significant modes upon which the integration scheme is operating. In this study, several pilot runs were done in order to decide the best mesh size to be used for the analysis in order to integrate accurately the response up to the third mode of vibration. Consequently, the basic FE mesh that shown in Figure 5.2 is chosen

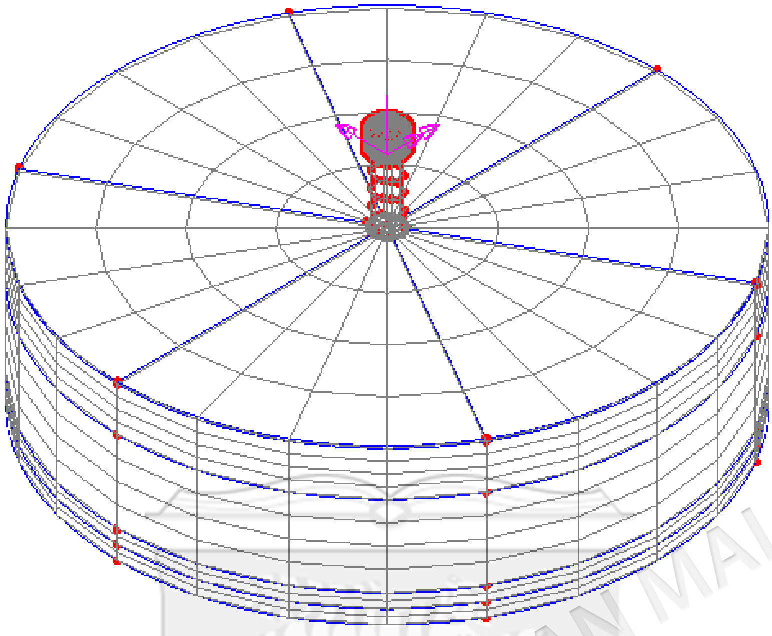

FIGURE 5.2 Mesh size adopted in this study for SSI

5.5.2 Integration Solution

In this study, the scheme of explicit is not used in order to avoid the use of small time steps which must be always smaller than a critical time step while in the implicit scheme, the time steps can generally be much greater than the explicit critical time step. Moreover, the implicit algorithm is generally used for inertial problems where the response is governed by the low frequency components, i.e. seismic response, as it has been considered the most effective (Bathe 1982; Beshara and Virdi 1991). In addition, it is of our interest to perform an iteration technique for each time step within the implicit scheme. As well as for non-linear dynamic response, especially under earthquake loading, which is highly path-dependent, then the analysis of a non-linear dynamic problem stringently requires iteration at each time step in order to obtain accurate results (Bathe 1982)

In this study, therefore, the implicit Newmark's (Newmark 1959) and Hilber Hughes Taylor (Hilber et al. 1977) approaches are employed

Where α, β and γ are parameters of the Newmark and Hilber Hughes Taylor methods as shown in Table 5.9 and Figure 5.3. If α, β and γ are chosen properly and the time step is small enough and representative of current practice for the implicit scheme, it can ensure the result is a good approximation to the actual dynamic response of the elevated tank under consideration.

The Hilber-Hughes-Taylor parameters α, β and γ can be varied to obtain optimum stability and accuracy. The integration scheme is unconditionally stable provided that $2\gamma \geq \alpha \geq 0.5$ and according to Bathe (1982), the optimal choice is presented in $\gamma = 0.25(\alpha + 0.5)^2$, therefore, in this study, the parameters presented in Table 5.7 and Figure 5.3 are chosen in order to obtain integration with good accuracy and unconditional stability as well as some numerical damping to damp out spurious numerical oscillations (Wood 1990). If $\alpha = 0$ this family of algorithms reduces to the Newmark family.

TABLE 5.9 Integration scheme parameters chosen for circular and rectangular tanks

Parameter	Newmark	Hilber-Hughes-Taylor
γ	0.6	0.6
β	0.25	0.3025
α	0.0	-0.1

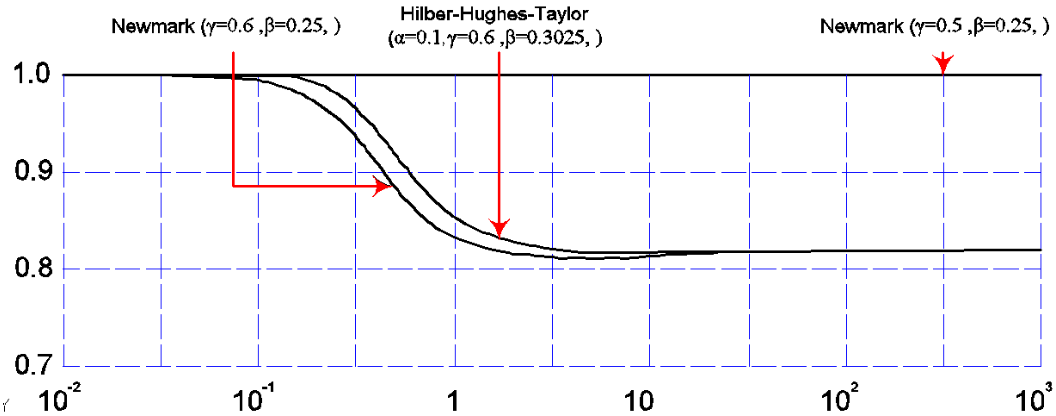

FIGURE 5.3 Spectral radii without structural damping

5.5.3 Time Step Used

With a proper choice of parameters, this algorithm is unconditionally stable, i.e. the error for any initial conditions does not grow without bound for any time step size Δt. However, time step size could be limited due to accuracy considerations.

First of all, for dynamic analyses, the response of higher modes includes time of impulsive mode, convective mode and third mode, may in some cases need to be considered. If the time step is greater than the limiting time step, the higher modes will not be integrated accurately. To accurately integrate all the relevant higher modes, the time step would need to be less than the limiting value for the highest mode considered. However, there is no exact value for the limiting time step but rather a range of values. The size of the ideal time step cannot be identified as it would depends on the actual accuracy required. For linear elastic systems, a time step of about $\Delta t = \left(\frac{1}{10} - \frac{1}{20}\right) T_n$ is used. In which T_n is the period of the highest structural mode required in the study.

It seems to be a good rule of thumb to ensure reasonably accurate numerical results (Bathe 1982, Chopra 1995). Theoretical limits on the time step required for stability of the solution have not been determined for non-linear systems and there is no guidance on the limiting time step required for non-linear analysis. However, as the issue concerned is about how well the shape of the oscillating motion is represented by the time stepping scheme, one could safely assume that there is no difference in this aspect for linear or non-linear analysis therefore the same limiting time step is assumed in this study. Furthermore, when postulating how the higher modes may influence the solution, the frequency content of earthquake loading should be considered (Bathe 1982). Assuming the maximum frequency contained in the earthquake loading is $\grave{f}_{max}$, the maximum frequency of the modes that may influence the solution are generally given as $f_{max} \cong 4\acute{f}_{max}$, and therefore the time step can be chosen to be $\Delta t < 0.5/f_{max}$ for the SDOF systems (Bathe 1982, LUSAS Manual 2007).

Finally, the time step also depends on the size of the finite element mesh (Bathe 1982, Pal 1998). Simply, the time step can be chosen as $\Delta t < T_n/\pi$ (Bathe 1982). Therefore, a time step size in the range of $\Delta t = \left(\frac{1}{10} - \frac{1}{20}\right) T_n$, and $0.5/f_{max}$ and T_n/π will be investigated in this study.

From the eigenvalue analysis of the circular elevated tank presented in Table 5.10, and Appendix IV (mode shapes) and the values of the natural frequency obtained are from the first 30 modes associated with the corresponding periods.

The maximum frequency of the artificially generated earthquake is $\grave{f}_{max} =$ 33.33Hz (see Table 4.1). Therefore, it depends upon which higher modes are considered in this study, the time step size is assume to be chosen accordingly with reference to $\Delta t = \left(\frac{1}{10} - \frac{1}{20}\right) T_n$, T_n/π and $0.5/f_{max}$. For the consideration of $0.5/f_{max}$, the limiting time step size is about 0.02 s. The time step size chosen accordingly with reference to $\Delta t = \left(\frac{1}{10} - \frac{1}{20}\right) T_n$ and T_n/π for the first sixth modes is shown in Table 5.10 and Table 5.11. In this study, a time step size of 0.02 s is chosen after many pilot runs with different time step sizes as shown in Figure 5.4 (Appendix V), (these value of time step is also tested to be used for rectangular tank). Although this time step is slightly larger than the time step $\Delta t = \left(\frac{1}{10} - \frac{1}{20}\right) T_n$, for capturing the sixth mode and $0.5/f_{max}$ for the frequency content of earthquake, it is chosen in order to reduce the computational effort required for the analyses. However, we will show that this time step is able to capture the tank responses with a reasonable accurate solution up to the sixth mode.

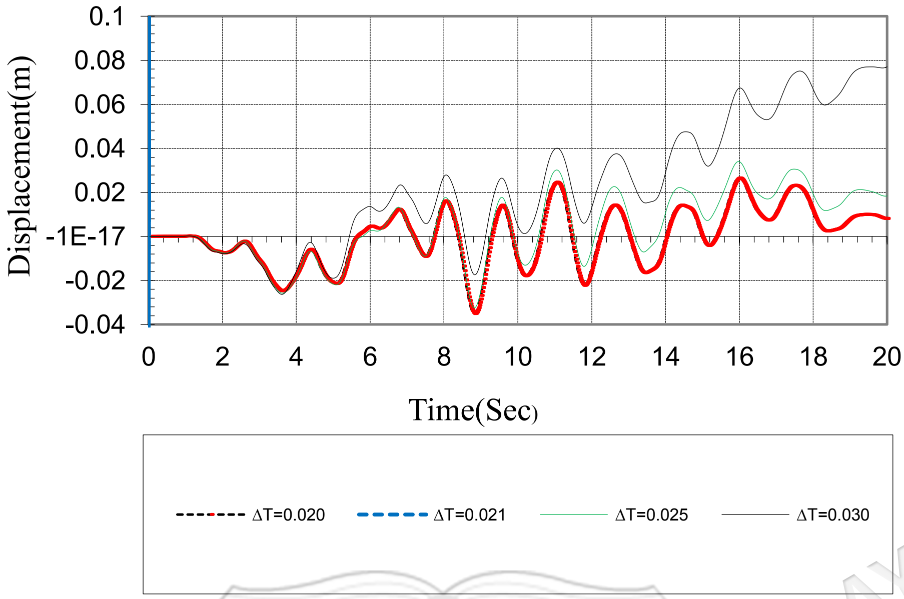

FIGURE 5.4 Convergence of time steps for circular tank

5.5.4 Viscous Damping Ratio

In this study, the value of viscous damping is assumed to be 0.05 for most of RC structures (Priestley et al. 1996; Wilson 2002) and the two natural circular frequencies adopted in the above calculation are 0.32 Hz and 1.77 Hz which is the first two fundamental frequencies obtained from the eigenvalue analysis. Thus the values of ξ and ω can be calculated from Figure 3.25 to be 0.075 and 3.16E-05, respectively. The characteristics of Rayleigh damping also same procedure for rectangular tank

It should be noted that ξ and ω (mentioned in Chapter III section 3.4.4) are constants set of equations, can be solved through model superposition. Such an assumption leads to a constant damping ratio for entire system, which is not usually pertinent to soils, whose damping depends strongly on the development of share strains and may vary abruptly over the geometrical domain of integration. For this reason, and when the shear strains are lower than the threshold value, a variable damping solution can be adopted, in which the Rayleigh assumption holds good.

5.5.5 Fourier Analysis

The Fourier analysis is also used to transform the seismic excitation data and results from the time domain to frequency domain. In analysing the elevated water tank under dynamic loading, the frequency response of the tank is usually regarded to be very important because it tells us how much response at a particular frequency is present in the time domain. In this study, the results obtained from the time stepping dynamic analysis are transformed into the frequency domain using this analysis. The following equation is used for the Fourier analysis.

The responses in frequency domain are obtained by transforming the acceleration responses using a MATLAB program. The program incorporated a built function for fast Fourier Transforms.

5.6 PERFORMING STATIC ANALYSIS

After evaluating all parameters that contributed significantly in the analysis of elevated concrete water tank, a static analysis is performed in two stages of analysis as following :-

Stage-1:- performing the static analysis to evaluate the state of stresses at the soil before the tank is constructed (in-situ soil stresses) as shown in Figure 5.5. The results are under self weight of the soil profile in which the load applied at gauss points (stress point) of the HX8 elements. The results stresses vary from zero to 1000 $\mathrm{KN/m^2}$ before the earthquake occurred.

Stage-2:- performing the static analysis to evaluate the state of stresses at the soil after the tank is constructed as shown in Figure 5.6. The results are under self weight of the soil profile + the self weight of elevated tank including the water in the container. The varying of stresses results are changed due to the placing of elevated tank

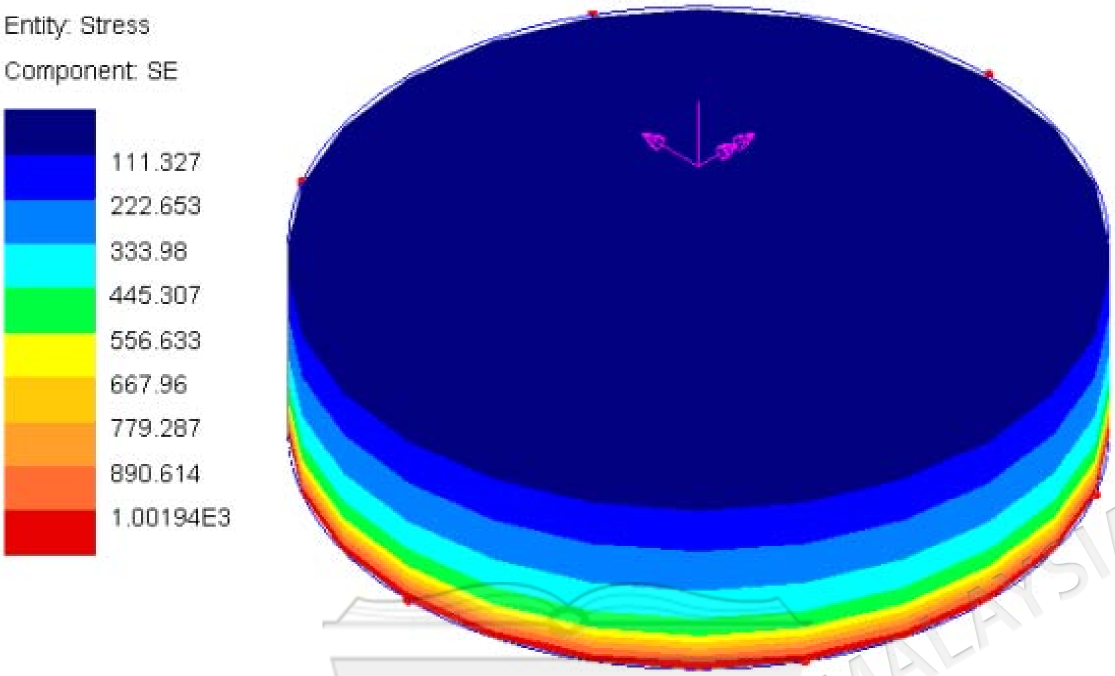

FIGURE 5.5 State of stress results in the soil before the tank constructed (KN/m^2)

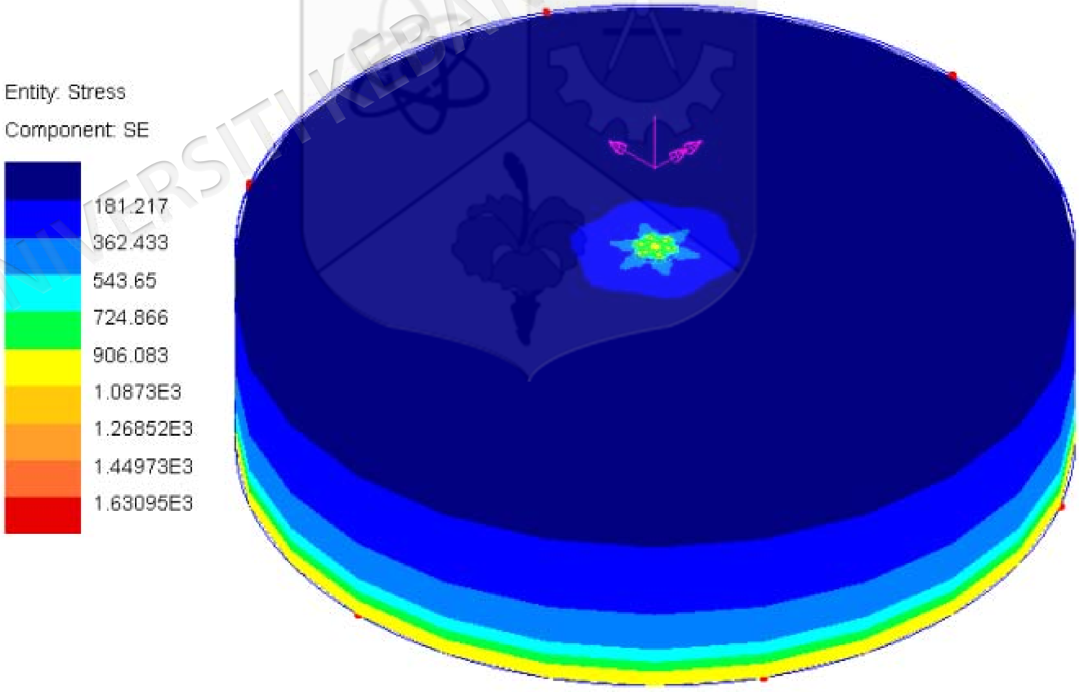

FIGURE 5.6 State of stress in the soil after the circular tank constructed (KN/m^2)

5.7 SUMMARY

This chapter discussed to the identification parameters to be used in this study and stated with defining the cases and to be conducted in this study, then presented its parameters of modal properties for circular and rectangular tanks. This chapter also presented identification parameters of the alternative masses distributed to be used in the FEM models, parameter identifications for FEM in case of linear and non-linear direct dynamic analysis. The identification of FE mesh, integration solution, and time step were also discussed. And performing of static analysis before moving to dynamic analysis was also conducted.

CHAPTER VI

ANALYSIS, RESULTS AND DISCUSSIONS

6.1 INTRODUCTION

After obtaining and examining the parameters to be used in this study, started from modal parameters of model properties of elevated tanks (rectangular and circular), the static analysis for static force equilibrium then the analyses continued with the dynamic studies. In this chapter, the results of 3-D dynamic numerical analyses in the forms of i) acceleration, ii) displacement, iii) strain, iv) stress and v) pore pressure are presented as well as the results of mechanical models in case of single and two degrees of freedom, the results then are used for comparisons with finite elements method. The results are presented in cases of embedment and with no embedment.

This chapter also presents the results of the alternative modification to Westergaard approach in the case of rectangular and circular elevated concrete water tank in clustered bar charts form. The results on the effects of the time history response of circular elevated concrete tank along the highest level of the tank passed on nonlinear direct dynamic analysis (step by step) are also presented in case of two dynamic scheme that mentioned before in case of embedment and no embedment.

Construction stages effects on the analysis of elevated concrete water tank (displacements, shear force at the base of the tank, axial force) are also presented in this chapter. The results of the circular elevated concrete water tank drafts at eight levels presents as in case of fixed and SSI effects are presented in case of two analysis scheme in case of embedment and no embedment. After these results a new frame work and instructions are obtained and presents to be used by engineers.

6.2 CASES OF MECHANICAL MODELS BASED ON SDOF (RESPONSE SPECTRUM)

The results of the fundamental period (T_i), base shear (V_{base}) and overturning moment (M_o) based on response spectrum method with assumption of no embedment in the case of circular elevated concrete water tank is given in Table 6.1 in which case-1 presented with K_s, L, and M_i. Whilst the results of case-2 with the SSI effects included its parameters K_θ and K_x are also presented in Table 6.1 .The same analysis are also carried out for rectangular tank of case-3 and case-4 .The results are presented in Table 6.2 with calculation of V_{base} and M_o based on and free vibration response spectrum method.

TABLE 6.1...Results obtained from SDOF (circular with no embedment)

Case-1				**Case-2**			
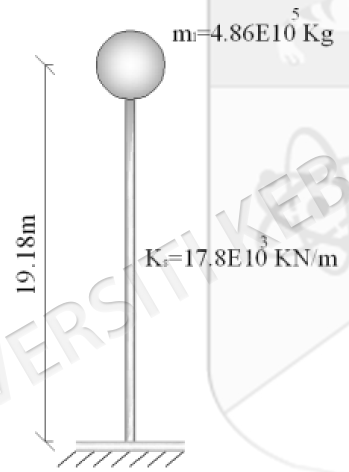				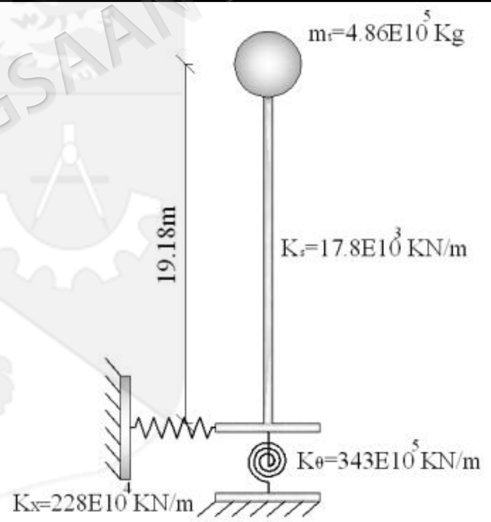			
Fixed				**SSI**			
Ti (Sec)	Tc (Sec)	Shear (KN)	Moment (KN.m)	Ti (Sec)	Tc (Sec)	Shear (KN)	Moment (KN.m)
1.038	-	92	1772	1.085	-	91	1753

TABLE 6.2 Results obtained from SDOF (rectangular with no embedment)

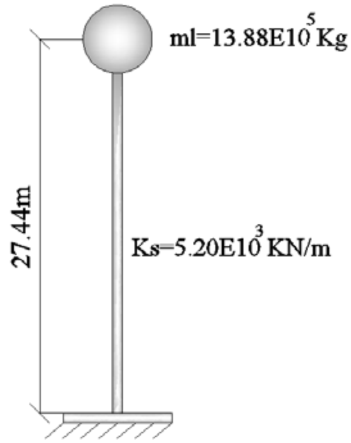

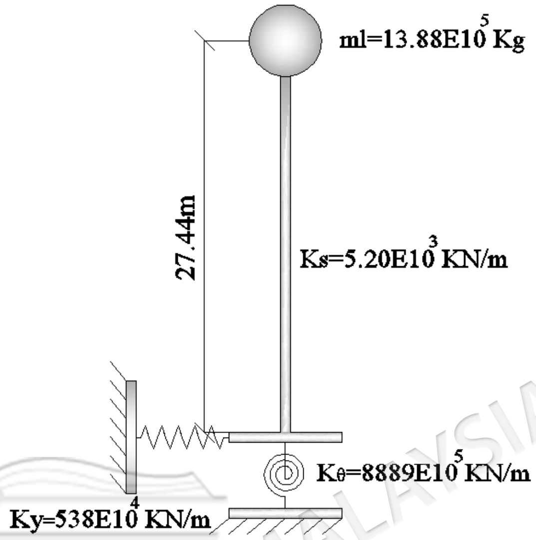

Case-3				Case-4			
Fixed				SSI			
Ti (Sec)	Tc (Sec)	Shear (KN)	Moment (KN.m)	Ti (Sec)	Tc (Sec)	Shear (KN)	Moment (KN.m)
3.240	-	95	2626	3.245	-	92	2546

6.3 CASES OF MECHANICAL MODELS BASED ON TWO DOF (RESPONSE SPECTRUM)

Table 6.3 shows the results of case-5 and case-6 for circular tank with assumption of embedment equal to zero. Both cases were idealized based on two DOF with FSI consideration in which carries same parameters of K_c and m_c Whilst for case-6, the results are obtained based on SSI assumptions with the parameters of K_θ and K_x The same technique and procedure were carried out for case-7 and case-8 The results are shown in Table 6.4 in which calculations of V_{base} and M_o were based on free vibration and response spectrum.

TABLE 6.3 Results obtained from two DOF (circular with no embedment)

Case-5				Case-6			
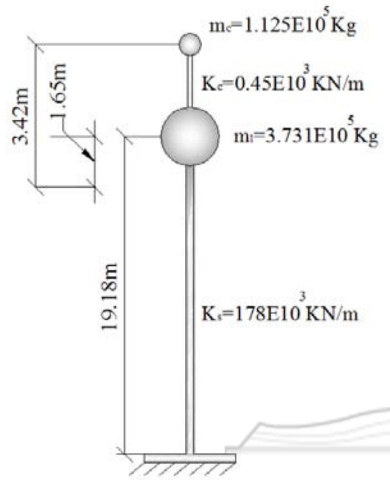				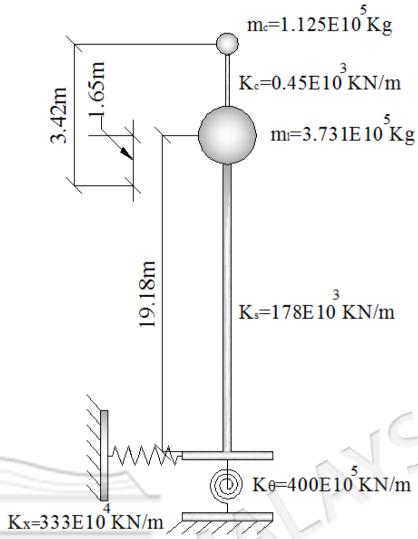			
Fixed				**SSI**			
Ti (Sec)	Tc (Sec)	Shear (KN)	Moment (KN.m)	Ti (Sec)	Tc (Sec)	Shear (KN)	Moment (KN.m)
0.900	3.140	82	1581	0.941	3.140	78	1517

TABLE 6.4 Results obtained from two DOF (rectangular with no embedment)

Case-7				**Case-8**			
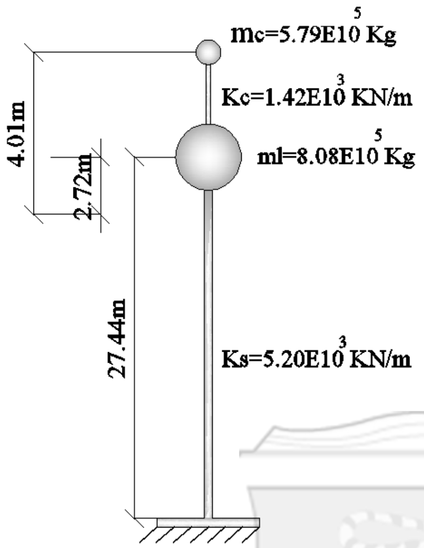				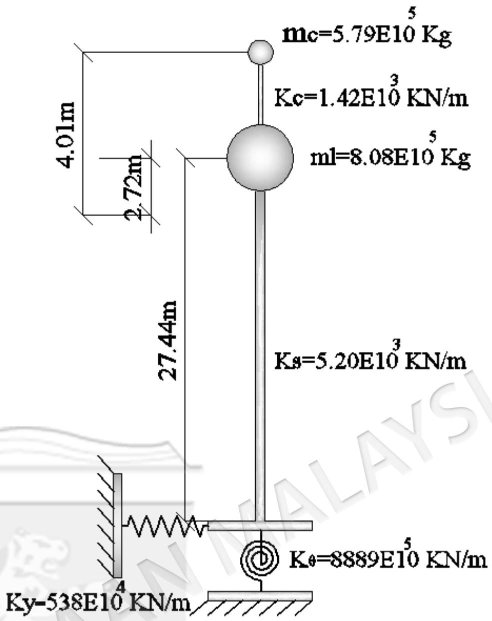			
Fixed				**SSI**			
Ti (Sec)	Tc (Sec)	Shear (KN)	Moment (KN.m)	Ti (Sec)	Tc (Sec)	Shear (KN)	Moment (KN.m)
2.20	4.01	89	2463	2.203	4.01	89	2448

6.4 CASES OF FINITE ELEMENTS METHOD (RESPONSE SPECTRUM)

Extending the calculations from two DOF to multi DOF and based on 3D-FE, Table 6.5 shows the results of case-9 which is based on fixed base approach. The results of T_c, T_i, V_{base} and M_o of the circular elevated tank through response spectrum analysis method were calculated with consideration of the FSI effects using added mass approach Westergaard. Same data were calculated for cases-10 but based on 3D SSI consideration with assumptions of the embedment equal to zero. Table 6.6 shows the same parameters with different values for rectangular tank and the results presented was carried out based on assumptions of embedment equal to zero.

TABLE 6.5 Results obtained from FEM (circular with no embedment)

Case-9				**Case-10**			
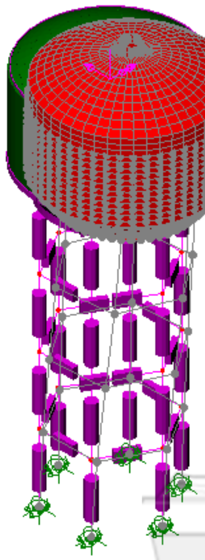				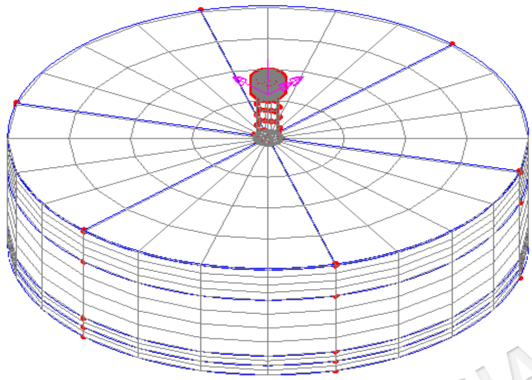			
Fixed				**SSI**			
Ti (Sec)	Tc (Sec)	Shear (KN)	Moment (KN.m)	Ti (Sec)	Tc (Sec)	Shear (KN)	Moment (KN.m)
0.98	3.14	75	1452	1.02	3.14	72	1388

TABLE 6.6 Results obtained from FEM (rectangular with no embedment)

Case-11				**Case-12**			
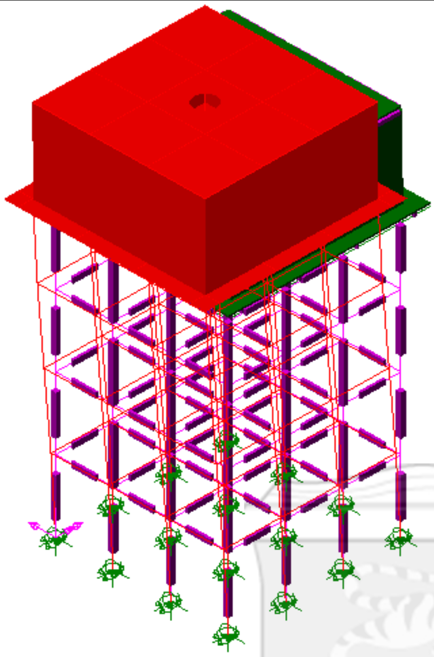				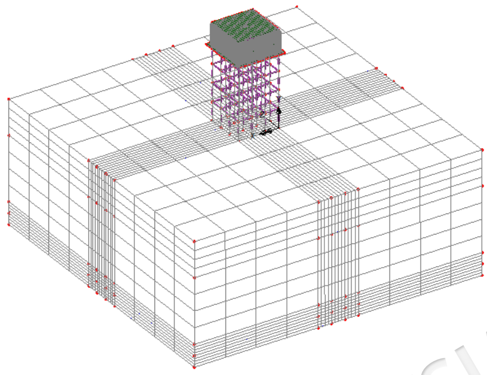			
Fixed				**SSI**			
Ti (Sec)	Tc (Sec)	Shear (KN)	Moment (KN.m)	Ti (Sec)	Tc (Sec)	Shear (KN)	Moment (KN.m)
2.274	3.98	81	2250	2.275	3.98	80	2228

6.5 CASES OF MECHANICAL MODELS SDOF AND 2DOF CASE OF EMBEDMENT (RESPONSE SPECTRUM)

Table 6.7 shows the results of case-13 for circular tank with assumption of embedment equal to 4m. Both cases were idealized based on SDOF and two DOF for case-13 and case-14 respectively, in which carries same parameters of K_s, K_θ and K_x .The results are shown in Table 6.7 in which calculations of V_{base} and M_o were based on free vibration and response spectrum.

TABLE 6.7 Results obtained from SDOF and two DOF (circular with embedment)

<table>
<tr><th colspan="4">Case-13</th><th colspan="4">Case-14</th></tr>
<tr><td colspan="4">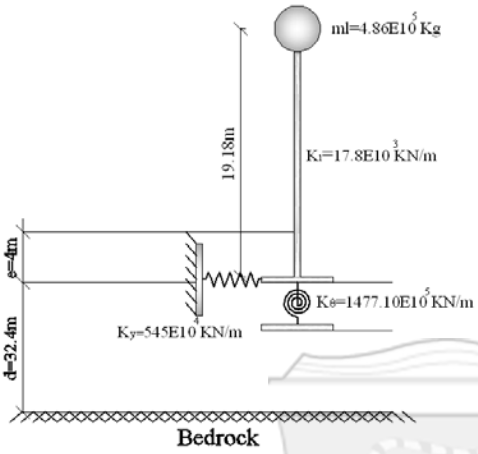
</td><td colspan="4">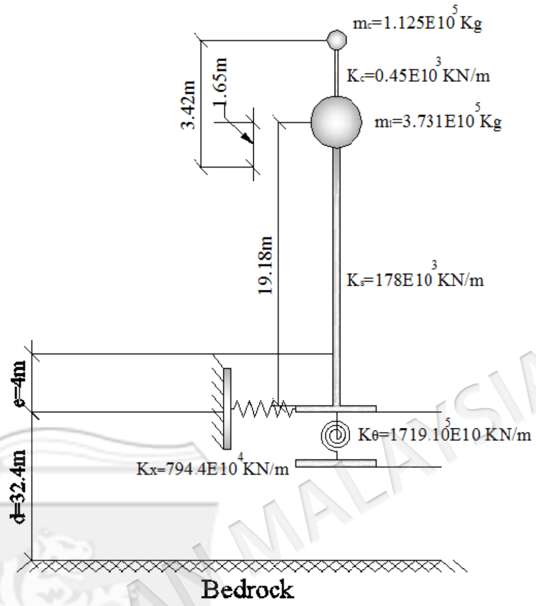
</td></tr>
<tr><td colspan="4">SSI</td><td colspan="4">SSI</td></tr>
<tr><td>Ti (Sec)</td><td>Tc (Sec)</td><td>Shear (KN)</td><td>Moment (KN.m)</td><td>Ti (Sec)</td><td>Tc (Sec)</td><td>Shear (KN)</td><td>Moment (KN.m)</td></tr>
<tr><td>1.051</td><td>-</td><td>86</td><td>1659</td><td>0.90</td><td>3.14</td><td>85</td><td>1641</td></tr>
</table>

TABLE 6.8 Results obtained from SDOF and two DOf (rectangular with embedment)

Case-15

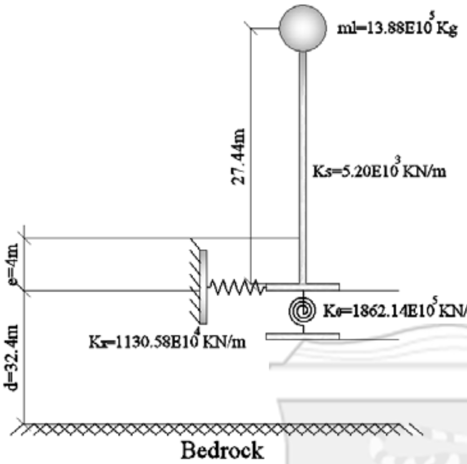

Case-16

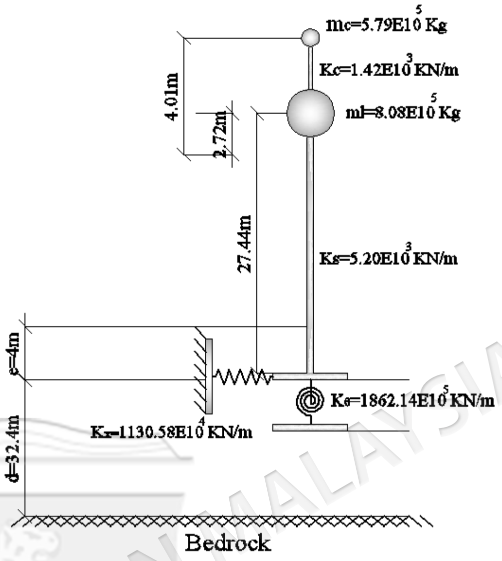

Case-15				**Case-16**			
SSI				**SSI**			
Ti (Sec)	Tc (Sec)	Shear (KN)	Moment (KN.m)	Ti (Sec)	Tc (Sec)	Shear (KN)	Moment (KN.m)
3.257	-	91	2475	2.212	4.01	88	2400

6.6 CASES OF FINITE ELEMENT IN CASE OF EMBEDMENT (RESPONSE SPECTRUM)

Extending the calculations from two DOF to multiple DOF and based on 3D-FE, Table 6.9 shows the simulation results of T_c, T_i, V_{base} and M_o for rectangular elevated tank case-17. The analysis was carried out based on SSI assumptions through free vibration and response spectrum with FSI consideration using added mass approach Westergaard. The same data was also used and calculated for case-18 of rectangular elevated tank. Both of cases 17 and 18 were embedment to 4m.

TABLE 6.9 Results obtained from FEM in case of linear and (circular and rectangular with embedment)

Case-17				Case-18			
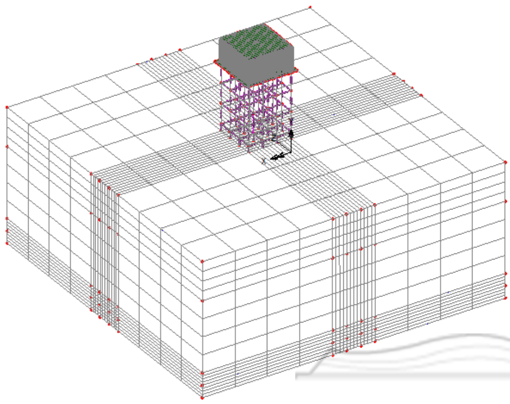				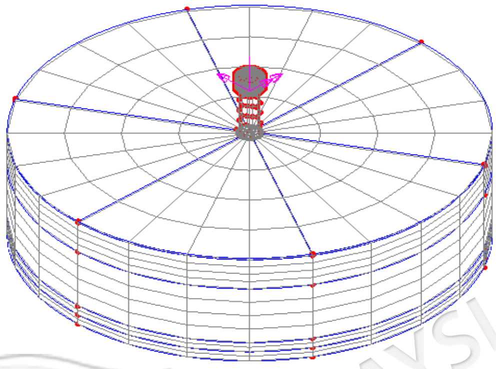			
SSI				SSI			
Ti (Sec)	Tc (Sec)	Shear (KN)	Moment (KN.m)	Ti (Sec)	Tc (Sec)	Shear (KN)	Moment (KN.m)
2.271	3.98	84	2307	0.92	3.14	67	1299

6.7 CASES OF FINITE ELEMENT METHOD (TIME HISTORY)

Table 6.10, Table 6.11, Table 6.13 and Table 6.14 shows the results of base shear (V_{base}) and overturning moment (M_o) respectively based on implicit time history analysis for circular and rectangular elevated concrete water tank. The simulation results ware obtained through FEM approaches with assumption of no embedment (Table 6.10) and with embedment (Table 6.11)

TABLE 6.10 Results obtained from FEM in case of linear nonlinear (rectangular with no embedment)

Case-19		Case-20	
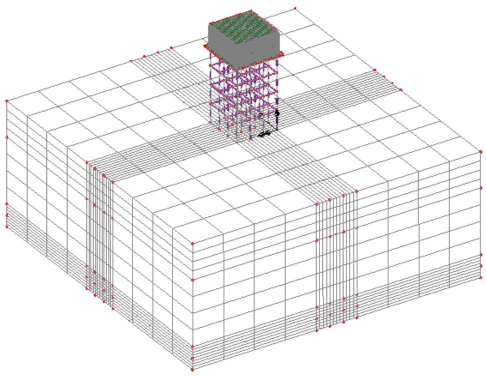		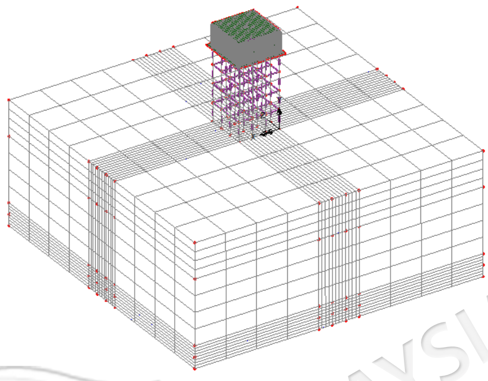	
SSI-Linear		**SSI-Nonlinear**	
Shear (KN)	Moment (KN.m)	Shear (KN)	Moment (KN.m)
78	2113	77	2101

TABLE 6.11 Results obtained from FEM in case of linear and nonlinear (rectangular with embedment)

Case-21		Case-22	
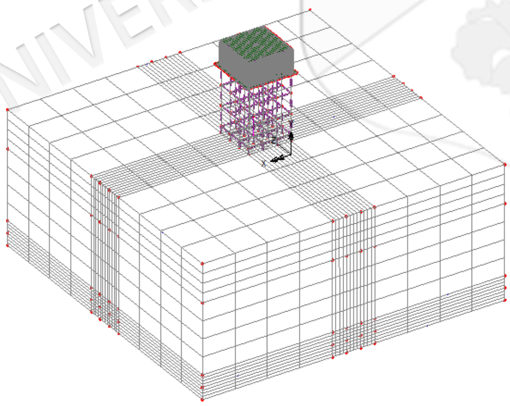		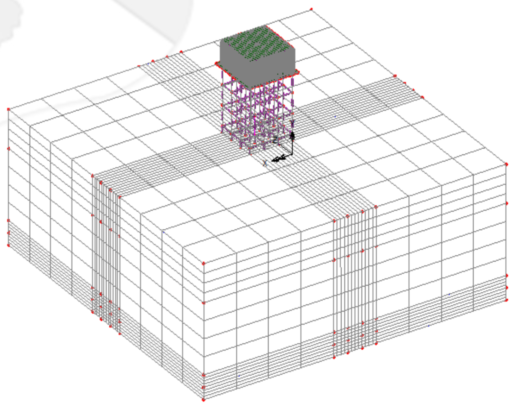	
SSI-Linear		**SSI-Nonlinear**	
Shear (KN)	Moment (KN.m)	Shear (KN)	Moment (KN.m)
77	2120	76	2099

TABLE 6.12 Results obtained from FEM in case of linear and nonlinear (circular with no embedment)

Case-23		Case-24	
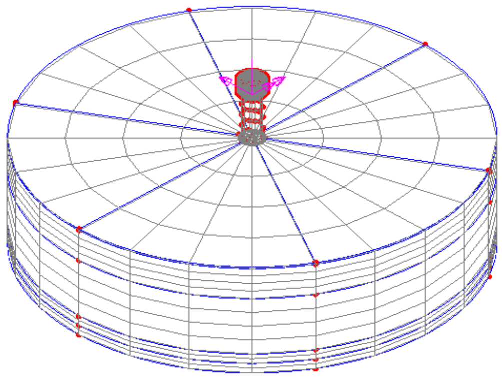		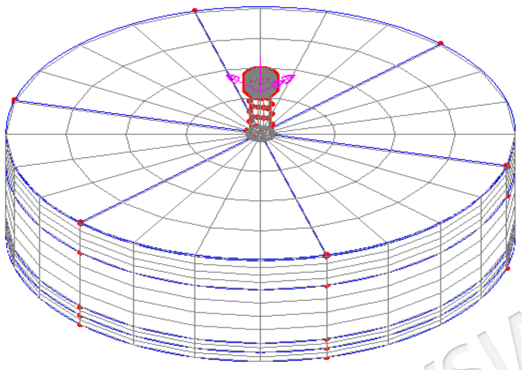	
SSI-Linear		**SSI-Nonlinear**	
Shear (KN)	Moment (KN.m)	Shear (KN)	Moment (KN.m)
71	1364	67	1316

Table 6.13 Results obtained from FEM in case of linear and nonlinear (circular with embedment)

Case-25		Case-26	
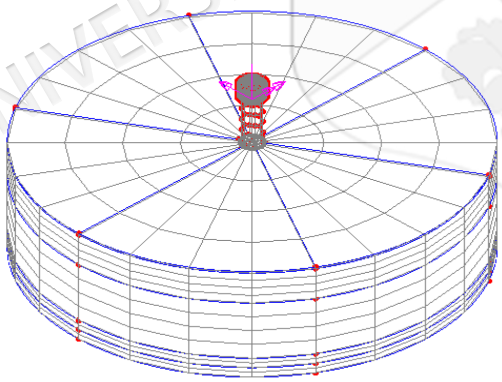		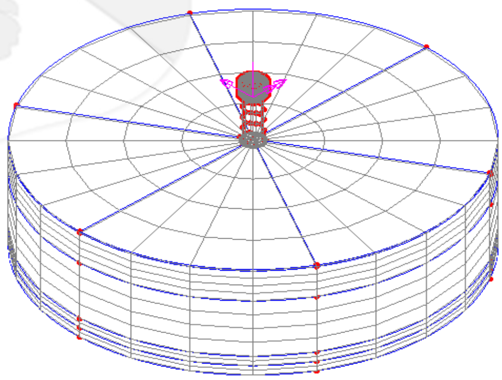	
SSI-Linear		**SSI-Nonlinear**	
Shear (KN)	Moment (KN.m)	Shear (KN)	Moment (KN.m)
66	1277	63	1231

6.8 ANALYSIS OF THE RESULTS (CIRCULAR AND RECTANGULAR TANK)

The following sections described and discussed the deviations of periods of impulsive and convective modes and forces (overturning moments and shear forces) created at the base of elevated tanks and their effects due to the idealization of elevated tank.

SSI effects are expected to bring about a reduction the longitudinal direction in the induced base shear and due to that the overturning moment in case of linear and nonlinear analysis (Seed, 1986). Wiliest the decreased as the foundation embedment increased SSI may produce either reduction of the base shear, depending on soil parameters (Livaoglu, 2007).

6.8.1 Period of Impulsive Mode

As shown in Figure 6.1 and in the case of elevated rectangular water tank, the results indicated that T_i for SDOF based on fixed base approach is 3.24 sec .Whilst small increment was around %1 due to consideration of SSI effects. In case of two DOF idealization and due to redistributions of the tank mass (two-DOF idealization), T_i has decreased abruptly by 32% and including of SSI consideration also affect T_i by less that 1%. In case of FEM simulation with multiple DOF T_i is remarkably far from SDOF and also relatively from two DOF (7%). Even for the case of SSI consideration, T_i gets small affects for FEM idealization.

The significant of these results are by considering SSI affects for the stiff soil in case of SDOF, two-DOF and FEM having minor effects to the T_i in which it can be ignored with acceptable losing in accuracy of results for this shape of typical elevated tank, but T_i based on SDOF instead to two DOF and FEM idealizations despite the ease of implement still unacceptable.

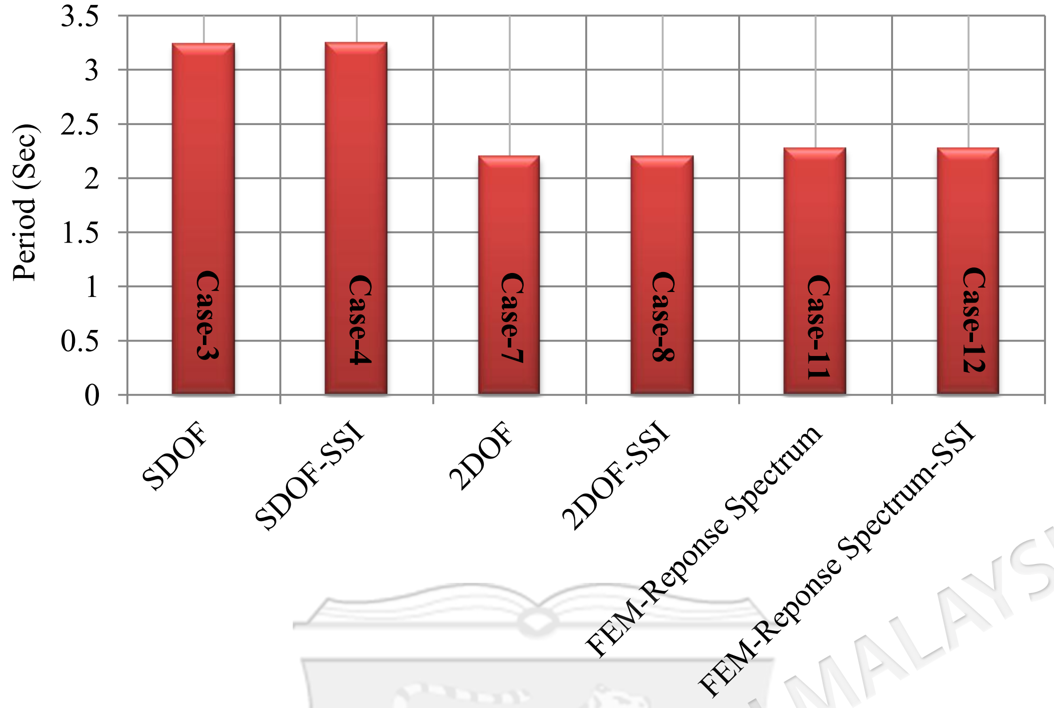

FIGURE 6.1 Periods of impulsive mode of the rectangular elevated tank

In the case of circular elevated concrete water tank and as shown in Figure 6.2, for SDOF T_i is given as 1.038 sec which is remarkably less than T_i in case of rectangular tank (because the stiffness of rectangular tank staging is remarkably higher tank the stiffness of staging in circular tank) and with SSI consideration the value of T_i significantly increased about 4.50%. In case of two DOF, T_i is obtained 0.9 sec and significantly increased for 4.55% due to SSI effects, similarly in case of FEM. The variation of using two DOF instead to SDOF affected T_i by 13.3% and 13.27% for SSI consideration respectively and in case of using FEM instead to SDOF affects T_i by 5.58% and, 5.60% due to SSI consideration. Through FEM simulation had significantly effects T_i by -8.88% and,-8.40 for SSI consideration when compared to 2DOF simulation.

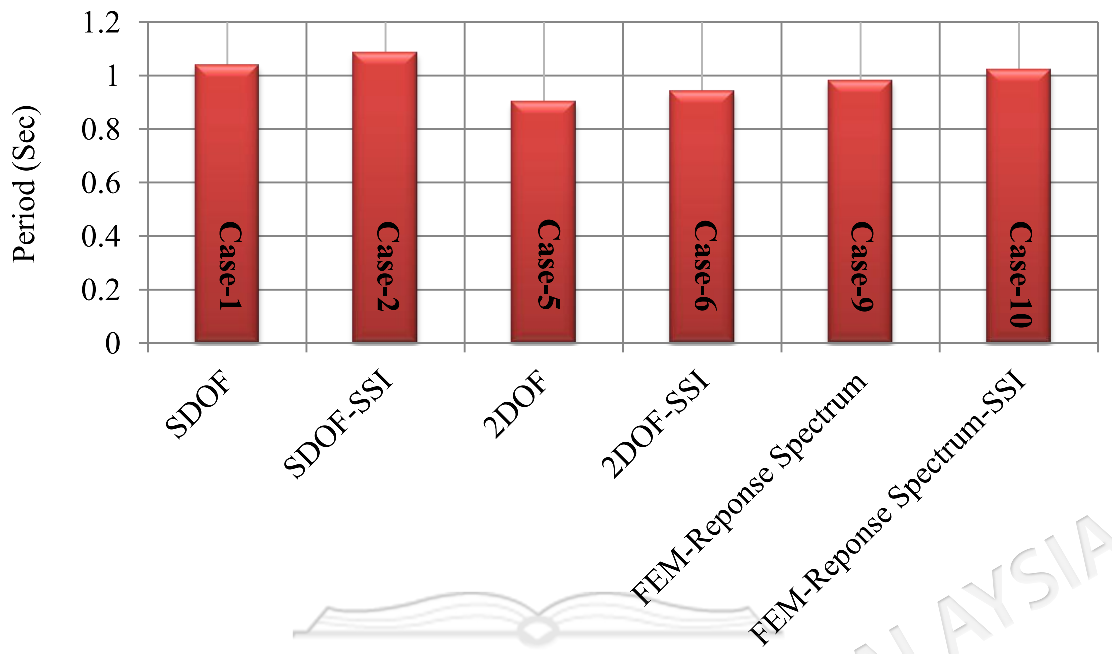

FIGURE 6.2 Periods of impulsive mode of circular elevated tank without embedment

In case of rectangular elevated concrete water tank with embedment assumptions, results are as shown in Figure 6.3, with SSI consideration. The deviation of using SDOF to two DOF and FEM are 32% and 30.27% respectively. Whilst the deviation of using two DOF to FEM is -2.67%

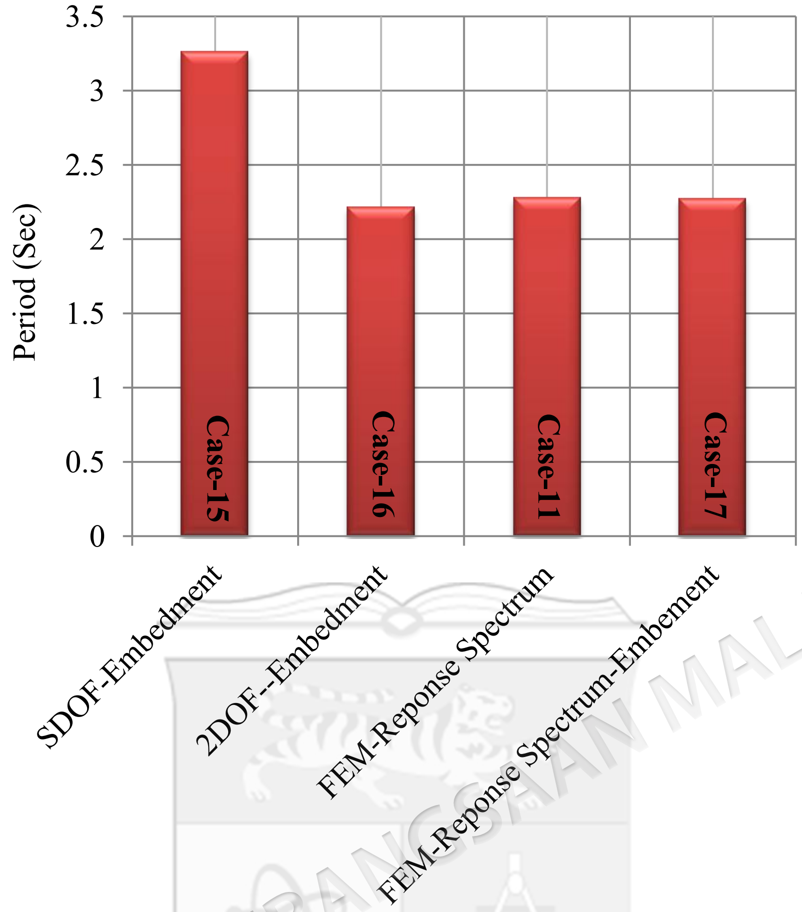

FIGURE 6.3 Periods of impulsive mode of the rectangular elevated tank with embedment

In case of circular elevated concrete water tank with embedment assumptions, and as shown in Figure 6.4, the results are based on accounting of SSI consideration. The deviation of using SDOF to two DOF and FEM are 10.47% and 10.46% respectively. Whilst the deviation of using two DOF to FEM is -0.11%

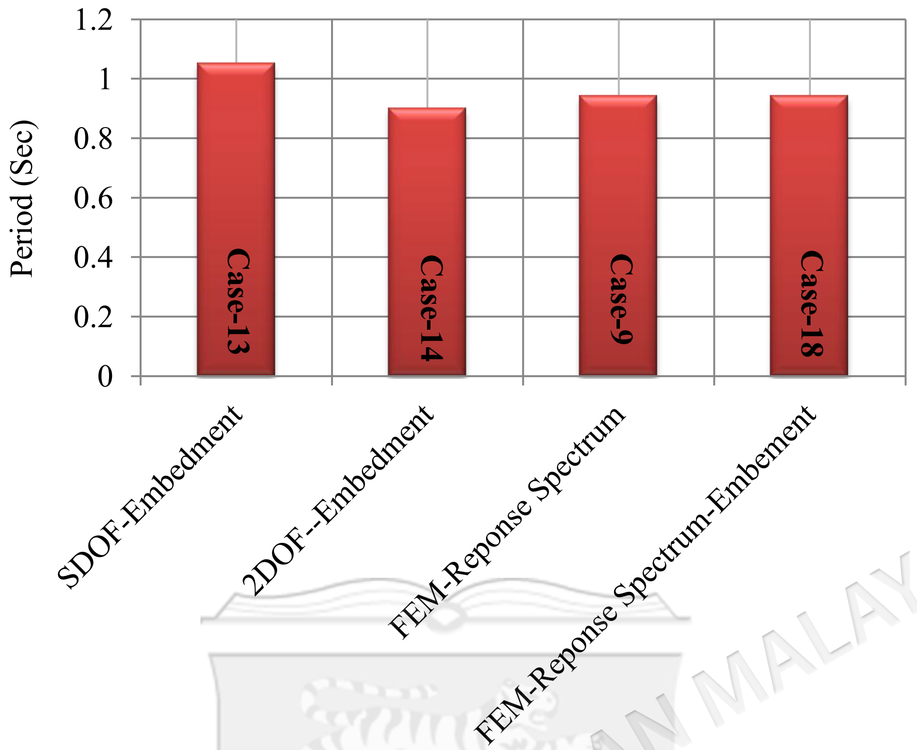

FIGURE 6.4 Periods of impulsive mode of the circular elevated tank with embedment

Generally from all of the cases presented was calculated based on Malaysian seismic data, and the results indicated that the variation between T_i for SODF and FEM are remarkably overestimated for which FSI is ignored. Whilst T_i calculated based on two DOF in which FSI effects is takes into account the results shows good correlation compared with FEM.

6.8.2 Period of Convective Mode

As shown in Figure 6.5, 6.6, 6.7 and 6.8 the results obtained are presented for the case of rectangular and circular tanks in case of embedment and without embedment. The results show that the period of convective mode for two DOF and FEM for all cases are less than 1% in which indicates that calculating the convective mode can be done based on two DOF without modelling the sloshing mass and it's stiffness. This can also be carried out in some conventional FEM software where the elements to be used are not available in the element library. The significant of these results are, although the calculateions period of convective mode in different ways which are differ in terms of the difficulty in building the model, especially FEM, but the values close dramatically to each other, in which it can be take this advantage to adopt the easiest ways to calculate the period.

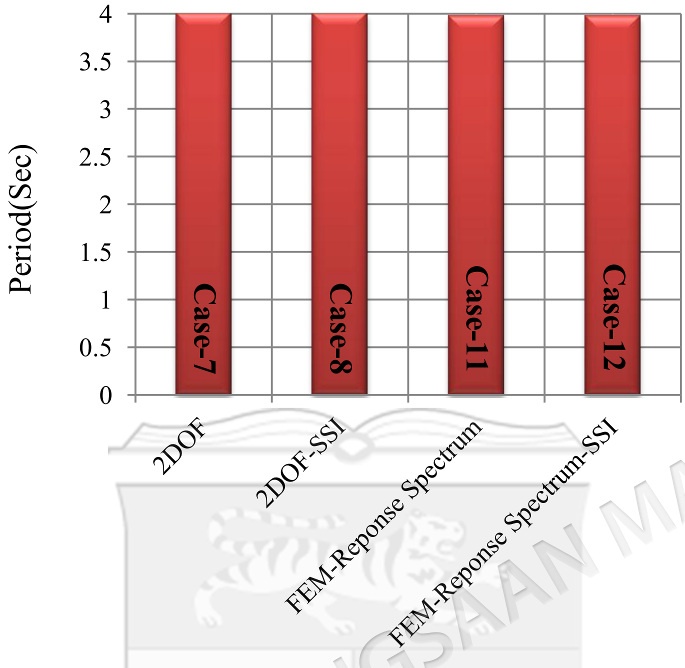

FIGURE 6.5 Periods of convective mode of the Rectangular elevated tank

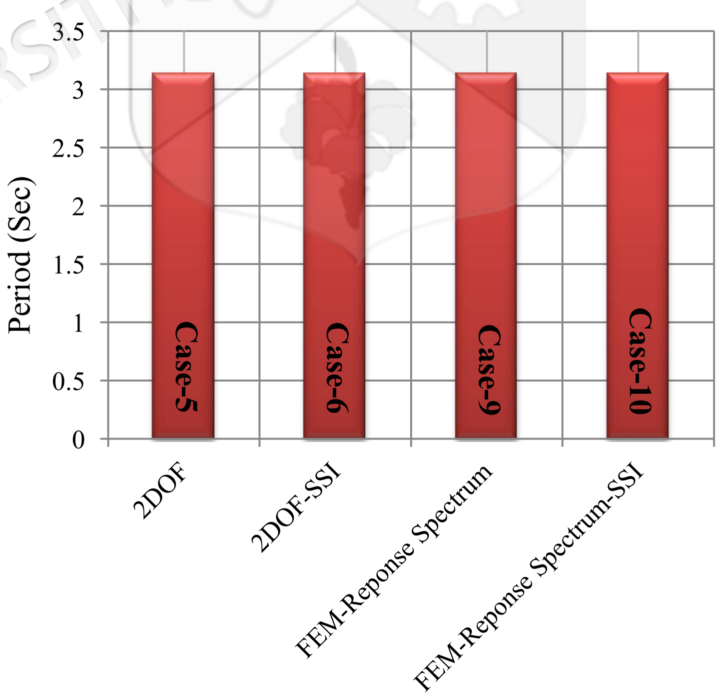

FIGURE 6.6 Periods of convective mode of circular tank

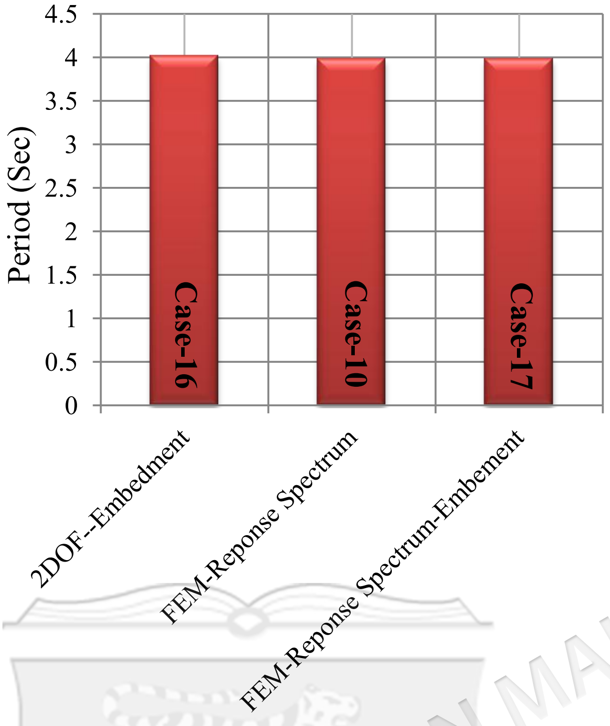

FIGURE 6.7 Periods of convective mode of the rectangular elevated tank with embedment

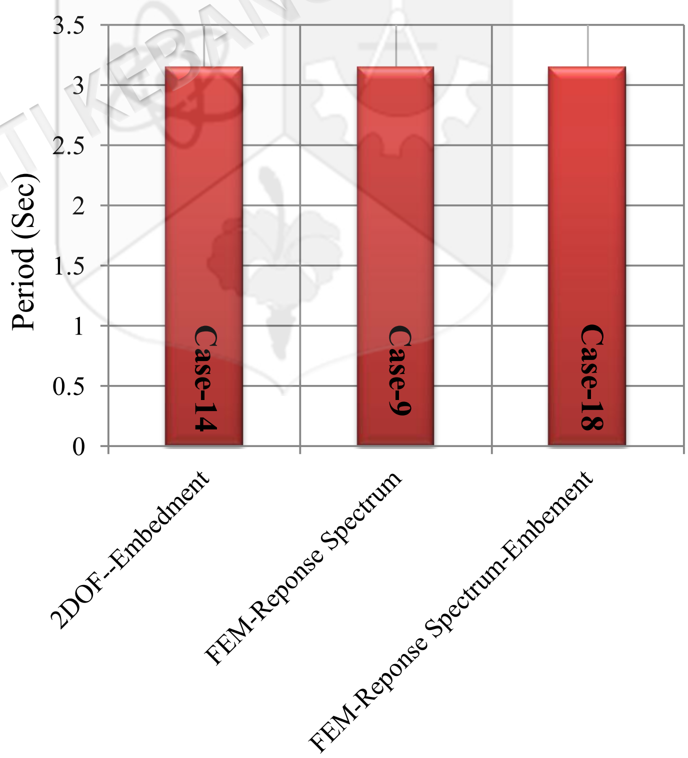

FIGURE 6.8 Periods of convective mode of the circular elevated tank with embedment

6.8.3 Base Shear Force

In the case of rectangular elevated tank as shown in Figure 6.9 the idealization of the tank based on SDOF shows an overestimated for base shear force when compared to nonlinear FEM (SSI) model which is 19.42%. Whilst with SSI consideration the deviation is 16.9% which is still an overestimating base shear. Changing the idealization to two DOF in which the base shear was calculated based on two mode shapes (convective + impulsive) the deviations become 13.53% for two DOF and 12.99% for SSI effects. Moving to multi DOF through FEM response spectrum method the results obtained have dropped abruptly from 4.73% and 3.75% respectively for case of FEM and FEM with SSI effects. Whilst for direct times history analysis gave 1.4% deviation

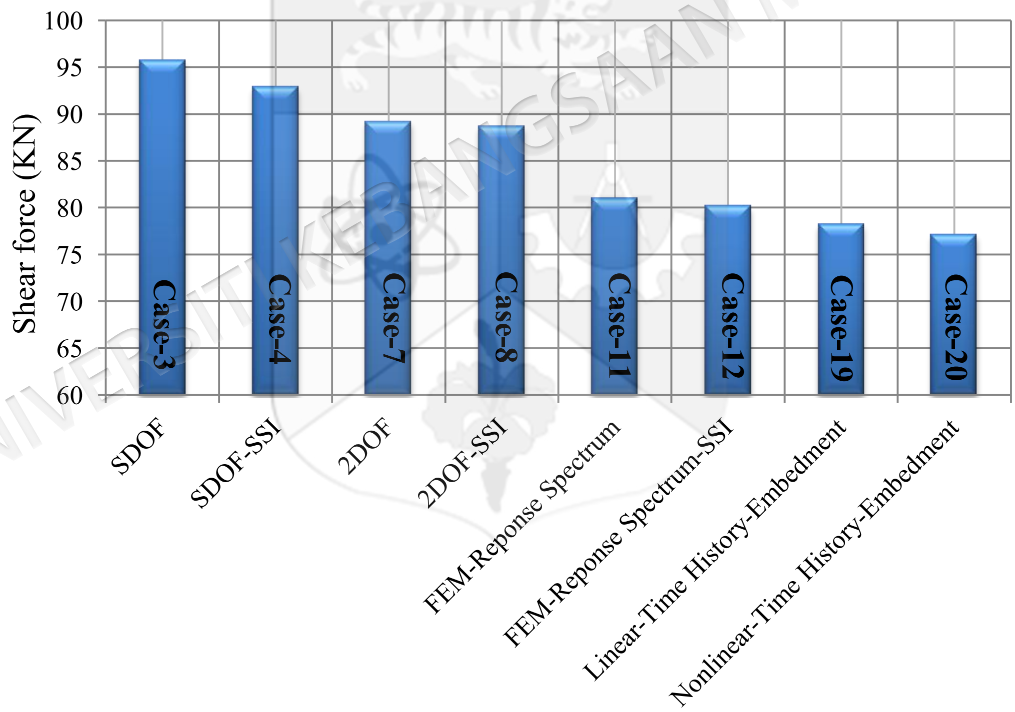

FIGURE 6.9 Base shear forces of the rectangular elevated tank

In the case of circular elevated tank as shown in Figure 6.10 in which the SDOF idealization has 27% and 26.21% deviations in case of fixed and with SSI which is remarkably far compared to rectangular tank. In case of two DOF the deviations results shows 17.5% and 14.08% (fixed and SSI) which are even still remarkably far.

Whilst in the case of FE response spectrum models the deviations of shear forces are 10.25% and 6.06% in case of fixed and SSI effects respectively. For direct time history approach the deviation 4.70% but computationally very expensive especially when take the nonlinearity (material) in consideration.

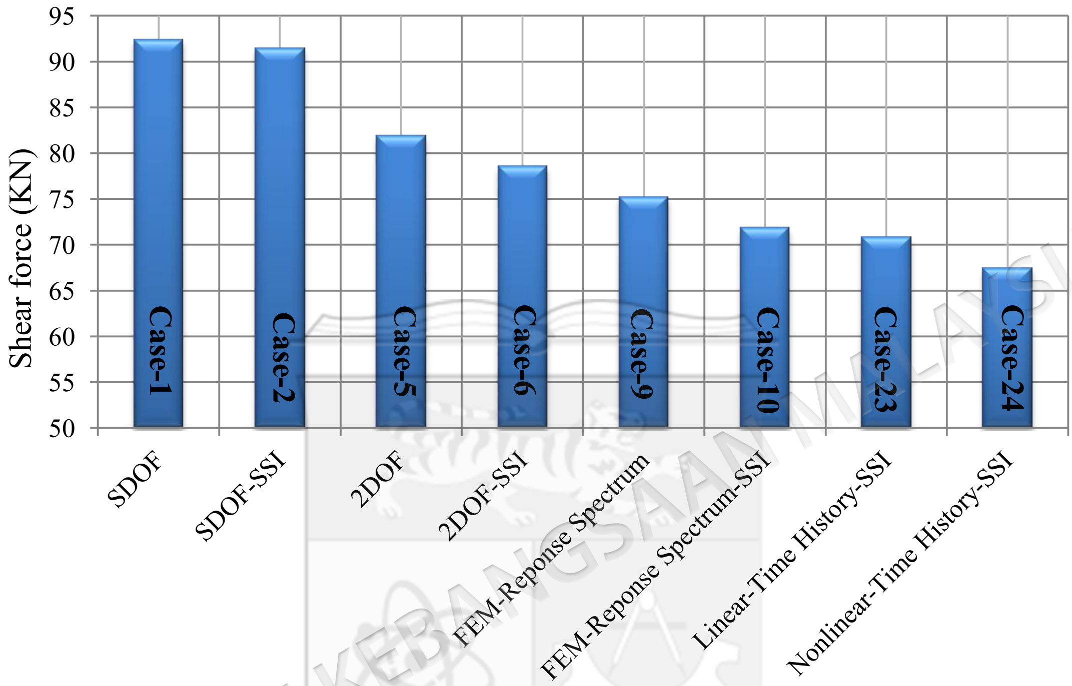

FIGURE 6.10 Base shear forces of circular elevated tank

In the case of rectangular tank with embedment and as shown in Figure 6.11, in which the SSI effects are considered to all cases, the results show that almost same scenario with the rectangular tank with embedment equal to zero with respect to the magnitudes of base shear forces. The results also shows small remarkably effects of embedment on the base shear compared to nonlinear dynamic analysis. Similarly for the circular tank as shown in Figure 6.11

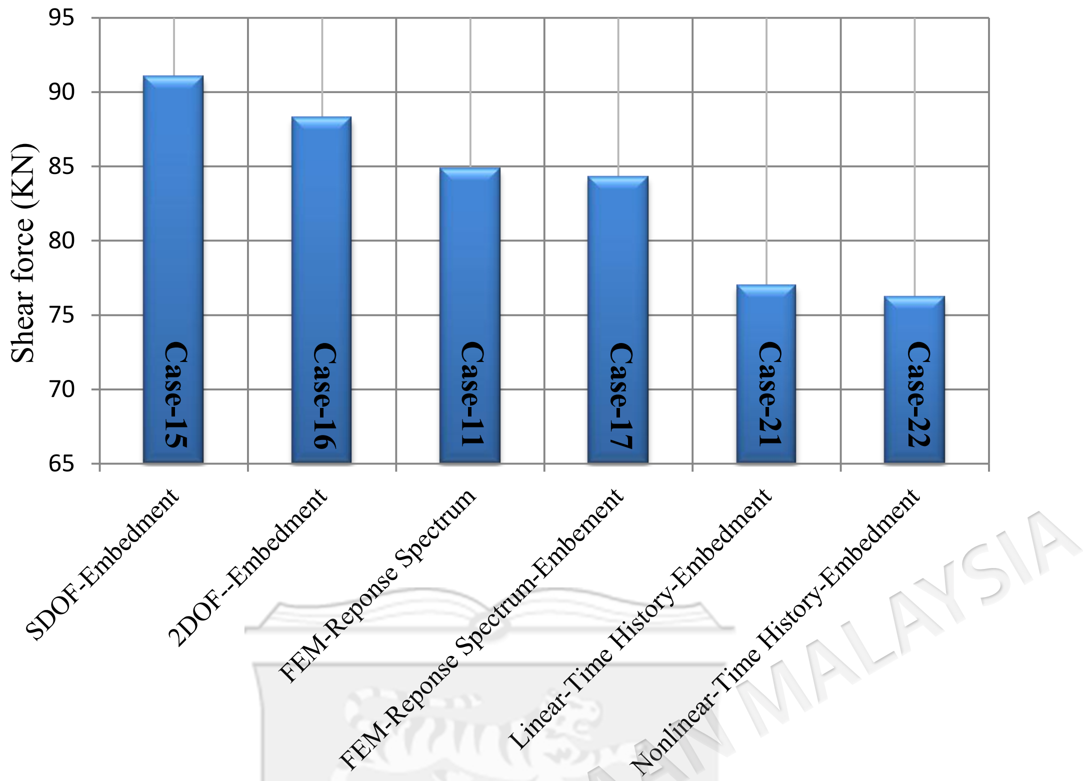

FIGURE 6.11 Base shear forces of the rectangular elevated tank with embedment

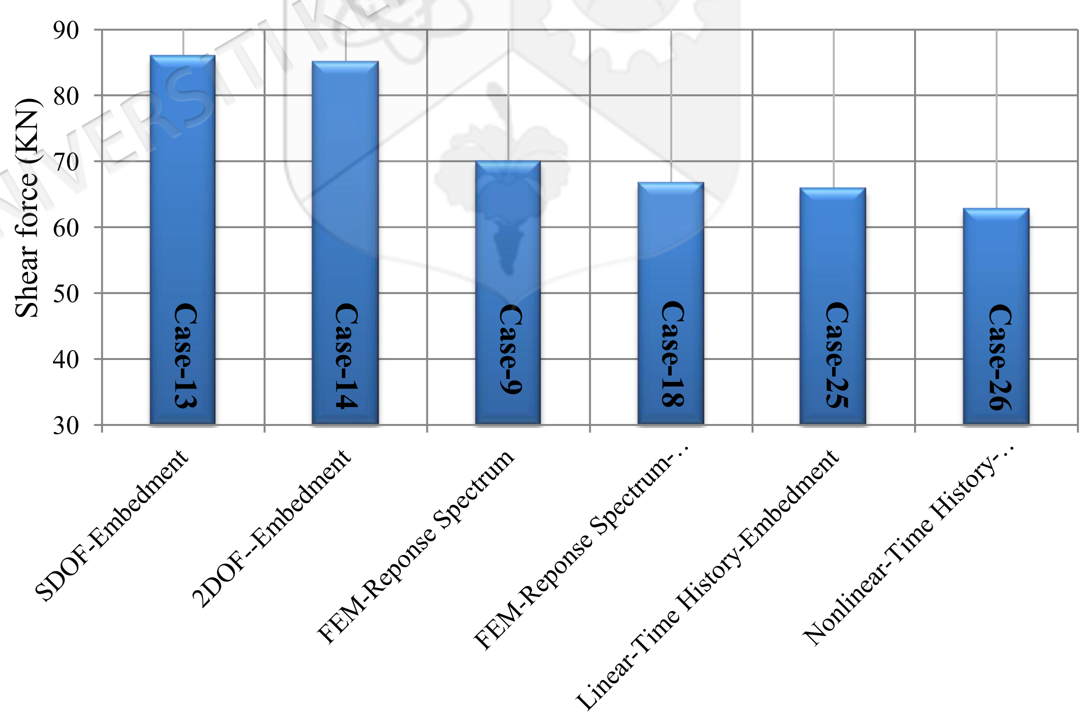

FIGURE 6.12 Base shear forces of the circular elevated tank with embedment

6.8.4 Overturning Moment

Figure 6.13, 6.14, 6.15 and 6.16 shows same scenario with base shear in overturning moment at base of elevated tank in case of rectangular and circular with embedment and without embedment.

It is well known that the bending moment is calculated from the shear forces. From the results obtained note that the difference between the values almost equal with a difference in the range of 1% in case of base shear either increase or decrease.

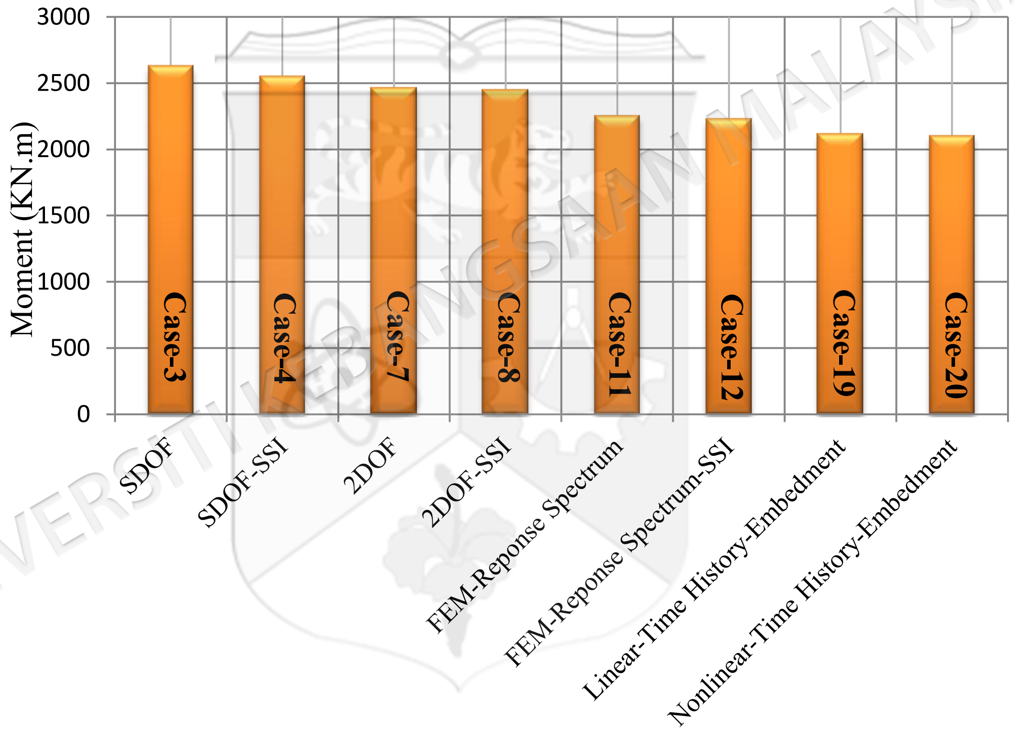

FIGURE 6.13 Overturning moment of the rectangular elevated tank

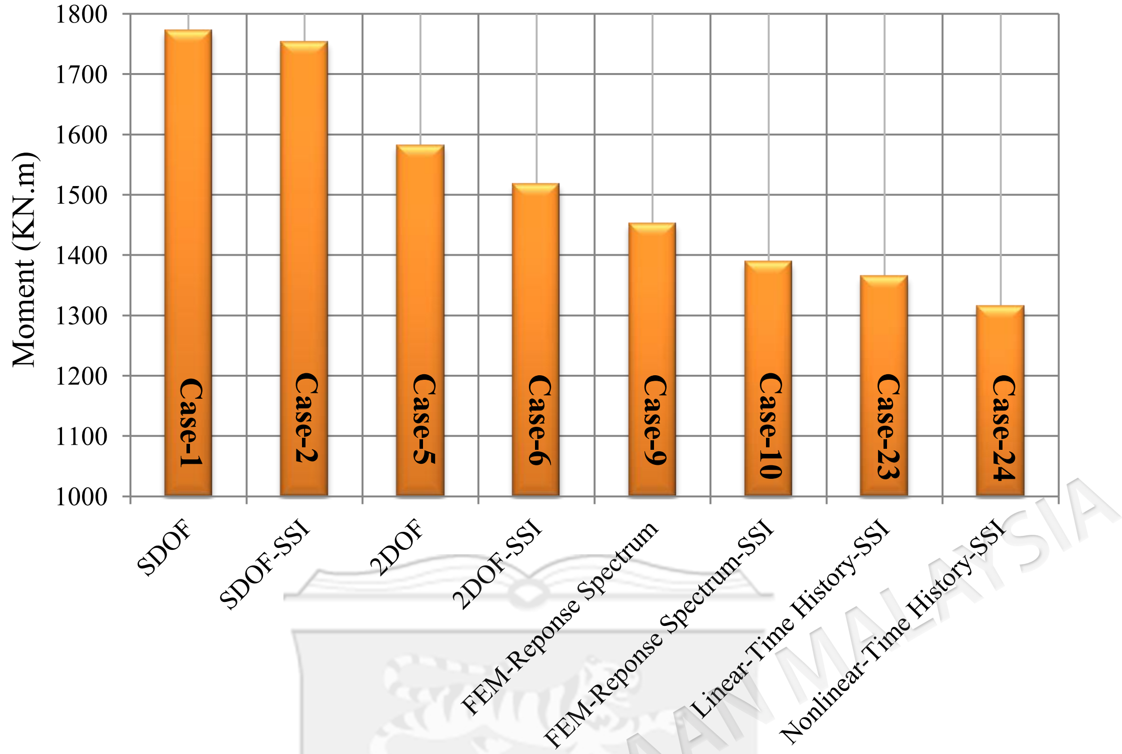

FIGURE 6.14 Overturning moment of circular elevated tank

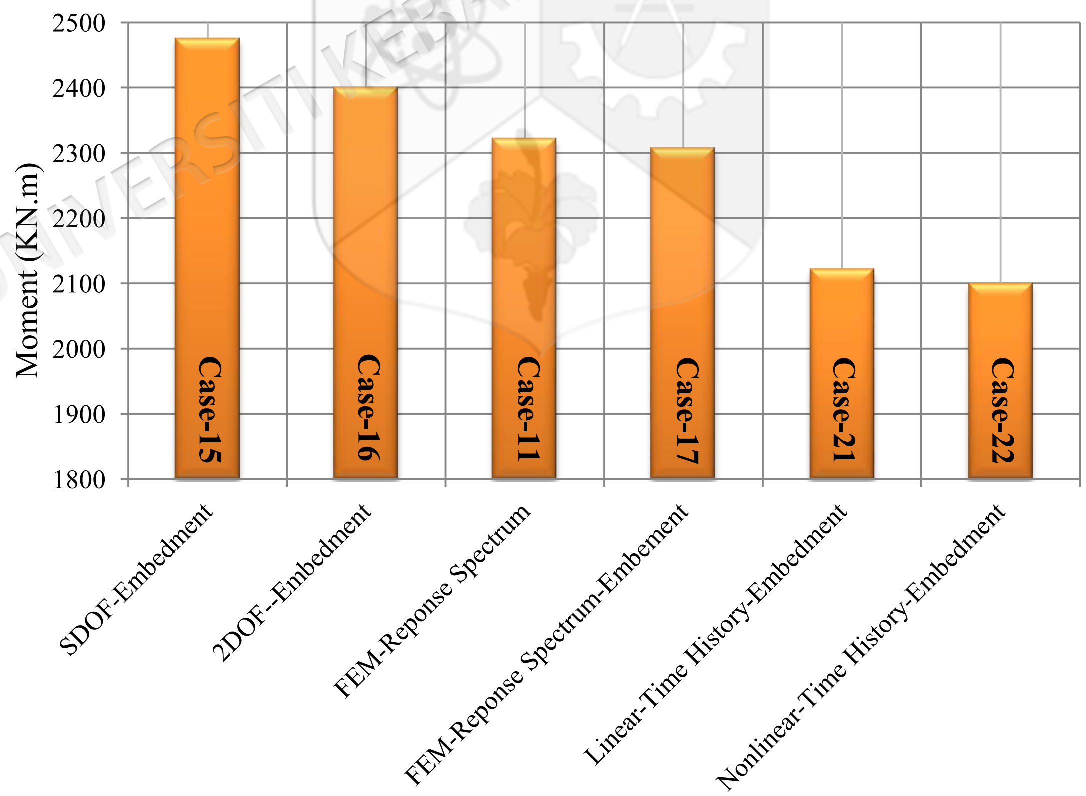

FIGURE 6.15 Moment forces of the rectangular elevated tank with embedment

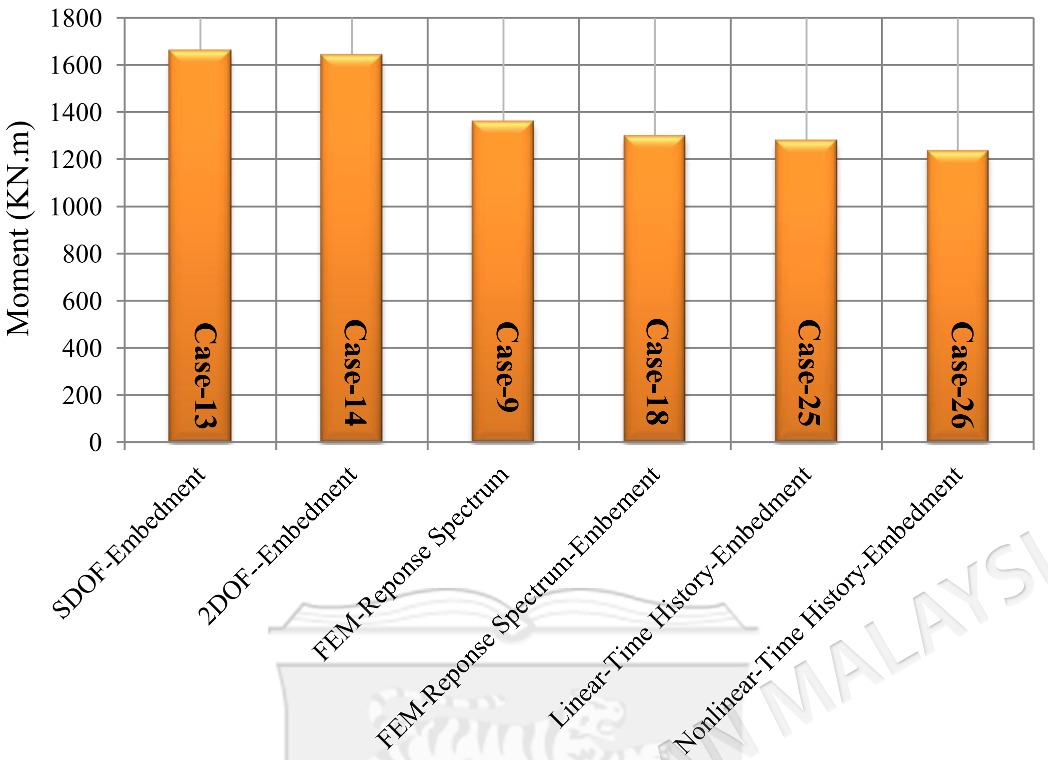

FIGURE 6.16 Moment forces of the circular elevated tank with embedment

6.9 ALTERNATIVE MASS DISTRIBUTED

The results showed in Figure 6.17 and 6.18 show the value of impulsive mode indicated that there is minor of rectangular and circular tanks respectively. There is only a small difference can be found between each case for rectangular and circular tank model, the deviation between values of impulsive mode of case-1(4) and Westergaard approach is around 0.4%. The same manner was found in case of circular tank where the deviation between case-1(4) and Westergaard was around 3% .Whilst the other cases are more accurate as the number of impulsive mass divided increase.

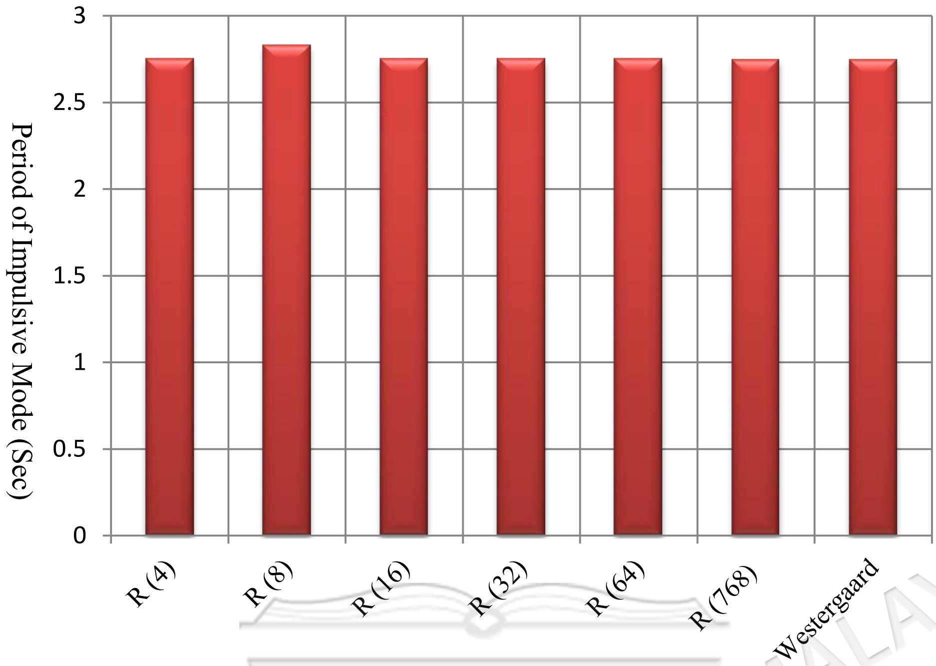

FIGURE 6.17 Values of impulsive mode for the rectangular tank

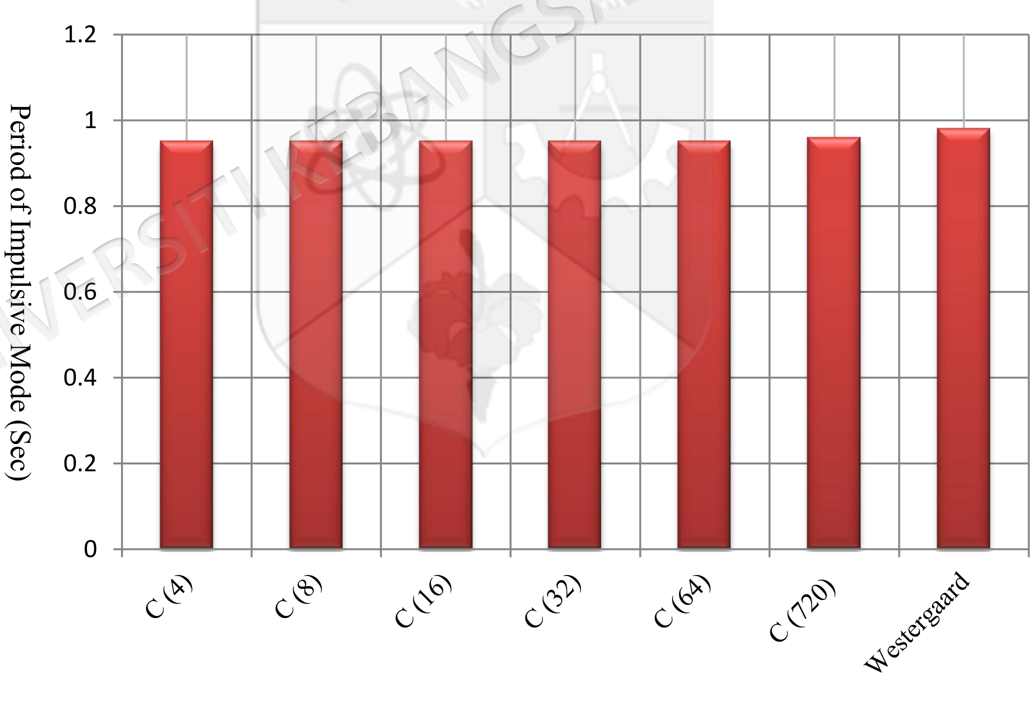

FIGURE 6.18 Values of impulsive mode for the circular tank.

6.10 RESULTS OF ANALYSIS THROUGH FULL TIME HISTORY (IMPLICIT) FOR CIRCULAR TANK

The response spectrum analysis conducted previously only considered the maximum amplitude of seismic effect, but dynamic analysis in the time domain can provide more information for earthquake-resistant design of structures. The latter approach consists of a step-by-step direct integration in which the time domain is discretized into a large number of small increments, and for each time interval the equations of motion are solved to obtain the structural responses (linearly or nonlinearly) such as displacements.

6.10.1 Effects of Nonlinear Soil Structure Interaction

Figure 6.19 indicates that the two cases have different waveforms in case of Newmark scheme and the peak responses of case fixed and nonlinear SSI are 0.036 and 0.026 m respectively in direction I. The reason of the different waveform is that the fundamental periods with the nonlinear SSI and fixed base approach. This phenomenon indicates that the responses of relative roof displacements are controlled by the fundamental mode. Same manner for direction II (Figure 6.20) in which the responses have same waveform and values. Similarly in the case of H H Tylor as shown in Figure 6.21 and 6.22 the effects also almost same as Newmark scheme

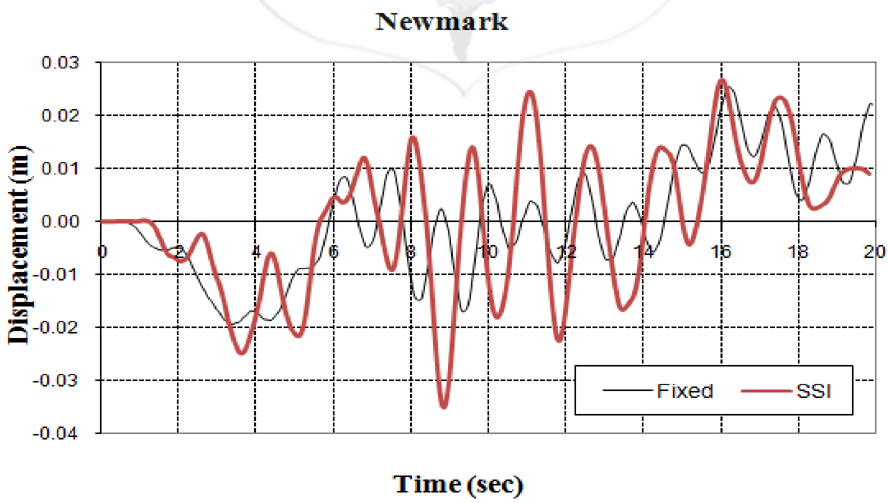

FIGURE 6.19 Time history response of the circular elevated concrete water tank using based on nonlinear soil structure interaction and fixed base approach (Newmark)

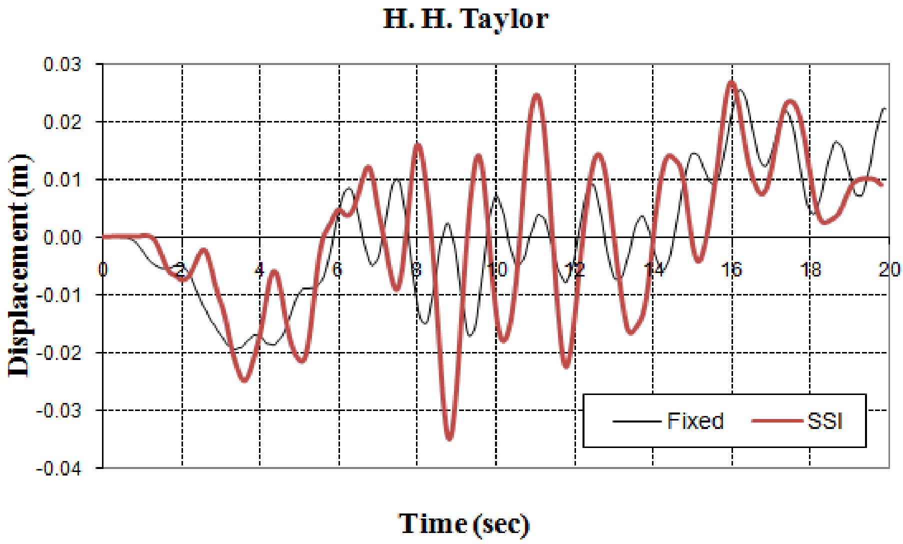

FIGURE 6.20 Time history response of the circular elevated concrete water tank using based on nonlinear soil structure interaction and fixed base approach (H H Tylor)

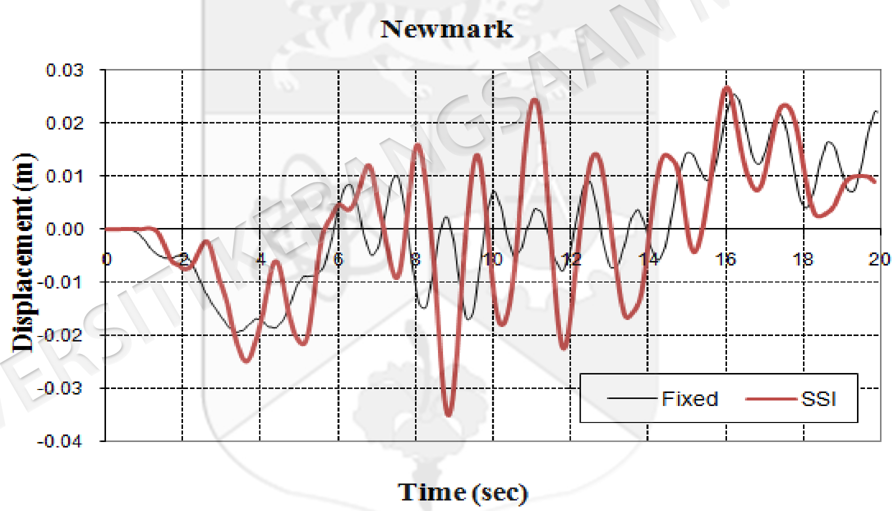

FIGURE 6.21 Time history response of the circular elevated concrete water tank using Newmark scheme Based on NSSI and fixed base approach

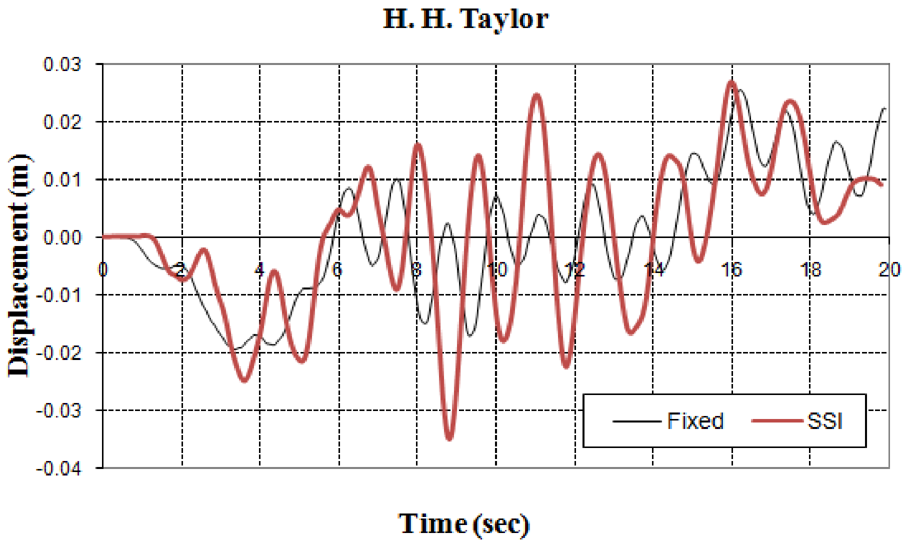

FIGURE 6.22 Time history response of the circular elevated concrete water tank using Newmark and H. H. Taylor scheme based on NSSI and fixed base approach

6.10.2 Effects of Accounting In-situ Soil Stresses and Structural Loading (Circular Tank)

The time history responses of the base shear at the base of circular elevated tank are shown in Figure 6.23 for which the Newmark scheme is adopted. The results are shown for three cases namely: A) considering the state of stress at the soil before the tank constructed (in-situ soil stress) and state of stress at the soil after the tank constructed. B) considering the state of stress at the soil after the tank constructed and ignoring in-situ soil stress C) ignoring A and B for the results, all the three cases have almost similar waveforms, and the peak responses of case A, B and C are 72.23, 72.93 and 73.22 KN respectively, in which indicated a minor effects compared to whole response of the tank, this effects gets 0.4% by ignoring B and 1.36% by ignoring A and B. By observing the results in Figure 6.24 where the Newmark scheme replaced to H H Tylor scheme does not make any change in the results. In case of embedment equal to 4 m the results. In case of embedment linear direct analysis the effects are little more in which this effect gets 0.63%by ignoring B and 1.84% by ignoring A and B in both direction and both analysis scheme (Appendix VI) Same scenario with the nonlinear dynamic analysis for both directions and analysis scheme (Appendix VI).

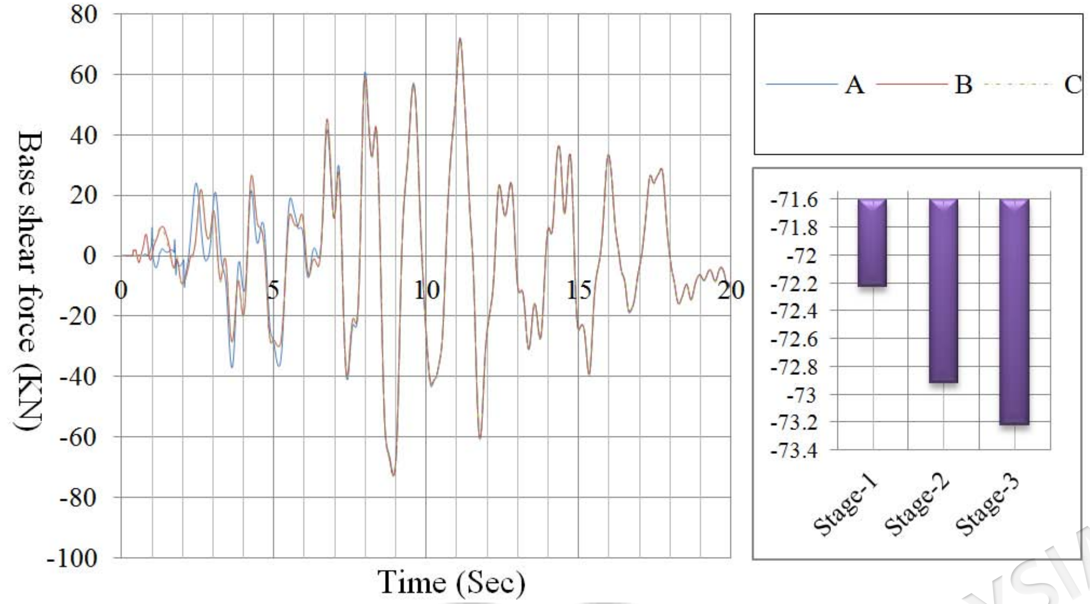

FIGURE 6.23 Time history response of circular elevated tank based on linear analysis (Newmark)

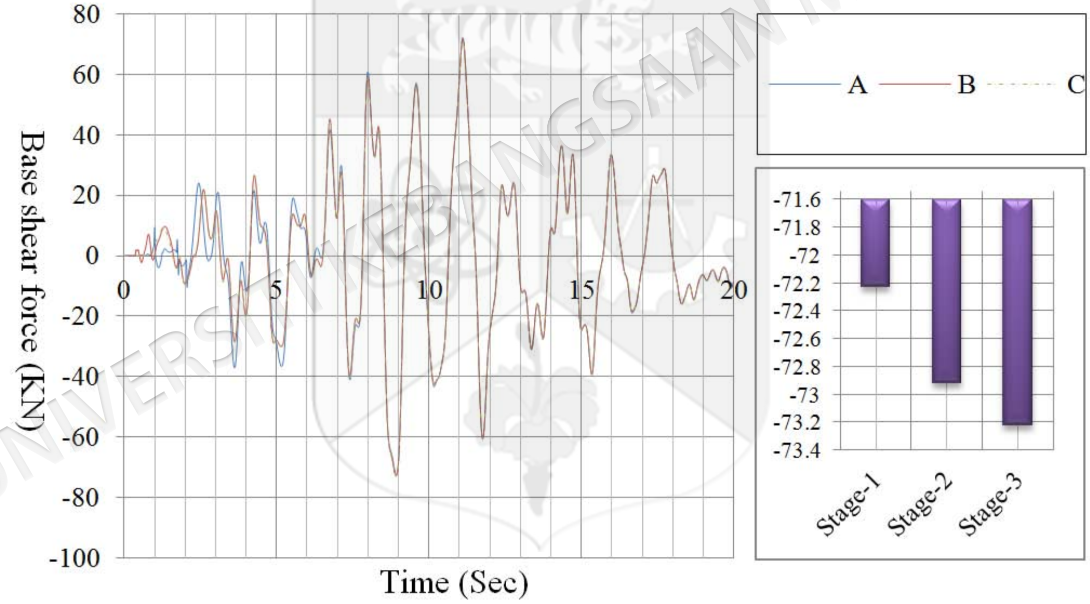

FIGURE 6.24 Time history response of circular elevated tank based on linear analysis (H H Tylor)

6.10.3 Maximum Displacement along Circular Elevated Tank

In order to evaluate the effect of embedment on the lateral behaviour of tank systems, the calculated roof displacements can be compared. It seems that the effects of embedment on the dynamic behaviour of tank systems not as significant, the roof displacements of the systems are significantly affected by the foundation embedment.

In these models, embedment causes a 17% decrease in roof displacement as shown in Figure 6.25 and 6.26 which is a pretty large reduction for such a structure. Same effects also presented in Appendix (VI) in which also the direction of seismic load and the analysis scheme considered

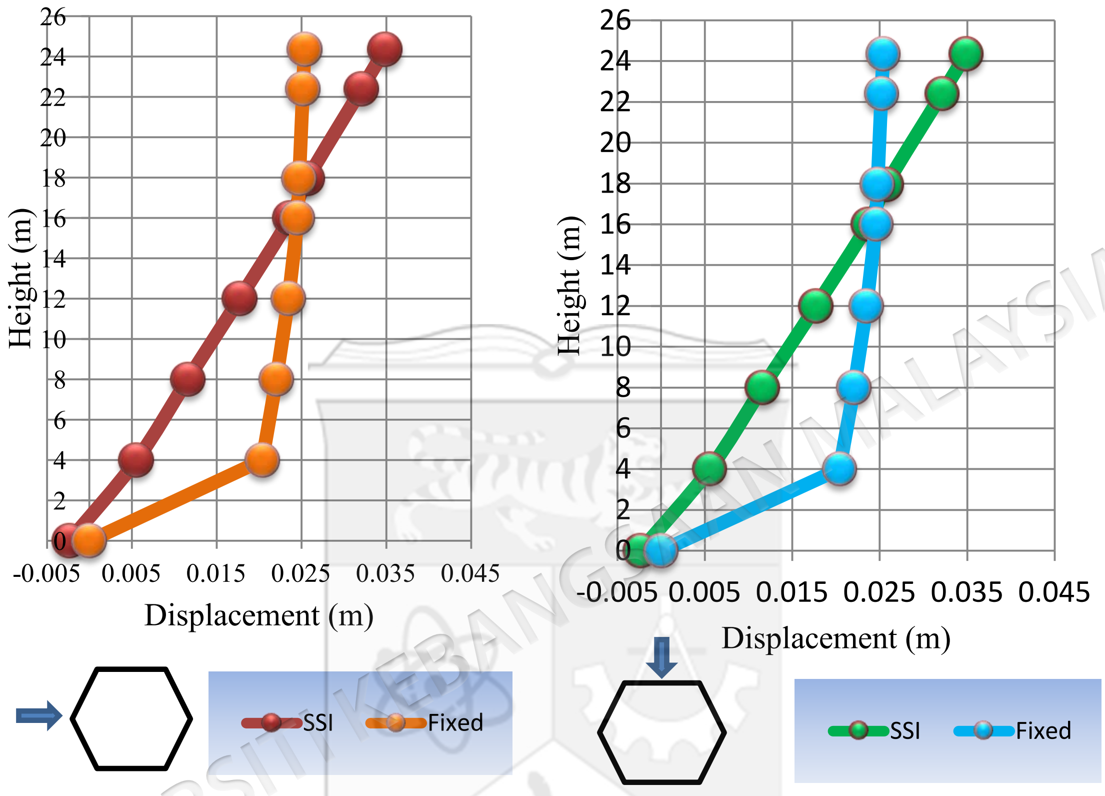

FIGURE 6.25 Maximum calculated displacements along the height of the circular elevated tanks without embedment

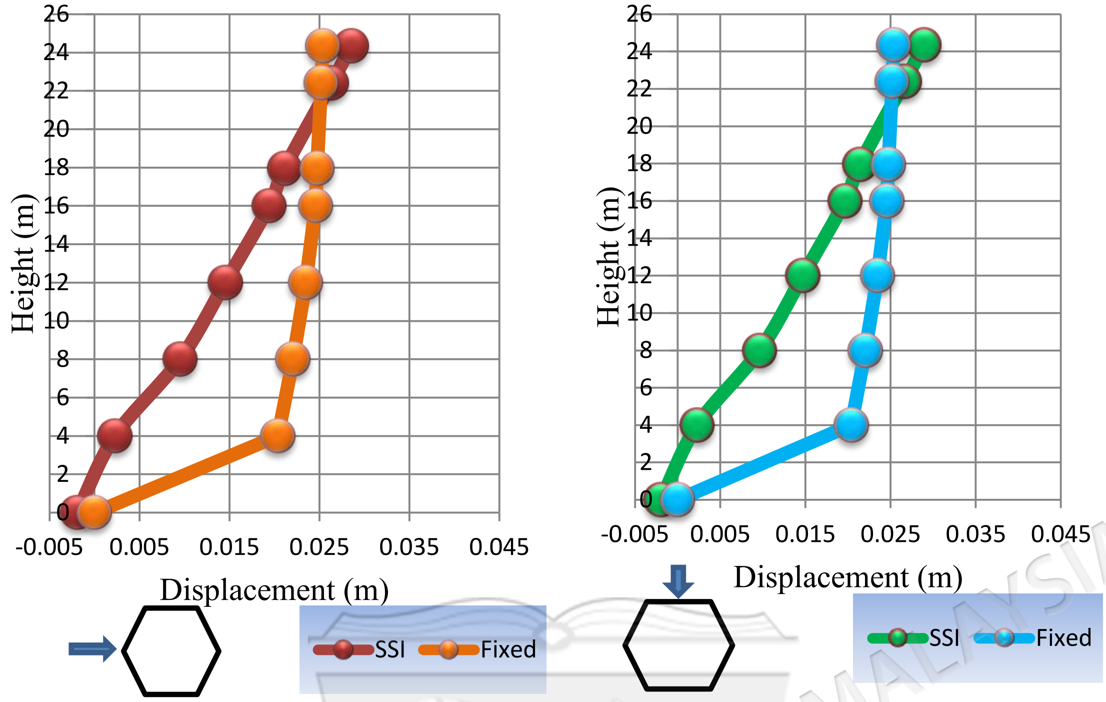

FIGURE 6.26 Maximum calculated displacements along the height of the circular elevated tanks with embedment

6.11 SUMMARY

In this chapter started presented the cases to be conducted in this study with its results (period of convective mode, period of impulsive mode, base shear and overturning moment) for mechanical and FEM simulations, the analyses of those results also were discussed for all cases. The modification of the Westergaard approach and suggested models, effects of nonlinear soil structure interaction, maximum displacement along circular elevated tank, and the effects of accounting in-situ soil stresses and structural loading for the circular tank also presented and discussed in this chapter.

CHAPTER VII

CONCLUSIONS AND RECOMMENDATIONS

7.1 INTRODUCTION

Based on the results obtained, this study has managed to achieve all the objectives that been mentioned in Chapter I. The analyses of the elevated concrete water tanks due to the Malaysian seismic event have also been carried out in accordance with the scope of work. In this study the applicability of using the analytical models based on SDOF, SDOF with SSI consideration, two DOF with FSI consideration and two DOF with SSI consideration has been evaluated. Comparisons with three dimensional nonlinear FE models in case of embedment and no embedment have been conducted in case of rectangular and circular elevated concrete water tank.

This study suggests an alternative suitable modification to Westergaard method, in order to simplify the SSI techniques to save the computation time and efforts. The suggested method is based of adding impulsive mass to the walls of tank in case of circular and rectangular shapes do not affected significantly the dynamic analysis of elevated tanks in which creates increasing in base shear force and overturning moment less than the deviations obtained. Therefore the proposed method is more applicable in case of easily to implement through FE models for dynamic analysis of elevated tank than Westergaard approach.

This study concerned on some of the parameters that may be able to affects the dynamic response of which to the technical reasons the circular tank has been chosen of this part of study. The effects of considering the state of stresses in the soil before (in-situ soil stresses) and after (structural loading) the tank constructed have been obtained under artificial acceleration motion in case of embedment and no embedment based on linear and nonlinear direct dynamic analysis approach has been used to compare these member forces against the Korean code requirements are based upon using elastic properties,

7.2 CONCLUSIONS

According to the results discussed in the previous sections, we can make conclusions as following.

1- Idealizing the elevated concrete water tanks based on single degree of freedom and subjected to local seismic load is still inapplicable to obtain the base shear and overturning moment at the base of tanks and may remain as overestimate analysis, in case of fixed base approach and SSI effects.

2- The simplified procedure that can be utilized for evaluating the dynamic characteristics and the seismic response of the elevated tank is relatively adequate by using two DOF. Furthermore analysis with two DOF procedures, also still also remains some overestimating in case of fixed base approach and SSI effects.

3- Calculation of the period of convective mode in which the implementation of its effects in FE model is relatively quite complicated and lacking some of elements to be used (joint elements) in some of commercial software, can be obtained the stiffness of spring based upon Housner's equation as mentioned equation chapter II and the time of convective mode can be obtained by equation (1) Chapter II.

4- The alternative modification to the Westergaard approach in which shows overall excellent correlation can be used to add the mass of water to the tank walls and obtained the base shear and overturning moment.

5- The results of FE model based on first mode (Impulsive mode) reveals very good correlation in case of fixed base and SSI approaches, this will obviously improve the way in which the develop FE models is more realistically behave instead to the mechanical models according to the real structure. A lot of work would be needed for these models to be developed to the extent that their real behaviour in the variety of possible loads combinations could be realised. It is hoped however that the results to date will give the designers a real insight into their structure and its behaviour under load such that they would wish to explore this interesting structure and more fully understand its complexity.

6- In the case of linear full dynamic analysis the results show excellent convergence but computationally more complicated. But questions raised by these analyses remain unanswered regarding the compatibility between time step, mesh size of the soil profile and damping in which needs an expensive computational.

7- A significant effect on the displacement was found for the circular elevated concrete water tank when nonlinear SSI is considered in the analysis and the responses have different waveforms. Whilst the analysis scheme (H H Tylor and Newmark) does not affect the response significantly.

8- The time history roof displacement of the circular tank decreases considerably (17%) by the foundation embedment. Accordingly, the roof displacement is probably the most critical parameter to be evaluated for this kind of structures. Although the base shear response does not change as much as roof displacement, a maximum 7.5% change in base shear for tank in which the base shear may also be critical parameter especially for softer soils, and strongly relative to the effect of embedment.

9- The embedment appears to affect the sloshing response the least, with a maximum 1% reduction in the time of convective mode, which is relatively small, compared to other response parameters.

10- Considering the state of stresses at the soil before and after the tank constructed having very minor effects on the whole response of the circular elevated concrete water tank in case of 3 dimensional FEM wit accounting SSI. This advantage can be used to avoid the computational of applied loading in the soil and tank (construction stages) in the seismic analysis.

7.3 DEVELOPMENT FRAME WORK FOR ANALYZING ELEVATED CONCRETE WATER TANKS

Analysis of elevated concrete water tanks under static loads requires the building of FE model as a first step in analyzing the tank under vertical loads. Then, the applied lateral loads on the FE model which include earthquake and wind loads are calculated for its effect that needs to move the mechanical models. Based on the results obtained, analysis of elevated concrete water tanks become more easily as shown in Figure 7.1. The process of analyzing the elevated concrete water tanks under seismic loads taking advantage of the results of the study in which computationally cheaper than conventional method and more accurate. The diagram shown in Figure 7.1 could help the engineers to conduct the dynamic response of elevated concrete water tanks more easily.

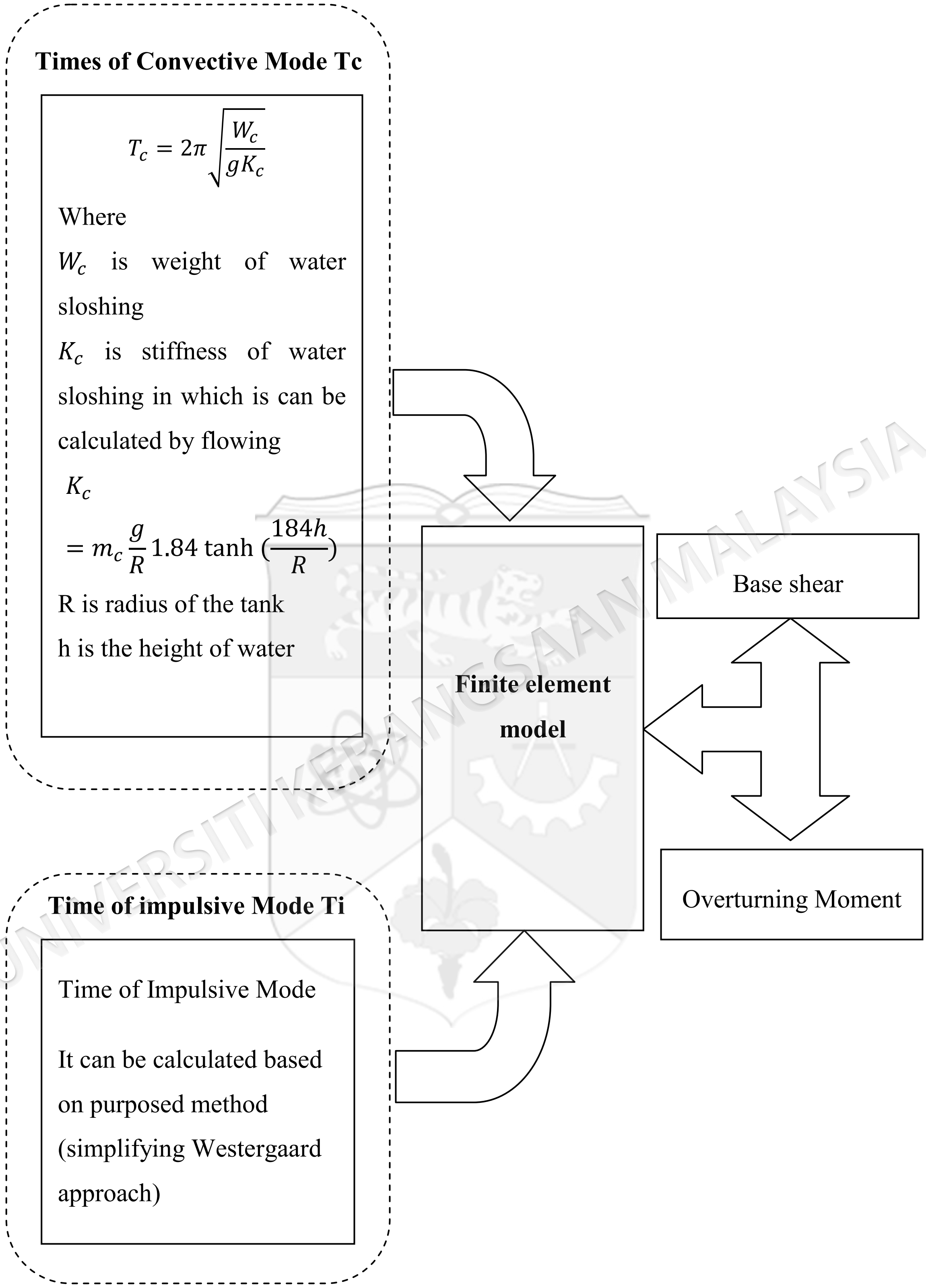

FIGURE 7.1 Developments New Frame Work for Analyzing Elevated Concrete Water Tanks

7.4 RECOMMENDATIONS FOR FURTHER WORK

1- It is recommended that more numerical examples be analyzed and evaluated for different soil types and foundation conditions so that the results from the procedure presented here can be generalized.

2- The use of 3 dimensional flow element for modelling water in the container which is available in some of commercial software such as ANSYS, ABAQUS, ADINA and COSMOS ...etc, to model fluid structure interactions. The modelling in this case more realistic, which is could effected the positively

3- Apply interface element instead of fully constrain between foundation and soil instead to fully fixed makes the results going to be more accurate.

4- Modelling the soil by coupling between FEM and boundary element method (BEM) in which take this approach allows taking the advantages of FEM and BEM and avoiding the disadvantages for which the model in this case especially modelling soil boundary makes the model more realistic.

REFERENCES

Abascal, R. & Domínguez, J. 1990. Dynamic response of two-dimensional flexible foundations allowed uplifting. *Comp Geomech* 9:113–129.

ACI 318. 2002. *Building Code Requirements for Reinforced Concrete*. Detroit: American Concrete Institute.

ACI 371R-98. 1995. *Guide to the Analysis Design and Construction of Concrete-pedestal Water Tower.* Detroit: American Concrete Institute.

Alarcón, E., Cano, J.J. & Domínguez, J. 1989. Boundary element approach to the dynamic stiffness functions of circular foundations. *Int. J. Numer. Anal. Methods Geomechs* 13: 645-664.

American Society of Civil Engineers (ASCE) 7-02. 2002. *Minimum Design Loads for Buildings and Other Structures*.

Applied Technology Council. 1978. *Structural Engineers Association of California*, United States. National Bureau of Standards. U.S. Dept. of Commerce, National Bureau of Standards: Technology & Engineering.

Apsel, R.J. & Luco, J.E. 1983. On the Green's functions for a layered halfspace: Part II. *Bull. Seism. Soc. Am.* 73: 931–951.

Atkinson, G.M. & Boore, D.M. 1997. Stochastic point-source modelling of ground motion in the Cascadia region. *Seismological Research Letters* 68: 74-85.

Aviles, J. & Perez-Rocha, E.L. 1998. Effect of foundation embedment during building-soil structure interaction. *Earthq. Eng. Struct. Dyn* 27:1523-1540.

Aviles, J. & Suarez, M. 2002. Effective periods and damping of building foundation systems including seismic wave effects. *Eng Struct* 24: 553–62.

Azlan, A., Hendriyawan, & Masyhur, I. 2005. Selection and development of appropriate attenuation relationship for peninsular Malaysia. *Proceeding Malaysian Science and Technology Congress*, Mid Valley, Kuala Lumpur.

Azlan, A., Suhana, S., Selvanayagam, P.N. & Zamri, D. 2006. Vulnerability of public buildings subjected to earthquake by finite element modeling. *Proceedings of the 6th Asia-Pacific Structural Engineering and Construction Conference (APSEC 2006)*, Kuala Lumpur, Malaysia.

Bathe, K.J. 1982. *Finite element procedures in engineering analysis*. New Jersey: Prentice-Hall.

Bathe, K.J. & Wilson, E.L. 1976. *Numerical Methods in Finite Element Analysis*. New Jersey: Prentice-Hall.

Bauer, H.F. 1964. *Fluid oscillations in the containers of a space vehicle and their influence upon stability*. NASA TR R 187.

Bellier, O., Bellon, H., Sébrier, M., Sutanto, & René, M. R. 1999. K–Ar age of the Ranau Tuffs: implications for the Ranau caldera emplacement and slip-partitioning in Sumatra (Indonesia). *Journal of Tectonophysics* 312:347–359

Beresnev, I.A. & Atkinson, G.M. 1998. FINSIM-A FORTRAN program for simulating stochastic acceleration time histories from finite faults. *Seismological Research Letters* **69**(1): 27-32.

Beshara, F.B. & Virdi, K.S. 1991. Non-linear finite element dynamic analysis of two-dimensional concrete structures. *Comp. & Struct* **41**(6):1281–1294.

Bommer, J.J. & Ruggeri, C. 2002. The specification of acceleration time-histories in seismic design codes. *European Earthquake Engineering* 1:3-17.

Bommer, J.J. & Acevedo, A.B. 2004. The use of real earthquake accelerograms as input to dynamic analysis. *Journal of Earthquake Engineering* **8**(1):43-91.

Boore, D.M. 2003. Simulation of ground motion using the stochastic method. *Pure and Applied Geophysics* 160:635-676.

BSSC (1994) NEHRP Provisions. 1994. Edition, *Building Seismic Safety Council*. Washington, D.C.

Chen, C.P. & Barber, R.B. 1976. Seismic design of liquid storage tanks to earthquakes. International Symposium on Earthquake Structural Engineering, *St. Louis, MO* 1231–1247.

Chen, W.F. & Mizuno, E. 1990. *Non-Linear Analysis in Soil Mechanics Theory and Implementation*. Netherlands: Elsevier.

Chopra, A.K. 2006. *Dnamics of Structures*. *Theory and applications to earthquake engineering*. Third Edition. New Jersey: Prentice-Hall.

Clough, G.W. & Schmidt, B. 1981. Design and performance of excavations and tunnels in soft clay. *In E.W. Brand & R.P. Brenner Eds* 569-631.

Clough, R.W. & Penzien, J. 1975. *Dynamics of Structures*. New York: McGraw-Hill, Inc.

Clough, R.W. & Penzien, J. 1993. *Dynamic of structure*. 2nd Edition. New York: McGraw-Hill.

Damatty, A.A., Saafan, M.S. & Sweedan, A.M. 2005. Dynamic characteristics of combined conical-cylindrical shells. *Thin Wall Struct* **43**(9):1380–1397.

Dieterman, H.A. 1988. Dynamics of tower liquid–structure–foundation interaction. Ph.D. Dissertation, TU Delft, Netherlands.

Dobry, R. & Gazetas, G. 1986, Dynamic response of arbitrary shaped foundations. *J. Geotech. Eng.–ASCE* **112**(2):109-135.

Domínguez, J. 1978. Dynamic stiffness of rectangular foundations. *Research Report R78-20*, Dept. Civ. Engrg. Massachusetts Inst. of Tech. Cambridge, Mass.

Domínguez, J. & Medina, F. 1989. Boundary elements for the analysis of the seismic response of dams including dam-water-foundation interaction effects. *Engrg. Anal* 6:158-163

Donea, J., Gıuliani, S. & Halleux, J.P. 1982. An arbitrary Lagrangian–Eulerian finite element method for transient dynamic fluidstructure interaction. *Computer Methods in Applied Mechanics and Engineering* 33:689–723.

Dussom, K.B., Hadj-Hamou, T. & Bakeer, R. 1991. QUAKE: An expert system for the selection of design earthquake accelerogram. *Computers and Structures*. **40**(1):161-167.

Dutta S.C., Jain, S.K. & Murty, C.V. 2000a. Assessing the seismic torsional vulnerability of elevated tanks with RC frame-type staging. *Soil Dyn Earthquake Eng* 19:183–197.

Dutta, S. & Mondal, A. 2004. Soil structure interaction in dynamic behaviour of elevated tanks with alternate frame staging configurations. *J Sound Vibrat* 277:825–53.

Dutta, S. C. & Majumdar, A. 2001b. Effect of soil–structure interaction on dynamic behaviour of elevated water tanks. *Proceedings Structural Engineering Convention (SEC-2001)*, October, Roorkee, India, pp.714–724.

Dutta, S.C. & Dutta, S. 2003. Inelastic seismic response of elevated tanks incorporating period lengthening due to soil-flexibility. *European Earthquake Engineering* 3:36-49.

Dutta, S.C., Jain, S.K. & Murty, C.V. 2001a. Inelastic seismic torsional behaviour of elevated tanks. *J Sound Vibrat* **242**(1):151–167.

Dutta, S.C., Jain, S.K. & Murty, V.R. 2000b. Alternate tank staging configurations with reduced torsional vulnerability. *Soil Dyn Earthquake Eng* 19:199–215.

Elnashai, A. S. & Sarno, L. D. 2008. *Fundamentals of Earthquake Engineering*. The Atrium, Southern Gate, Chichester, West Sussex United Kingdom: John Wiley & Sons, Ltd.

Elsabee, F. & Morray, J.P. 1977. Dynamic behavior of embedded foundations. Rpt. No. R77-33, Dept. of Civil Engrg. MIT, Cambridge, Mass.

Eurocode-8, 2003. *Design of structures for earthquake resistance-Part 1. 1:General rules—Seismic action and general requirements for structures-Part 4: Silos, tanks and pipelines*: European Committee for Standardization.

FEMA-368/369. 2000. The 2000 NEHRP *Recommended Provisions for New Buildings and Other Structures, Part 1: Provision and Part 2: Commentary*. Washington: Federal Emergency Management Agency.

Fenves, G. & Chopra, A.K. 1984. Earthquake analysis of concrete gravity dams including reservoir bottom absorption and dam-water-foundation rock interaction. *Earthquake Engineering and Structural Dynamics* **12**(5):663-80.

Ferritto, J. M. 1992. N-1844 Ground motion amplification and seismic liquefaction: A study of treasure Island and the Loma Prieta Earthquake, Naval Civil Engineering Laboratory, Port Hueneme, CA June.

Gasparini, D.A. & Vanmarcke, E.H. 1976. Simulated earthquake motions compatible with prescribed response spectra. Evaluation of Seismic Safety of Buildings Report No. 2, Department of Civil Engineering, Massachusetts Institute of Technology, USA.

Gazetas, G. & Tassoulas, J.L. 1987. Horizontal stiffness of arbitrary shaped embedded foundations. *Journal of GT Division*, *ASCE* **113**(5): 458–475

Goto, Y. & Shirasuna, T. 1980. Studies on earthquake response of grouped underground tanks in soft ground. *The 7th World Conference on Earthquake Engineering*, Istanbul.

Gürsoy, S. & Durmu, A. 2009. Investigation of linear and nonlinear of behaviors of reinforced concrete cantilever retaining walls according to the earthquake loads considering soil-structures interactions, *Structural Engineering and Mechanics* **31**(1):75-91.

Gulkan, P. & Sozen, M.A. 1974. In-elastic responses of reinforced concrete structures to earthquake motions, *Proceedings of the ACI* **71**(12):605-610.

Haroun, M.A. & Ellaithy, M.H. 1985. Seismically induced fluid forces on elevated tanks. *J Tech Top Civil Eng* **111**(1):1–15.

Haroun, M.A. & Housner, G.W. 1981. Seismic design of liquid storage tanks. *ASCE Journal of Technical Councils* **107** (1):191–207.

Haroun, M.A. & Temraz, M.K. 1992. Effects of soil-structure interaction on seismic response of elevated tanks. *Soil Dyn Earthquake Eng* **11**(2):73–86.

Hemsley, J.A. 1999. *Elastic Analysis of Raft Foundations*. London: Amer Society of Civil Engineers.

Hilber, H.M., Hughes, T.J. & Taylor, R.L. 1977. Improved numerical dissipation for time integration algorithms in structural dynamics. *Int. J. Earthquake Engrg. and Struct Dyn* 5:283–292.

Hillmer, P. & Schmid, G. 1988. Calculation of foundation uplift effects using a numerical Laplace transform. *Earthquake Engineering and Structural Dynamics* 16:789-801.

Housner, G.W. 1955. Properties of strong ground motion earthquakes. *Bulletin of Seismological Society of America* 45:187-218.

Housner, G.W. 1963. Dynamic behaviour of water tanks. *Bulletin of the Seismological Society of the America* 53:381–387.

IBC-2003. 2003. *International Building Code*. Virginia: International Code Council.

Idriss, I.M. & Sun, J. 1991. *User's manual for SHAKE91 for Geotech. Modeling*. University of California.

Imai, T. & Tonoghi, K. 1982. Correlation of N-value with s-wave velocity and shear modulus, Proc. *2nd European Symp on Penetration Testing* 67-72.

Jennings B., Jennings, P.C. & Bielak, J. 1973. Dynamics of building soil interaction. *Bull. Seismol. Soc. Am* 63:9–48.

Karabalis, D.L. & Beskos, D.E. 1984. Dynamic response of 3D rigid surface foundations by time domain boundary element method. *Earthquake Eng. Struc. Dyn* 12:73-93.

Kowalsky, M.J., Priestley, M.J. & MacRae, G.A. 1995. Displacement-based design of R.C. bridge columns in seismic regions. *Earthquake Engineering and Structural Dynamics* 24:1623-1643.

Krinitszky, E.L. & Chang, F.K. 1979. State-of-the-art for assessing earthquake hazards in the United States: specifying peak motions for design earthquakes, Miscellaneous Paper S-73-1, Report 7, U.S. Army Corps of Engineers Waterways Experiment Station, Vicksburg, Mississippi.

Kuo, J.S. 1982. Fluid-structure interactions: Added mass computation for incompressible fluid, UCB/EERC-82/09 Report, University of California, Berkeley.

Kwok, A.O., Stewart, J.P., Hashash, Y.M.A., Matasovic, N., Pyke, R., Wang, Z. & Yang, Z. 2007. Use of exact solution of wave propagation problems to guide implementation of nonlinear seismic ground response analysis procedures. *J. Geotech. Geoenv. Eng. ASCE* **133**(11):1385-1398.

Lee, W.V. 1980. Effect of foundation embedment on soil-structure interaction. *The 7th World Conference on Earthquake Engineering*, Istanbul.

Ronald, T. & Eguchi. 1986. Lifeline seismic risk analysis - Case studies. *Proceedings of the Session Sponsored by the Technical Council of Lifeline Earthquake Engineering of the American Society of Civil Engineers in American Society of Civil Engineers.*

Livaoglu, R. & Dogangun, A. 2006a. Simplified seismic analysis procedures for elevated tanks considering fluid-structure-soil interaction. *J Fluids Struct* **22**(3):421–39.

Livaoglu, R. & Dogangun, A. 2007a. Effect of foundation embedment on seismic behavior of elevated tanks considering fluid–structure-soil interaction. *Soil Dynamics and Earthquake Engineering* 27: 855–863.

Livaoglu, R. & Dogangun, A. 2004 A Simple seismic analysis procedure for fluid-elevated tank-foundation/soil systems. *6th International Congress on Advances in Civil Engineering*. Bogazici University, Istanbul, Turkey.

Livaoglu, R. & Dogangun, A. 2006c. The effects of local site classes on the dynamic behavior of elevated tanks with frame and shaft supporting structures, *7th International Conference on Advances in Civil Engineering*. Yıldız Technical University, Istanbul, Turkey.

Livaoglu, R. & Dogangun, A. 2006b. Dynamic behavior and seismic performance of elevated tanks due to ground types defined in EC-8 and TEC-06. *First European Conference on Earthquake Engineering and Seismology*. Geneva, Switzerland.

Livaoglu, R. & Dogangun, A. 2007b. An investigation about effects of supporting systems on fluid-elevated tanks interaction, *International conference on earthquake engineering and seismology (IIEES).* Tehran, Iran.

Livaoglu, R. & Dogangun, A. 2008. Sloshing response of the cylindrical elevated tanks with frame staging system on different soil conditions, Flow Induced Vibration, Zolotarev & Horacek eds. Institute of Thermo mechanics. Prague.

Livaoglua, R. & Dogangun, A. 2007b. Seismic behavior of cylindrical elevated tanks with a frame supporting system on various subsoil. *Indian Journal of Engineering &Materials sciences* 14:133-145.

LUSAS FEA 14.1. 2007. *LUSAS User Manual Version 14.1*. United Kingdom.

LUSAS software option for plus versions in dynamic analysis. 2007. (online) .http://www.lusas.com/products/options/dynamic.html . (15 june 2008).

Macleod, I.A. 2005. *Modern Structural Analysis Modelling Process and guidance*. London: Thomas Telford Ltd.

Mandal, A. & Dutta, S.C. 2002. Effect of soil–structure interaction on dynamic characteristics of elevated tank with annular ring-type foundation, *Proceedings National Seminar on Role of IT in Fire and Disaster.*

Marashi, E.S. & Shakib, H. 1997. Evaluations of dynamic characteristics of elevated water tanks by ambient vibration tests. *Proceedings of the 4th International Conference on Civil Engineering*, Tehran, Iran.

Mohammadi, M. & Karabalis, D.L. 1990. 3-D soil-structure interaction analysis by BEM: Comparison studies and computational aspects. *Soil Dynamics and Earthquake Engineering* **9**(2):96-108

Morris, A. & Rahman, A. 2008. *A Practical Guide to Reliable Finite Element Modelling.* The Atrium, Southern Gate, Chichester, West Sussex, England: John Wiley & Sons Ltd.

Nasser, M. 2009. Seismic response of R/C frames considering dynamic soil-structure interaction. *18th International Conference on the Application of Computer Science and Mathematics in Architecture and Civil Engineering. Weimar*, Germany.

Newmark, N.M. & Hall, W.J. 1982. Earthquake spectra and design. Engineering Monographs on Earthquake Criteria, Structural Design and Strong Motion Records, Vol. 3, *Earthquake Engineering Research Institute*, University of California, Berkeley, CA, USA.

Newmark, N.M. & Rosenblueth, E. 1971. *Fundamentals of earthquake engineering*. New York: Prentice-Hall.

Newmark, N.M. 1959. A method of computation for structural dynamics. *Journal of the Engineering Mechanics, ASCE* **85**(3): 67-94.

Ohsaki, Y. & Iwasaki, R. 1973. Dynamic shear modules and Poisson's ratio of soil deposits. *Soils and Foundn* 13:61–73.

Ohta, Y. & Goto, N. 1978. Empirical shear wave velocity equations in terms of characteristic soil indexes. *Earthquake Engg. Struct. Dyn* 6:167–187.

Ottenstreuer, M. 1982. Frequency dependent dynamic response of footings, in proc. soil dynamics and earth. engng. *Conf. Southampton, Springer-Verlag,* England.

PLAXIS-GiD Version 1. 2008. *Material Models Manual*. Netherland.

Priestley, M.J. 2003. *Myths and fallacies in earthquake engineering*. Italy: Rose School.

Priestley, M.J., Seible, F. & Calvi, G.M. 1996. *Seismic Design and Retrofit of Bridges.* New York: John Wiley and Sons.

Resheidat, R.M. & Sunna, H. 1986. Behavior of elevated storage tanks during earthquakes. *Proceedings of the 3rd US National Conference on Earthquake Engineering* 21:43–54.

Scaled accelerograms and equivalent response spectra: corps of engineers, Waterways Experiment Station, Misc. Paper S-73-1, Report 14, Vicksburg, MS 391 80, 88 pp.

Schnabel, P.B., Lysmer, J. & Seed, B.H. 1970. Shake, a program for earthquake response analysis of horizontally layered sites. Rep. No. EERC 72-12, *Earthquake Engineering Research Center*, College of Engineering, University of California, Berkeley.

Seed, H.B. & Idriss, I.M. 1969. Soil modeling and damping factors for dynamic response analyses. Report No. EERC 70–10, *Earthquake Research Center*. University of California, Berkeley, California

Seismic Design Guidelines for Concrete Buildings in Malaysia JKR. 2007. Government of Malaysia.

Shakib, F. Omidinasab, and Ahmadi, M.T. 2010. Seismic demand evaluation of elevated reinforced concrete water tanks. *International Journal of Civil Engineerng* **8**(3):204-220.

Shibata, A. & Sozen, M. 1976. Substitute structure method for seismic design in R/C. *J. Struct. Div* **102**(1):1–18.

SIMQKE User Manual, 1976. NISEE Software Library, University of California, Berkeley, USA.

Sinha, B.P., Gerstle, K.H. & Tulin, L.G. 1964. Stress-strain relations for concrete under cyclic loading. *ACI Journal* **61**(2):195-210.

Stewart, J. & Kwok, A. 2008. Nonlinear seismic ground response analysis: code usage protocols and verification against vertical array data. *Geotechnical Engineering & Soil Dynamics IV, ASCE Geotechnical Special Publication*. 181: 24.

Stewart, J.P. & Fenves, G.L. 1998. System identification for evaluating soil structure interaction effects in buildings from strong motion recordings. *J. Earthquake Engrg. Struct. Dyn* **27**(8):869-885.

Stewart, P.J., Seed R.B. & Fenves, G.L. 1999. Seismic soil-structure interaction in buildings. II: empirical findings. *J Geotechn Geoenviron Eng* **125**(1):38–48.

Takewaki, I., Takeda, N. & Uetani, K. 2003. Fast practical evaluation of soil-structure interaction of embedded structure. *Soil Dyn. Earthq. Eng* 23:195-202.

Tapan, K.S. 2009. *A Fundamentals of Seismic Loading on Structures*. United Kingdom: John Wiley & Sons.

Time-history dynamic analysis of concrete hydraulic structures. 2003. *US Army Corps of Engineers engineering and design*. EM 1110-2-6051, engineer manual.

UBC 97. 1997. *Uniform building Code, volume 2. structural Engineering Design Provisions*. Virginia: International Code Council

Vanmarcke, E.H. 1979. State-of-the-Art for assessing earthquake hazards in the United States, Representation of Earthquake Ground Motions.

Veletsos, A.S. & Shivakumar, P. 1993. Sloshing response of layered liquids in rigid tanks. *Earthquake Engng. Struct. Dyn* 22:801–821.

Veletsos, A.S. 1977. *Dynamics of structure-foundation systems. structural and geotechnical mechanics*. New Jersey: Prentice Hall.

Westergaard, H.M. 1931. Water pressures on dams during earthquakes. Proceedings of the ASCE 57, 1303.

Wieschollek, M., Kopp, M., Hoffmeister, B. & Feldmann, M. 2011. Seismic design of spherical liquid storage tanks. *iii eccomas Thematic Conference on Computational Methods in Structural Dynamics and Earthquake Engineering*, Greece.

Wilson, E.L. 2002. *Three dimensional static and dynamic analysis of structures*. Berkeley, California, USA: CSI Publication.

Wilson, E.L. & Khalvati, M. 1983. Finite elements for the dynamic analysis of fluid-solid systems. *International Journal of Numerical Methods in Engineering* 19: 1657–1668.

Wolf, J.P. 1994. *Foundation Vibration Analysis Using Simple Physical Models*. New Jersey: Prentice-Hall.

Wolf, J.P. 2002. Some cornerstones of dynamic soil-structure interaction, *Eng. Struct* 24:13-28.

Zeng, Y., Anderson, J.G. & Yu, G. 1994. A composite source model for computing realistic synthetic strong ground motions. *J. Res. Lett* 21:725-728.

Zienkiewicz, O.C. & Bettes, P. 1978. Fluid-structure dynamic interaction and wave forces; an introduction to numerical treatment. *International Journal of Numerical Methods in Engineering* 13:1–16.

LIST OF PUBLICATIONS

Gareane A.I., S.A. Othman, O. Karim, & A. Kasa, 2007. Seismic response of elevated concrete water tank and their interaction with soil and water. *Regional engineering postgraduate conference (EPC)*, Malaysia.

Gareane, A.I., S.A. Othman, O. Karim, & A. Kasa, 2008. Investigate the seismic response of elevated concrete water tank, *Regional engineering postgraduate conference (EPC)*, Malaysia.

Gareane, A.I., S.A. Othman, O. Karim, & A. Kasa, 2008. Simulation study on the fundamental frequency of elevated water tank. *International technical conference (ITC) JKAS-JPZ-CAU*, Berjaya Time square, Malaysia.

Gareane, A.I., S.A. Othman, O. Karim, & A. Kasa, 2009. Dynamic behavior of elevated concrete water tank with alternate impulsive mass configurations. *Proceedings of the 2nd WSEAS international conference on engineering mechanics, structures and engineering geology*, Greece.

Gareane, A.I., S.A. Othman, O. Karim, & A. Kasa, 2010. Effects of nonlinear soil structure interaction on the seismic response of elevated tank. *International technical conference (ITC) JKAS-JPZ-CAU*, South Korea.

Gareane, A.I., S.A. Othman, O. Karim, & A. Kasa, 2010. Capability of LUSAS software to handle 3D continuum nonlinear soil structure interaction due to seismic load. *Regional Engineering Postgraduate Conference (EPC)*, Equatorial hotel Bangi, Malaysia.

Gareane, A.I., S.A. Othman, O. Karim, & A. Kasa, 2011, Study the fluid structure interaction due to dynamic response of elevated concrete water tank. *Australian journal of basic and applied sciences* **5**(9): 1084-1087.

Gareane, A.I., S.A. Othman, O. Karim, & A. Kasa, 2011, Behaviour of Elevated Concrete Water Tank Subjected to Artificial Ground Motion. *Electronic journal of geotechnical engineering (EJGE)* 16 (Bund. D).387-406.

APPENDIX I

Tanks details

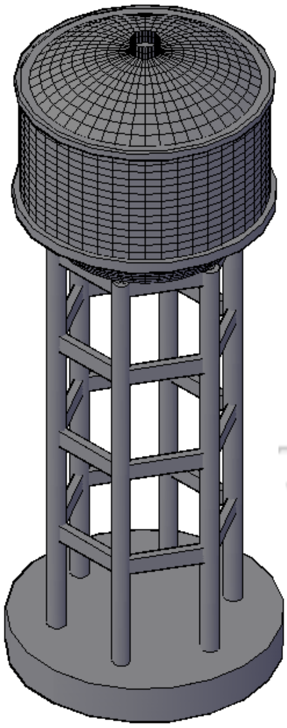

3 Dimensions

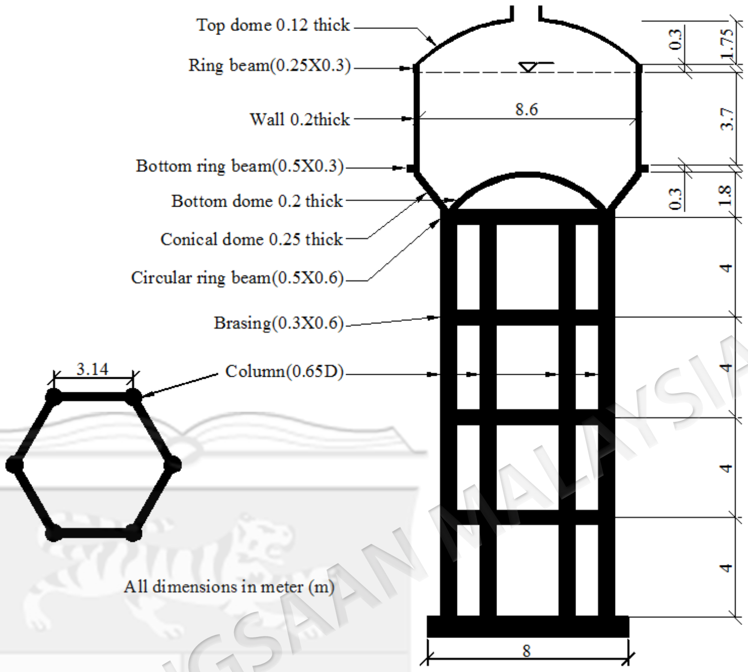

Section

Circular elevated concrete water tank

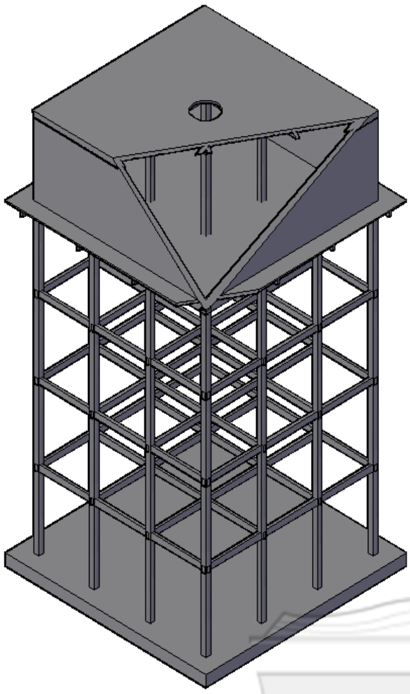

3 Dimensions

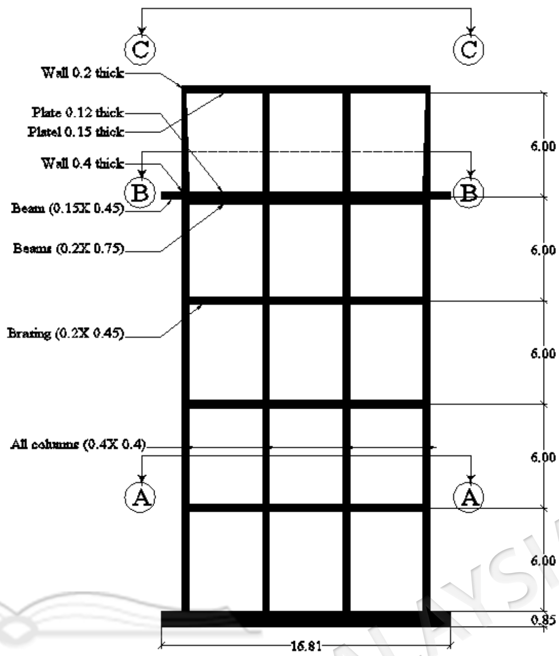

Section

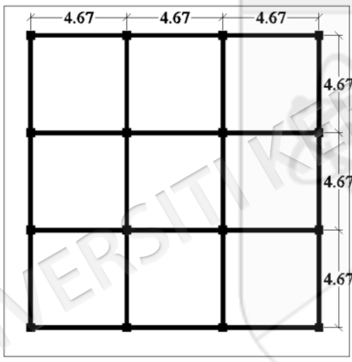

Section (A-A)

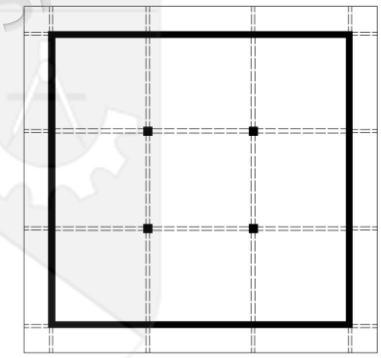

Section (B-B)

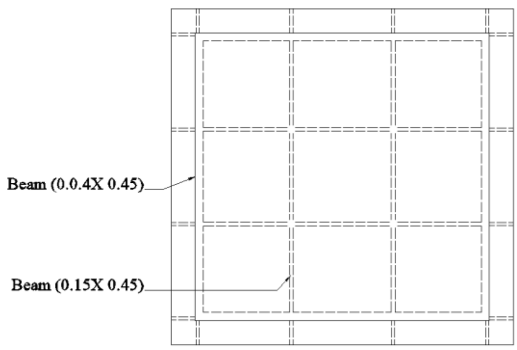

Section (C-C)

Rectangular elevated concrete water tank

APPENDIX II

Flow chart of Gasparini and Vanmarcke approach

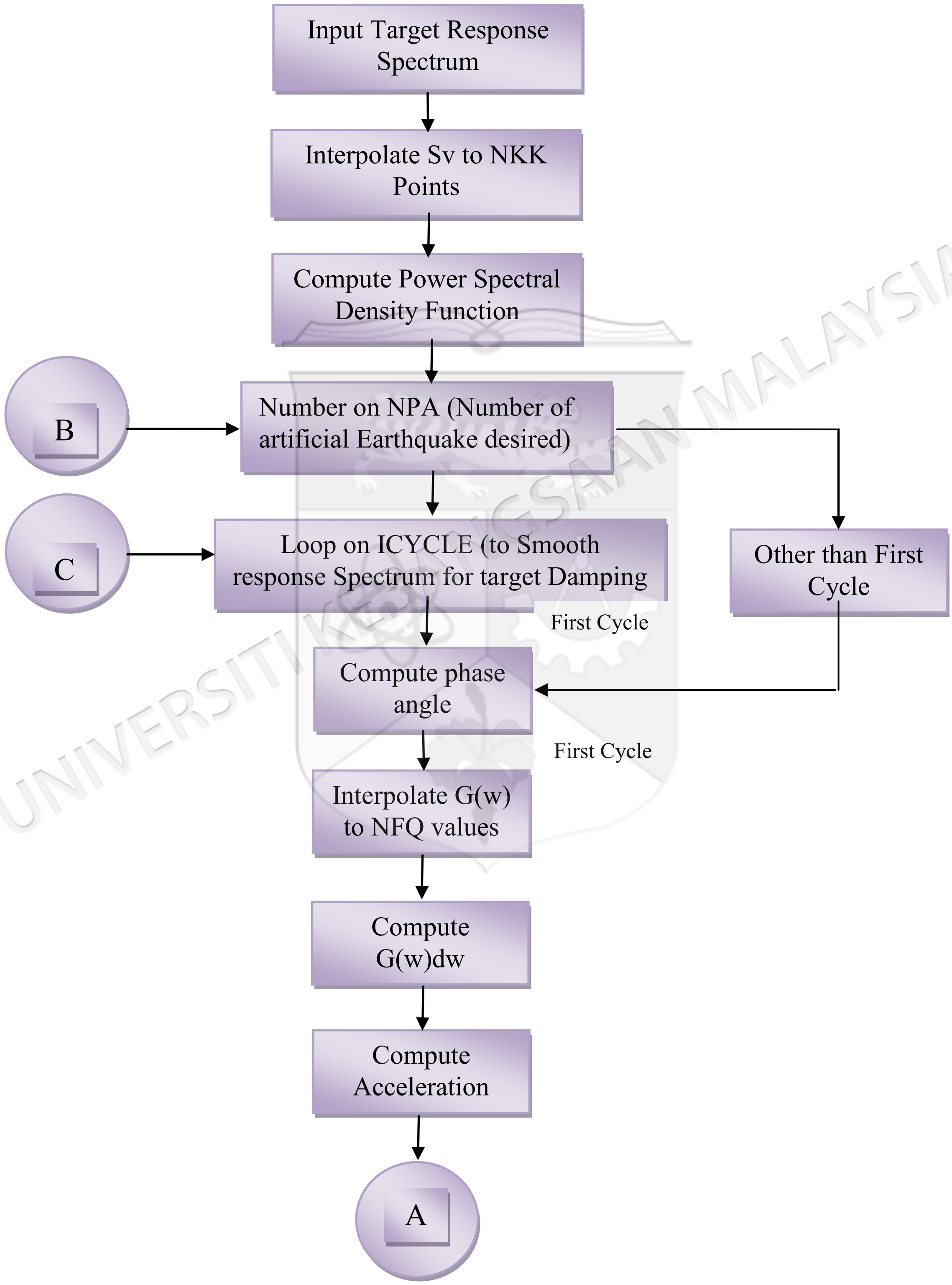

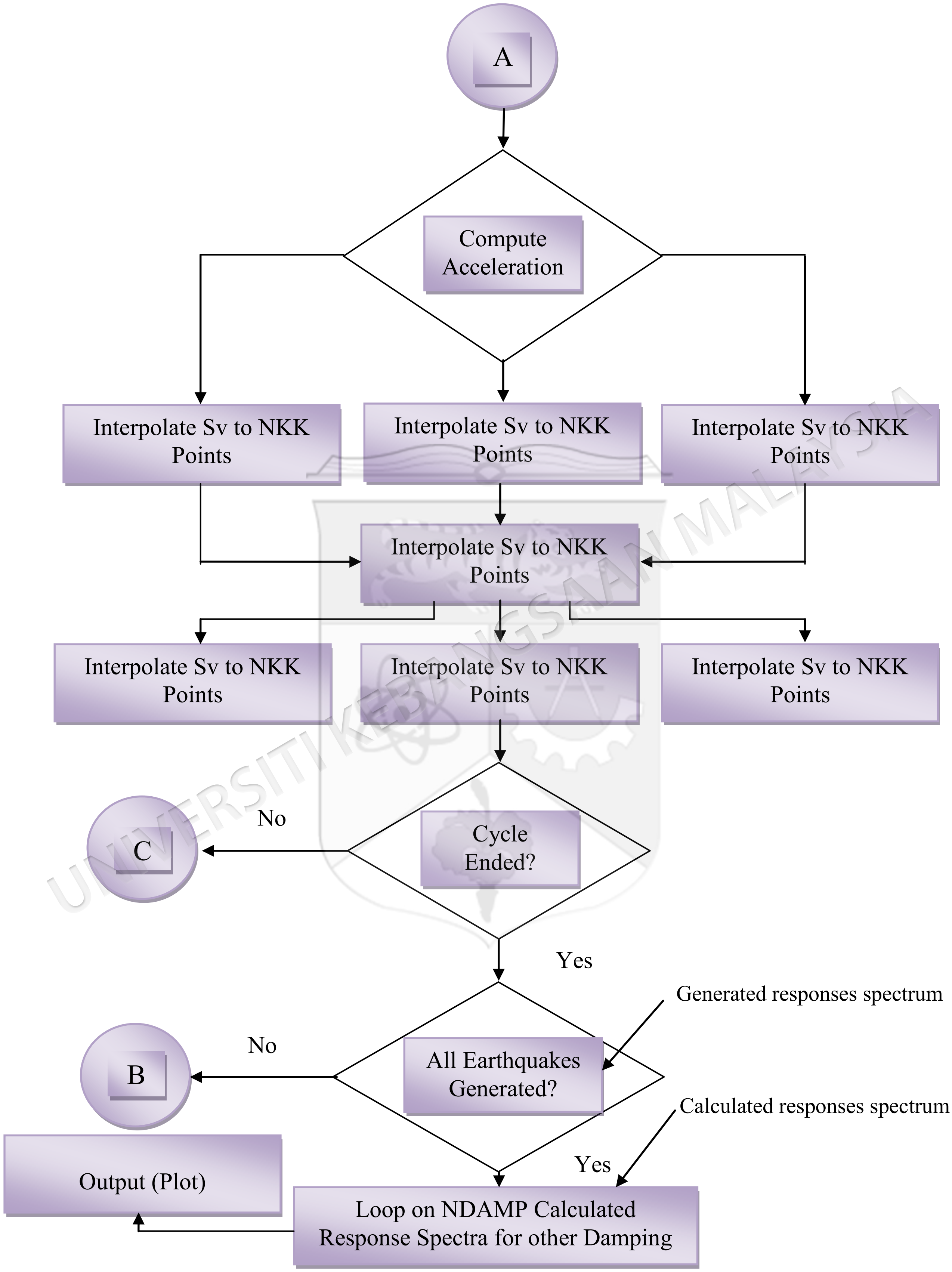

Source: SIMQKE theory manual

APPENDIX III

Soil profile parameters

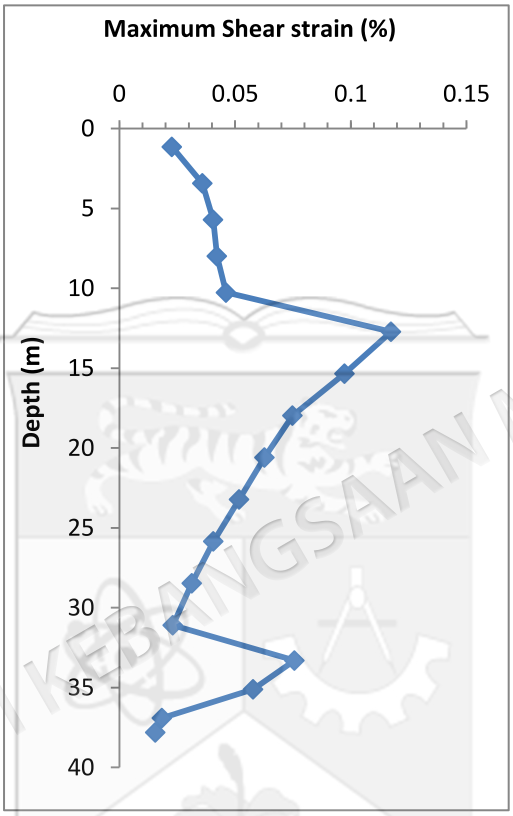

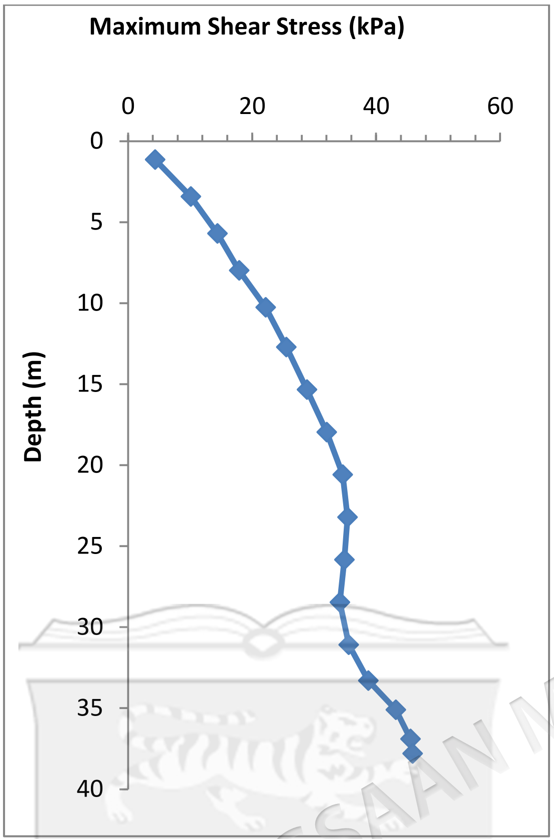
Maximum Shear Stress (kPa)
0
20
40
60
Depth (m)
0
5
10
15
20
25
30
35
40

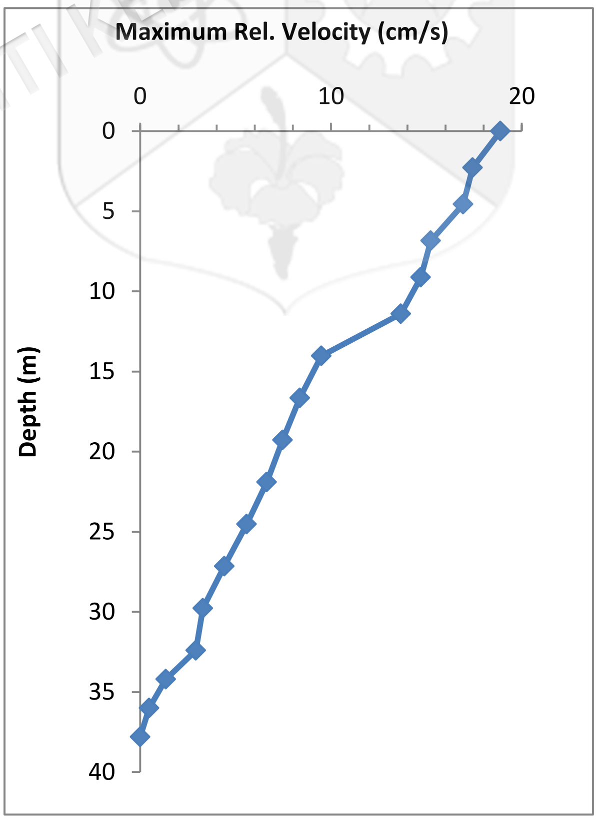
Maximum Rel. Velocity (cm/s)
0
10
20
Depth (m)
0
5
10
15
20
25
30
35
40

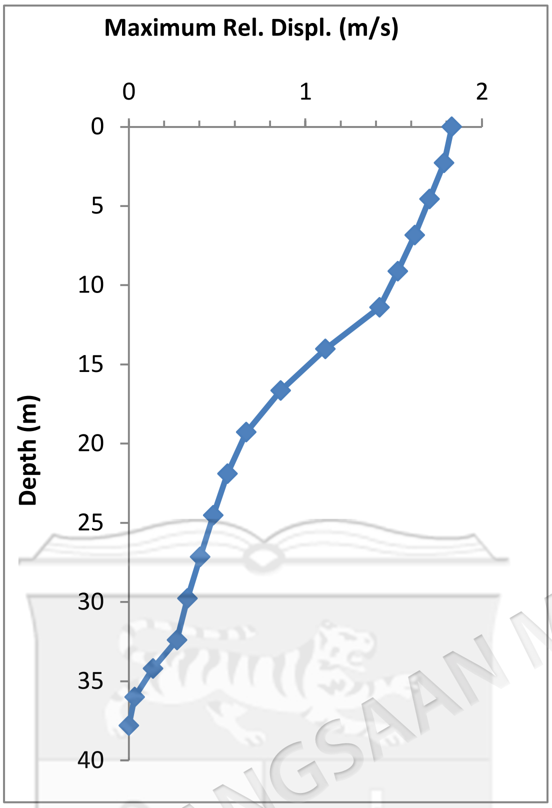
Maximum Rel. Displ. (m/s)
0
1
2
0
5
10
15
20
25
30
35
40
Depth (m)

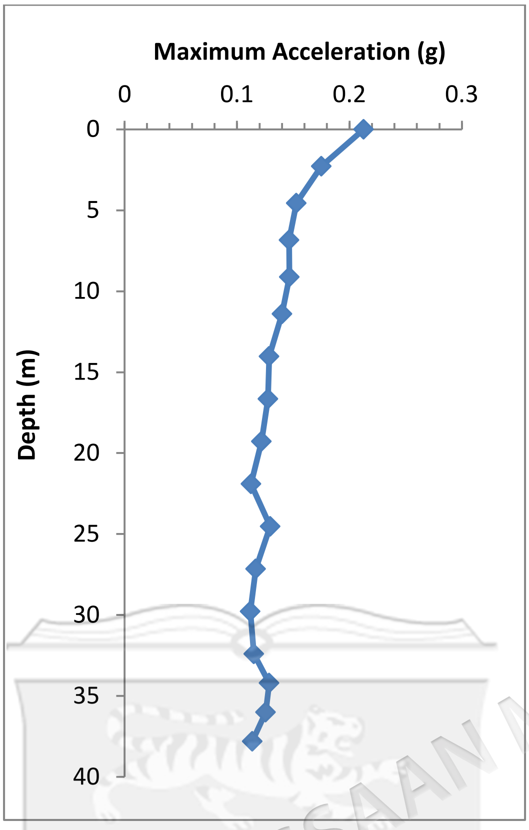
Maximum Acceleration (g)
0
0.1
0.2
0.3
Depth (m)
0
5
10
15
20
25
30
35
40

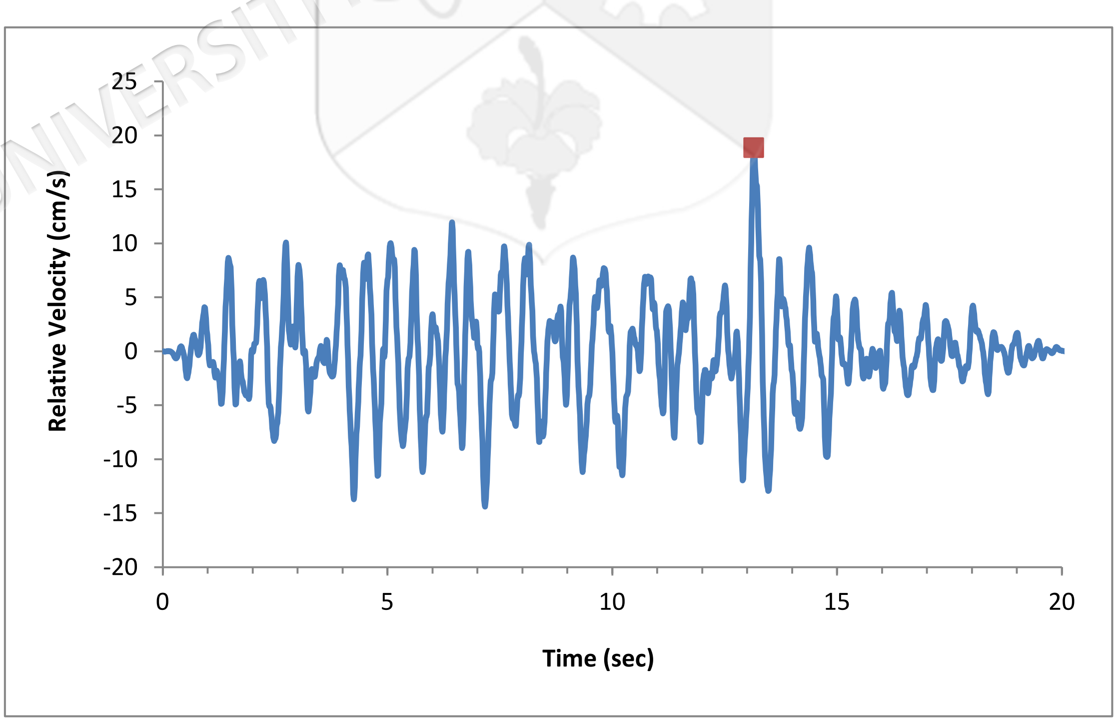
Relative Velocity (cm/s)
25
20
15
10
5
0
-5
-10
-15
-20
0
5
10
15
20
Time (sec)

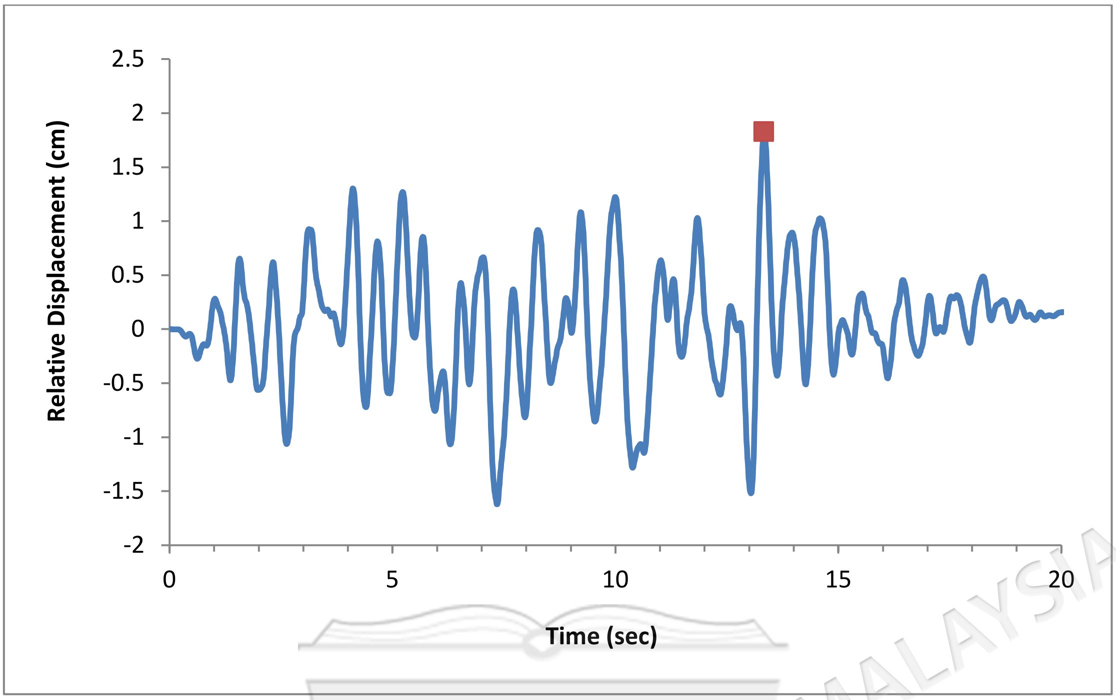
Relative Displacement (cm)
2.5
2
1.5
1
0.5
0
-0.5
-1
-1.5
-2
0
5
10
15
20
Time (sec)

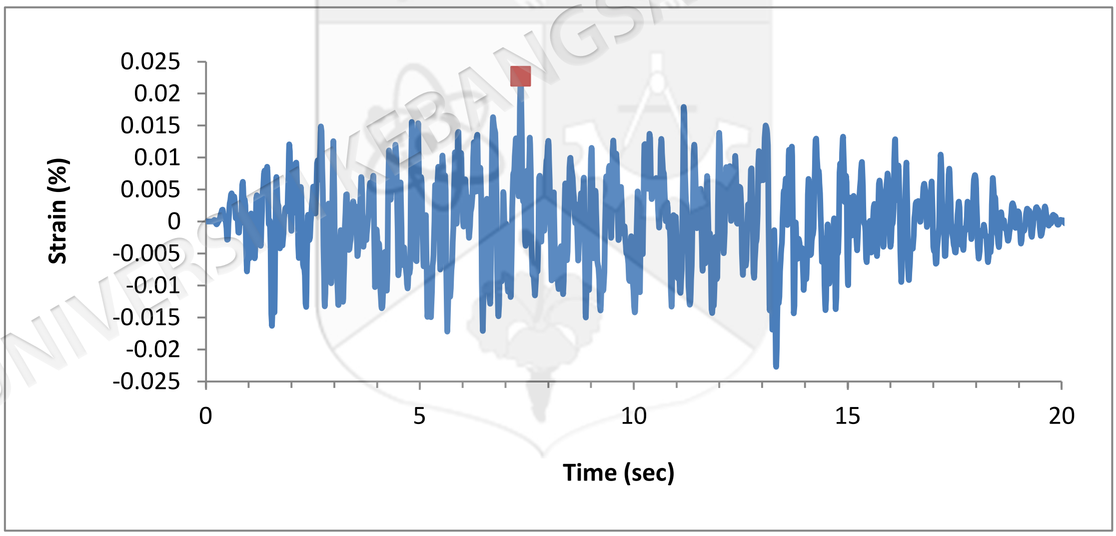
Strain (%)
0.025
0.02
0.015
0.01
0.005
0
-0.005
-0.01
-0.015
-0.02
-0.025
0
5
10
15
20
Time (sec)

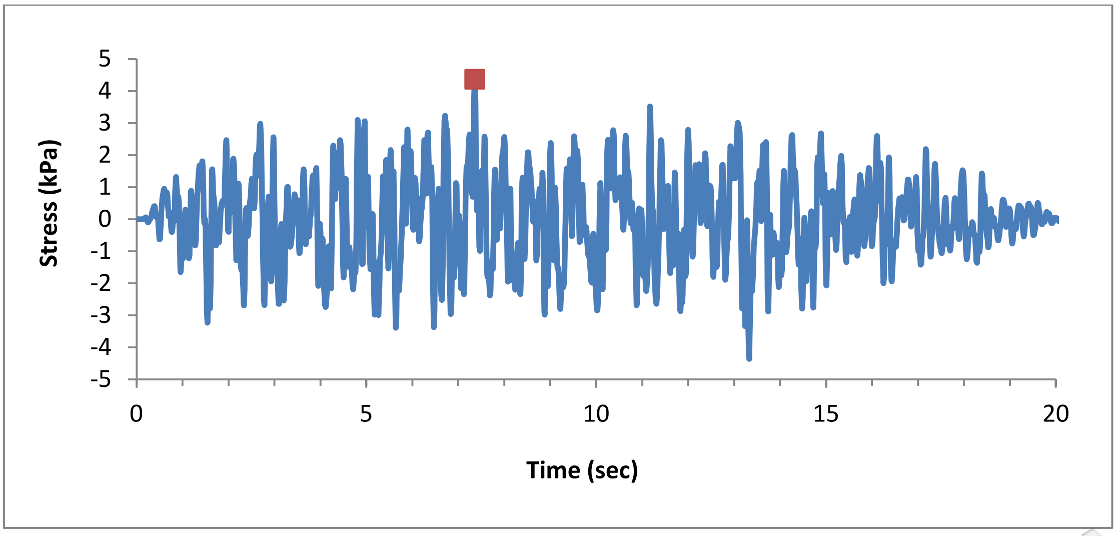
Stress (kPa)
5
4
3
2
1
0
-1
-2
-3
-4
-5
0
5
10
15
20
Time (sec)

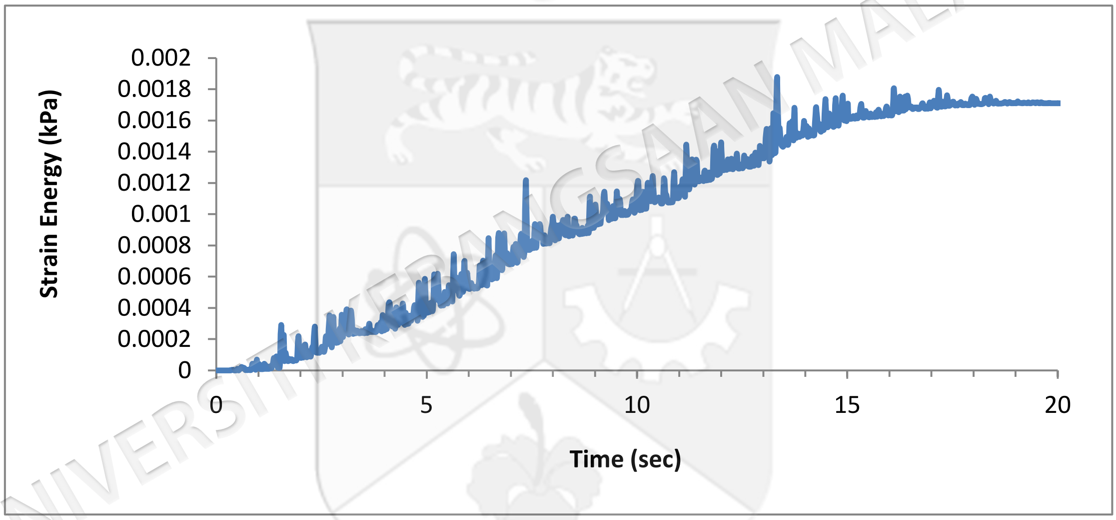
Strain Energy (kPa)
0.002
0.0018
0.0016
0.0014
0.0012
0.001
0.0008
0.0006
0.0004
0.0002
0
0
5
10
15
20
Time (sec)

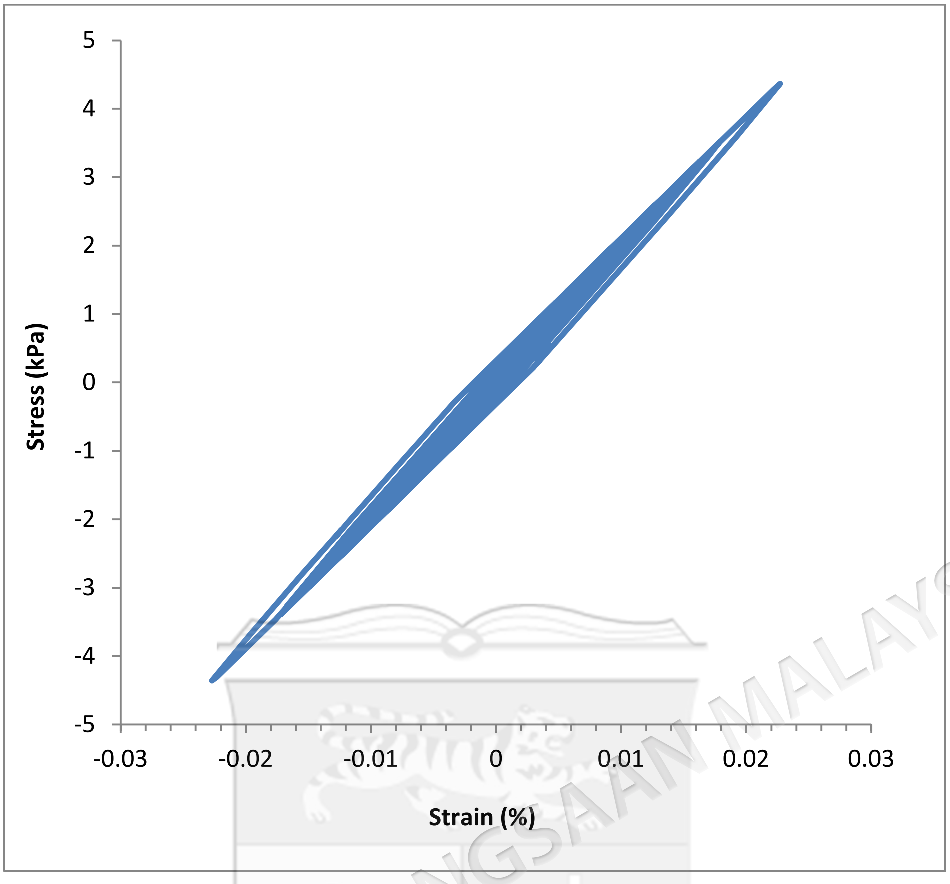

Stress (kPa)
5
4
3
2
1
0
-1
-2
-3
-4
-5
-0.03
-0.02
-0.01
0
0.01
0.02
0.03
Strain (%)

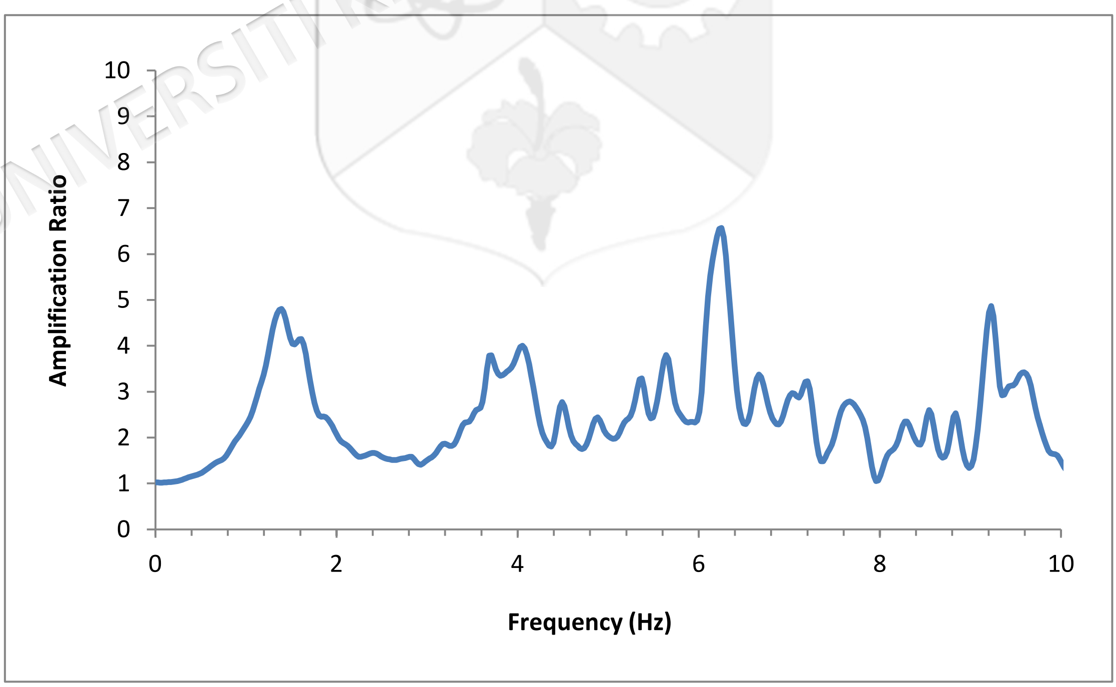

Amplification Ratio
10
9
8
7
6
5
4
3
2
1
0
0
2
4
6
8
10
Frequency (Hz)

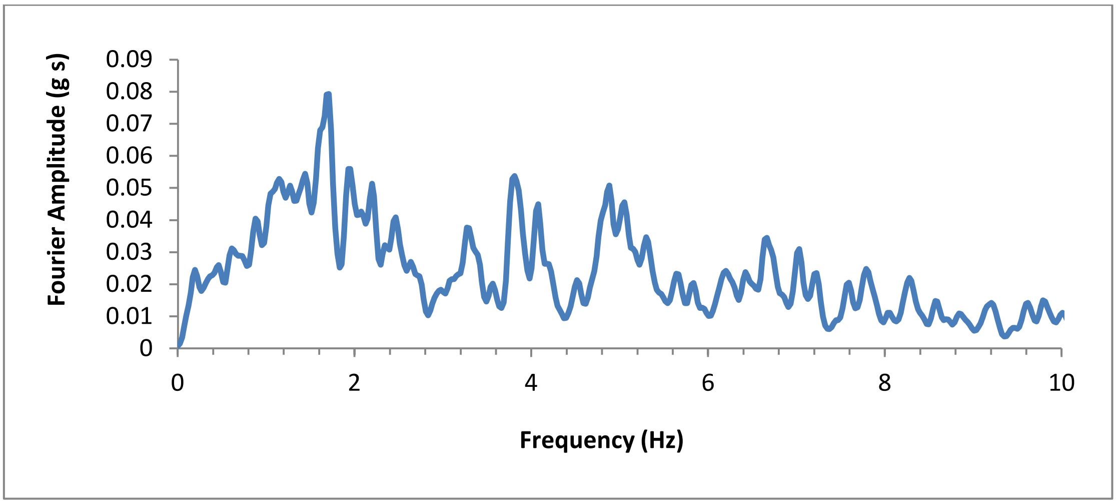
Fourier Amplitude (g s)
0.09
0.08
0.07
0.06
0.05
0.04
0.03
0.02
0.01
0
0
2
4
6
8
10
Frequency (Hz)

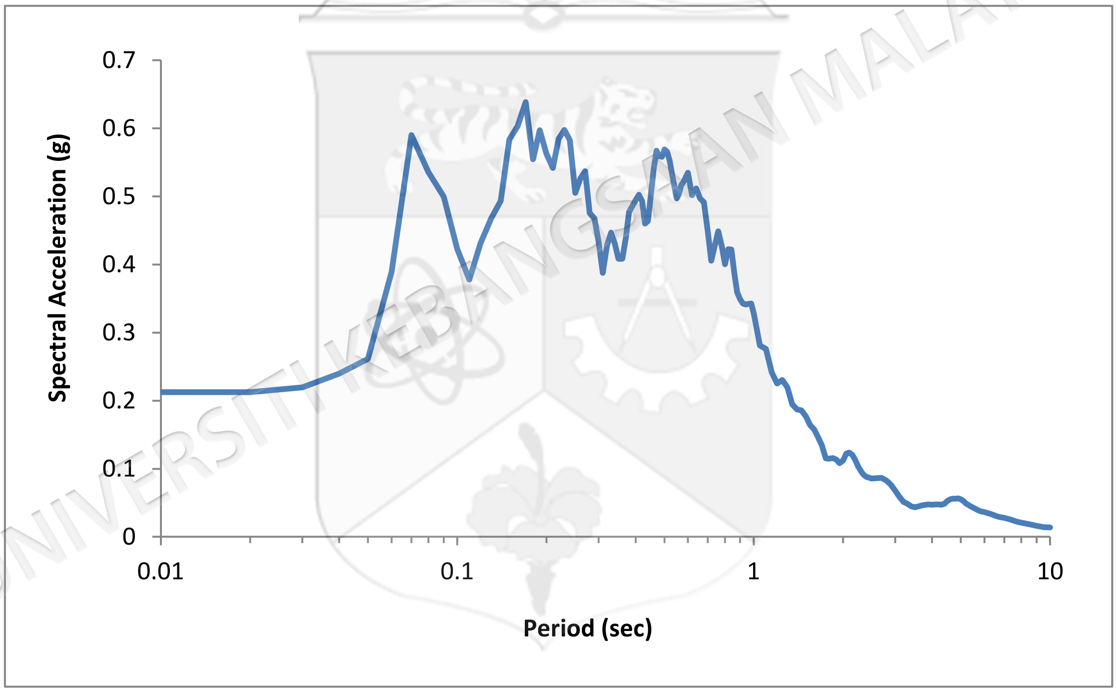
Spectral Acceleration (g)
0.7
0.6
0.5
0.4
0.3
0.2
0.1
0
0.01
0.1
1
10
Period (sec)

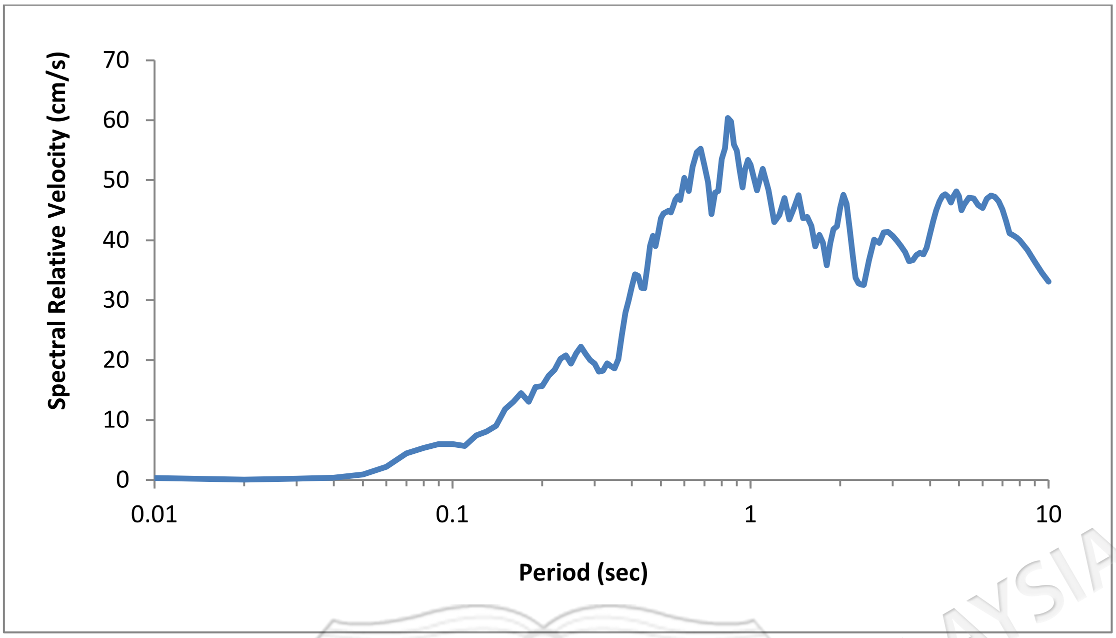
Spectral Relative Velocity (cm/s)
70
60
50
40
30
20
10
0
0.01
0.1
1
10
Period (sec)

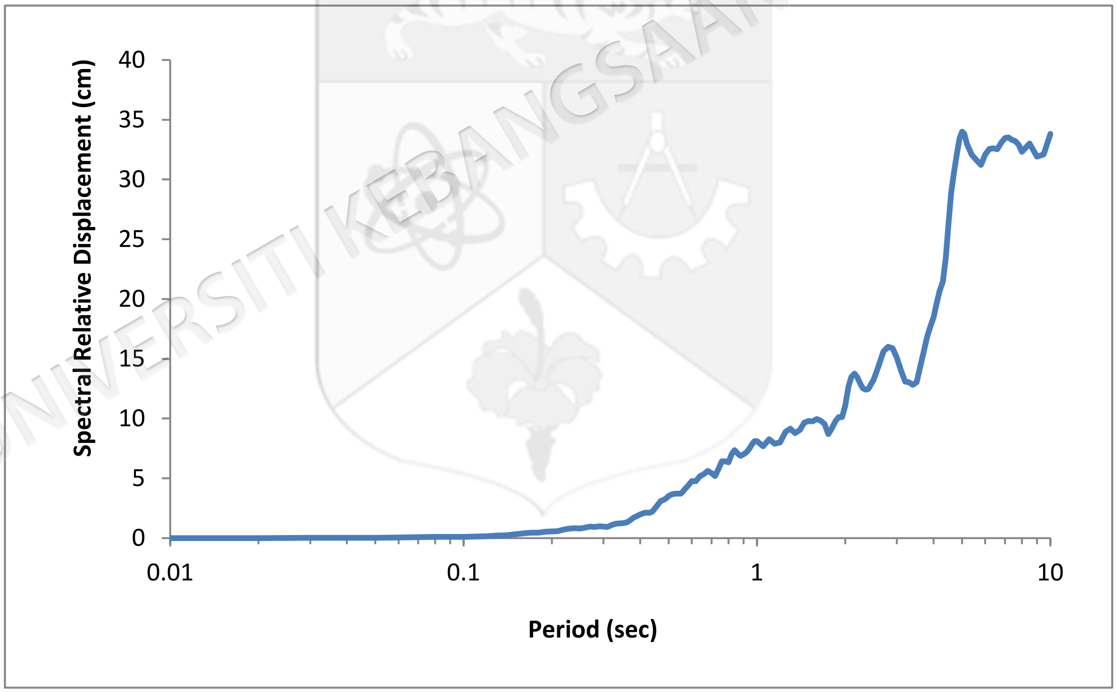
Spectral Relative Displacement (cm)
40
35
30
25
20
15
10
5
0
0.01
0.1
1
10
Period (sec)

APPENDIX IV

Mode shapes (fixed base approach) of the circular tank

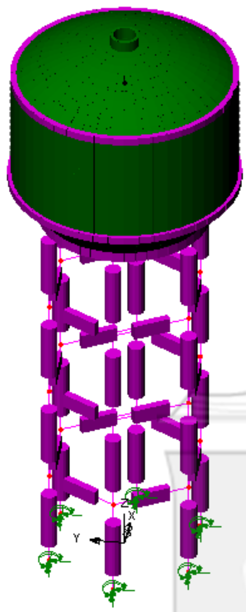

Mode (1) Frequency =0.315180

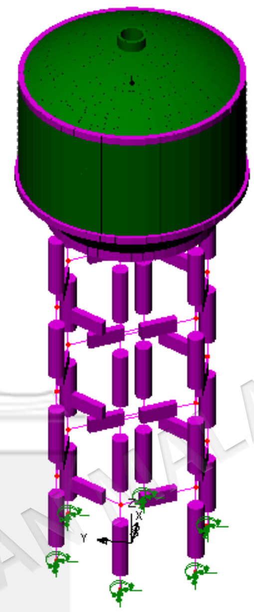

Mode (2) Frequency =0.315180

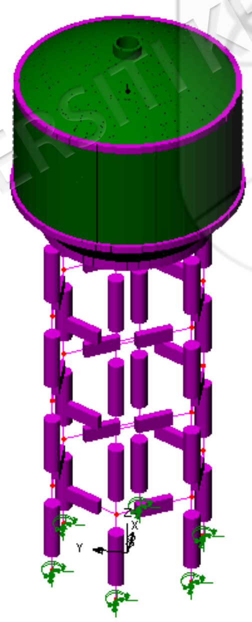

Mode (3) Frequency =0.318588

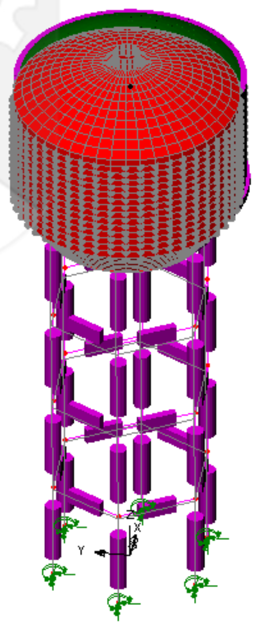

Mode (4) Frequency =1.77077

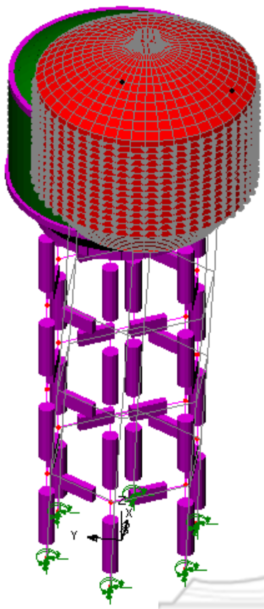

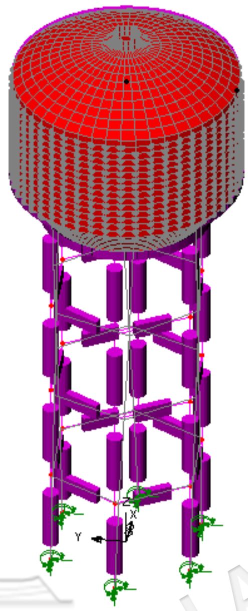

Mode (5) Frequency =1.77079

Mode (6) Frequency =2.09683

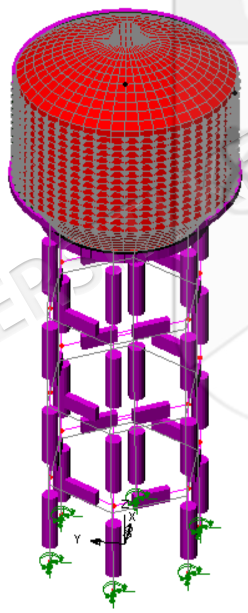

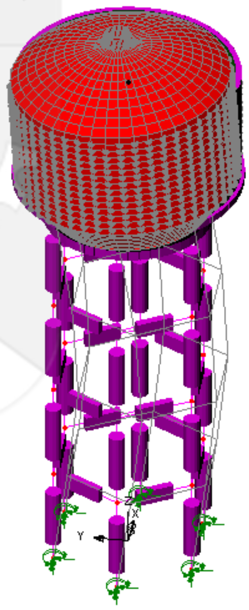

Mode (7) Frequency =10.1249

Mode (8) Frequency =10.1251

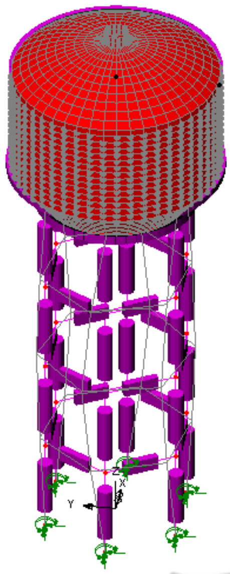

Mode (9) Frequency =13.3404

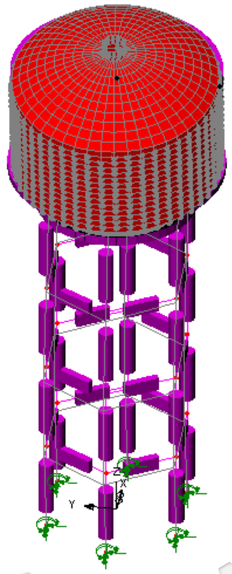

Mode (10) Frequency =13.8596

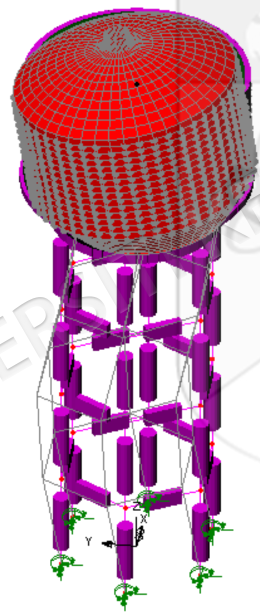

Mode (11) Frequency =13.8597

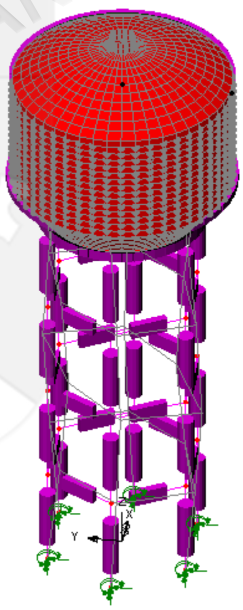

Mode (12) Frequency =14.8626

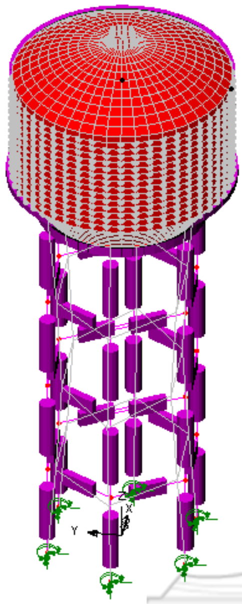

Mode (13) Frequency =14.8626

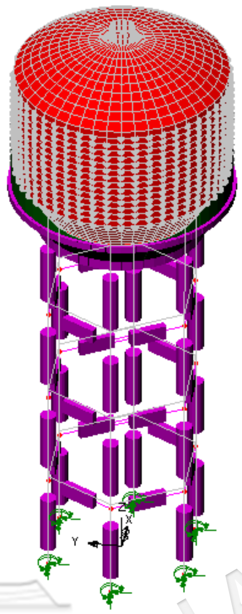

Mode (14) Frequency =14.9227

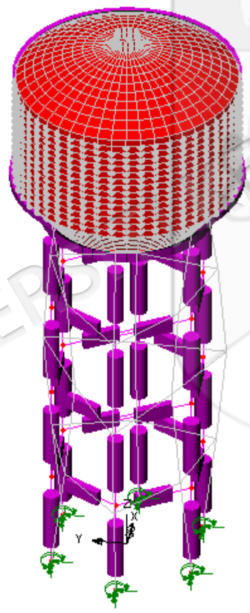

Mode (15) Frequency =14.9229

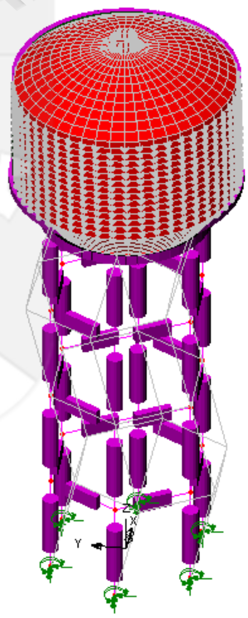

Mode (16) Frequency =18.5600

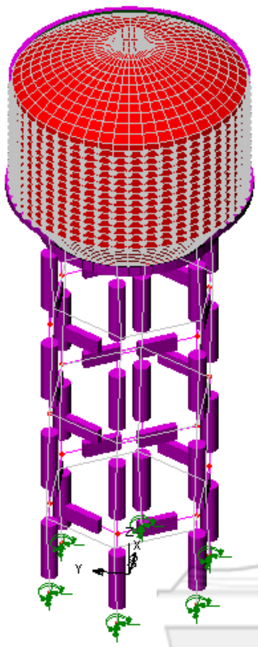

Mode (17) Frequency =19.3535

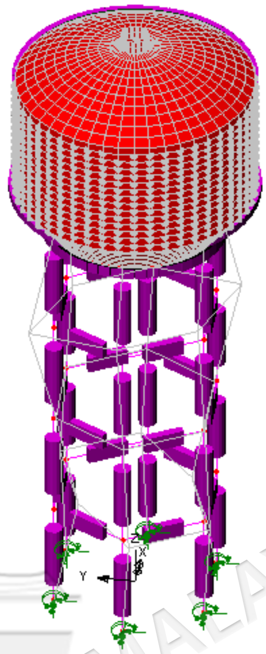

Mode (18) Frequency =20.4382

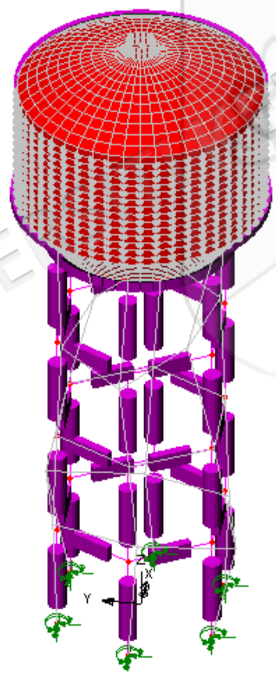

Mode (19) Frequency =20.6770

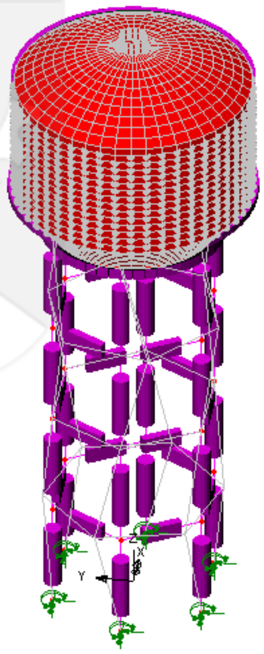

Mode (20) Frequency =20.6770

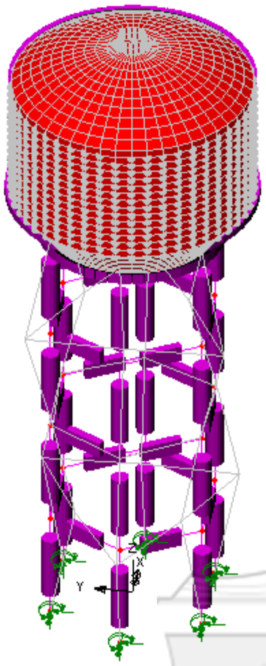

Mode (21) Frequency =20.6948

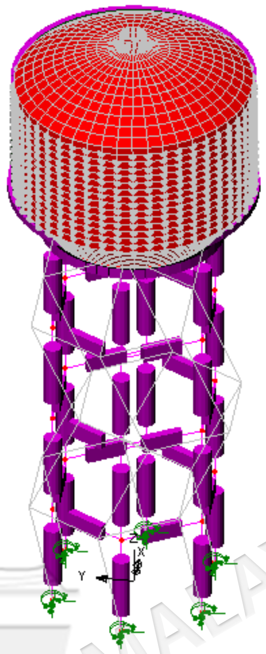

Mode (22) Frequency =20.6948

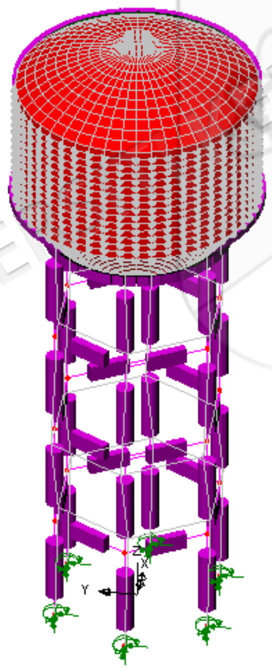

Mode (23) Frequency =21.2969

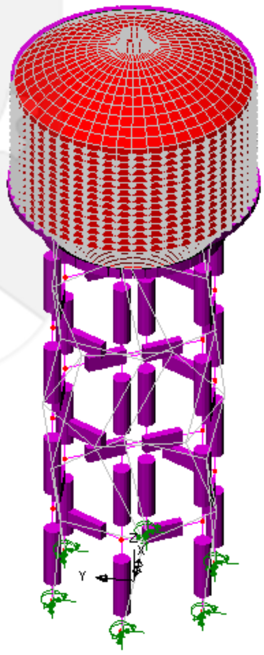

Mode (24) Frequency =21.6098

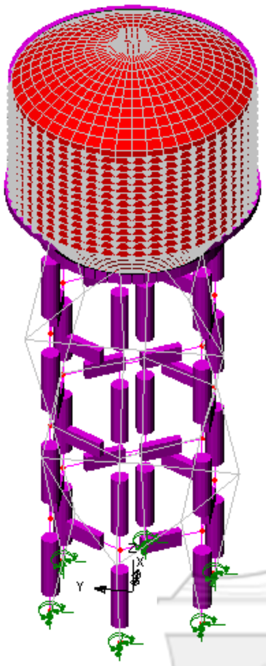

Mode (25) Frequency =23.8928

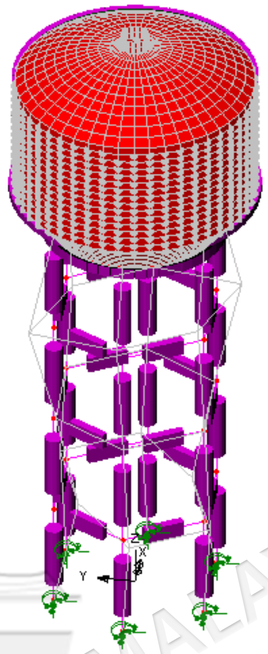

Mode (26) Frequency =23.8928

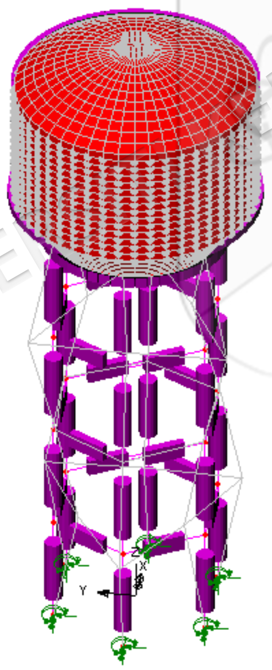

Mode (27) Frequency =25.1404

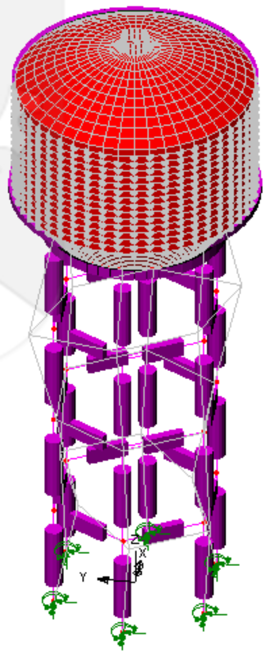

Mode (28) Frequency =25.1404

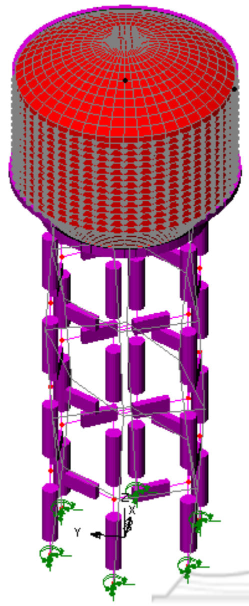

Mode (29) Frequency =26.2133

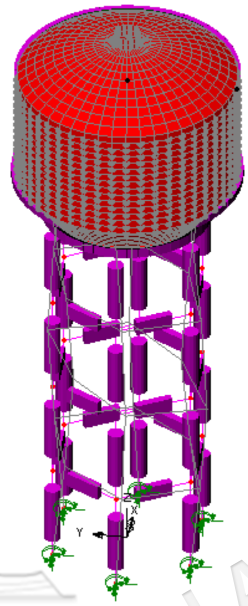

Mode (30) Frequency =26.2133

Mode shapes (Fixed Base Approach) of the rectangular Tank

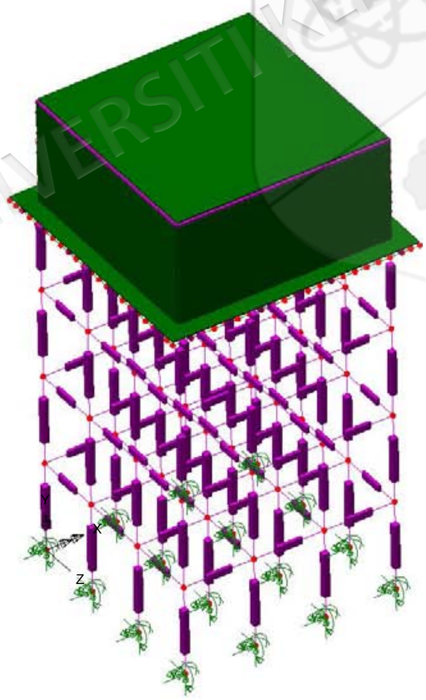

Mode (1) Frequency =0.36441

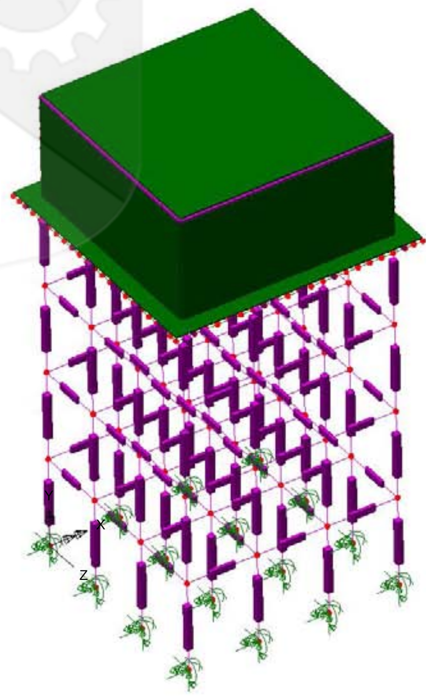

Mode (2) Frequency =0.36441

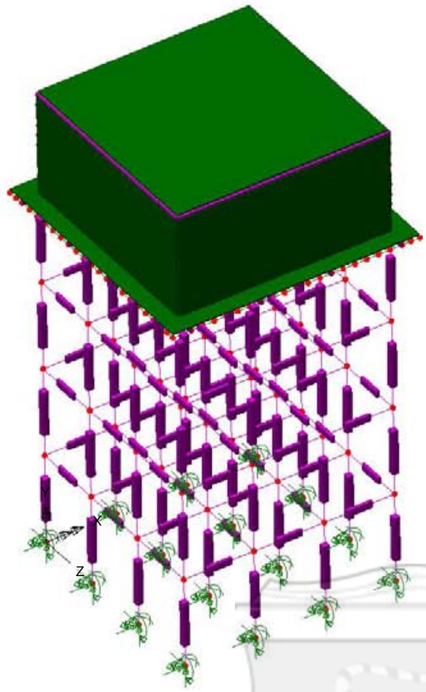

Mode (3) Frequency =0.366072

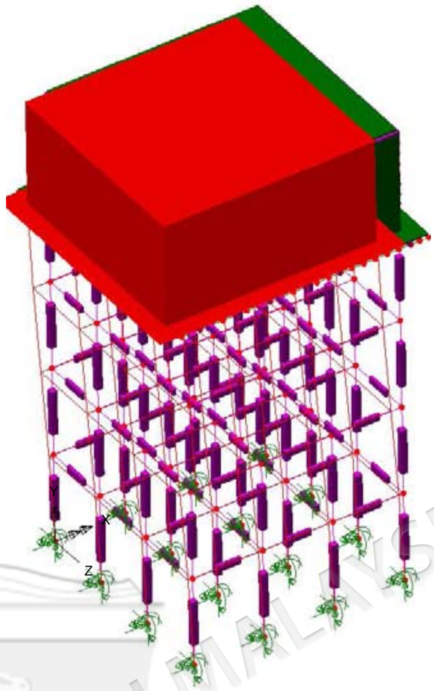

Mode (4) Frequency =2.96197

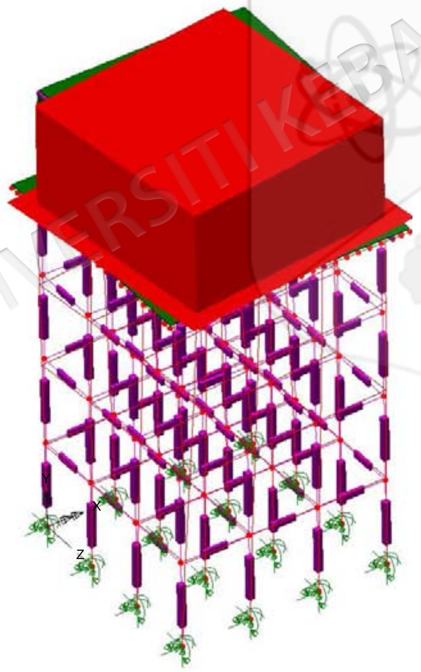

Mode (5) Frequency =2.96197

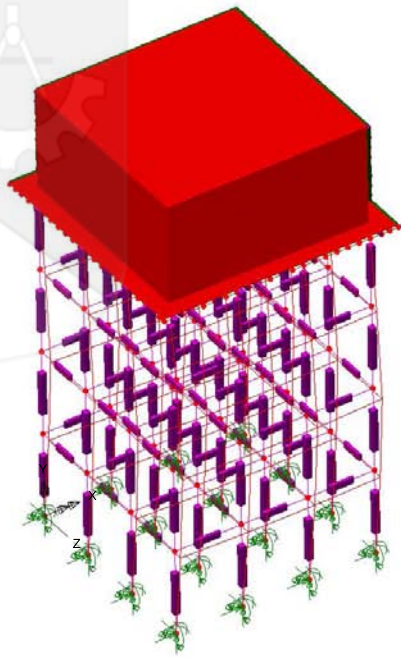

Mode (6) Frequency =3.21988

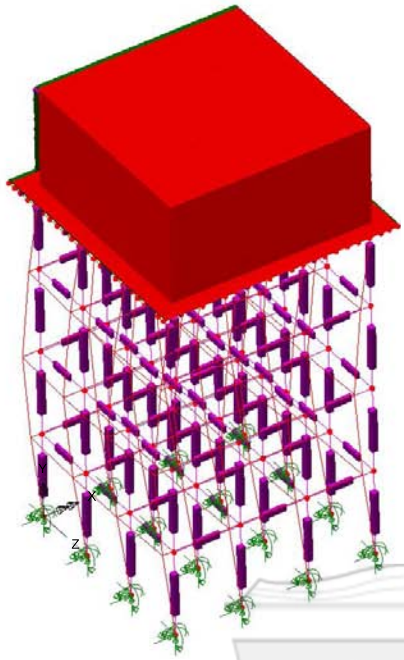

Mode (7) Frequency =3.63345

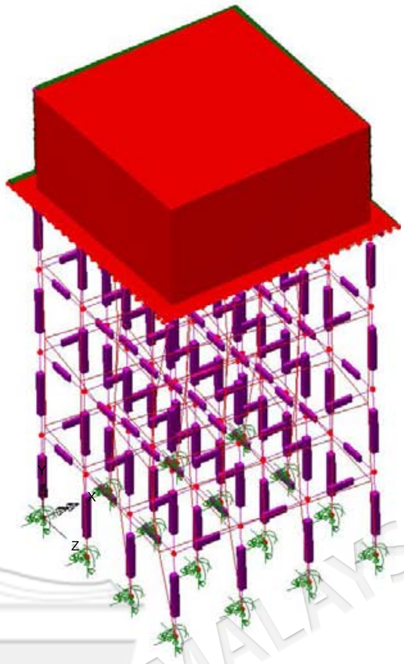

Mode (8) Frequency =4.43994

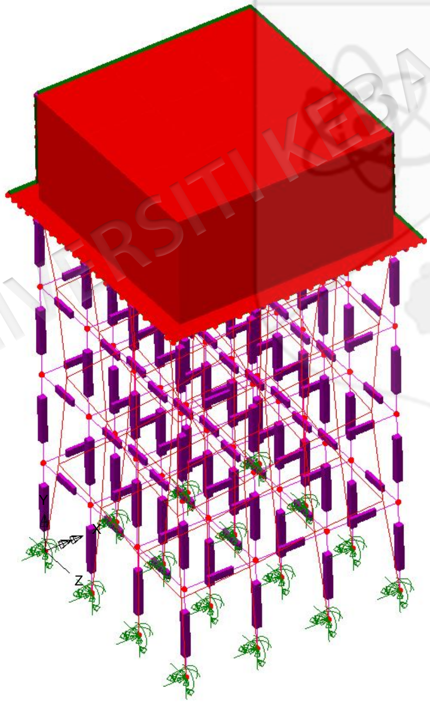

Mode (9) Frequency =4.43994

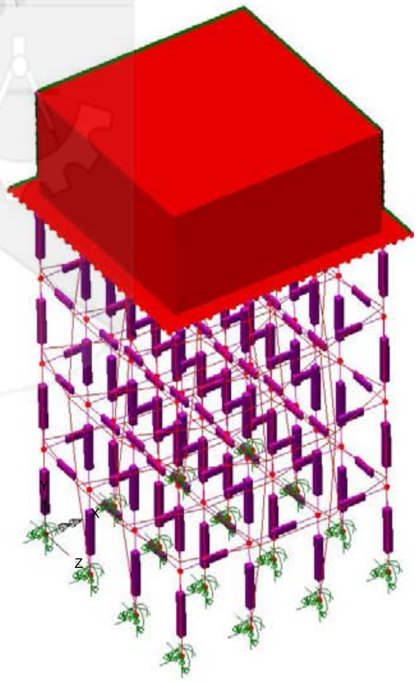

Mode (10) Frequency =5.60893

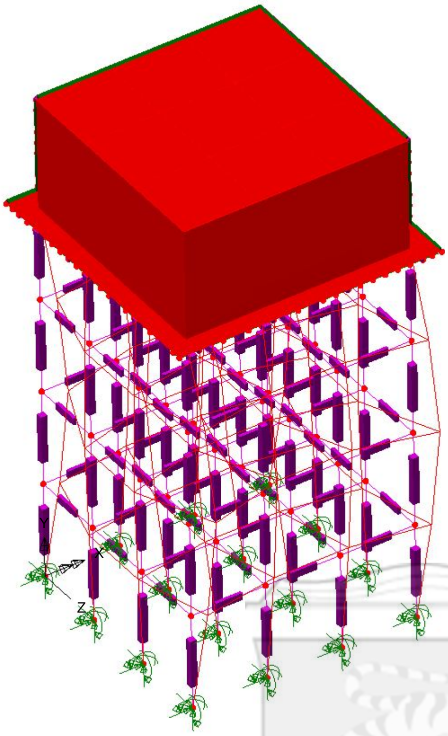

Mode (11) Frequency =5.81082

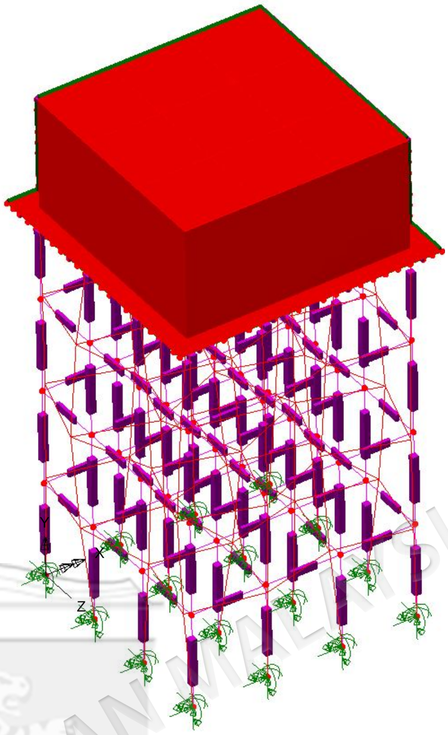

Mode (12) Frequency =6.2347

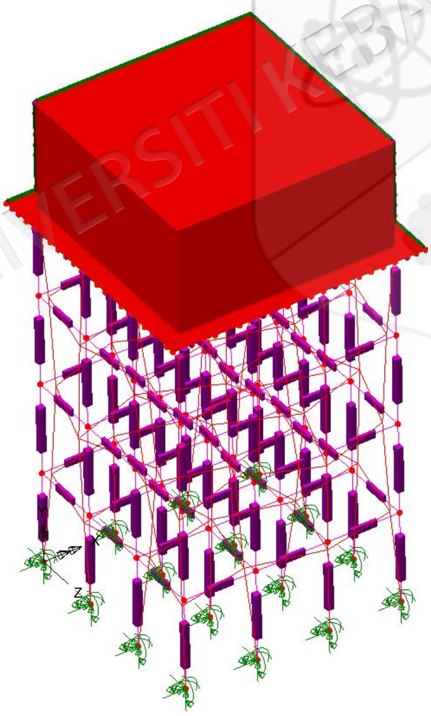

Mode (13) Frequency =6.2347

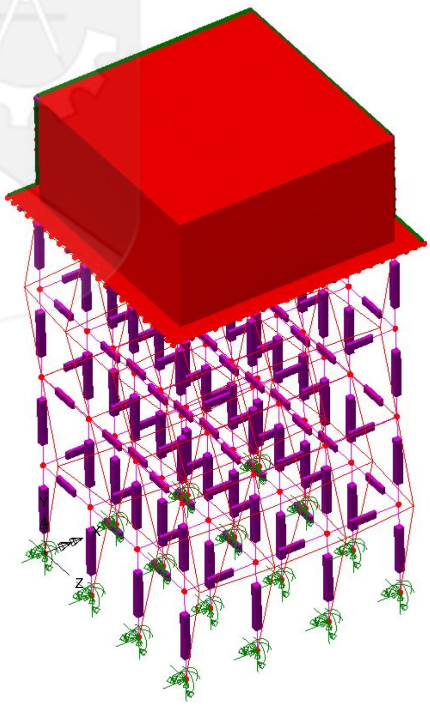

Mode (14) Frequency =6.77073

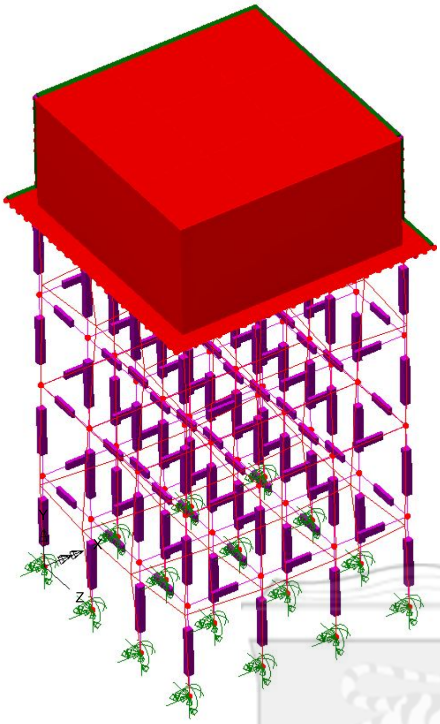

Mode (15) Frequency =6.89623

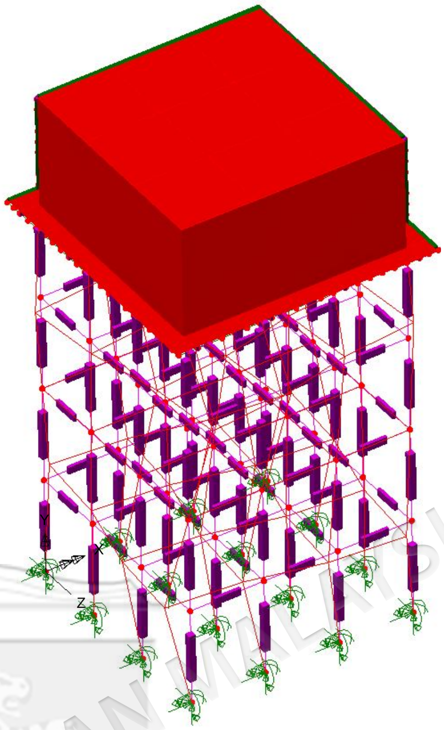

Mode (16) Frequency =7.07538

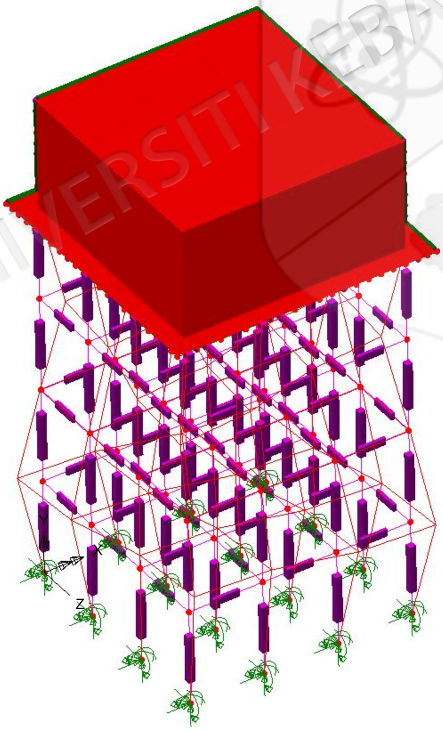

Mode (17) Frequency =7.07538

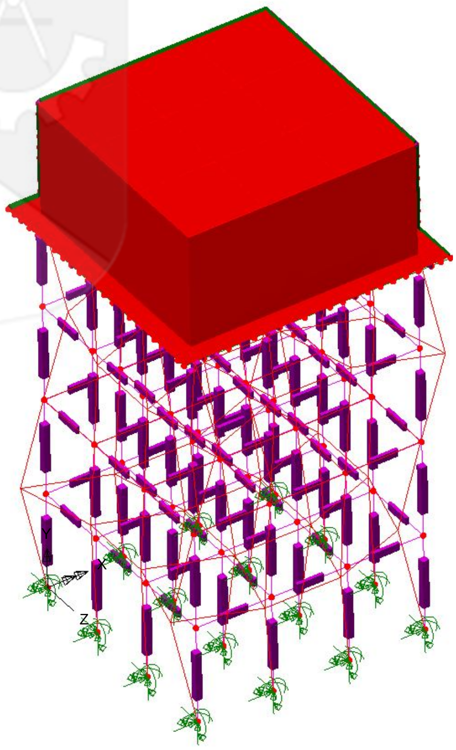

Mode (18) Frequency =7.38955

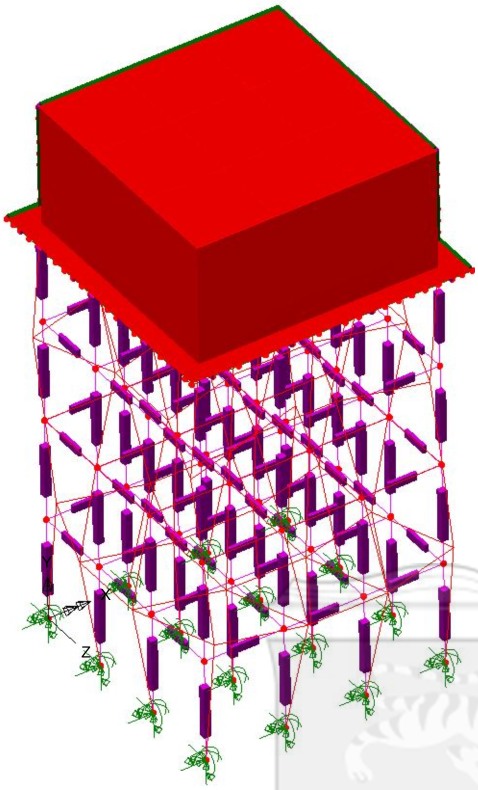

Mode (19) Frequency =7.62554

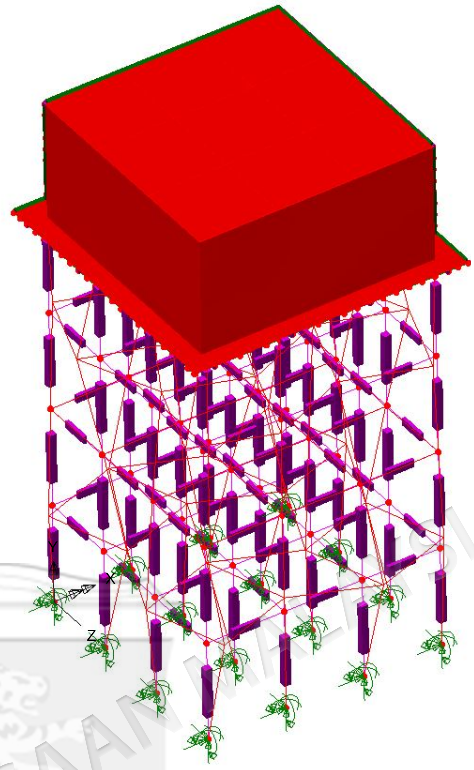

Mode (20) Frequency =7.62554

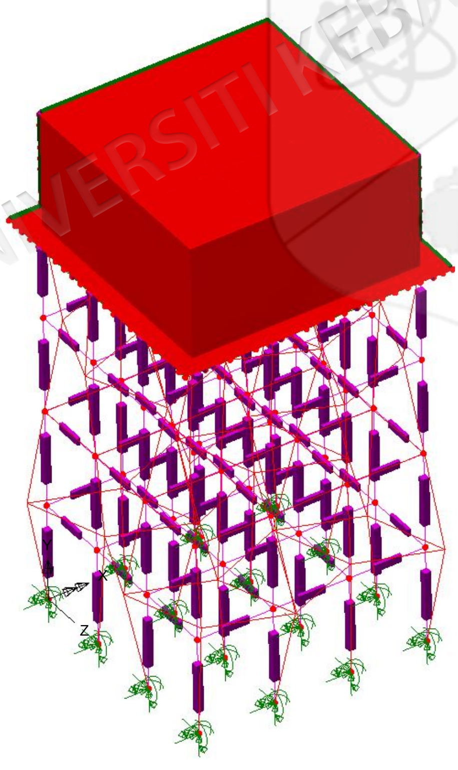

Mode (21) Frequency =7.94581

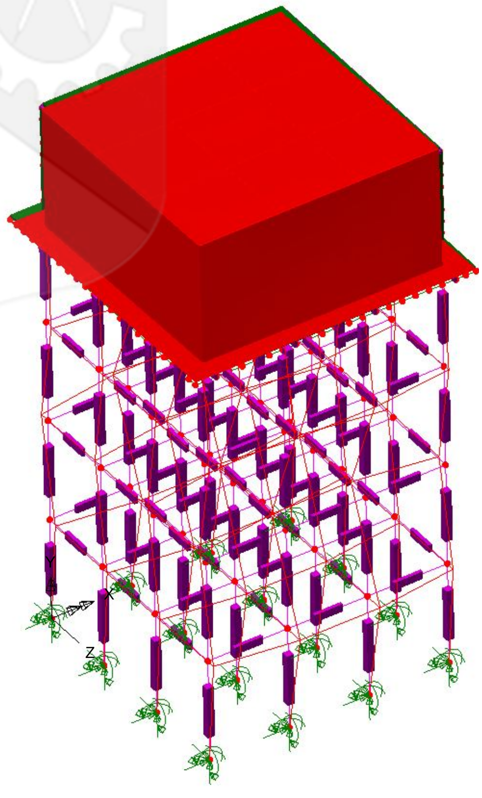

Mode (22) Frequency =8.4026

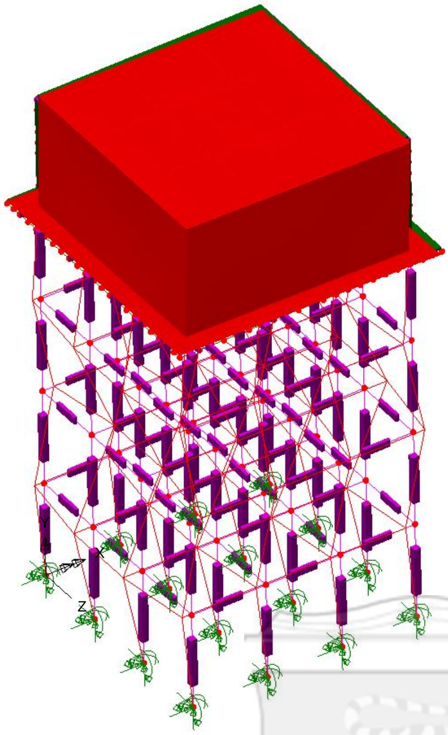

Mode (23) Frequency =8.51107

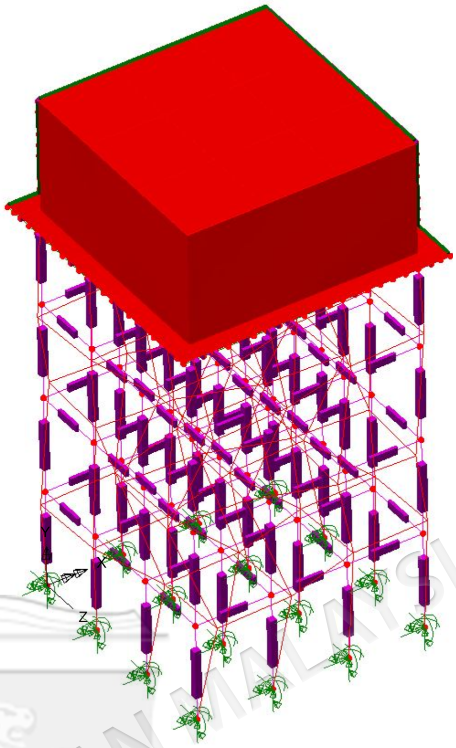

Mode (24) Frequency =8.60545

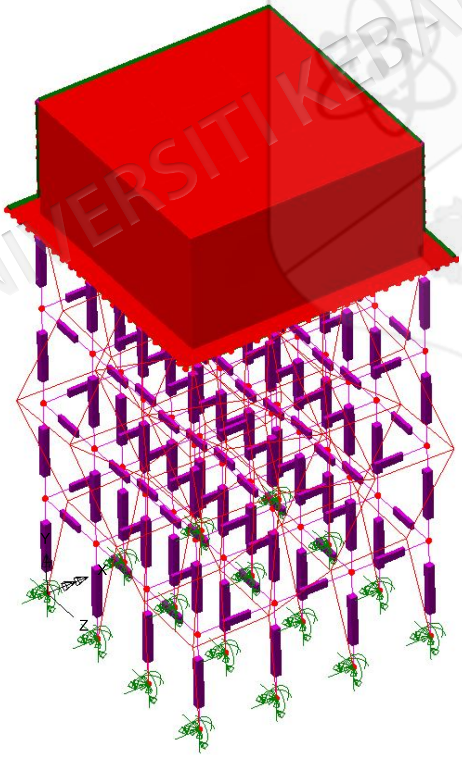

Mode (25) Frequency =9.27687

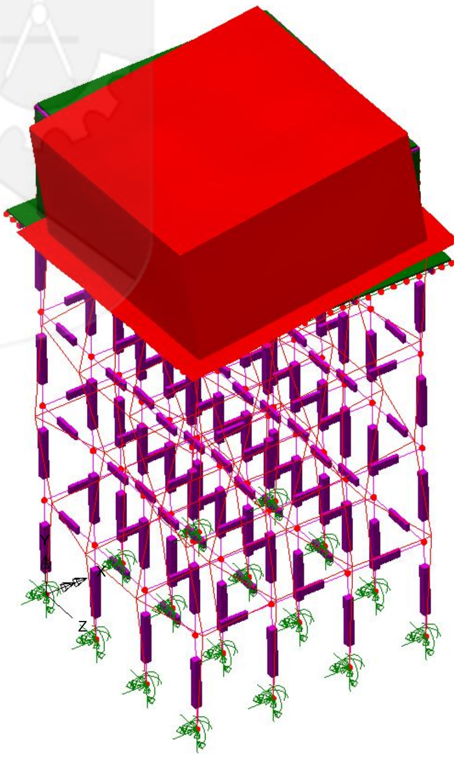

Mode (26) Frequency =9.27687

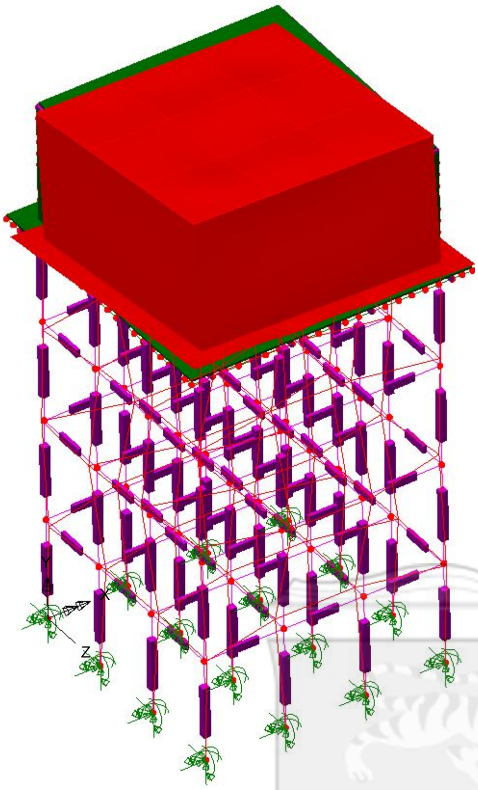

Mode (27) Frequency =9.88078

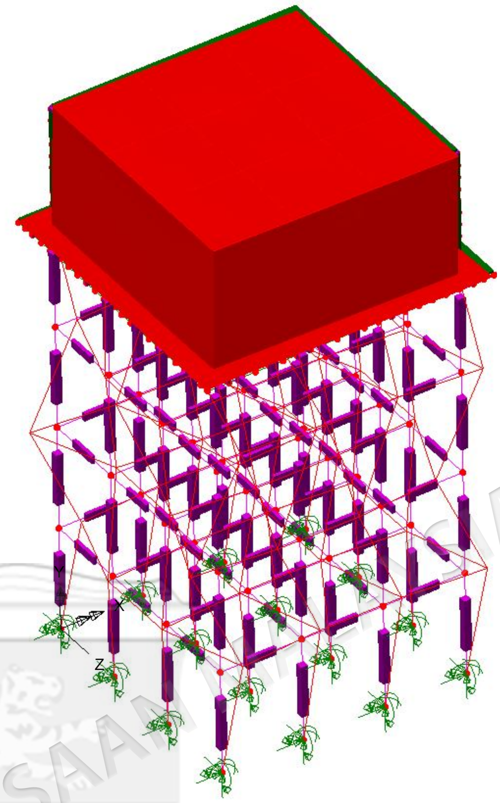

Mode (28) Frequency =9.88078

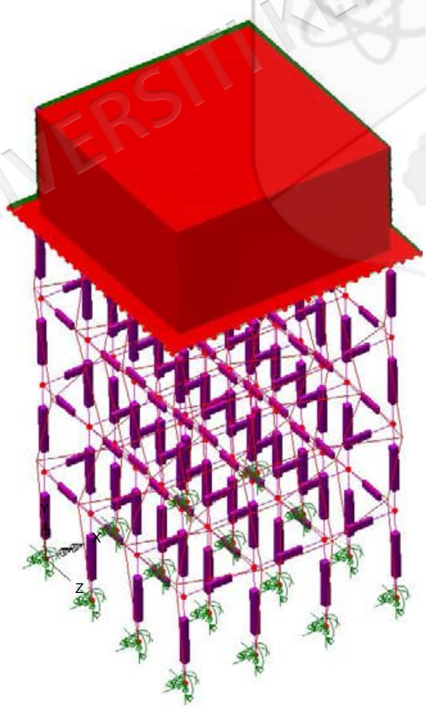

Mode (29) Frequency =10.3899

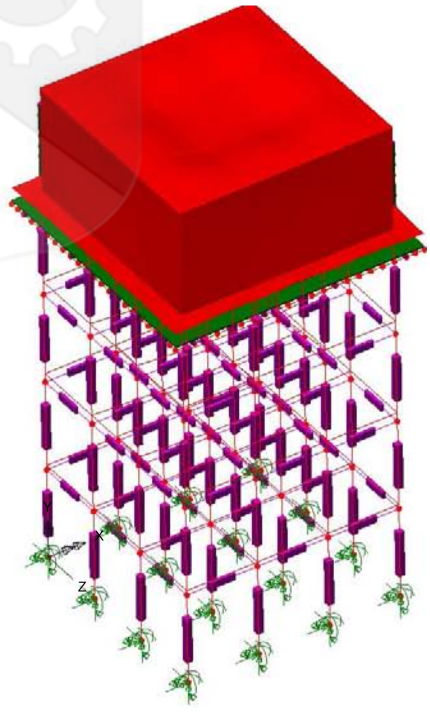

Mode (30) Frequency =10.4493

Mode shapes numbers associated with natural frequency of circular elevated tank

Mode	Eigenvalue	Error norm
1	3.92173	0.368704E-10
2	3.92174	0.410935E-10
3	4.00700	0.117464E-09
4	123.790	0.196172E-09
5	123.793	0.855875E-09
6	173.574	0.574413E-09
7	4047.10	0.433935E-09
8	4047.22	0.536257E-09
9	7025.83	0.572588E-09
10	7583.32	0.555571E-09
11	7583.51	0.140874E-09
12	8720.71	0.109772E-09
13	8720.71	0.508307E-10
14	8791.31	0.775633E-10
15	8791.53	0.245285E-09
16	13599.2	0.228732E-10
17	14786.9	0.347568E-09
18	16490.9	0.193371E-08
19	16878.6	0.469065E-08
20	16878.6	0.992196E-08
21	16907.6	0.417538E-07
22	16907.6	0.172940E-06
23	17905.7	0.418928E-09
24	18435.8	0.880205E-09
25	22536.8	0.102084E-07
26	22536.8	0.997615E-06
27	24952.0	0.329903E-06
28	24952.0	0.765652E-06
29	27127.0	0.118648E-06
30	27127.0	0.331645E-07

Mode shapes numbers associated with natural frequency of rectangular elevated tank

Mode	**Eigenvalue**	**Error norm**
1	5.24253	1.18E-09
2	5.24253	4.58E-10
3	5.29046	8.05E-10
4	346.354	9.09E-12
5	346.354	7.80E-12
6	409.298	7.91E-12
7	521.192	5.29E-12
8	778.239	3.57E-11
9	778.239	1.94E-11
10	1242.00	8.84E-12
11	1333.02	2.97E-11
12	1534.59	9.79E-12
13	1534.59	6.83E-12
14	1809.80	1.06E-11
15	1877.51	2.01E-11
16	1976.33	6.56E-09
17	1976.33	4.57E-08
18	2155.74	1.60E-11
19	2295.62	1.17E-09
20	2295.62	2.74E-11
21	2492.51	2.06E-11
22	2787.33	3.88E-11
23	2859.75	4.12E-11
24	2923.52	1.02E-11
25	3397.53	5.97E-11
26	3397.53	9.37E-08
27	3854.27	2.68E-11
28	3854.27	1.12E-07
29	4261.68	1.42E-09
30	4310.55	1.51E-10

APPENDIX V

Results of convergence study of time step along circular elevated concrete water tank

Time history response with various time steps at level 24.50 m

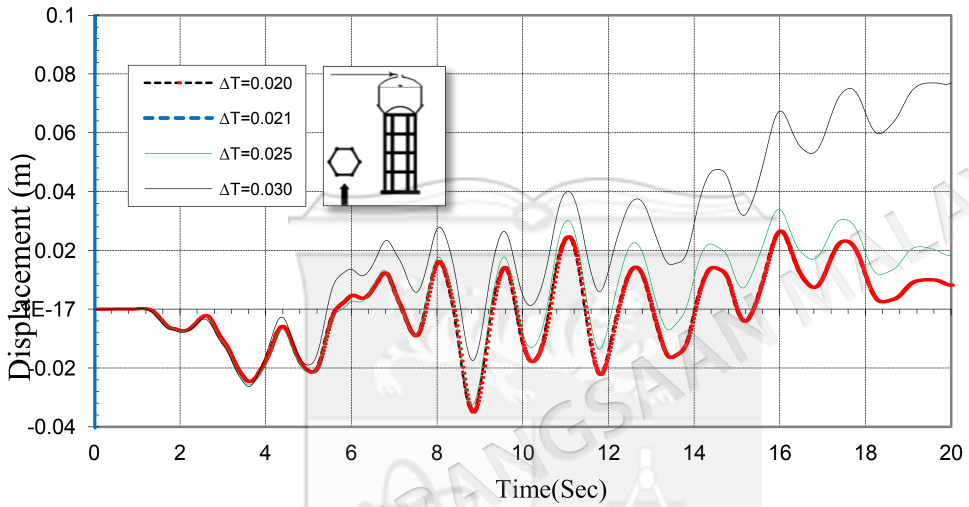

Time history response with various time steps at level 22.25 m

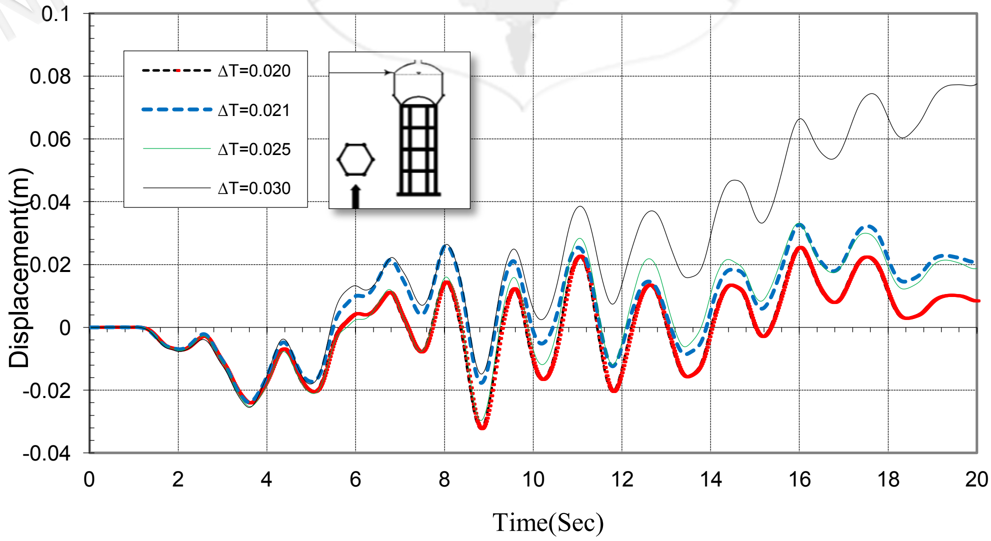

Time history response with various time steps at level 18.25 m

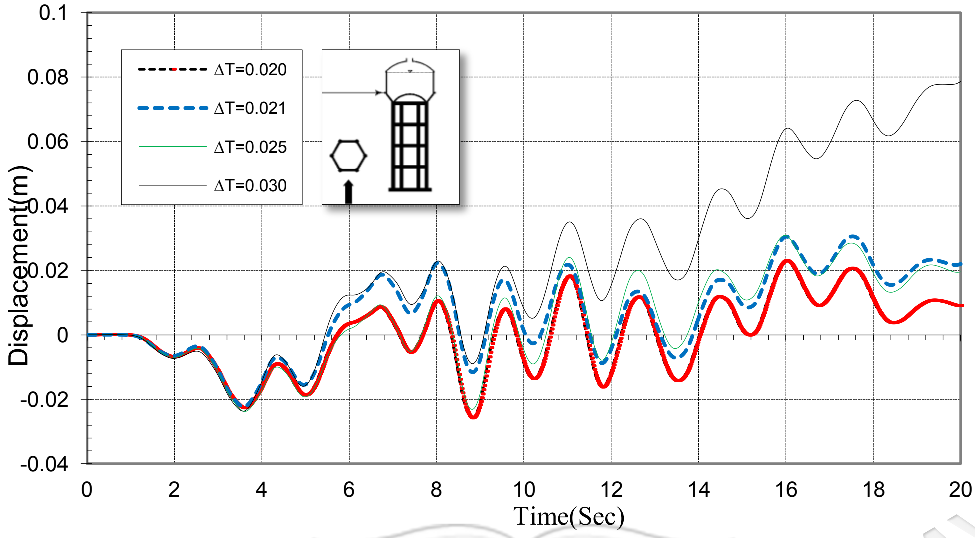

Time history response with various time steps at level 16.00 m

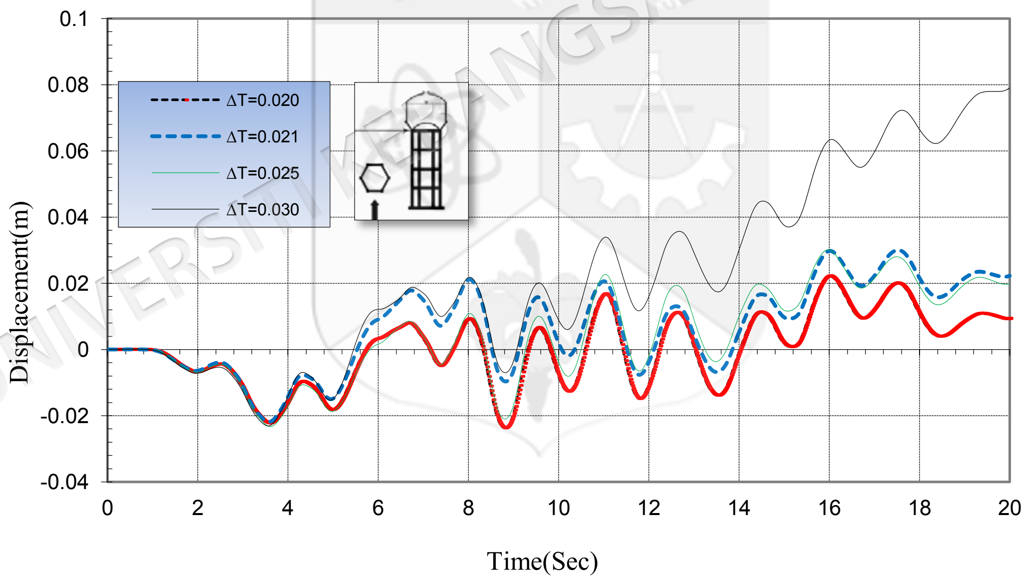

Time history response with various time steps at level 12.00 m

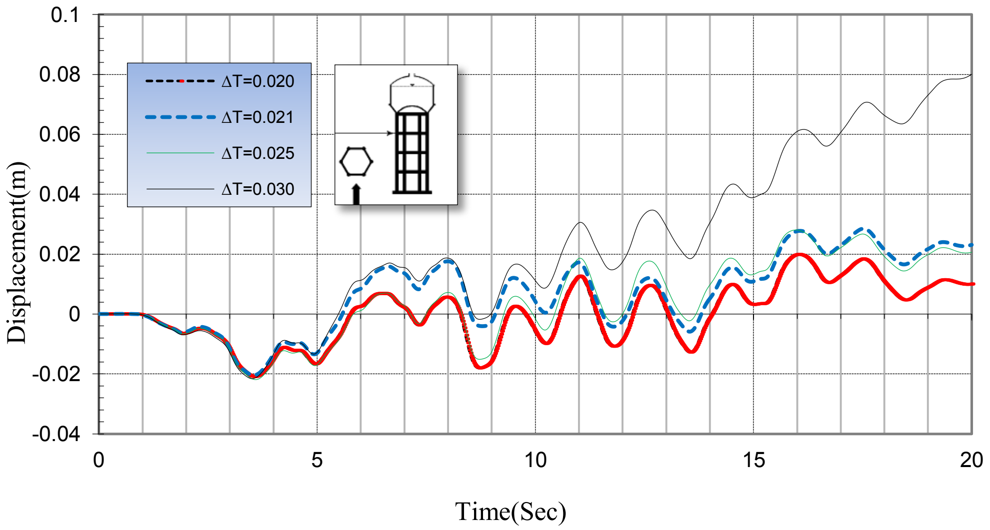

Time history response with various time steps at level 6.00 m

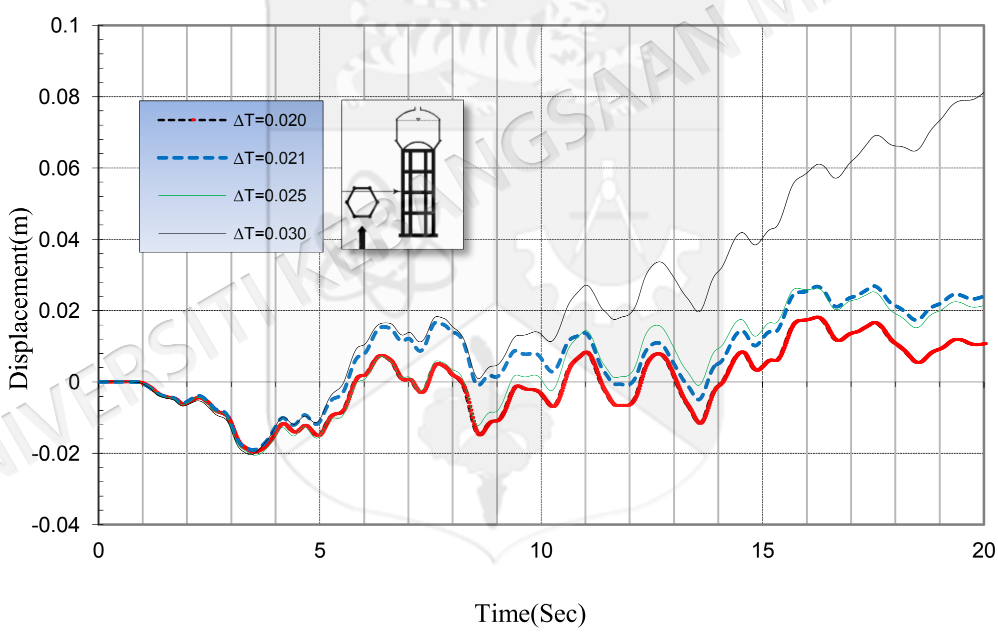

Time history response with various time steps at level 4.00 m

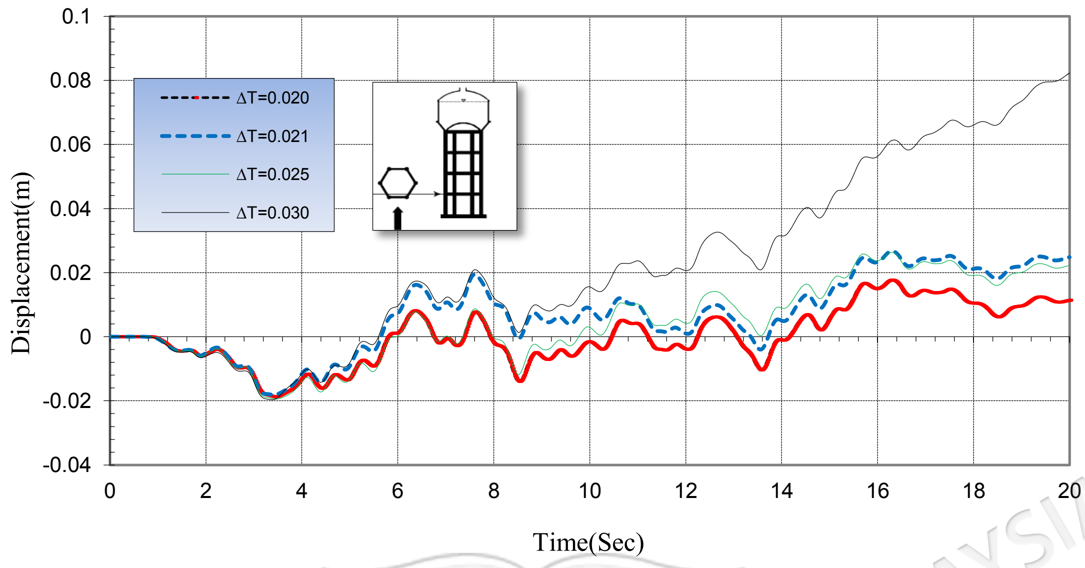

Time history response with various time steps at level 0.00 m

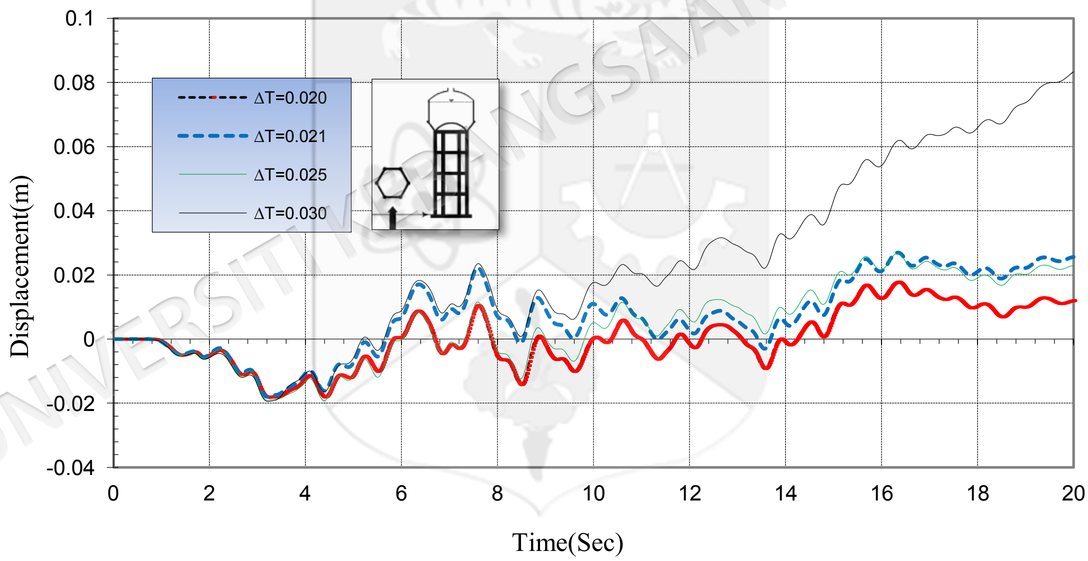

APPENDIX VI

Base shear time histories of the construction stages

Linear analysis (Newmark) direction I

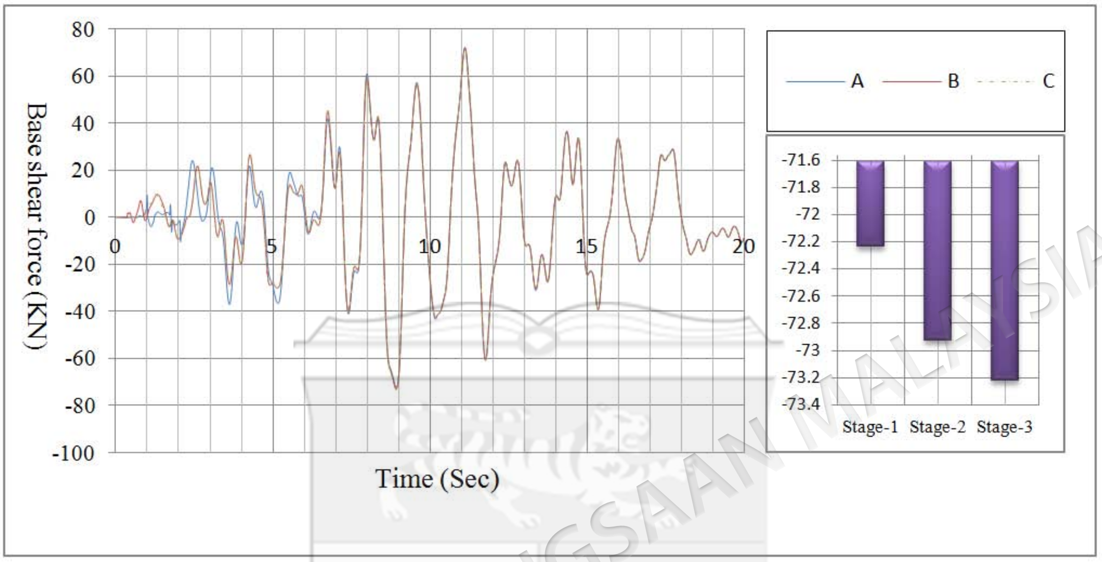

Linear Analysis (Newmark) direction II

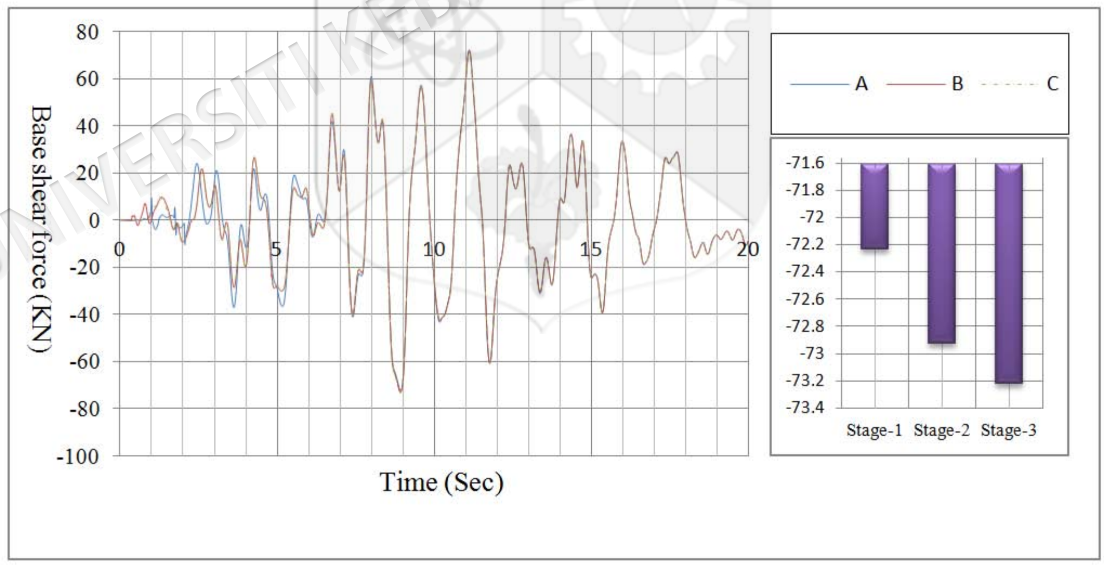

Linear analysis (H H Tylor) Direction I

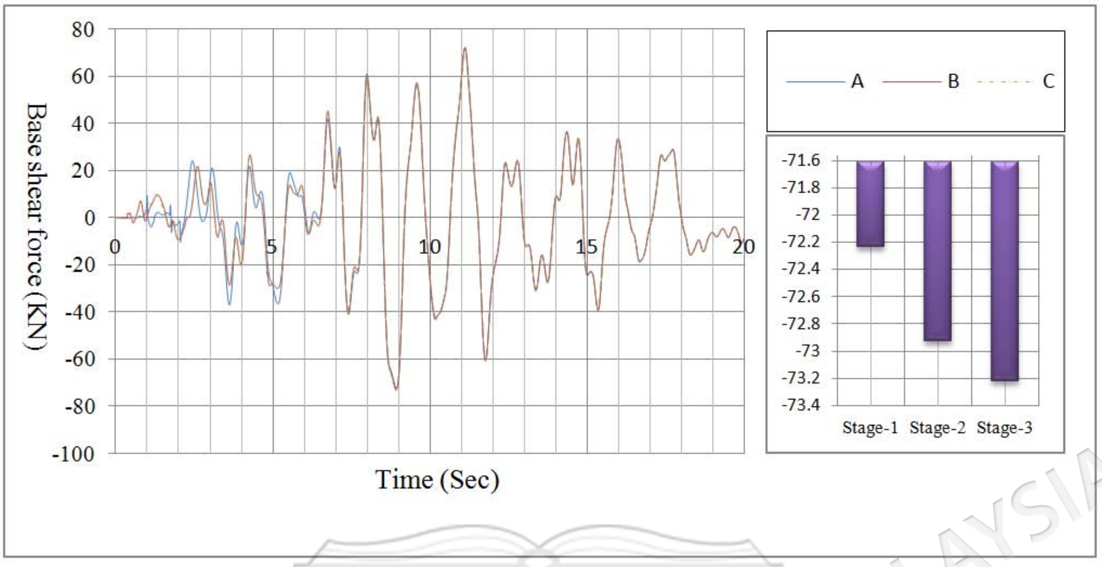

Linear Analysis (H H Tylor) Direction II

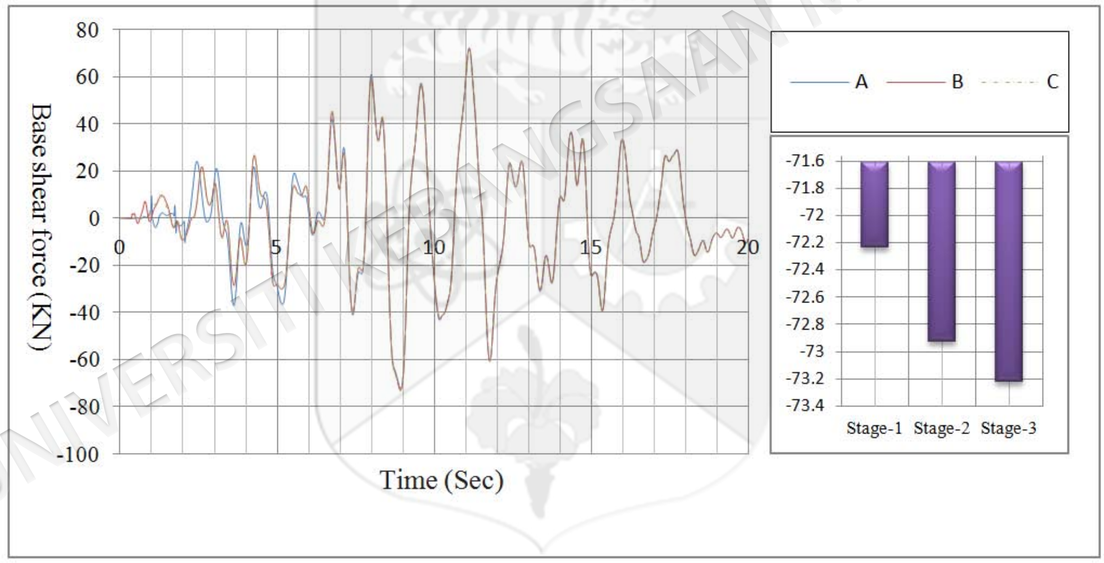

Linear analysis with embedment (Newmark) Direction I

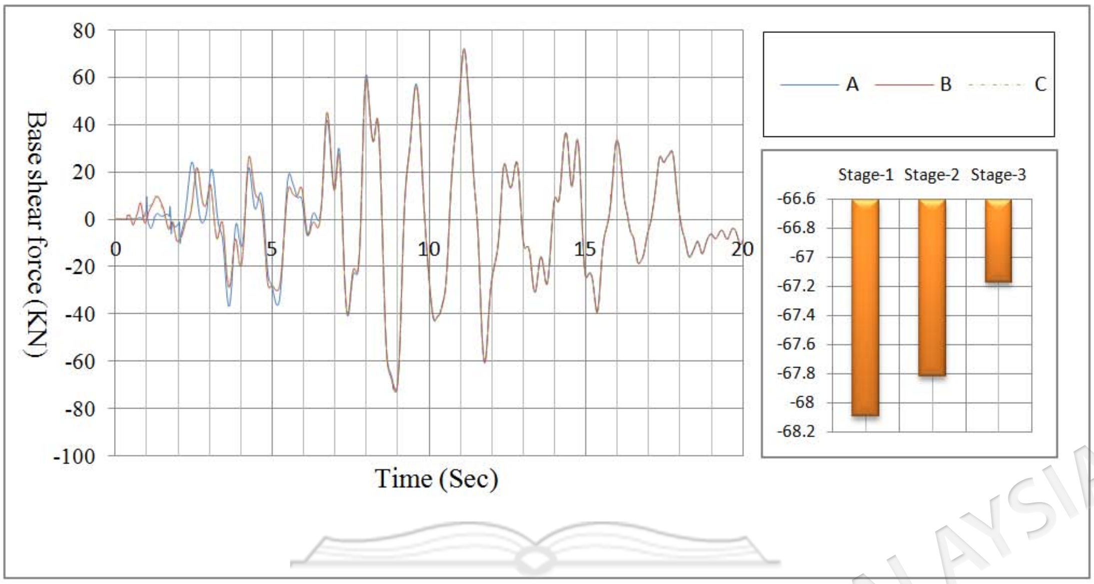

Linear analysis with embedment (Newmark) Direction II

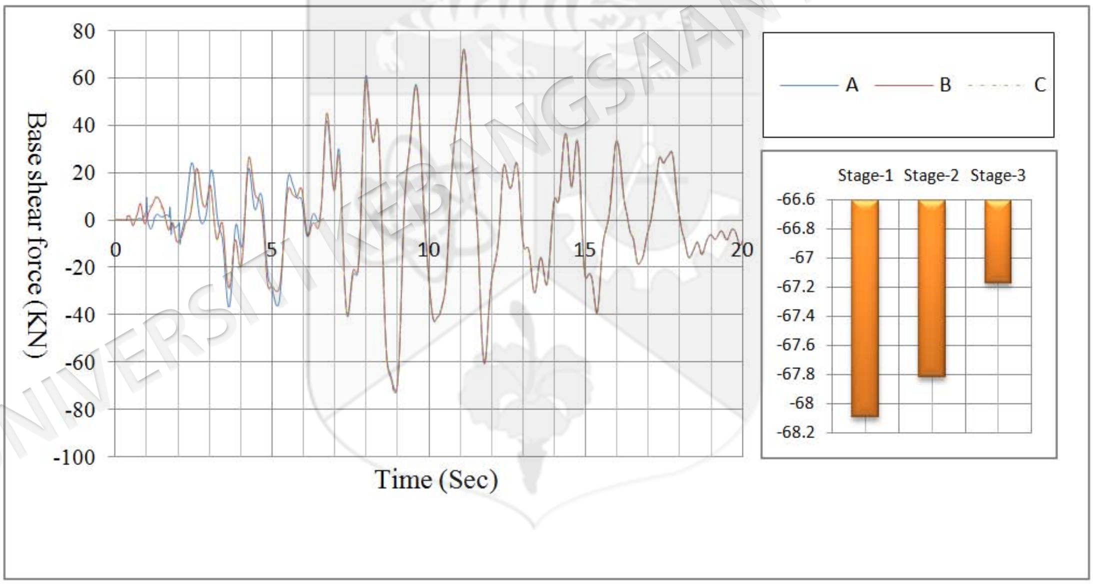

Linear analysis with embedment (H H Tylor) Direction I

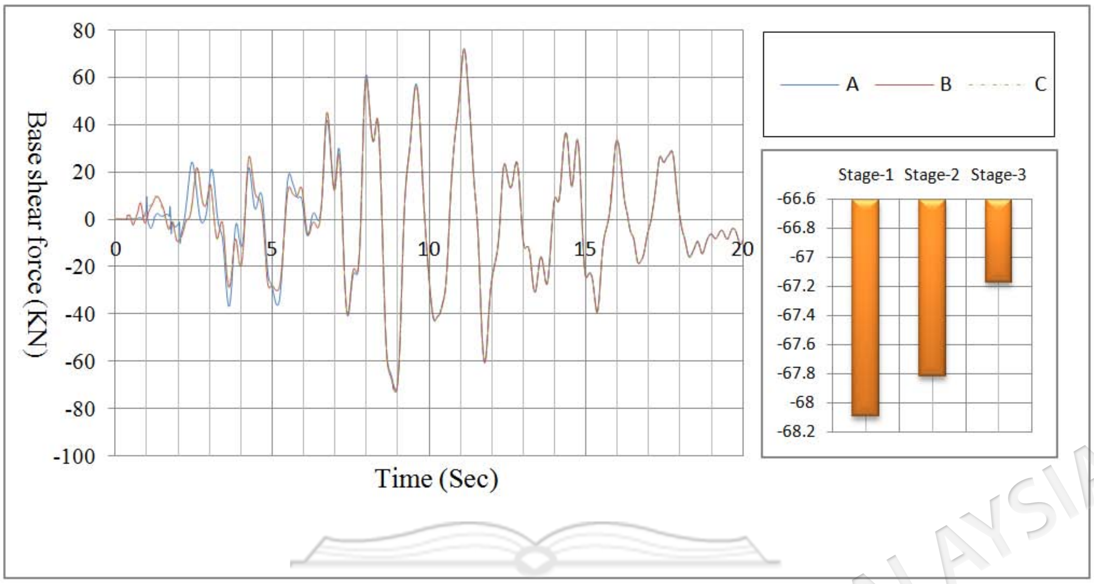

Linear analysis with embedment (H H Tylor) Direction II

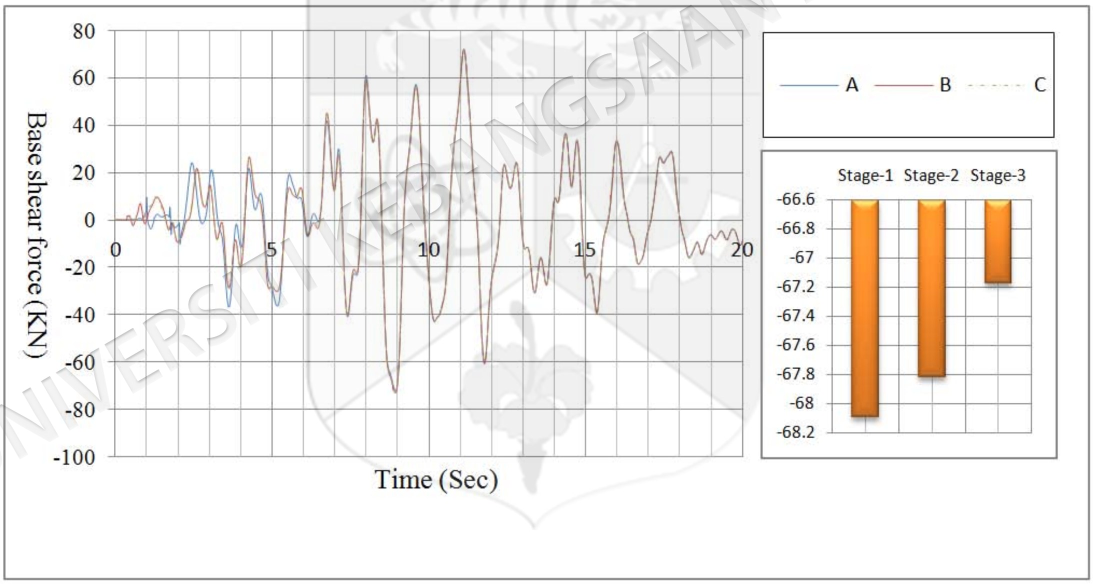

Nonlinear analysis (Newmark) Direction I

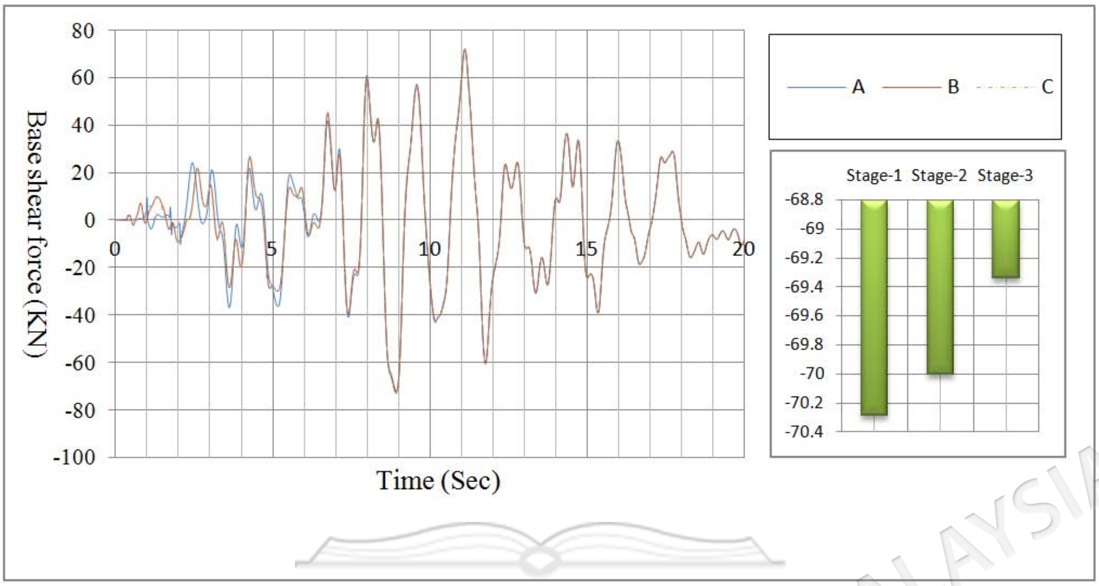

Nonlinear analysis (Newmark) Direction II

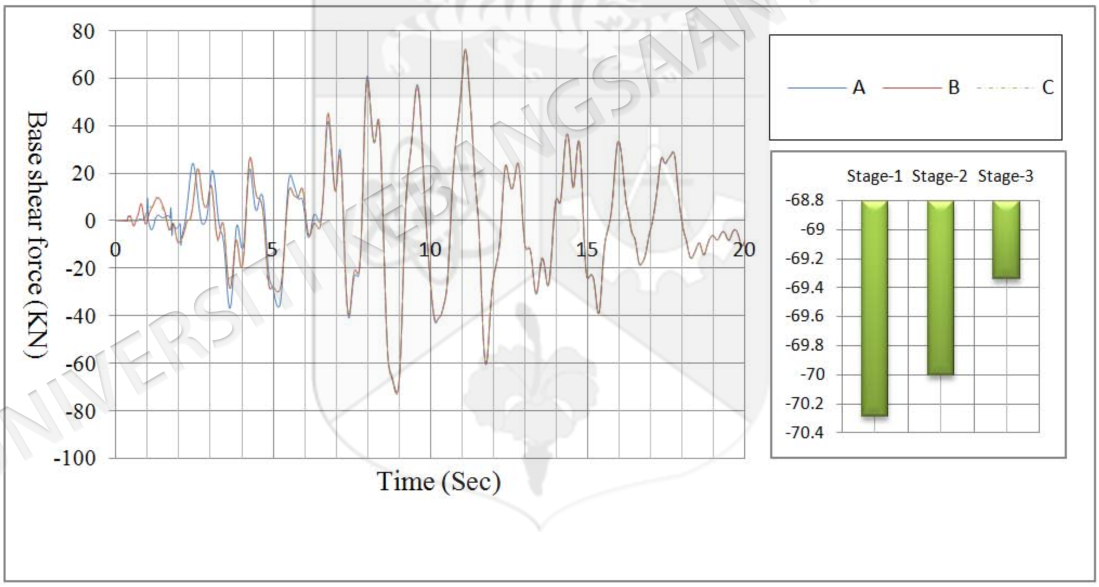

Nonlinear analysis (H H Tylor) Direction I

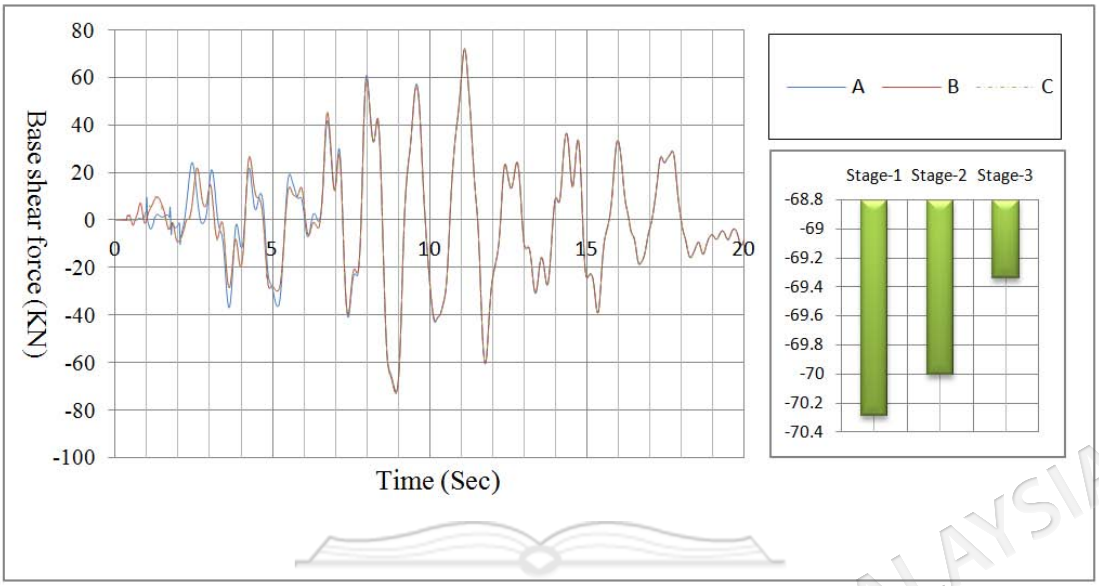

Nonlinear analysis (H H Tylor) Direction II

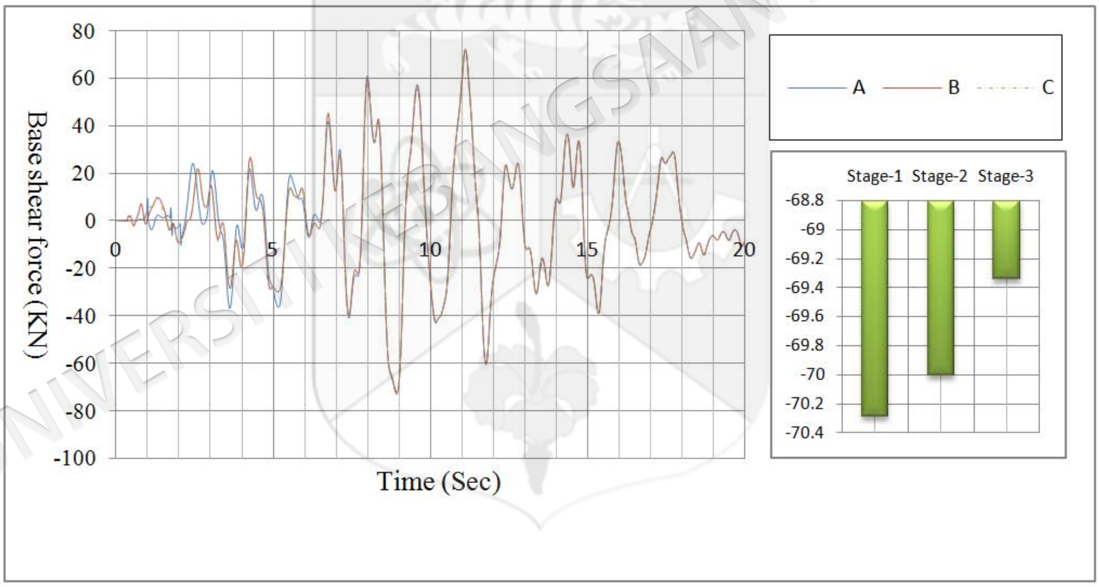

Nonlinear analysis with embedment (Newmwrk) Direction I

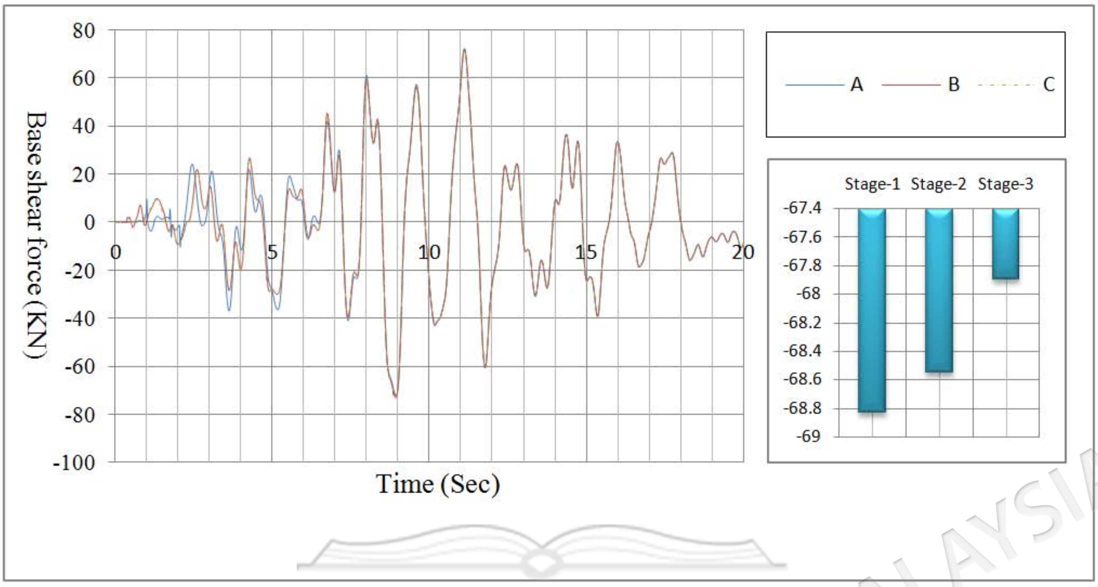

Nonlinear analysis with embedment (Newmwrk) Direction II

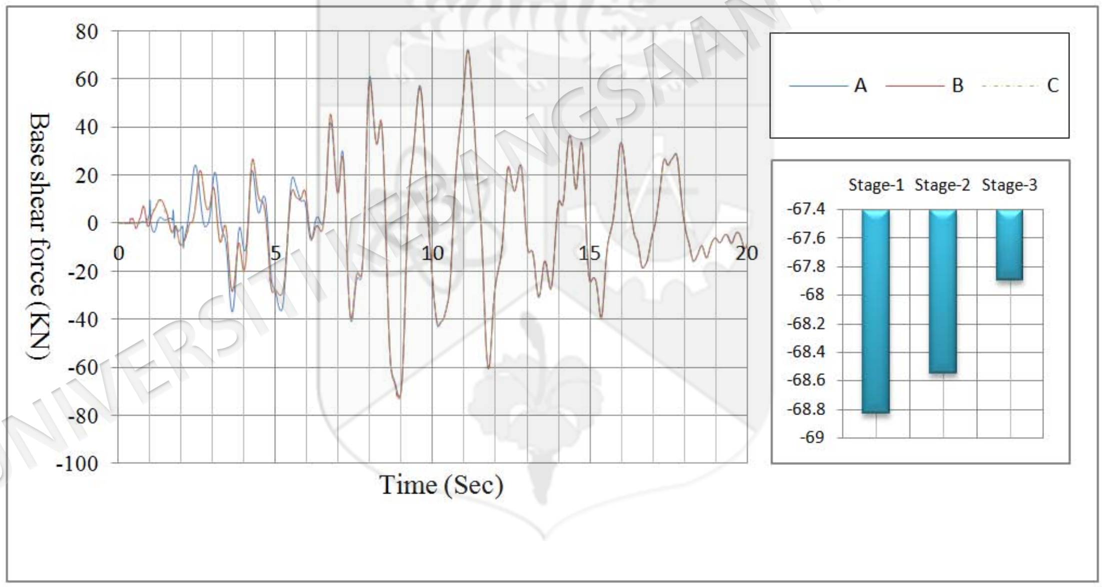

Nonlinear analysis with embedment (Newmark) Direction I

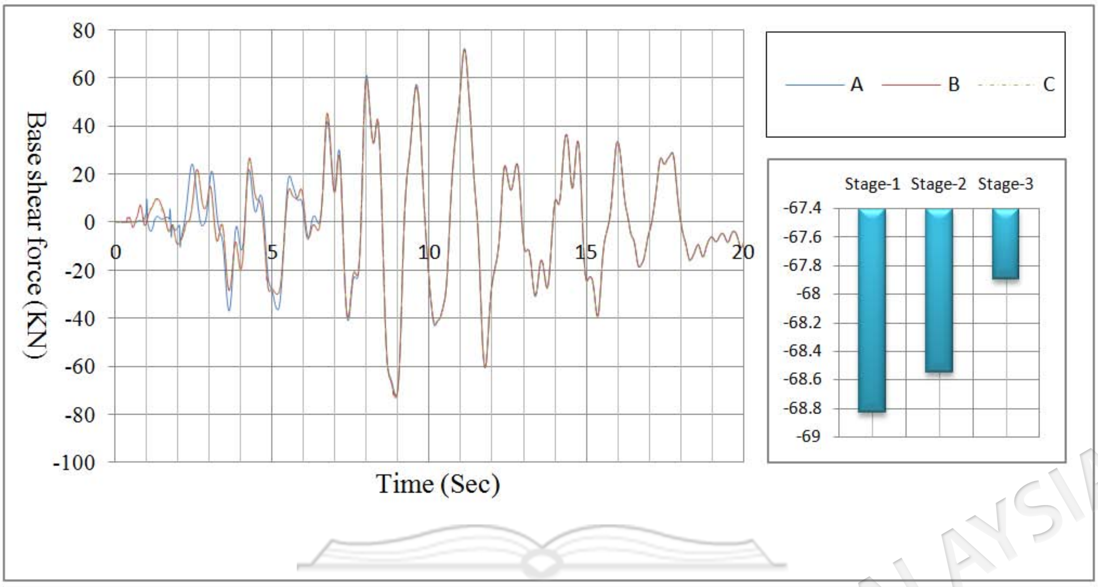

Nonlinear analysis with embedment (Newmark) Direction II

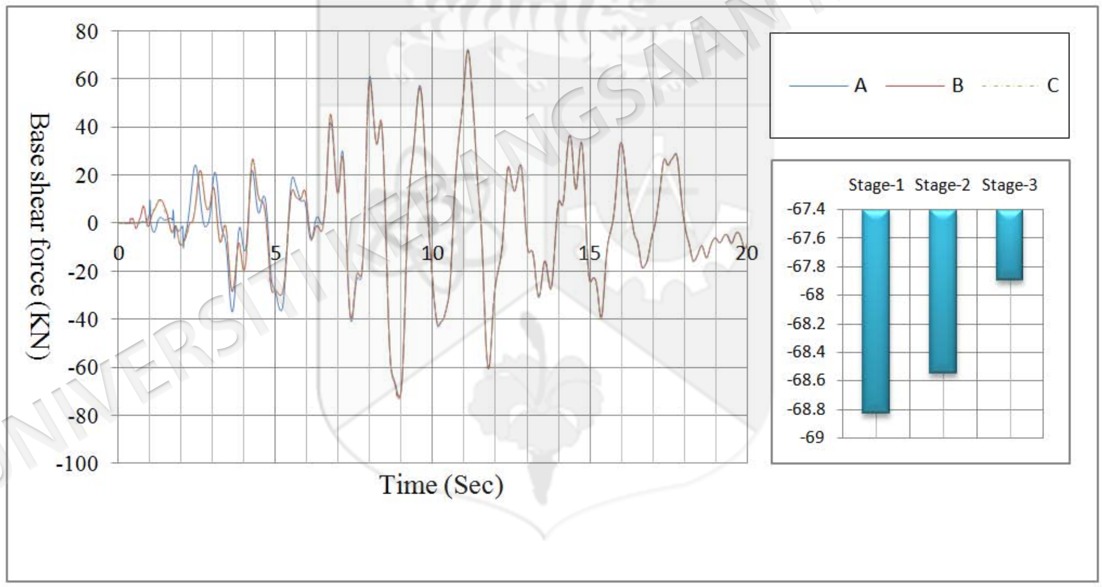

Drafting along elevated circular concrete water tank

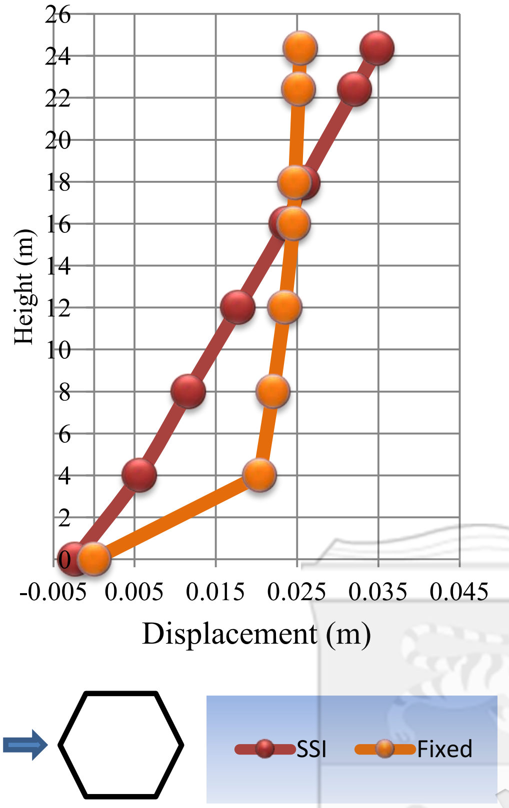

Linear analysis (Newmark) x Direction

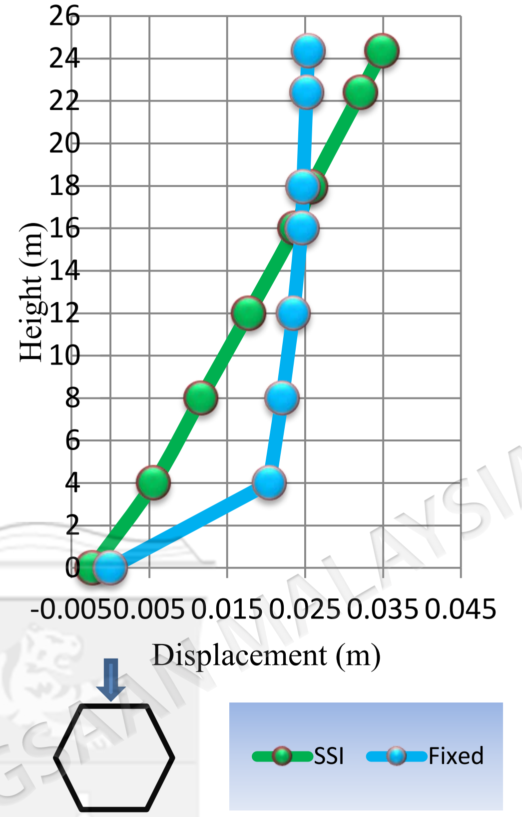

Linear analysis (Newmark) Y Direction

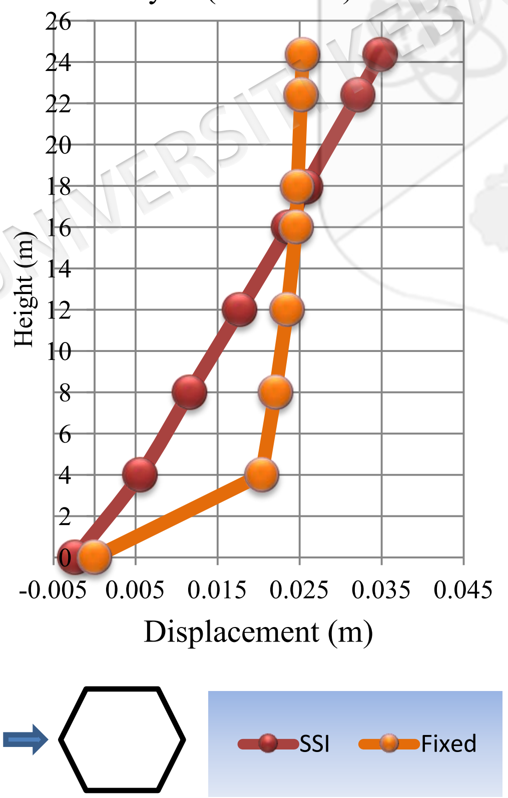

Linear analysis (H. H. Tylor) x Direction

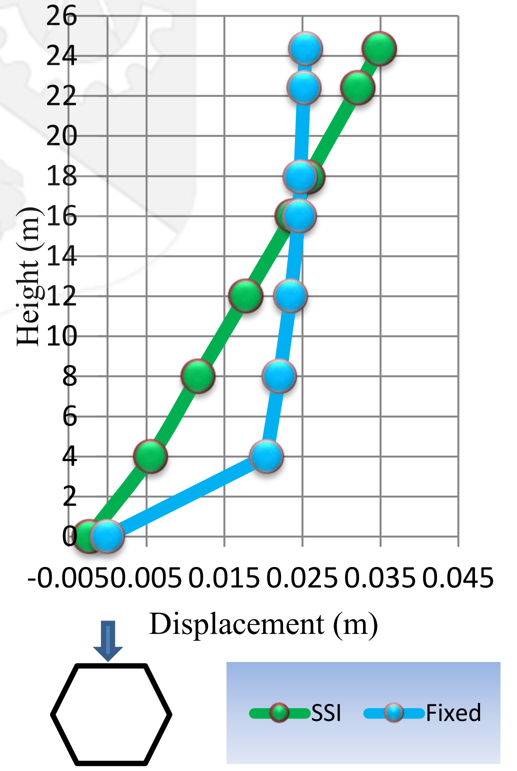

Linear analysis (H. H. Tylor) Y Direction

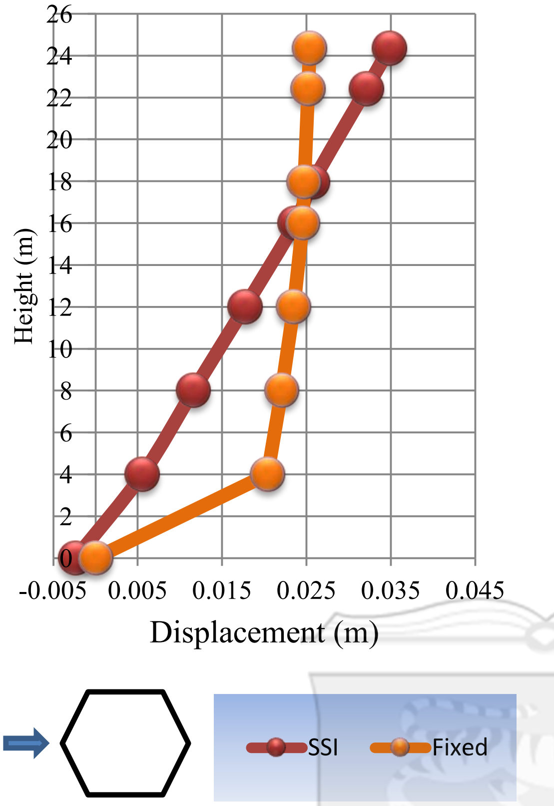

Nonlinear analysis (Newmark) x Direction

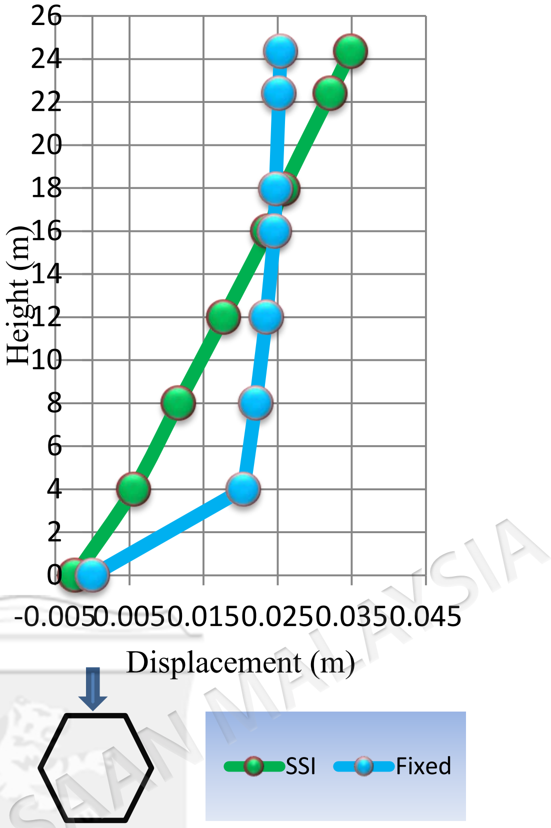

Nonlinear analysis (Newmark) Y Direction

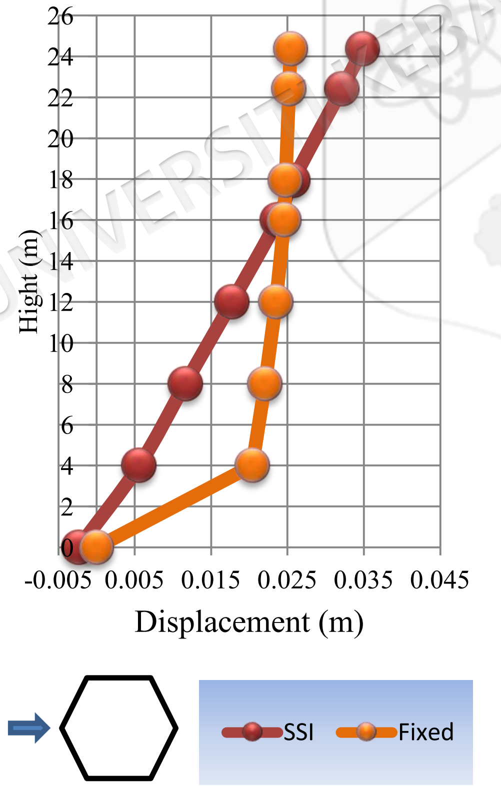

Nonlinear analysis (H. H. Tylor) x Direction

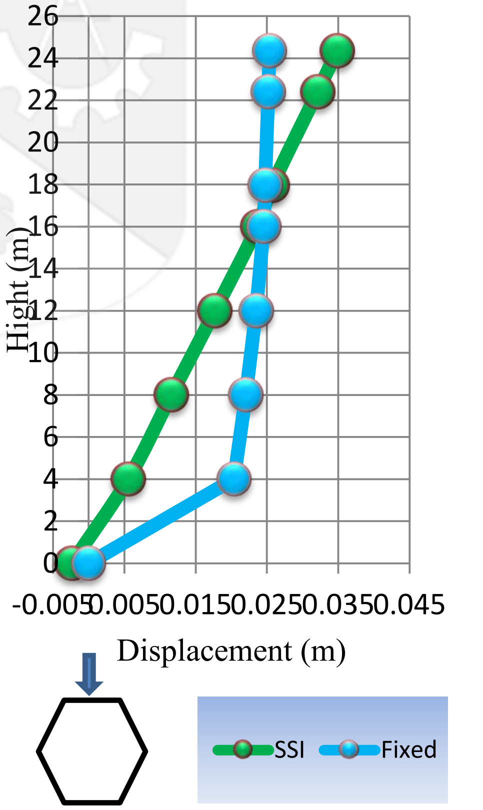

Nonlinear analysis (H. H. Tylor) y Direction

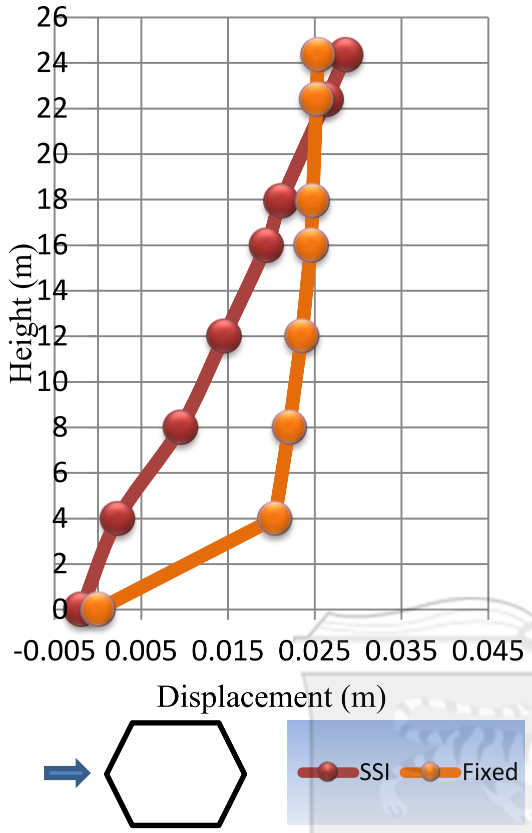

Linear analysis (Newmark) X Direction (Embedment)

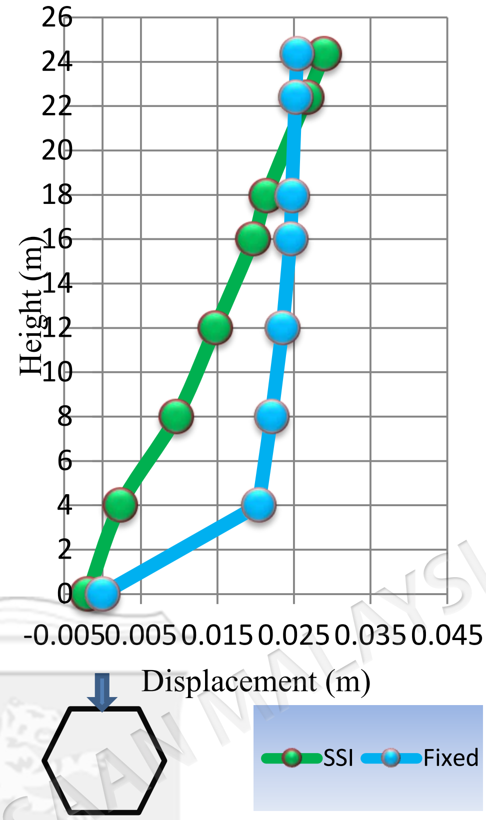

Linear analysis (Newmark) Y Direction (Embedment)

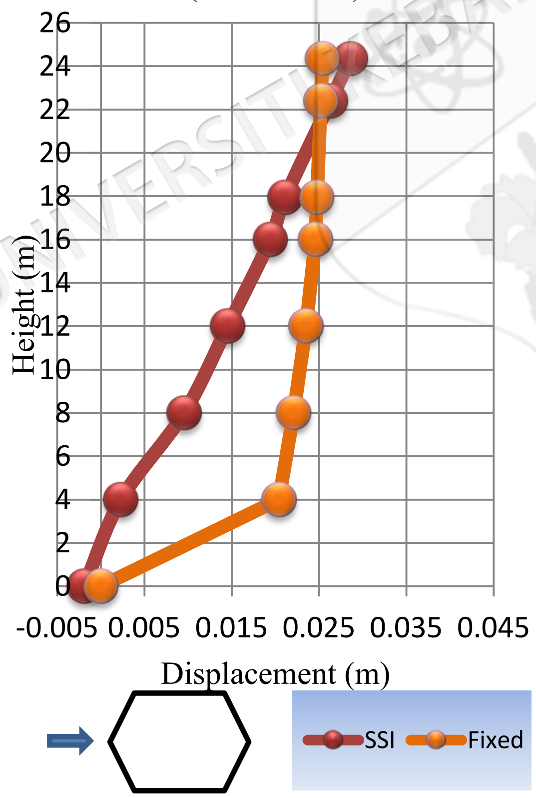

Linear analysis (H. H. Tylor) X Direction (Embedment)

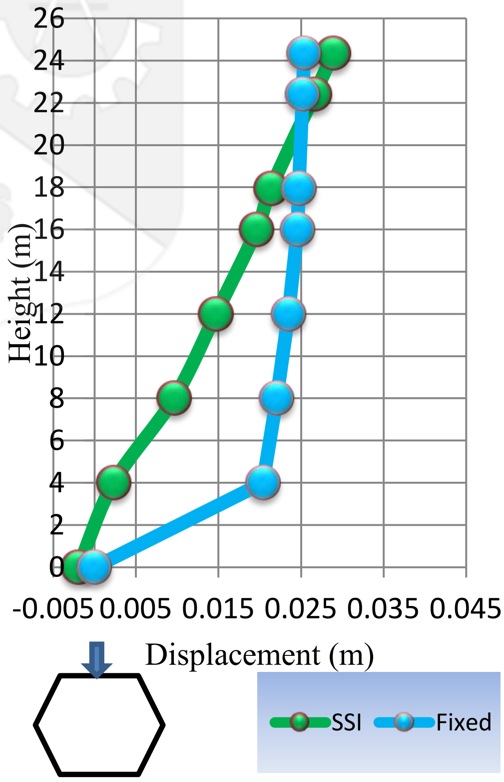

Linear analysis (H. H. Tylor) Y Direction (Embedment)

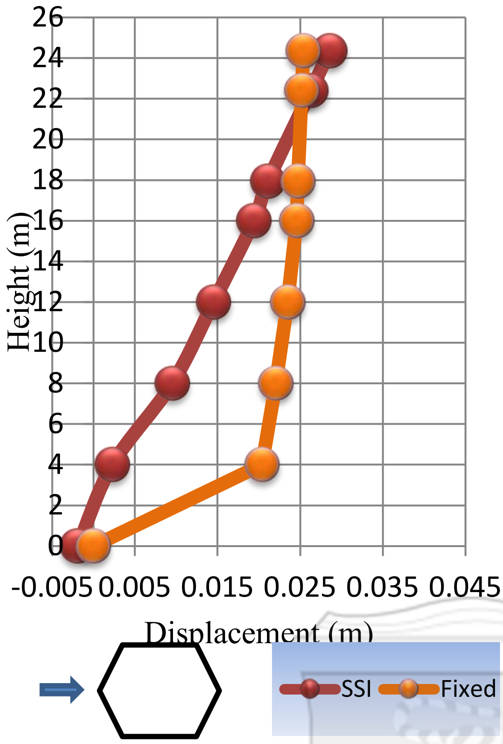

Nonlinear analysis (Newmark) X Direction (Embedment)

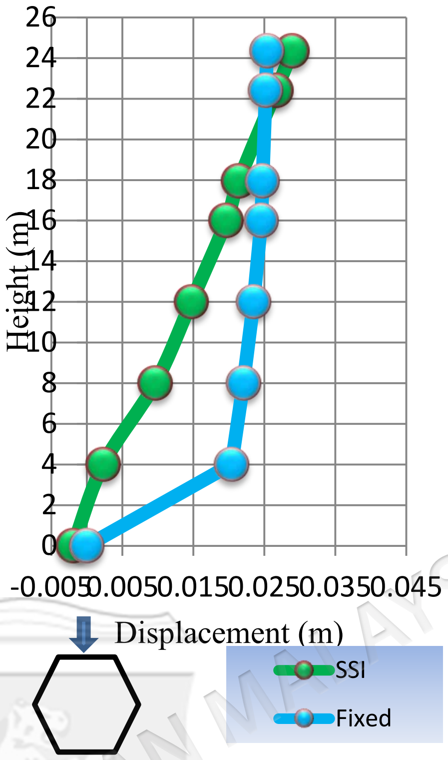

Nonlinear analysis (Newmark) Y Direction (Embedment)

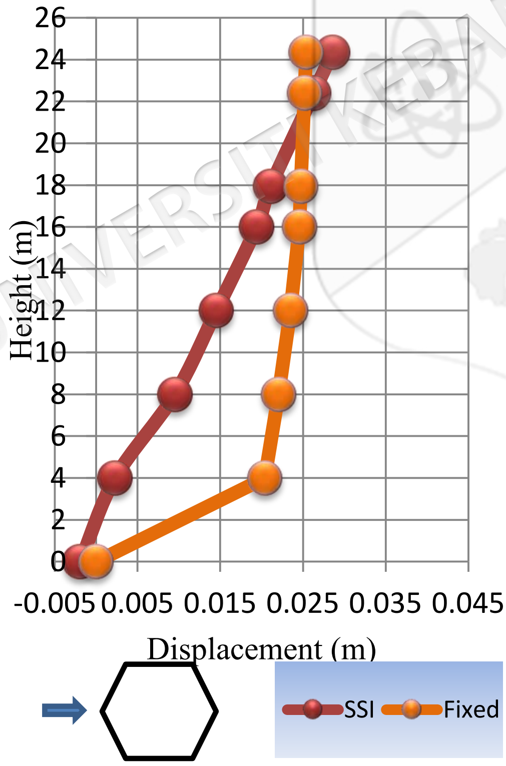

Nonlinear analysis (H. H. Tylor) X Direction (Embedment)

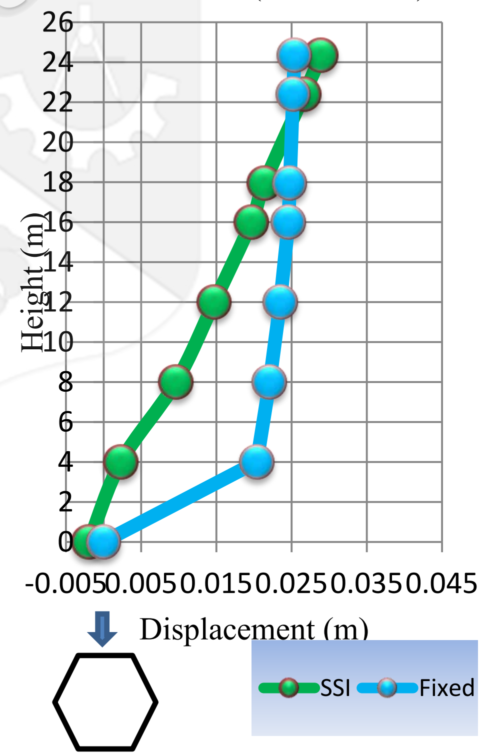

Nonlinear analysis (H. H. Tylor) Y Direction (Embedment)